

Process based modelling of the nutrient dynamics in a tidal dominated coastal area

Dissertation
Zur Erlangung des Doktorgrades
der Mathematisch-Naturwissenschaftlichen Fakultät
der Christian-Albrechts-Universität zu Kiel

vorgelegt von

Piyamarn Leangruxa

Kiel
September 2004

Referent:	Prof. Dr. Roberto Mayerle
Koreferent:	Prof. Dr. Franciscus Colijn
Tag der mündlichen Prüfung:	10 November 2004
Zum Druck genehmigt	Kiel, October 2005

Acknowledgements

The author wishes to express her deepest gratitude and profound appreciation to her supervisor, Prof. Dr. Roberto Mayerle. His exemplary guidance, continuous supports and close supervision throughout her research are most deeply appreciated. Special gratitude is also extended to Dr. Karl-Juergen Hesse for his invaluable advice and all kind of supports.

Grateful acknowledgements are extended to the colleagues of the Coastal Research Laboratory and the Research and Technology Centre Westcoast for their invaluable friendship and continuous encouragement.

The sincerely appreciation is especially due to Ms. Britta Egge for her assistance during the laboratory analysis. The support of the entire crew during the measuring campaigns is well acknowledged.

Finally, the author is indebted to her family for all kind of supports, trust and encouragement which made her research possible.

Abstract

The Northern German Wadden Sea is characterized as a natural eutrophic system, which is subjected to an additional anthropogenic nutrient input deriving mainly from the discharge of the Elbe river through its seaward border. Information about the distribution and transport of the nutrients near to the coast is still insufficient, since most of the previous measurements were restricted to the tidal inlets only. The aim of the present study is to set up a nutrient dynamic model which takes into account the main Wadden Sea specific processes governing the dissolved inorganic nutrient distribution in the shallow area. Investigations were carried out in a semi-enclosed tidal flat area known as the Meldorf Bight. The hydrodynamics in the area is mainly dominated by tidal forcing with the mean tidal range of about 3.5m. During low tide the tidal flat area is dry and it is flooded during high tide.

First, seasonal nutrient gradients and their transport patterns were evaluated. The seasonal cycle of dissolved inorganic nitrogen compounds corresponds to the usual pattern in temperate seas with maxima in winter and minima in spring and summer. In the case of phosphate, high concentrations prevailed also in late summer, which is a result of remobilization from the temporary iron hydroxide sediment buffer. Nutrient concentrations during ebb tide were slightly higher than the concentrations during flood tide indicating the importance of local sources near the coast. Due to a strong tidal mixing, the vertical variation of nutrient concentrations was found to be insignificant. Computed net transports of nutrients were found to be slightly different for spring, summer and winter. Export of phosphate was observed in late summer.

Results from small scale spatial measurements and from tidal nutrient cycles were used as a data basis to set-up the nutrient dynamic model. The Delft3D modelling system (Delft Hydraulics, The Netherlands) was employed for the numerical analysis of the flow and nutrient dynamics. The model was set-up for the simulation of nitrate, ammonium and phosphate gradients. Measured nutrient concentrations at the model open sea boundaries were used as input data. A sensitivity analysis with respect to the model parameters such as the dispersion coefficient was carried out. Due to the complexity of the natural processes, only the seasonal dominant ones were selected for the calibration.

The model results were compared to the measured data. There is a good agreement in winter when the nutrients are conservative and biological processes are minimal. During spring the influence of local freshwater discharge deriving from the hinterland drainage was found to be significant. The model is capable of capturing the impact due to the freshwater releases. Main nutrient trends are relatively well estimated, especially for nitrate and phosphate. In summer, denitrification of nitrate as well as ammonification and phosphorus remineralisation were accounted for in the model calibration. Although the trends in ammonium are well predicted by the model, some discrepancies between the measured and computed concentrations are still significant. However, the results of model validation confirm the ability of the calibrated model in predicting the short term nutrient distribution in the investigation area.

Kurzfassung

Das nördliche deutsche Wattenmeer stellt ein natürlich eutrophes System dar, welches einem zusätzlichen antropogenen Nährstoffeintrag unterliegt, der hauptsächlich über den seewärtigen Rand aus dem Elbeästuar in das Gebiet eindringt. Unsere Kenntnisse der Nährstoffgradienten und -transporte in den flachen küstennahen Bereichen dieses Gebietes sind noch sehr lückenhaft, da sich frühere Messungen meist auf die Tidenrinnen beschränkten. Die vorliegende Untersuchung hat die Entwicklung eines Nährstoffdynamik-Modells zum Ziele, welches die wichtigsten wattenmeerspezifischen Steuerfaktoren der anorganisch gelösten Nährstoffverteilung berücksichtigt. Die Untersuchungen wurden in einem halbabgeschlossenen, flachen Wattenmeergebiet nördlich der Elbmündung, der Meldorfer Bucht, durchgeführt. Die Hydrodynamik dieses Gebietes wird hauptsächlich durch die Gezeitenbewegung bestimmt, welche durch einen mittleren Tidenhub von ca. 3,5m gekennzeichnet ist.

In mehreren Feldmessungen wurden die saisonalen Gradienten und Transporte der anorganisch gelösten Stickstoffkomponenten und des Phosphats bestimmt. Der saisonale Verlauf der Stickstoffkomponenten entspricht dem für temperierte Meeresgebiete üblichen Zyklus mit Maxima im Winter und Minima im Frühling und Sommer. Im Phosphatverlauf wurden im Spätsommer sehr hohe Konzentrationen beobachtet, die auf eine Remobilisierung aus dem temporären Eisenhydroxid-Sedimentpuffer zurückgeführt werden. Die mittleren Nährstoffkonzentrationen waren während der Ebbtide meist höher als zur Flutphase, welches auf die Bedeutung lokaler Nährstoffquellen entlang der Küste hinweist. Signifikante Unterschiede in den Nährstoffkonzentrationen zwischen Oberflächen- und Tiefenwasser waren aufgrund der gezeitenbedingt starken Vertikaldurchmischung nicht vorhanden. In den berechneten Nettotransporten der Nährstoffe ergaben sich leichte saisonale Unterschiede. Im Spätsommer wurde ein Phosphatexport aus der Bucht in das vorgelagerte Gebiet beobachtet.

Die kleinräumigen saisonalen Flächenaufnahmen und die tidenzyklischen Erhebungen stellten die Datengrundlage für die Entwicklung des Nährstoffdynamik-Modells dar. Das Delft3D Modellsystem (Delft Hydraulics, Niederlande) wurde für die numerische Analyse der Strömungs- und Nährstoffdynamik angepasst. Das Modell wurde für die Simulation der Nitrat-, Ammonium- und Phosphatgradienten eingesetzt. Als Antrieb wurden die tidenzyklischen Nährstoffkonzentrationen an der offenen Modellgrenze verwendet. Es wurde eine Sensitivitätsanalyse bezüglich der einzelnen Modellparameter, wie dem Dispersionskoeffizienten, durchgeführt. Aufgrund der Komplexität der natürlichen Prozesse wurden nur die saisonal bedeutenden Faktoren für die Kalibrierung des Modells ausgewählt.

Die Modellberechnungen wurden mit den Felddaten verglichen. Es bestand eine gute Übereinstimmung im Winter, da sich die Nährstoffe zu dieser Jahreszeit aufgrund der reduzierten biologischen Aktivität weitgehend konservativ verhalten. Im Frühling wurde ein deutlicher Einfluss lokaler Einträge aus der Hinterlandentwässerung beobachtet. Das Modell konnte diesen Einfluss gut reproduzieren, speziell für Nitrat und Phosphat. Für die Simulation der Sommersituation wurden Denitrifikations- und Remineralisierungsprozesse

in die Modell-Kalibrierung einbezogen. Die Genauigkeit der Modellberechnungen war zufriedenstellend. Obgleich die Trends der Ammoniumkonzentrationen recht gut reproduziert werden konnten, bestehen hier noch deutliche Diskrepanzen zwischen den Modell- und den Felddaten. Die Ergebnisse der Modellvalidierung bestätigen jedoch, dass das kalibrierte Modell in der Lage ist, die Nährstoffverteilung in der Meldorfer Bucht kurzfristig vorherzusagen.

Contents

Acknowledgements	V
Abstract	VII
Kurzfassung	IX
Contents	XI
List of figures	XIII
List of tables	XVII
1 Introduction	1
1.1 Background	1
1.2 Outline of the dissertation	3
2 State of knowledge	5
2.1 Nutrient dynamics in the Wadden Sea	5
2.2 Modelling of nutrient dynamics	6
3 Investigation area	13
3.1 Introduction	13
3.2 Description of the study site	13
3.2.1 Bathymetry	17
3.2.2 Hydrodynamics	18
3.2.3 Sediment distribution	18
4 Field measurements	21
4.1 Materials and methods	21
4.1.1 Determination of nutrient concentrations	25
4.1.2 Determination of salinity	26
4.2 Results of field measurements: Nutrient transports	26
4.2.1 Tidal conditions	26
4.2.2 Tidal variation of dissolved inorganic nutrient concentrations	28
4.3 Small scale nutrient distribution	35
4.3.1 Tidal conditions	35
4.3.2 Winter nutrient distribution	37
4.3.3 Spring nutrient distribution	42
4.3.4 Summer nutrient distribution	48
4.4 Discussion of the measured results	54

5	Numerical modelling	57
5.1	Introduction.....	57
5.2	Modelling system.....	57
5.2.1	Flow model.....	57
5.2.2	Nutrient dynamics model	60
5.3	Meldorf Bight Model	65
5.3.1	Model domain, grid and bathymetry	66
5.3.2	Model dimensions	66
5.3.3	Tidal flow model.....	67
5.3.3.1	Model set-up	67
5.3.3.2	Sensitivity studies	67
5.3.3.3	Model calibration.....	67
5.3.3.4	Model validation	67
5.3.4	Nutrient dynamics model	68
5.3.4.1	Model set-up	68
5.3.4.2	Sensitivity studies	69
5.3.4.3	Selection of open sea boundary conditions	73
5.3.4.4	Model calibration.....	80
5.3.4.5	Model validation	91
5.3.4.6	Discussion of the results	98
6	Model application	101
6.1	Introduction.....	101
6.2	Sewer station	101
6.3	Freshwater input.....	102
6.4	Remineralisation of ammonium and phosphate in sediment	105
6.5	Discussion of the model application	107
7	Conclusions and recommendations	109
	References	111
	Appendix A	119
	Appendix B.....	131
	Erklärung.....	143
	Lebenslauf	145

List of figures

Figure 2.1: Spatial coverage of ecological modelling in the North Sea	9
Figure 3.1: Investigation area.....	14
Figure 3.2: The Meldorf Bight and its surroundings	14
Figure 3.3: Natural basins classified according to watersheds (Spiegel, 1997)	15
Figure 3.4: The Buesum harbour and important sites along the coast.....	15
Figure 3.5: Dike with sheep and tidal flat area in the Meldorf Bight	16
Figure 3.6: Eastern polder basin and the Meldorf Harbour	17
Figure 3.7: Bathymetry of the investigation area	18
Figure 3.8: Sediment grain size in the Meldorf Bight by Reimers (1999).....	19
Figure 4.1: Location of cross-section G-H at the Piep intertidal channel during the seasonal nutrient transport measurements in 2001	22
Figure 4.2: Location of sampling stations on the cross-section G-H at the Piep intertidal channel.....	22
Figure 4.3: Sampling locations during the small scale seasonal nutrient investigation in 2002	24
Figure 4.4: Water level, current magnitude and flow discharge on 21 June 2001.....	27
Figure 4.5: Water level, current magnitude and flow discharge on 29 June 2001.....	27
Figure 4.6: Water level, current magnitude and flow discharge on 12 September 2001.....	27
Figure 4.7: Water level, current magnitude and flow discharge on 14 November 2001	27
Figure 4.8: DIN concentrations at the cross section G-H in the Piep intertidal channel during the measuring campaigns performed in 2001	28
Figure 4.9: PO ₄ concentrations at the cross section G-H in the Piep intertidal channel during the measuring campaigns performed in 2001	28
Figure 4.10: Vertical variation of NO ₂ , NO ₃ , NH ₄ and PO ₄ at station G on 21 June 2001	29
Figure 4.11: Vertical variation of NO ₂ , NO ₃ , NH ₄ and PO ₄ at station H on 21 June 2001	30
Figure 4.12: Vertical variation of NO ₂ , NO ₃ , NH ₄ and PO ₄ at station G on 29 June 2001	30
Figure 4.13: Vertical variation of NO ₂ , NO ₃ , NH ₄ and PO ₄ at station H on 29 June 2001.....	31
Figure 4.14: Vertical variation of NO ₂ , NO ₃ , NH ₄ and PO ₄ at station G on 12 September 2001	31
Figure 4.15: Vertical variation of NO ₂ , NO ₃ , NH ₄ and PO ₄ at station H on 12 September 2001	32
Figure 4.16: Vertical variation of NO ₂ , NO ₃ , NH ₄ and PO ₄ at station G on 14 November 2001.....	32
Figure 4.17: Vertical variation of NO ₂ , NO ₃ , NH ₄ and PO ₄ at station H on 14 November 2001.....	33
Figure 4.18: Water transports during the measurements in 2001 at the cross section G-H in the Piep intertidal channel.....	34
Figure 4.19: DIN transports at the cross section G-H in the Piep intertidal channel in 2001.....	34
Figure 4.20: PO ₄ transports at the cross section G-H in the Piep intertidal channel in 2001	35
Figure 4.21: Water level, current magnitude and direction on 13 February 2002	35
Figure 4.22: Water level, current magnitude and direction on 14 February 2002	36
Figure 4.23: Water level, current magnitude and direction on 7 May 2002	36
Figure 4.24: Water level, current magnitude and direction on 8 May 2002	36

Figure 4.25: Water level, current magnitude and direction on 21 August 2002	36
Figure 4.26: Water level, current magnitude and direction on 22 August 2002	37
Figure 4.27: Nutrient concentrations at grid stations on 13 February 2002	38
Figure 4.28: Nutrient concentrations at grid stations on 14 February 2002	38
Figure 4.29: Nutrient concentrations at landbased stations on 13 February 2002	39
Figure 4.30: Nutrient concentrations at landbased stations on 14 February 2002	39
Figure 4.31: Distribution of NO ₃ , NH ₄ and PO ₄ in winter 2002	40
Figure 4.32: Correlation of DIN and PO ₄ with salinity in winter 2002.....	40
Figure 4.33: Comparisons of nutrient concentrations at the outlet and outfall of the sewage plant and at Buesum Mole in winter 2002	41
Figure 4.34: NO ₂ concentration at ship 1 and ship 2 in winter 2002.....	41
Figure 4.35: NO ₃ concentration at station ship 1 and ship 2 in winter 2002	41
Figure 4.36: NH ₄ concentration at station ship 1 and ship 2 in winter 2002	42
Figure 4.37: PO ₄ concentration at station ship 1 and ship 2 in winter 2002.....	42
Figure 4.38: Nutrient concentrations at grid stations on 7 May 2002.....	43
Figure 4.39: Nutrient concentrations at grid stations on 8 May 2002.....	43
Figure 4.40: Nutrient concentrations at landbased stations on 7 May 2002	44
Figure 4.41: Nutrient concentrations at landbased stations on 8 May 2002	44
Figure 4.42: Distribution of NO ₃ , NH ₄ and PO ₄ in spring 2002.....	45
Figure 4.43: Correlation of DIN and PO ₄ with salinity in spring 2002.....	45
Figure 4.44: Comparisons of nutrient concentrations at the outlet and outfall of the sewage plant and at Buesum Mole in spring measurements 2002.....	46
Figure 4.45: NO ₂ concentration at station ship 1 and ship 2 in spring 2002	46
Figure 4.46: NO ₃ concentration at station ship 1 and ship 2 in spring 2002	47
Figure 4.47: NH ₄ concentration at station ship 1 and ship 2 in spring 2002	47
Figure 4.48: PO ₄ concentration at station ship 1 and ship 2 in spring 2002.....	47
Figure 4.49: NO ₂ and NO ₃ concentrations at the automatic sampler station in spring 2002.....	47
Figure 4.50: NH ₄ and PO ₄ concentrations at the automatic sampler station in spring 2002	48
Figure 4.51: Nutrient concentrations at grid stations on 21 August 2002	49
Figure 4.52: Nutrient concentrations at grid stations on 22 August 2002	49
Figure 4.53: Nutrient concentrations at landbased stations on 21 August 2002	50
Figure 4.54: Nutrient concentrations at landbased stations on 22 August 2002	50
Figure 4.55: Distribution of NO ₃ , NH ₄ and PO ₄ in summer 2002	51
Figure 4.56: Correlation of DIN and PO ₄ with salinity in summer 2002.....	51
Figure 4.57: Comparisons of nutrient concentrations at the outlet and outfall of the sewage plant and at Buesum Mole in summer measurements 2002.....	52
Figure 4.58: NO ₂ concentration at stations ship 1 and ship 2 in summer 2002.....	52
Figure 4.59: NO ₃ concentration at stations ship 1 and ship 2 in summer 2002.....	52
Figure 4.60: NH ₄ concentration at stations ship 1 and ship 2 in summer 2002.....	53
Figure 4.61: PO ₄ concentration at stations ship 1 and ship 2 in summer 2002	53
Figure 4.62: NO ₂ and NO ₃ concentrations at the automatic sampler station in summer 2002.....	53

Figure 4.63: NH₄ and PO₄ concentrations at the automatic sampler station in summer 2002	53
Figure 5.1: Grid and bathymetry of the Meldorf Bight model.....	66
Figure 5.2: Effect of time step on NO₃ concentrations	70
Figure 5.3: Effect of time step on NH₄ concentrations	70
Figure 5.4: Effect of time step on PO₄ concentrations.....	70
Figure 5.5: Effect of the open boundary on NO₃ concentrations.....	71
Figure 5.6: Effect of the open boundary on NH₄ concentrations	71
Figure 5.7: Effect of the open boundary on PO₄ concentrations.....	71
Figure 5.8: Effect of the dispersion coefficients on NO₃ concentrations	72
Figure 5.9: Effect of the dispersion coefficients on NH₄ concentrations	72
Figure 5.10: Effect of the dispersion coefficients on PO₄ concentrations.....	72
Figure 5.11: Effect of the denitrification rate on NO₃ concentrations	73
Figure 5.12: Effect of the remineralisation on PO₄ concentrations.....	73
Figure 5.13: Comparison of measured and computed NO₃ concentrations before high water (a) and after high water (b) in winter 2002	75
Figure 5.14: Comparison of measured and computed NH₄ concentrations before high water (a) and after high water (b) in winter 2002	75
Figure 5.15: Comparison of measured and computed PO₄ concentrations before high water (a) and after high water (b) in winter 2002	76
Figure 5.16: Comparison of measured and computed NO₃ concentrations before high water (a) and after high water (b) in spring 2002.....	77
Figure 5.17: Comparison of measured and computed NH₄ concentrations before high water (a) and after high water (b) in spring 2002.....	77
Figure 5.18: Comparison of measured and computed PO₄ concentrations before high water (a) and after high water (b) in spring 2002.....	78
Figure 5.19: Comparison of measured and computed NO₃ concentrations before high water (a) and after high water (b) in summer 2002.....	79
Figure 5.20: Comparison of measured and computed NH₄ concentrations before high water (a) and after high water (b) in summer 2002.....	79
Figure 5.21: Comparison of measured and computed PO₄ concentrations before high water (a) and after high water (b) in summer 2002.....	80
Figure 5.22: Measured data versus preliminary model results for NO₃ on 13 February 2002.....	82
Figure 5.23: Measured data versus preliminary model results for NH₄ on 13 February 2002.....	82
Figure 5.24: Measured data versus preliminary model results for PO₄ on 13 February 2002	83
Figure 5.25: Comparisons of measured and computed concentrations of NO₃ at the grid stations before high water (a) and after high water (b) on 13 February 2002	83
Figure 5.26: Comparisons of measured and computed concentrations of NH₄ at the grid stations before high water (a) and after high water (b) on 13 February 2002	84
Figure 5.27: Comparisons of measured and computed concentrations of PO₄ at the grid stations before high water (a) and after high water (b) on 13 February 2002	84
Figure 5.28: Measured data versus preliminary and calibrated model results for NO₃ on 7 May 2002	85
Figure 5.29: Measured data versus preliminary and calibrated model results for NH₄ on 7 May 2002	85
Figure 5.30: Measured data versus preliminary and calibrated model results for PO₄ on 7 May 2002	85

Figure 5.31: Comparisons of measured data, preliminary and calibrated model results for NO₃ at the grid stations before high water (a) and after high water (b) on 7 May 2002.....86

Figure 5.32: Comparisons of measured data, preliminary and calibrated model results for NH₄ at the grid stations before high water (a) and after high water (b) on 7 May 2002.....87

Figure 5.33: Comparisons of measured data, preliminary and calibrated model results for PO₄ at the grid stations before high water (a) and after high water (b) on 7 May 2002.....87

Figure 5.34: Measured data versus preliminary and calibrated model results for NO₃ on 21 Aug. 200288

Figure 5.35: Measured data versus preliminary and calibrated model results for NH₄ on 21 Aug. 200288

Figure 5.36: Measured data versus preliminary and calibrated model results for PO₄ on 21 Aug. 2002.....88

Figure 5.37: Comparisons of measured and computed concentrations of NO₃ at the grid stations before high water (a) and after high water (b) on 21 August 200289

Figure 5.38: Comparisons of measured and computed concentrations of NH₄ at the grid stations before high water (a) and after high water (b) on 21 August 200290

Figure 5.39: Comparisons of measured and computed concentrations of PO₄ at the grid stations before high water (a) and after high water (b) on 21 August 200290

Figure 5.40: Measured data versus validated model results for NO₃, NH₄, PO₄ on 14 February 2002.....92

Figure 5.41: Measured data versus validated model results for NO₃, NH₄ and PO₄ on 8 May 2002 ...92

Figure 5.42: Measured data versus validated model results for NO₃, NH₄ and PO₄ on 22 August 2002.....93

Figure 5.43: Comparisons of measured and validated concentrations of NO₃ at the grid stations before high water (a) and after high water (b) on 14 February 200294

Figure 5.44: Comparisons of measured and validated concentrations of NH₄ at the grid stations before high water (a) and after high water (b) on 14 February 200294

Figure 5.45: Comparisons of measured and validated concentrations of PO₄ at the grid stations before high water (a) and after high water (b) on 14 February 200295

Figure 5.46: Comparisons of measured and validated concentrations of NO₃ at the grid stations before high water (a) and after high water (b) on 8 May 2002.....95

Figure 5.47: Comparisons of measured and validated concentrations of NH₄ at the grid stations before high water (a) and after high water (b) on 8 May 2002.....96

Figure 5.48: Comparisons of measured and validated concentrations of PO₄ at the grid stations before high water (a) and after high water (b) on 8 May 2002.....96

Figure 5.49: Comparisons of measured and validated concentrations of NO₃ at the grid stations before high water (a) and after high water (b) on 22 August 200297

Figure 5.50: Comparisons of measured and validated concentrations of NH₄ at the grid stations before high water (a) and after high water (b) on 22 August 200297

Figure 5.51: Comparisons of measured and validated concentrations of PO₄ at the grid stations before high water (a) and after high water (b) on 22 August 200298

Figure 6.1: Effect of increased nutrient discharge from the sewage plant on nutrient levels on the surrounding area (a) nitrate (b) ammonium (c) phosphate concentrations of scenarios 1 and 2102

Figure 6.2: Effect of freshwater input on (a) nitrate (b) ammonium (c) phosphate concentration on the Meldorf Bight.....104

Figure 6.3: Effect of nutrient release from the sediment on (a) ammonium and (b) phosphate concentrations in sediment of scenarios 1 and 2106

Figure 6.4: Discrepancies between scenarios 1 and 2 for ammonium and phosphate concentrations.....106

List of tables

Table 2.1: Modelling systems.....	8
Table 2.2: Dedicated ecological models in the North Sea area	8
Table 2.3: Comparisons of space and time scales for ecological modelling in the North Sea	11
Table 4.1: Sampling data of the measuring campaigns performed in 2001	23
Table 4.2: Sampling data of the measuring campaigns performed in 2002	25
Table 5.1: Selection of boundary condition for the nutrient simulation in winter	74
Table 5.2: Selection of boundary condition for the nutrient simulation in spring.....	76
Table 5.3: Selection of boundary condition for the simulation in summer	78
Table 5.4: Calibration strategy	81
Table 5.5: Summary of the discrepancies obtained from calibration and validation results	91
Table 6.1: Scenarios of sewage water release into the Meldorf Bight.....	101
Table 6.2: Scenarios of freshwater discharges into the Meldorf Bight.....	102
Table 6.3: Scenarios of the remineralisation of NH₄ and PO₄ in sediment at the Meldorf Bight.....	105

1 Introduction

1.1 Background

Coastal regions are environmentally, economically and politically important areas supporting a diverse range of industries and large population centres. As society has increasingly populated along the coasts, the deterioration of the coastal environment has become a critical issue. One of the most significant problems is the over enrichment of coastal waters with nutrients. Introduction of excess nitrogen and phosphorus to the area may lead to eutrophication effects by unbalancing organic supply to the marine ecosystem. One of the most negative effects of eutrophication encompasses oxygen deficiency in bottom waters followed by mass mortality of fish and benthic organisms.

Human activities on land affect both the quantities and qualities (ratios) of nutrient input to the coastal seas. One of the major sources of nutrient enrichment is due to current agricultural practices. The bulk of these nutrient inputs are from diffuse sources, such as soil leakage of mineral fertilizer and wet deposition of atmospheric nitrogen compounds. These inputs are much more difficult to reduce than inputs from point sources, as the case for sewage plants. In order to achieve a successful reduction in diffuse nutrient inputs, current agricultural practices and land use forms, which are characterised by continuous cultures without crop rotation and intensive industrial cattle breeding, have to be transformed and supplemented by additional measures such as the creation of wetlands and vegetation belts as natural nutrient sinks.

The Oslo and Paris Convention (OSPAR) for the protection of the marine environment of the north-east Atlantic established in 1992 a strategy to combat the eutrophication problem in the coastal area. An agreement was made among the governments of the continental countries bordering the North Sea upon the Second International North Sea conference in 1987 to reduce anthropogenic nutrient inputs into rivers and coastal waters by 50% of the level of 1985 within a period of 10-years. Up to now this agreement has been successfully achieved for phosphorus loads but not for nitrogen, because most of the nitrogen inputs are from diffuse sources as mentioned above. In the River Elbe, phosphorus loads have been reduced by about 60%, whereas nitrogen reduction only accounts for about 30% (Behrendt et. al., 2003). Therefore, it is questionable if the ambitious goal of OSPAR, "to achieve by the year 2010 a healthy marine environment where eutrophication does not occur" can be reached.

A more recent but legislative regulation is the EU Water Framework Directive (WFD) which was decided by the European Union in 2000. The purpose of the directive is to develop a framework for the protection of inland surface waters, transitional waters, coastal waters and ground waters which prevents further deterioration, protects and enhances the ecological quality of aquatic systems. It aims at receiving a "good ecological status" and a "good chemical status" for European waters by the year 2015.

In order to fulfil the requirement from the Atlantic OSPAR convention and the European WFD, an assessment of the actual state of the aquatic ecosystem is scheduled as a first step. In the case of OSPAR the coastal seas have to be classified into three eutrophication categories: problem areas, potential problem areas and non-problem areas.

The German Bight including the Wadden Sea area is among the most eutrophied areas in the world. The Wadden Sea forms a direct interface between the soft north west European main land and the North Sea. It is a naturally eutrophied area which receives a constant import of particulate organic matter from the adjacent German Bight. In addition, a substantial nutrient input, derived from the freshwater discharge of the major rivers, is also entering the region. However, due to its dynamic nature and the navigation difficulties in conducting ship surveys, only little information is available on small scale nutrient patterns and nutrient transports. To fulfil the requirement from the regulating frameworks, spatial field measurements and monitoring programs were conducted only at selected sites in the Wadden Sea and adjacent areas.

In the northern German Wadden Sea, which is the area of interest in the present study, nutrient investigations were limited to single point monitoring stations such as the permanent station of the Alfred Wegener Institut/Biologische Anstalt Helgoland (AWI-BAH) in List/Sylt and the Buesum Mole monitoring station operated by the Research and Technology Centre Westcoast (FTZ). Other measurements, such as the spatial surveys carried out in the framework of the SYNDWAT and TRANSWATT projects, are restricted to the tidal inlets only. By contrast, our knowledge about nutrient transports and gradients above the tidal flats and in the very shallow nearshore areas is very scarce.

The difficulties and limitations of field measurements in covering the appropriate spatial and temporal scales of nutrient dynamics require the need for an additional tool to fill the gaps of knowledge and to predict possible consequences of measures taken to mitigate the eutrophication effect.

The purpose of this study is to assess seasonal nutrient transports and distribution in the Meldorf Bight, a shallow semi-enclosed area of the northern German Wadden Sea subjected to the estuarine influence of the Elbe river discharge and to several local nutrient inputs deriving from the hinterland. On this data basis, a numerical model for the simulation of nutrient dynamics in the area is set-up.

With the help of the numerical model it will thus be able to simulate the consequences of different options that can be taken to improve the water quality and to determine the optimal decisions in both economical and environmental senses. Furthermore, specific sources and sinks and their interaction can be identified, and as a consequence, recommendations for future in depth research activities can be made.

The main tasks of this study comprise:

- Field investigations in order to determine the seasonal gradients and tidal transports of dissolved inorganic nutrients in the Meldorf Bight.
- To set-up, calibrate, validate and apply a nutrient dynamics model for the simulation of seasonal nutrient distributions over a period of several days.

The measurements and lab analysis were carried out at the Research and Technology Centre Westcoast, University of Kiel, Germany. Simulations were carried out at the Coastal Research Laboratory, University of Kiel, Germany, with the Delft3D Modelling System developed at Delft Hydraulics, the Netherlands. A coupling of a depth-integrated two-dimensional flow model and a nutrient dynamics model was employed. The three major components of dissolved inorganic nutrients, nitrate, ammonium and phosphate, were modelled. Accuracy of the computed results is determined by means of comparisons with in situ nutrient concentrations.

1.2 Outline of the dissertation

This dissertation is divided into seven chapters. After the introduction, which gives the background, aim and scope of the study, the state of knowledge concerning the available information on nutrient dynamics in the Wadden Sea in terms of measured conditions and modelling approaches is summarised in chapter 2. Dedicated ecological models, including their spatial extend and resolutions are presented. Details of the investigation area including its surroundings are introduced in chapter 3. Major sources of nutrient inputs are also presented. Field measurements are presented in chapter 4. In this chapter, information on materials and methods are given, the measured data are presented and results are discussed. Results from field measurements were used to develop the assumptions for the model development as well as to use the data to calibrate and validate the model. The description of the model and its results are presented in chapter 5. Details of the modelling system, the model settings and the processes and parameters considered are summarised. Sensitivity studies with respect to several model parameters are illustrated. Furthermore, comparisons of the preliminary model results to measured data are presented. Finally the results from the calibration and validation are given and discussed. Chapter 6 presents model applications which can be applied to real cases. Three features were applied: inputs from a sewer station, freshwater inputs and nutrient release due to the remineralisation in the sediments. Finally, in chapter 7, conclusions and recommendations for future developments are presented.

2 State of knowledge

2.1 Nutrient dynamics in the Wadden Sea

The Northern German Wadden Sea forms a natural eutrophic interface between the coastal current of the southeastern North Sea and the soft mainland, which receives products of terrestrial, limnetic and marine processes. It is subjected to a substantial anthropogenic nutrient input deriving mainly from the freshwater discharge of the river Elbe, which accounts for an annual load of 144,000t N and 6,800t P in an average over the last 10 years (Bergemann, pers. com.). Other sources of nutrients are the numerous small rivers, streams and polders draining the agricultural hinterland and the coastal sewage plants. With an estimated share of about 1 to 2% from total nutrient loads (van Beusekom et. al., 2001), these nutrient inputs are quantitatively small when compared to the main river loads. However, they are of local importance, because they reach the Wadden Sea directly, whereas a considerable fraction of river discharge passes through the estuary towards the open German Bight.

In addition to high loads of dissolved nitrogen and phosphorus, the Wadden Sea also receives a considerable amount of particulate organic nutrients deriving mainly from the adjacent coastal water of the North Sea due to hydrodynamic processes such as tidal asymmetry, estuarine circulation and surface transport of particulate matter caused by the predominant westerly winds in the region (Postma, 1983, Hesse et. al., 1992). De Jonge and Postma (1974) suggested that the import of organic matter into the Wadden Sea had increased since the beginning of the fifties by a factor of 3 whereas the autochthonous production had remained unchanged. At present, it is assumed that about one third of the organic matter import into the Wadden Sea is derived from freshwater sources and two-thirds are imported from the open sea (van Beusekom and De Jonge, 1998). Subsequent remineralisation of this particulate organic matter is almost equally divided between the Wadden Sea sediment and the water column (Postma, 1983). The resulting amounts of dissolved inorganic nitrogen and phosphorus substantially add to the nutrient demand of algae growth in the region, especially in summer. For the Northern German Wadden Sea the import of particulate organic material was estimated to be in the range of $100 \text{ g C m}^{-2} \text{ yr}^{-1}$, resulting in a release of excess phosphate of $1,700 \text{ t P yr}^{-1}$ for the whole region (Dick et. al., 1999).

A fraction of the inorganic phosphate which is released by the remineralisation of organic matter is buried in the aerobic Wadden Sea sediments through adsorption on an insoluble iron-hydroxide complex (Dick et. al., 1999; van Beusekom et. al., 1999) The increasing import of organic matter during the growing season and the rising temperatures in summer lead to an enhanced decomposition intensity and thus to an increasing oxygen demand in the sediment with subsequent microbial sulphate reduction under anaerobic conditions. Iron hydroxides are thus reduced and iron sulphide is formed, resulting in a remobilization of phosphate which diffuses from the pore water into the water column, a process which can be enhanced by erosive storm events. This massive release of phosphate in summer is evident by strongly increased phosphate concentrations in the

water column of the Wadden Sea. Hickel (1989) suggested that the high phosphate concentrations in summer are an indicator for increased eutrophication of the Wadden Sea.

As a consequence of biological uptake, temporary storage and remobilization from the sediment, the seasonal cycle of phosphate in the Wadden Sea is characterised by a summer maximum, minima in spring and high concentrations in winter. It is thus different from the typical cycle of phosphate in open temperate seas, such as the North Sea, which usually exhibits an annual minimum during summer. Due to tidal mixing and turbulent diffusion considerable amounts of phosphate are exported from the Wadden Sea to the adjacent North Sea waters, thereby promoting algal growth in these waters (Hesse et. al., 1992).

Postma (1966) and Helder (1974) were the first to describe the seasonal cycle of nitrogen in the Wadden Sea. They found a clear annual cycle of dissolved inorganic nitrogen with low concentrations in spring and summer and high concentrations in autumn and winter. In the seaward areas of the Wadden Sea in summer, dissolved inorganic nitrogen can drop down to concentrations limiting algal growth (Hesse et. al., 1995). This may not only be due to nitrogen uptake by the phytoplankton, but also to intensive denitrification processes in the sediment and the water column, which is estimated to amount up to $50 \mu\text{M N m}^{-2} \text{ h}^{-1}$ (Hesse et. al., 1995).

Strong tidal currents, high wind speeds and a shallow, well mixed water column are the main physical factors responsible for the transport and distribution of the nutrient inputs in the area, resulting in a highly variable and complex shape of the spatial gradients. Highest concentrations are usually observed in those parts of the Wadden Sea which are directly subjected to continental runoff and at sites of silt accumulation, which are usually found in the nearshore area. It was estimated that in winter about 70% of the dissolved inorganic nitrogen and 55% of the dissolved inorganic phosphate pool in the Northern Wadden Sea are of anthropogenic origin (Hesse et. al., 1995).

2.2 Modelling of nutrient dynamics

Field measurements are cost and time consuming and can thus not provide the temporal and spatial resolutions one may want to have. The development of a computer model may fill this gap and support the scientists in interpreting the data. A model may be used as an analytical tool for the determination of sources and sinks and may provide a rough quantitative estimation of a specific process which is hard to achieve by means of field measurements only. It may thus constitute a pathfinder for further analytical research to be conducted. Furthermore, a computer model can be used as a prognostic tool to simulate scenarios related to changes in environmental conditions, in particular due to anthropogenic factors, and to estimate the consequences. The ability to deduce future environmental problems on the basis of field measurements alone is limited, therefore the use of an adequate simulation model in combination with field measurements constitutes an adequate strategy.

After successful development of hydrodynamic models in which flow dynamics and physical circulation can be well computed, these models have been further extended to ecological aspects. The development of an ecological model for the North Sea area was

initially based on box models or a zero-dimensional model. Box models are simple representations of complex aquatic systems which focus on fluxes between boxes and transformations within a box which are considered relatively homogeneous. A collection of simple box models can be linked together horizontally and vertically to represent the major features of the whole area. It is a simple but effective water quality management tool that can incorporate higher order two and three-dimensional models results. Box models are used mainly for two purposes: for studying the complex of a coupled process and for studying the sensitivity of a biological system. The box model is usually a relatively simple model of the ecosystem. It is often developed within a project for a special region. Only a few components are involved and the computation is limited to only a few parameters.

In contrast to its advantage on simplification, a box model has also a limitation for a prediction due to insufficient resolution. The model should be developed and extended to increase horizontal and vertical resolution for a better exchange calculation. It must also be capable of handling more complex biochemical processes. However, there is an agreement that the model complexity should be investigated under the given quality of the available data. Increasing the model complexity means that more input data are required to allow for the computation of more complex biochemical processes.

To overcome the transport and mixing resolutions, higher order model complexity has been introduced. Simple one-dimensional model were initially established to improve the understanding of the spring bloom, considering the seasonal changes in both physical and biological dynamics. Models were extended to two- and three -dimensional modelling when computer power reached a stage where the necessary trophic resolution could be combined with the desired spatial and temporal resolution. An advantage of three-dimension modelling compared to one-dimensional modelling is that all transport processes are included. The first differential three-dimensional ecological models were developed for the East Seto Inland Seas in the Pacific (Kishi and Ikeda, 1986), for the mid-Atlantic Bight (Walsh et. al., 1988) and for the limnic system of Lake Okeechobee in Florida (Dickinson et. al., 1992). Global three-dimensional biogeochemical modelling started in the late 1980s on the basis of dynamical ocean circulation modelling. However, for some areas and purposes the use of one-dimensional models is still adequate but many of them have been extended to two- or three-dimensional models.

Numerical modelling was mainly developed and applied to the coastal and estuarine areas. One of the most well known models is the Estuarine, Coastal and Ocean Model (ECOM-3D), which was developed by Blumberg and Mellor (1980, 1987) to simulate the effect of tides, winds and density gradients on water levels and three-dimensional currents. Later in 1987, Hydroqual linked this model with a steady state water quality model for eutrophication and anoxia in Chesapeake Bay. This model is a close relative of the Princeton Ocean Model (POM) which was pioneered by Alan Blumberg and George Mellor starting in 1977.

The CE-QUAL-W2 is a dynamic two dimensional model developed for stratified water bodies developed by Environmental and Hydraulics Laboratories, U.S. Army Corps of Engineers in 1986 (Environmental and Hydraulics Laboratories, 1986). The model consists of flow and water quality modules. Application of the model was applied to the Savannah estuary between Georgia and South Carolina, USA (Hall, 1987, Johnson et. al.,

1989). The impact of changes in waste loads on dissolved oxygen concentrations was determined.

The eutrophication models developed by Delft Hydraulics were established in 1991 for the Dutch MANS project (MANS, 1991). The DELWAQ model was constructed for the transport of conservatively mixed matter. The DYNAMO model was developed to simulate the nutrient pool and the model ECOLUMN-BLOOM II for the simulation of phytoplankton blooms. Examples of the different modelling system are presented in Table 2.1.

Table 2.1: Modelling systems

Models	Year	Model description	Institution
POM	1977	Princeton Ocean Model	Princeton University, USA
ECOM-3D	1987	Estuarine, Coastal and Ocean Model	Hydroqual, USA
CE-QUAL-W2	1986	A two-dimensional laterally averaged, Hydrodynamic and water quality model	Environmental and Hydraulics Laboratories, U.S. Army Corps of Engineers
ECOLUMN DYNAMO DELWAQ	1991	Ecological water column model Dynamic eutrophication model Delft Hydraulic Water Quality Model	Delft Hydraulics, the Netherlands

In the North Sea and adjacent coastal area, the problem of eutrophication was initially investigated by means of the box model. The use of numerical methods to construct a dedicated numerical model for a certain area was later developed to enhance the transport and mixing procedures. Extending of the one-dimensional model to two- or three-dimensional models was initiated during the 1990s. Table 2.2 presents the institutions with dedicated ecological models developed for the North Sea area. The spatial extension of the model in the North Sea can be traced from Figure 2.1.

Table 2.2: Dedicated ecological models in the North Sea area

Models	Year	Model description	Institution
NORWECOM	1993	Norwegian Ecological Model System	IMR, Bergen
GHER	1994	Geo-Hydrodynamics and Environment Research Model	MUMM, Liege
ECOHAM	1995	Ecological North Sea Model Hamburg	IFM, Hamburg
ERSEM	1995	European Regional Seas Ecosystem Model	EU-MAST Project
COHERENS	1999	Coupled Hydrodynamical Ecological model for Regional Northwest European Shelf seas	EU-MAST Project
POL3dERSEM	2000	Proudman Oceanographic Laboratory 3d ERSEM Model	POL, Liverpool PML, Plymouth

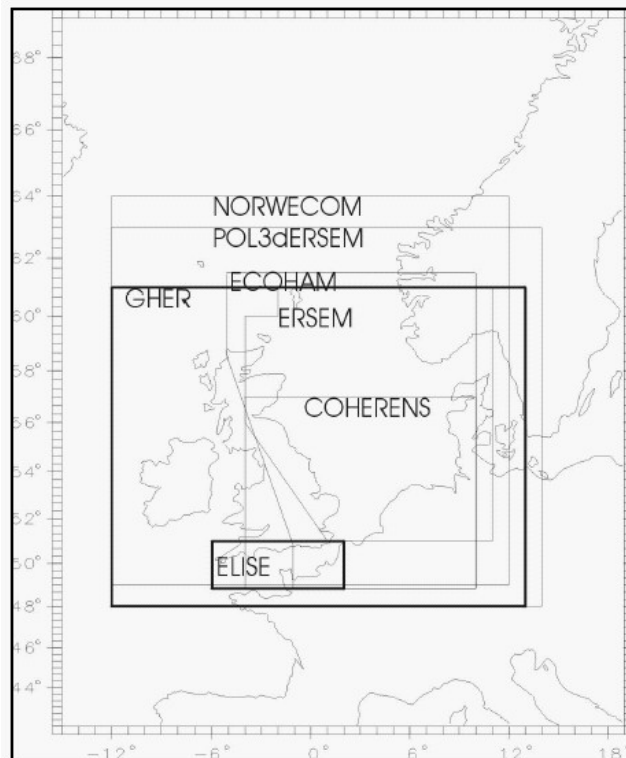


Figure 2.1: Spatial coverage of ecological modelling in the North Sea

The first three-dimensional ecosystem model for the North Sea was the NORWECOM in 1993, followed by the GHER model in 1994, ECOHAM and ERSEM in 1995. The NORWECOM was used to simulate mesocosm experiments and also phytoplankton dynamics. The model was extended to estimate primary production in space and time over the greater North Sea with a spatial resolution of about 20km over the spatial extent of 1,600km. Aksnes et. al., (1995) tested this model by comparing the prediction results for algae blooms with field observations. It was found that the model was able to reproduce the blooms satisfactory. The model was used to reproduce the distribution of primary production in the year 1985 (Skogen, Eriksrod and Svendsen, 1997). Fairly good agreement was obtained. Skogen and Moll (2000) applied this model to simulate the primary production during the period of 1985-1994 and compared it to the model results obtained from ECOHAM. It was found that both models produced similar results. The model was extended to NORWECOM2 to include oxygen, silicate shells and suspended particulate matter. The model was validated by using observed nutrient data in the North Sea for the period of 1980-1989. Simulated silicate and phosphate data were found to be reliable whereas simulated nitrogen showed disagreements with corresponding field data.

The GHER was applied for the northwest European continental shelf and coupled with a meso-scale circulation model. Initially it was developed by Delhez and Martin in 1994. The ecological module contained in this modelling system comprises the state variables of nitrogen-nutrients, phyto- and zooplankton biomass and detritus. The spatial resolution was approximately 18km with a spatial extent of 1,400km. The computed results for the phytoplankton biomass were not evaluated. Later in 1998, the model was improved and used to simulate primary production. Satisfied and non-satisfied regimes were characterized according to the dynamic response of the primary production to physical forcing.

ECOHAM is a three-dimensional model for estimating the annual primary production in the North Sea (Moll, 1995, 1997b and 1998b). It is a spatial extension of the one dimensional water column model developed by Radach and Moll (1993). The mechanism for nutrient regeneration was represented by immediate remineralisation of part of the dead organic matter in the water and by a linear process for the decomposition of detritus at the bottom. The coupling of the benthic nutrient reservoir to the water column was achieved by physical transfer of nutrients into the water column as prescribed by boundary conditions. The model was developed with a spatial resolution of about 20km and a spatial extent of 1,400km. The simulation was applied for the annual cycle in 1986. The development of the spring bloom was traced starting in the continental coastal zone, then extending into the area of the Baltic outflow along the Norwegian trench and finally covering the whole North Sea. The amount of the annual primary production was also estimated. Phosphate budgets derived from the simulation of the annual cycle in 1986 were validated with two sets of data (Moll, 1998a). It was found that a combination of the physical processes of horizontal advection and vertical turbulent diffusion enhanced the ability of the model to simulate the distribution of nutrients.

The ERSEM model was initially developed under the MAST project as a box model with a quasi three-dimensional spatial structure. It contains 85 boxes each in the horizontal surface and bottom layers and covered a spatial extent of 1,100km with a grid space of 110km. Radach and Lenhart (1995) described the nutrient dynamics in the North Sea by applying this model to calculate the fluxes and budgets of nutrients. It was found that the nutrient conditions regarding import and export fluxes in the North Sea are balanced. The model was applied for a long term simulation covering the period 1955-1993 to reproduce the effects of eutrophication in the North Sea (Pätsch and Radach, 1997). It was found that the model is able to simulate the food web in the eutrophic zone. The model was also applied to simulate the consequences due to a 50% reduction of nutrient loads from the major rivers around the North Sea (Lenhart, Radach and Ruardij, 1997 and Lenhart, 1999). This nutrient reduction resulted in a small decrease of primary production in the North Sea. Nitrogen budgets near the river mouth were found to be reduced by 15-20%. Zooplankton grazing on bacteria and mortality of phytoplankton remained unaffected.

Another model which was developed under the MAST project is the COHERENS. It was developed in 1999 for the northwest European shelf and covered a spatial extent of 900km with a grid space of 7km. Its purpose was to simulate the physical circulation, biological activity, sediment and contaminant transport. The model was applied for the simulation of the annual cycle in 1989 in the southern North Sea. Simulation of the spring bloom and the annual chlorophyll maximum produced good results.

In 2000, the previous ERSEM model was extended and applied for the northwest European continental shelf to illustrate the spatial and temporal variations in physical and chemical driving forces, so called POL3dERSEM (Allen et. al., 2001). A finer spatial resolution of 12km was applied and the area covered a spatial extent of 1,700km. The model was applied to determine the temporal development of the spring bloom in the North Sea. Comparisons of the simulated results with measured monthly mean data showed a good agreement. With the development of the POL3dERSEM, a new standard in three-dimensional modelling was set due to the complex trophic relations of ERSEM and the integration to a fully three-dimensional modelling system. For the finest resolution of 7 to 12km, the fluid motion was found to be well resolved. Table 2.3 shows a comparison of the space and time resolution in ecological modelling of the North Sea.

Table 2.3: Comparisons of space and time scales for ecological modelling in the North Sea

Models	Spatial resolution (km)	Temporal resolution (sec)	Spatial extent (km)	Temporal range (years)
NORWECOM	20	900	1600	1985-1994
GHER	18	-	1400	1989
ECOHAM	20	900	1400	1985-1994
ERSEM	110	86400	1100	1955-1993
COHERENS	7	600	900	1989
POL3dERSEM	12	1080	1700	1995

Ecological modelling usually contains the most important source and sink terms. Processes such as nutrient remineralisation in the sediment are taken into account by simplifying the natural process to a simple mathematical equation. Especially in shallow coastal regions, the benthic remineralisation process may be a major factor controlling nutrient dynamics in the water column. Except for the COHERENS model, all of the models listed in Table 2.2 have included this process. However, due to a lack of adequate field information on nutrient concentrations in the sediment, the sediment process can not be represented realistically in the model. Instead, the remineralisation rate is usually derived from the laboratory scale. The sediment process is recommended to be dynamically included only in long term simulations.

In general, the three-dimensional ecosystem models have given an improved understanding of the interaction of processes regulating biological production. Such models can also be applied to predict the consequences resulting from specific changes in the system and provide a conceptual framework for testing different hypotheses. The models are able to simulate the process of primary production and its functions for the pelagic and benthic system. Cycling of matter and interaction of different processes are well represented. Finally the inter-relation of each process and the corresponding consequences for the whole system can be visualized and an overall picture of the ecosystem can be drawn. Especially the latter is a major advantage of three-dimensional modelling compared to a more simplified model such as the box or one-dimensional models.

However, these advantages are counteracted by a lack of data either for prescribing these parameters or to validate the simulations. Complexity of the model parameters creates difficulties in handling and processing the data. Intensive measurements are required to narrow the range of parameters. Furthermore, most of the available ecological models are developed for the large scale domain. For small scale investigations, both measurements and modelling are still under development.

3 Investigation area

3.1 Introduction

The German Wadden Sea is a shallow coastal area with extensive tidal flats bordering the German west coast. It covers an area of about 8,000km² with the seaward border defined by the 10m isobath. The environment of the Wadden Sea is very dynamic and the forces of wind and water lead to the formation and erosion of the typical landscape elements of the area, the tidal flats, salt marshes, sandbanks and islands. Four major rivers enter the German Wadden Sea, which are the Elbe (mean discharge 718m³/s), the Weser (mean discharge 327m³/s), the Ems (mean discharge 106m³/s) and the River Rhine via the Ijssel (mean discharge 726m³/s). The total annual average freshwater volume which enters the Wadden Sea is about 60km³ with a total catchment area of approximately 230,000km². Together with the freshwater discharge, the Wadden Sea is subjected to a high load of pollutants and contaminants deriving from the human activities in the catchment.

Since 1986 the German Wadden Sea has owned the status of a national park and since 1990 it is officially considered as a man and biosphere reserve. For this reason, the natural system of the German Wadden Sea is well preserved and a regular monitoring program has been set-up. However, the area is still under pressure deriving from different anthropogenic activities. The most important are fishery (mainly shrimps), aquaculture (mainly blue mussels), navigation and tourism. Oil drilling and sand mining occur in a few areas.

The coastal stripe around the German Wadden Sea is well known for its agricultural activity. The use of mineral fertilisers during the growing season lead to high amounts of diffuse nutrient inputs into the system. These nutrient loads are strongly varying in time and space and thus difficult to assess directly. The trophic state of the estuarine part of the Northern German Wadden Sea is mainly influenced both by diffuse nutrient inputs entering the area directly from the coastline and by variable inputs deriving from the Elbe river plume.

3.2 Description of the study site

The investigation area is the Meldorf Bight on the German Wadden Sea coast located between the Elbe and Eider estuaries. It covers an area of about 400km² and is surrounded by a dike-protected coastline (Figure 3.1 and Figure 3.2). The study site is a semi-enclosed bay considered from its topography as a natural basin (Figure 3.3). The bay is subjected to a strong estuarine influence by the Elbe river. About 50% of the area gets dry at low water and the model domain is submerged at high water. The hydrodynamics of the domain are controlled by the combined effect of tides, wind driven currents and wind waves. The long term averaged water temperatures vary from 4 to 8°C in winter and from 14 to 18°C in summer. Due to the influence of the freshwater input mainly from the river Elbe, salinity in the area is found to be strongly diluted when compared to that of the

central North Sea (35 PSU). Averaged salinity in the study area varies from 20 to 29 PSU in winter and from 25 to 33 PSU in summer. Due to a strong tidal mixing, vertical stratification of temperature and salinity is not significant.

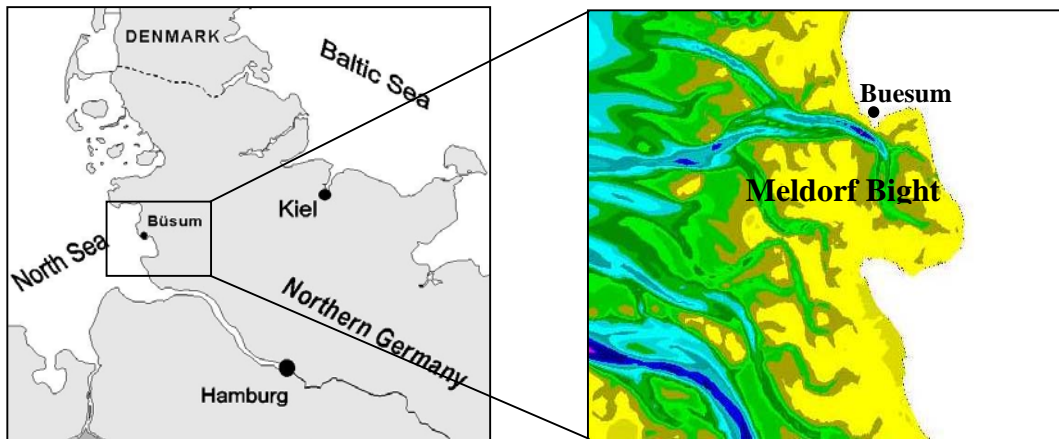


Figure 3.1: Investigation area

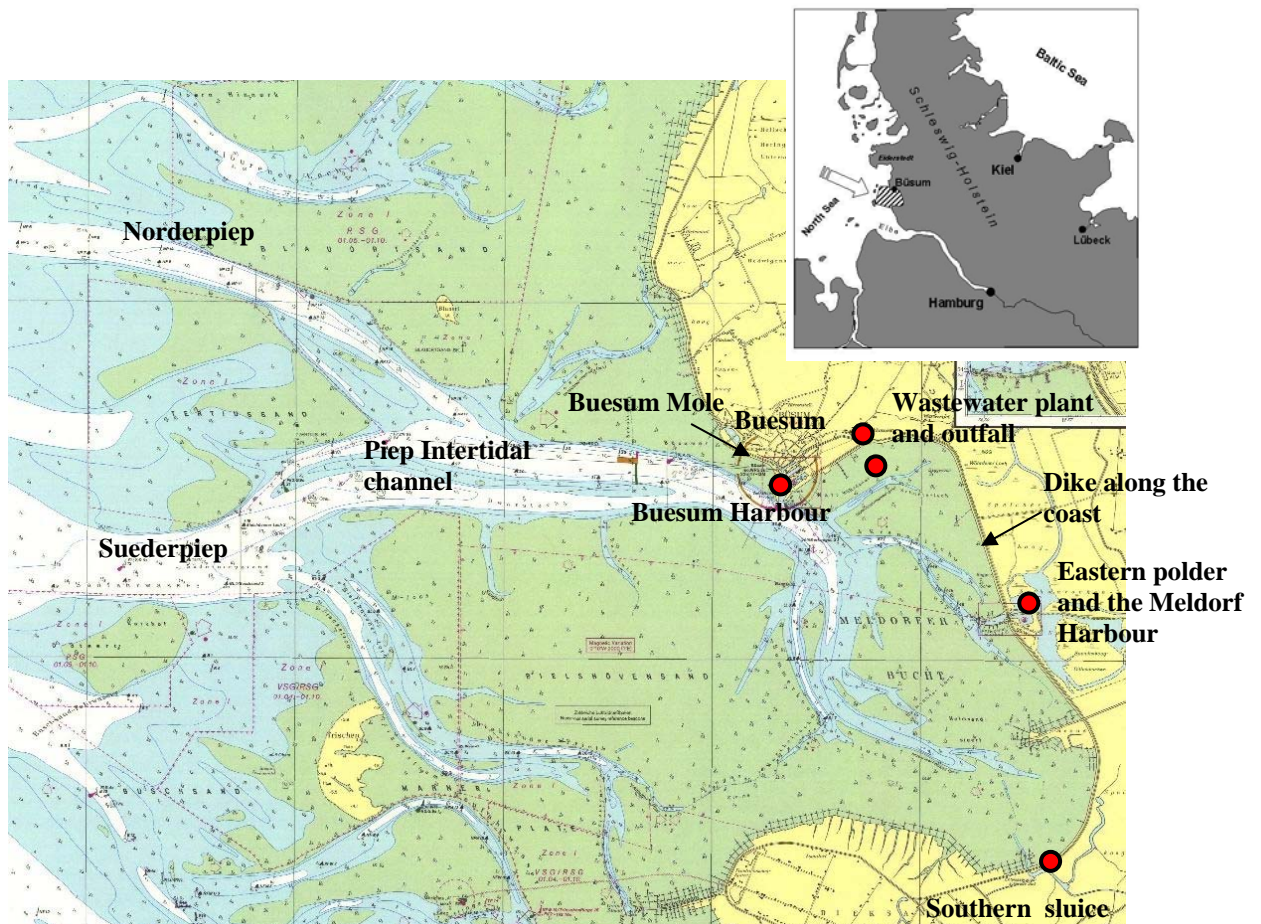


Figure 3.2: The Meldorf Bight and its surroundings

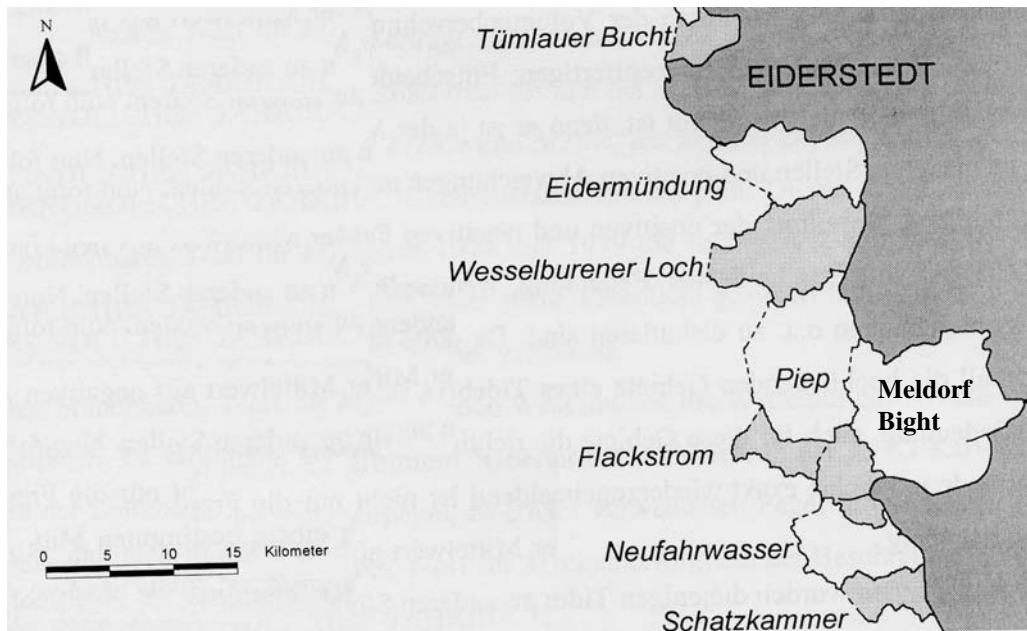


Figure 3.3: Natural basins classified according to watersheds (Spiegel, 1997)

At the north western border of the study area, the city of Buesum is situated. The total area of the city is approximately 15,770km² with 15km of coastline. Apart from its main fishery and agricultural activities, the city also has an importance as a tourist attraction spot on the German Wadden Sea national park. The city is a resort city in which population varies between 3000 in winter up to 6 times more in summer. This gives a significant concern in sewage waste which is distinctly increased during the tourist season. The city has also a small harbour with a ferry travelling to the island of Helgoland (Figure 3.4). Recreation is densely located along the beaches. The beach has sometimes been closed due to hygienic problems in the water related to the sewage discharge. Water quality of the bathing area has to be regularly monitored in order to avoid health problems.



Figure 3.4: The Buesum harbour and important sites along the coast

The sewage plant of Buesum has the capacity for treating the domestic wastewater of about 25,000 inhabitants (assuming that 1 inhabitant produces 170-litre wastewater/day).

It disposes of a biological treatment process for the removal of organic waste in an aerated sludge and settlement basin. The treated water is pumped through a 30m tube into the adjacent Wadden Sea in front of the sewage plant. Due to the pronounced fluctuation in tourist activities, the Buesum sewage plant has to cope with a rather varying load of waste water. The total amount of waste water may vary between 1500m³ during the slack period to 5000m³ per day during the tourist season.

Along the coastline, a dike has been constructed to protect the coastal area. Tourism, sheep farming, fishery and harbour activities including those of fish processing and grain storage are the main activities along the study area (Figure 3.5).



Figure 3.5: Dike with sheep and tidal flat area in the Meldorf Bight

Apart from the estuarine influence deriving from the Elbe River and the discharge from the sewage plant, the area is also subjected to direct freshwater discharge from a polder basin. It is located in the eastern part near the Meldorf Harbour (Figure 3.6). There are 5 small sluice gates which can be automatically opened during low tide to release the water inside the basin to the sea. Another smaller source is a sluice located at the southern part of the bay. The discharge from the eastern polder basin is about 10 times higher than the discharge released from the sluice in the south. The releasing rate depends on the meteorological conditions such as precipitation, wind conditions and the tidal phase. The water inside the polder basin is characterised by high nutrient concentrations due to draining from the agricultural hinterland (Agatha et. al., 1994). The agricultural activity is thus one of the main factors controlling the nutrient concentration of the polder water. Systematic monitoring programs concerning physical and biochemical parameters of the polder basin are missing.



Figure 3.6: Eastern polder basin and the Meldorf Harbour

3.2.1 Bathymetry

The bathymetry of the study area is presented in Figure 3.7. The transports of water and nutrients between the area and the German Bight are mainly subjected to the main tidal inlets (Norderpiep and Suederpiep) which intersect further landward and form the major channel, the Piep. The mean water depths of the sub-channels range between 10 to 20m. The deepest location is at the main tidal channel with a depth of about 25m. Inside the bight, there are three small channels emanating from the main Piep intertidal channel (Wöhrdener Loch, Kronenloch and Sommerkoog-Steertloch). Scattering of small tidal creeks which split from the small channels are generally found in the tidal flat.

Along the coast, muddy Wadden flats dominate, which are subjected to wet and dry processes during high and low tides. Plane bed with ripples and sand dunes can also be observed in the area. Approximately 15km of sandbanks exists along the coast. Mega ripples with lengths less than 10m and sand dunes with lengths up to 20m are found mainly in the Norderpiep. In the Suederpiep channel mega ripples and sand dunes with lengths up to 20m can be found. Mega ripples of 10 to 12m length and 0.2 to 0.4m height are found in the Piep (Mayerle et. al., 2002).

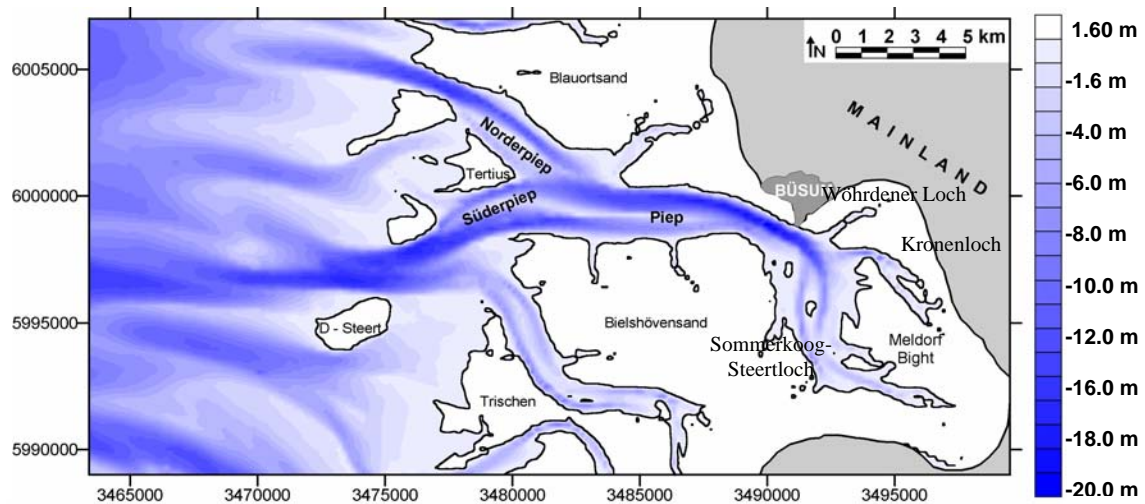


Figure 3.7: Bathymetry of the investigation area

3.2.2 Hydrodynamics

The hydrodynamic conditions of the study area are governed by a semi-diurnal tidal cycle. The tidal cycle repeats twice daily with the duration of 12 hours and 25 minutes for a cycle of flood and ebb tides (Reineck, 1978). About half of the area is submerged during ebb tide. The direction of the flood current is towards the east and southeast of the Meldorf Bight, whereas the ebb current is directed towards the west and northwest. Westerly winds prevail in the area. On the tidal flats, the local morphology has a strong influence on the direction of the currents. However, strong winds may influence the speed and direction of the water masses distinctly. Wave conditions of the investigation area are mainly generated by local wind and also swell waves from the open North Sea. The tidal range is about 3-3.5m and mean velocity is about 1.5m/s. Wave heights up to 3 to 4m are found at the outer region. A mixture of North Sea water and continental runoff enters the Meldorf Bight. The coastal water body is strongly mixed due to the strong tidal currents.

3.2.3 Sediment distribution

The sediment of the Meldorf Bight consists of mainly fine to very fine sand. Silt and clay are also presented. The bed sediment size varies from 80-170 μ m. Suspended sediment can be found with a grain size ranging from 6-86 μ m. (Mayerle et. al., 2002 and Poerbandono, 2003). In the tidal flat region, cohesive sediment is dominant. Very fine sand with an average grain size of 90 to 110 μ m is found. In the channel bed, medium to fine sand with consolidated mud are present. Figure 3.8 shows the sediment grain size distribution of the investigation made by Reimers in 1999. Reimers found a median grain size of 150 to 230 μ m on the southern part of Tertiussand and the shoal D-Steert. On the northeastern part of Tertiussand and western part of Blauortsand, grain sizes between 110 and 150 μ m were found.

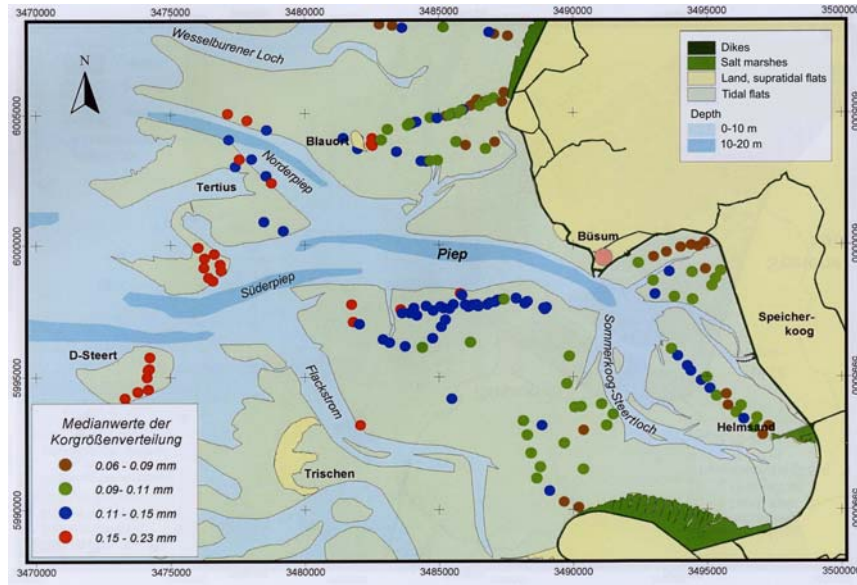


Figure 3.8: Sediment grain size in the Meldorf Bight by Reimers (1999)

4 Field measurements

4.1 Materials and methods

In order to improve our understanding of the nutrient characteristics of the area, two measuring strategies were designed which are aimed to determine 1) seasonal nutrient transports and 2) small scale seasonal nutrient distributions. Data of the latter were used to set up the numerical model to simulate nutrient dynamics in the Meldorf Bight.

1. Preliminary measurements: Seasonal nutrient transports

The first approach was conducted in 2001. The nutrient variability over the tidal cycle was determined in the surface and bottom waters and combined with water transports in order to compute nutrient transport budgets. The method was adopted from Dick et. al., (1999) who calculated budgets for the transports of water and heat as well as for dissolved nutrients and particulate matter between the coastal waters of the German Bight and the North Frisian Wadden Sea.

The quantification of net transports allows conclusions on the nature and extent of the main physical and biochemical processes influencing nutrient transfer in the Wadden Sea and allows for a direct comparison with measurements of relevant internal biological transformation rates such as primary production and remineralisation (Tillmann et. al., 2000, Rick et. al., 1999) as well as biogeochemical processes such as porewater leakage and sediment denitrification (van Beusekom et. al., 1999).

The measurements were performed in June, September and November 2001 on a cross-section (cross-section G-H) of the Piep intertidal channel near Buesum on the North Sea coast (Figure 4.1). The channel width at the cross section is about 2,500m with a maximum depth of approximately 15m with a sand bank in the middle (Figure 4.2). Water samples for dissolved inorganic nutrient analysis (N, P) were collected with a 5-litre Niskin bottle at two fixed stations at either side of the sand bank from the water surface and at the depth of about 1m above the bottom at half hour intervals over the tidal cycle. In addition, vertical CTD profiles were obtained using a ME multiprobe calibrated against standard water. Table 4.1 shows the details of all measurement periods.

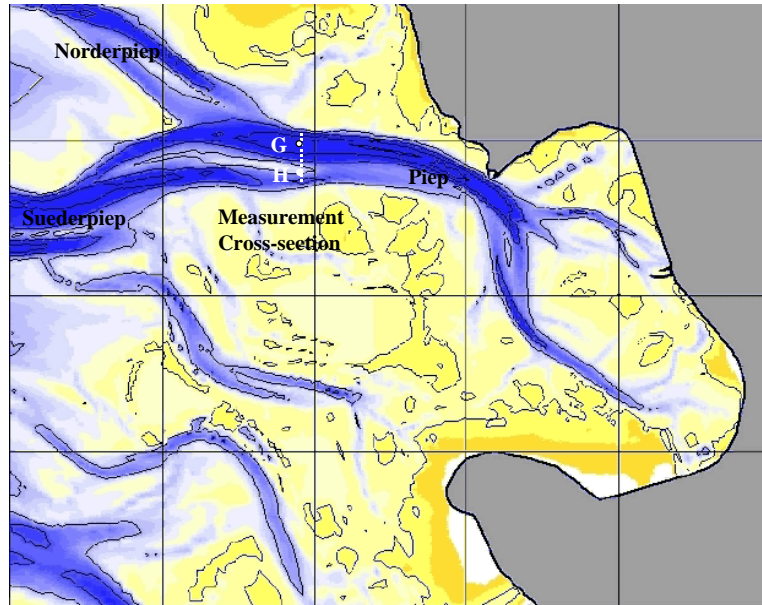


Figure 4.1: Location of cross-section G-H at the Piep intertidal channel during the seasonal nutrient transport measurements in 2001

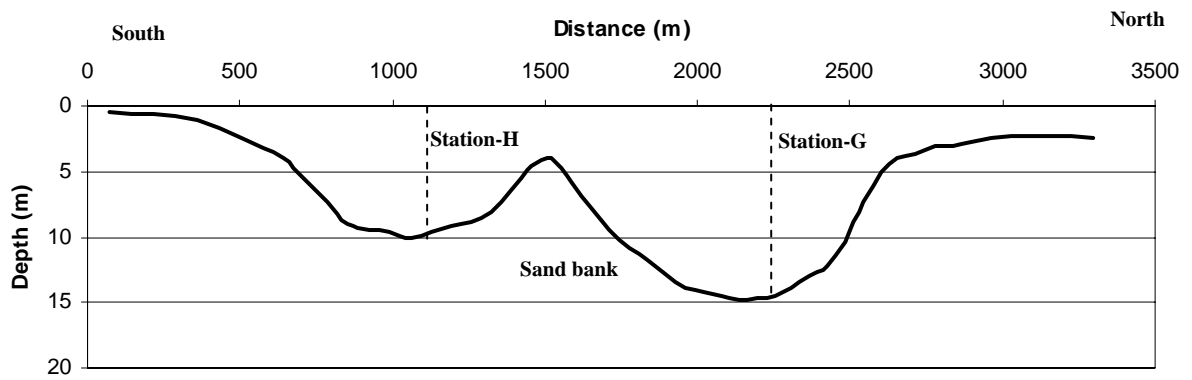


Figure 4.2: Location of sampling stations on the cross-section G-H at the Piep intertidal channel

Table 4.1: Sampling data of the measuring campaigns performed in 2001

Date	Tide	Time (hrs)	Station	Position	No. of CTD profiles	No. of Bottom water samples	No. of Surface water samples
21.06.01	Neap	6:54-19:25	G	54.14 N 8.73 E	12	12	12
			H	54.12 N 8.73 E	19	19	19
29.06.01	Spring	7:59-20:12	G	54.13 N 8.73 E	12	12	12
			H	54.12 N 8.73 E	4	4	4
12.09.01	Spring	7:13-19:59	G	54.14 N 8.73 E	13	13	13
			H	54.12 N 8.73 E	12	12	12
14.11.01	Spring	5:51-18:16	G	54.14 N 8.73 E	10	10	10
			H	54.12 N 8.73 E	11	11	11
Total					93	93	93

A total of 93 CTD profiles with 93 surface and bottom water samples were taken during the measuring campaigns. Conclusions from the measured results provided the basis to design the measurement strategies for the second approach and were used to define the configuration of the nutrient dynamics model described in chapter 5.

Hydrodynamic conditions during the measurements were obtained from the Meldorf Bight Flow Model developed at Corelab, University of Kiel (Palacio et. al., 2001, Mayerle and Palacio, 2002). The two-dimensional depth-integrated flow model of the Delft3D modelling system was employed. Details of the Delft3D Modelling system are described in chapter 5.

2. Intensive measurements: Small scale seasonal nutrient distributions

The second strategy aimed at investigating the small scale spatial gradients of dissolved inorganic nitrogen and phosphorus in the area and the tidal variation of these bioelements at the seaward boundary of the bight. It provides the basis for the development, calibration and validation of the numerical model for the simulation of nutrient distribution in the study area.

The measurements were performed in February, May and September 2002. Each of the seasonal measuring campaigns was subdivided into two assessments, which were performed on two consecutive days. The first assessment focused on the tidal variation of nutrient concentrations at the seaward edge of the bight and on the nutrient distribution in the area. These data were used to develop the boundary conditions of the model and for model calibration. The assessment on the second day was restricted to the evaluation of the spatial nutrient gradients in the model domain for the validation of the model. Additional data such as the freshwater influence and sediment-pore water analysis were also taken into account in this study.

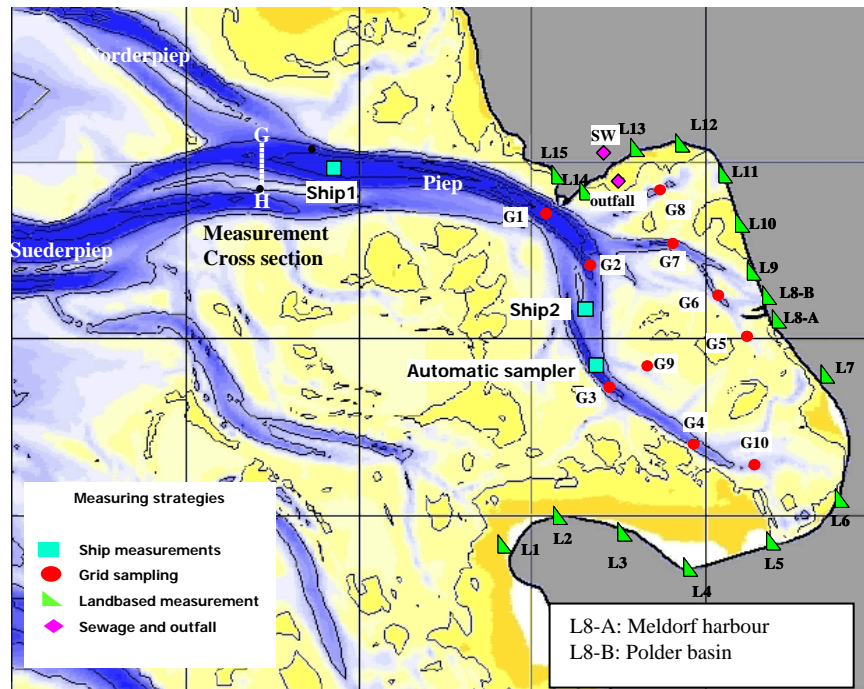


Figure 4.3: Sampling locations during the small scale seasonal nutrient investigation in 2002

Two ships and one additional automatic sampler were used in the nutrient measurements at the seaward boundary at moored stations over a tidal cycle (Figure 4.3). CTD profiles and water samples for nutrient and salinity analyses were taken, the latter with a 5-litre Niskin bottle at 1m below the water surface at half hour interval. In order to check the homogeneity of vertical distributions, additional bottom water samples were taken at 1m above the sea bottom at 3-hour intervals. The small scale spatial nutrient distribution was assessed on a grid of 10 stations (G1-G10) using a high-speed rubber boat. The grid sampling was performed from the water surface with a 2-litre PE bottle at approximately 2 hours before and after high tide. In addition, a total of 16 landbased stations (L1-L15) was sampled at the same period to determine the very near shore gradients at sites that could not be reached with the boat due to very shallow water depth.

In order to assess the influence of local nutrient discharges, additional landbased stationary measurements were performed at the Buesum Mole as well as at the outlet of the sewage plant and in front of the outfall with a frequency of half an hour over the tidal cycle. In addition water discharges from the sewage plant were recorded. The surface water in front of the outfall was sampled only during high water because the area is falling dry during low water. A total of about 540 water samples was collected throughout the measurements. Table 4.2 shows the details of the seasonal sampling campaigns.

Table 4.2: Sampling data of the measuring campaigns performed in 2002

Period	Type of measurements	No. of stations	No. of water samples	
			Surface	Bottom
Winter (13-14/02/2002)	Ships and automatic sampler	2	49	9
	Grid measurements	8	32	-
	Landbased measurements	16	26	-
	Buesum Mole	1	25	-
	Sewage and outfall	2	35	-
Spring (7-8/05/2002)	Ships and automatic sampler	3	73	9
	Grid measurements	10	37	-
	Landbased measurements	16	32	-
	Buesum Mole	-	-	-
	Sewage and outfall	2	18	-
Summer (21-22/08/2002)	Ships and automatic sampler	3	73	10
	Grid measurements	10	37	-
	Landbased measurements	16	31	-
	Buesum Mole	1	25	-
	Sewage and outfall	2	19	-
Total (540 samples)		92	512	28

As it was the case for the first measuring strategy, hydrodynamic conditions during the measurements were obtained from the Meldorf Bight Flow Model.

4.1.1 Determination of nutrient concentrations

For the analysis of nutrient concentrations, surface water samples were filtered on board through a pre-washed glass microfibre filter (Whatman GFF, pore size 0.7 μ m). The filtrate was poured into PE bottles and immediately frozen at -20 °C. The concentrations of dissolved inorganic nutrients (NO₂, NO₃, NH₄ and PO₄) were analysed in the laboratory of the Research and Technology Centre Westcoast Buesum according to the method of Grasshoff (1983) using an UVIKON XC spectrophotometer.

- Determination of nitrite

The standard method for the determination of nitrite in seawater is based on the reaction of nitrite with an aromatic amine leading to the formation of a diazonium compound which couples with a second aromatic amine. The product is an azo dye which is quantified by spectrophotometry. This method is very sensitive and is unaffected by the presence of other constituents which normally occur in seawater. Sulphanilamide hydrochloride is used as the amino compound, which after diazotization is coupled with N-(1-naphthyl)-ethylene diamine dihydrochloride. A spectrophotometer wave length of 542nm is used to determine the concentration. The samples containing high nitrate concentrations exceeding 3 μ mol/l were diluted.

- Determination of nitrate

Nitrate in seawater is reduced quantitatively to nitrite when a sample is run through a column containing cadmium filing coated with metallic copper. The nitrite produced is determined by diazotizing with sulfanilamide and coupling with N-(1-naphthyl)-ethylenediamine to form a highly colored azo dye which can be measured

spectrophotometrically. The sample is diluted if the concentration exceeds $15\mu\text{mol/l}$. A spectrophotometer wave length of 542nm can be used to determine the concentration.

- Determination of ammonium

Ammonium reacts in moderately alkaline solution with hypochlorite to give monochloramine which, in the presence of phenol and catalytic amounts of nitroprusside ions and excess of hypochlorite, gives indophenol blue. A spectrophotometer wave length of 630nm is used to determine the concentration.

- Determination of phosphate

The method is based on the reaction of the ions with an acidified molybdate reagent to yield a phosphomolybdate heteropoly acid, which is then reduced to a highly coloured blue compound. Ascorbic acid is the common reagent. A spectrophotometer wave length of 882nm is used to determine the concentration.

During the analysis of nutrient concentrations, blank and known standard samples were parallel analysed. The purpose was to control the accuracy of the analysis.

4.1.2 Determination of salinity

For the determination of salinity, a WTW conductivity meter (Model Cond 330i) was used. Calculation of the salinity was made according to the UNESCO Practical Salinity Scale 1978-PSS78 (Lewis, 1980).

4.2 Results of field measurements: Nutrient transports

4.2.1 Tidal conditions

In order to calculate seasonal nutrient transports, tidal variation of nutrient concentrations in June, September and November 2001 were investigated on a cross section of the main tidal inlet of the Meldorf Bight, the Piep (see section 4.1, Figure 4.1) and combined with computed water transports. Figures 4.4 to 4.7 show water level, current magnitude and flow discharge across the section as calculated with the flow model. The time of sampling during the tidal cycle is indicated by red dots in the figures. The tidal range is characterised by range of 3 to 4m. with the maximum current magnitude of about 1.5m/s . The maximum flow discharge at the tidal inlet over the tidal cycle ranges between $25,000\text{-}30,000\text{m}^3/\text{s}$.

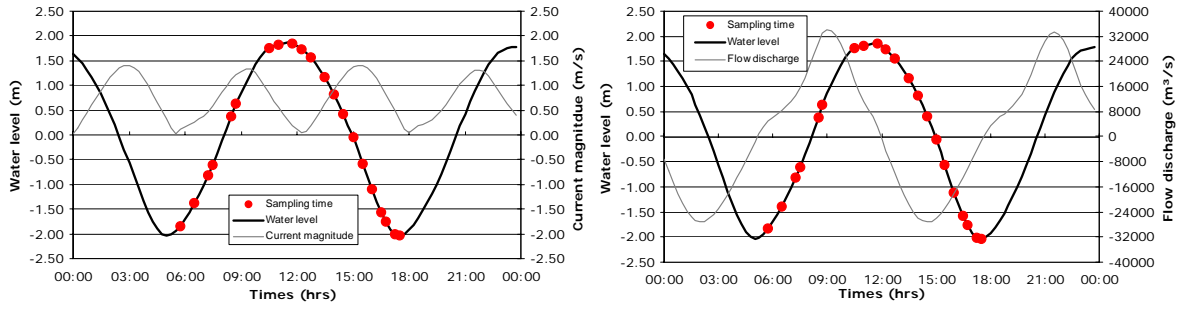


Figure 4.4: Water level, current magnitude and flow discharge on 21 June 2001

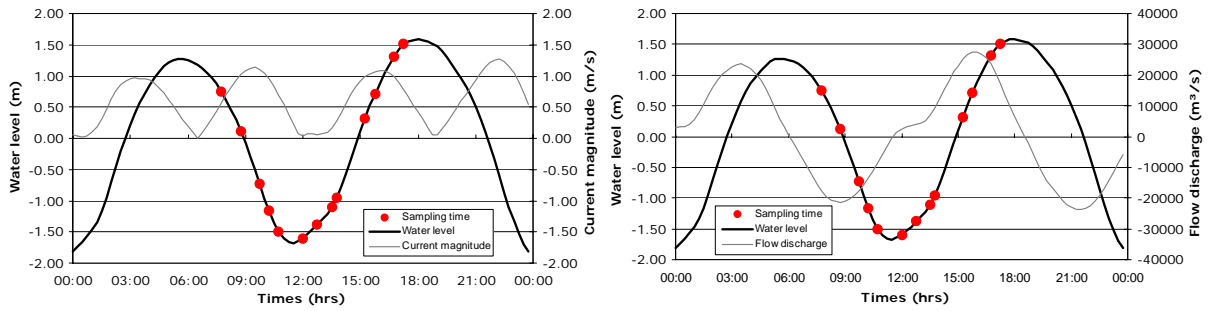


Figure 4.5: Water level, current magnitude and flow discharge on 29 June 2001

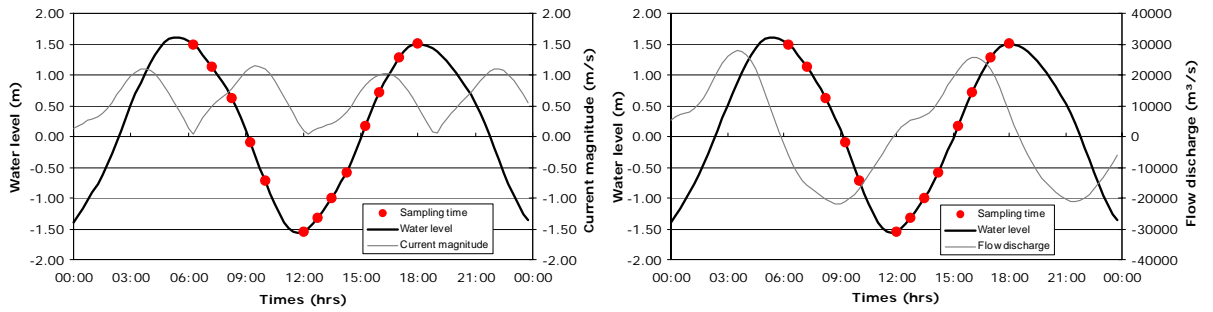


Figure 4.6: Water level, current magnitude and flow discharge on 12 September 2001

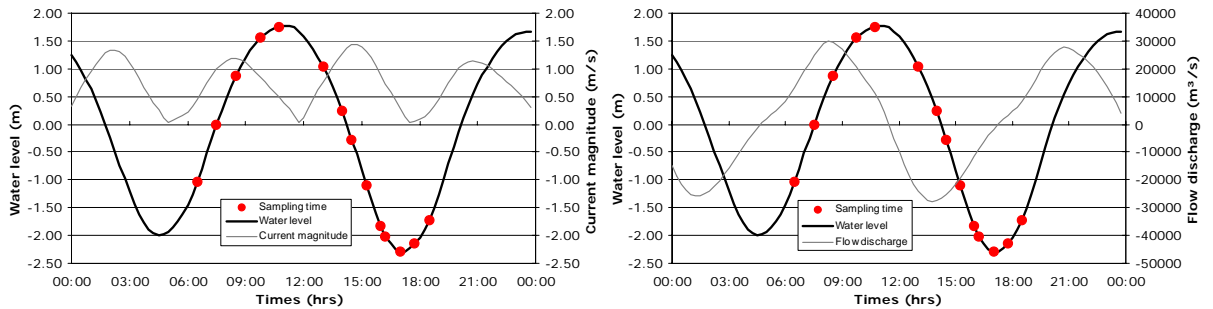


Figure 4.7: Water level, current magnitude and flow discharge on 14 November 2001

4.2.2 Tidal variation of dissolved inorganic nutrient concentrations

Variation of the surface concentrations of the dissolved inorganic nitrogen compounds and of dissolved phosphate over the tidal cycle at stations G and H in the tidal inlet are shown in Figures 4.8-4.9. In general, concentrations are scattered without significant dependencies on the tidal phase. However, there is a tendency of elevated nitrate concentrations during high tide and higher concentrations of ammonium and phosphate during low tide.

Differences in the tidal pattern between stations G and H of the cross section were found to be small. Discrepancies are normally under 10% with a maximum of about 20-30%. Highest lateral variations of nutrient concentrations are found in spring especially for the concentrations of nitrogen compounds.

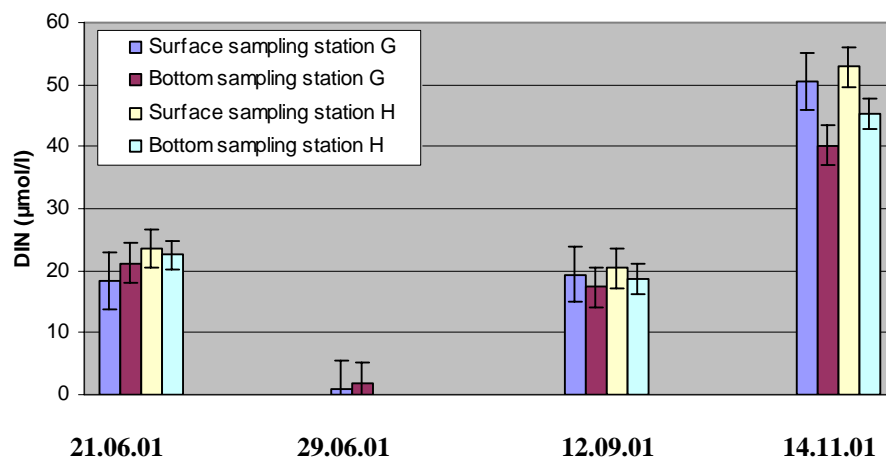


Figure 4.8: DIN concentrations at the cross section G-H in the Piep intertidal channel during the measuring campaigns performed in 2001

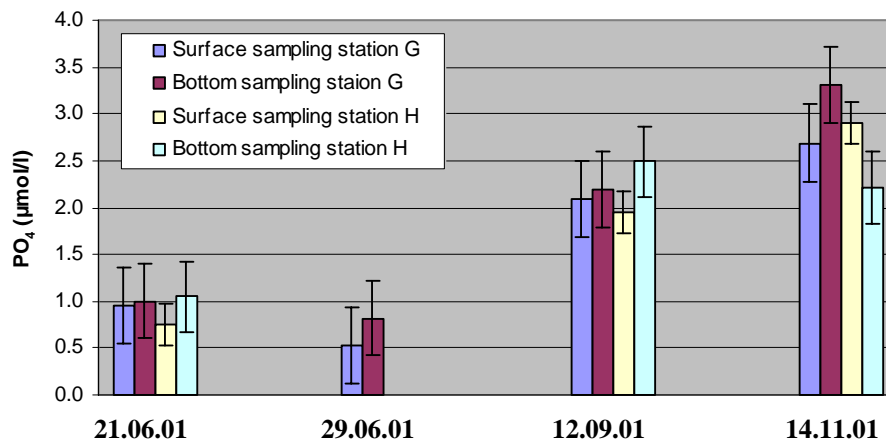


Figure 4.9: PO₄ concentrations at the cross section G-H in the Piep intertidal channel during the measuring campaigns performed in 2001

Vertical variation

As it was the case in the comparison between stations G and H, there were no significant differences between bottom and surface nutrient concentrations. (Figure 4.10 to Figure 4.17). Vertical variations were found to be much smaller than the tidal variation. Slightly higher vertical variations of phosphate are observed at station H during all measurement periods, which may be an indicator of phosphate released from the sediment. The discrepancies are found to vary between 25-40%. By contrast, at station G, the discrepancies in vertical phosphate concentrations are smaller (8-23%) For the nitrogen compounds vertical discrepancies of about 5-25% were found. An exception was observed for the intermediary nitrification product nitrite at station H in spring. Surface concentrations were much higher, accounting for a vertical difference of about 45%.

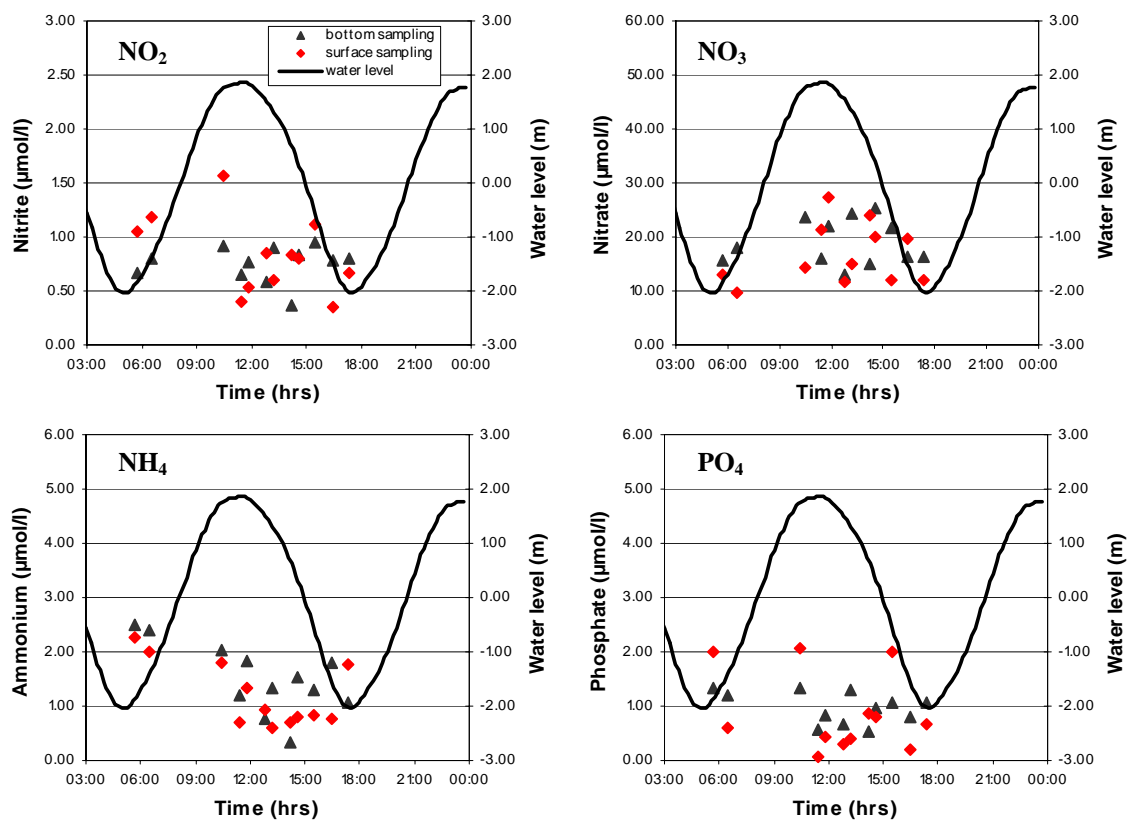


Figure 4.10: Vertical variation of NO_2 , NO_3 , NH_4 and PO_4 at station G on 21 June 2001

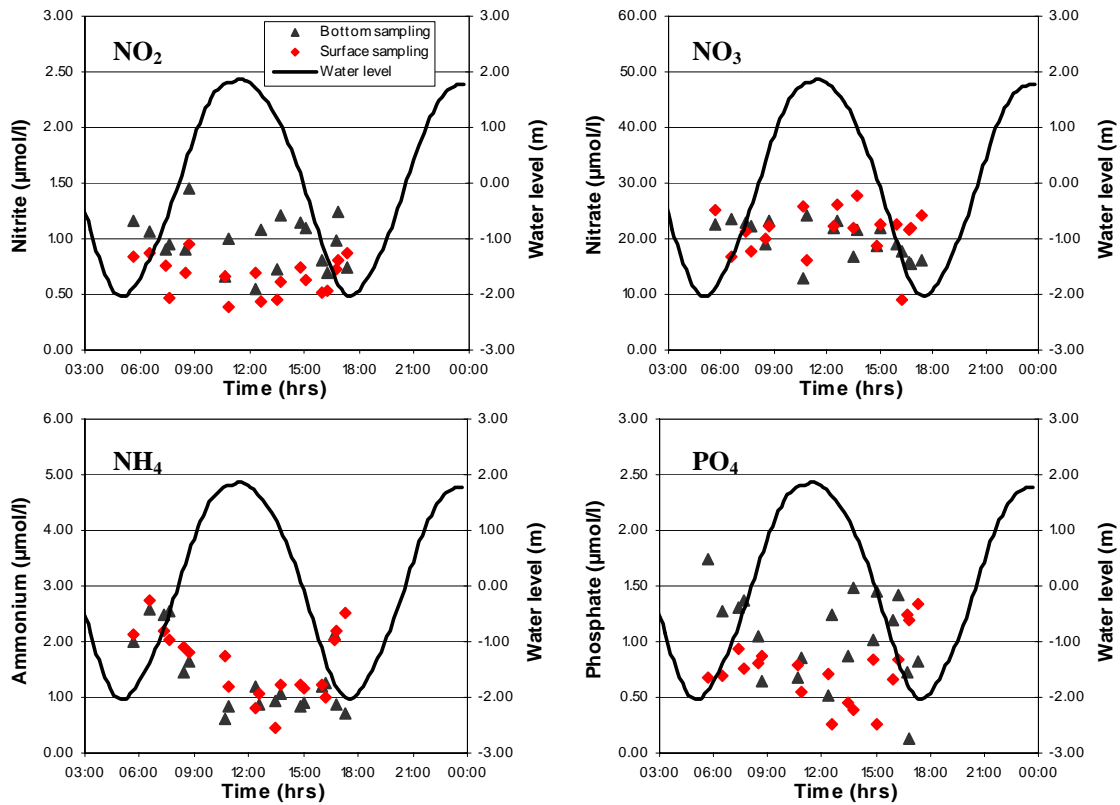


Figure 4.11: Vertical variation of NO_2 , NO_3 , NH_4 and PO_4 at station H on 21 June 2001

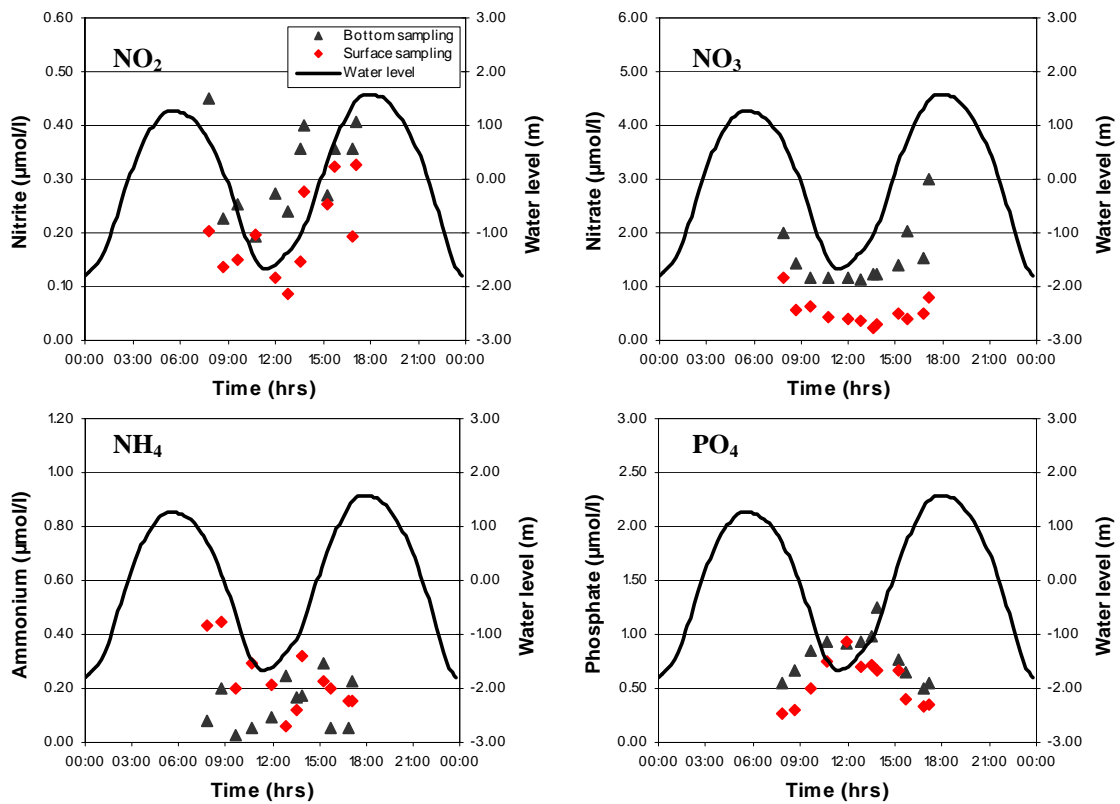


Figure 4.12: Vertical variation of NO_2 , NO_3 , NH_4 and PO_4 at station G on 29 June 2001

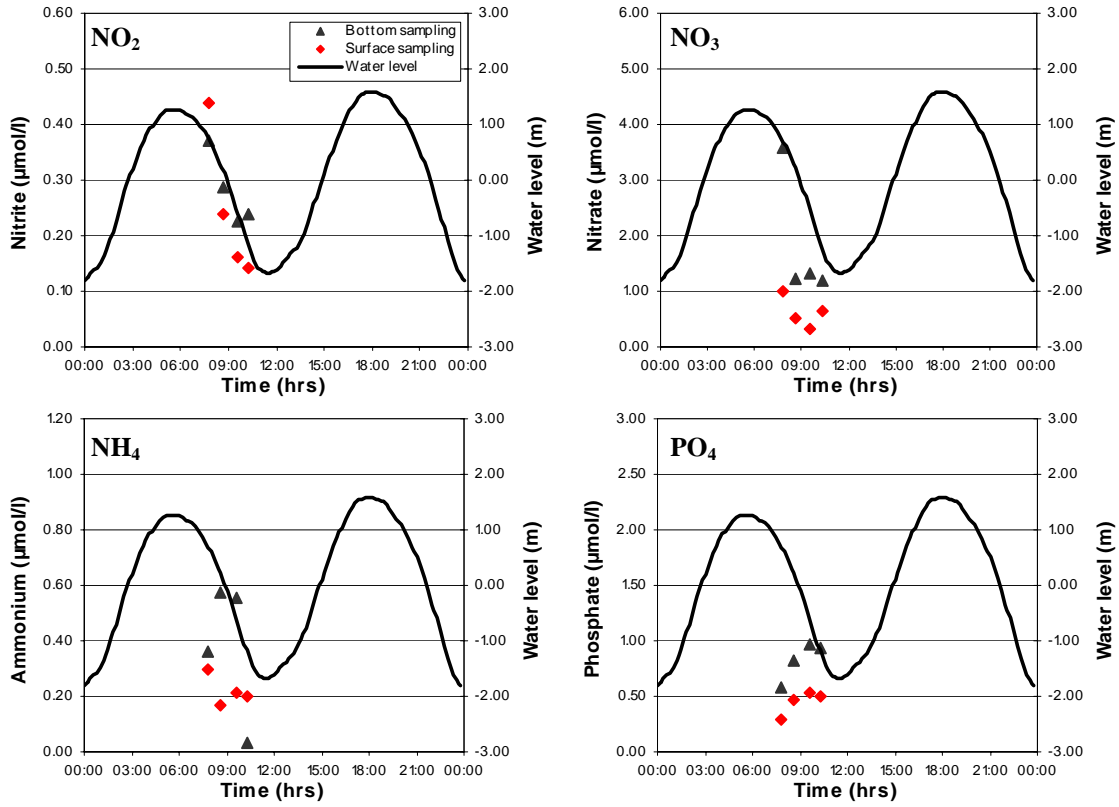


Figure 4.13: Vertical variation of NO_2 , NO_3 , NH_4 and PO_4 at station H on 29 June 2001

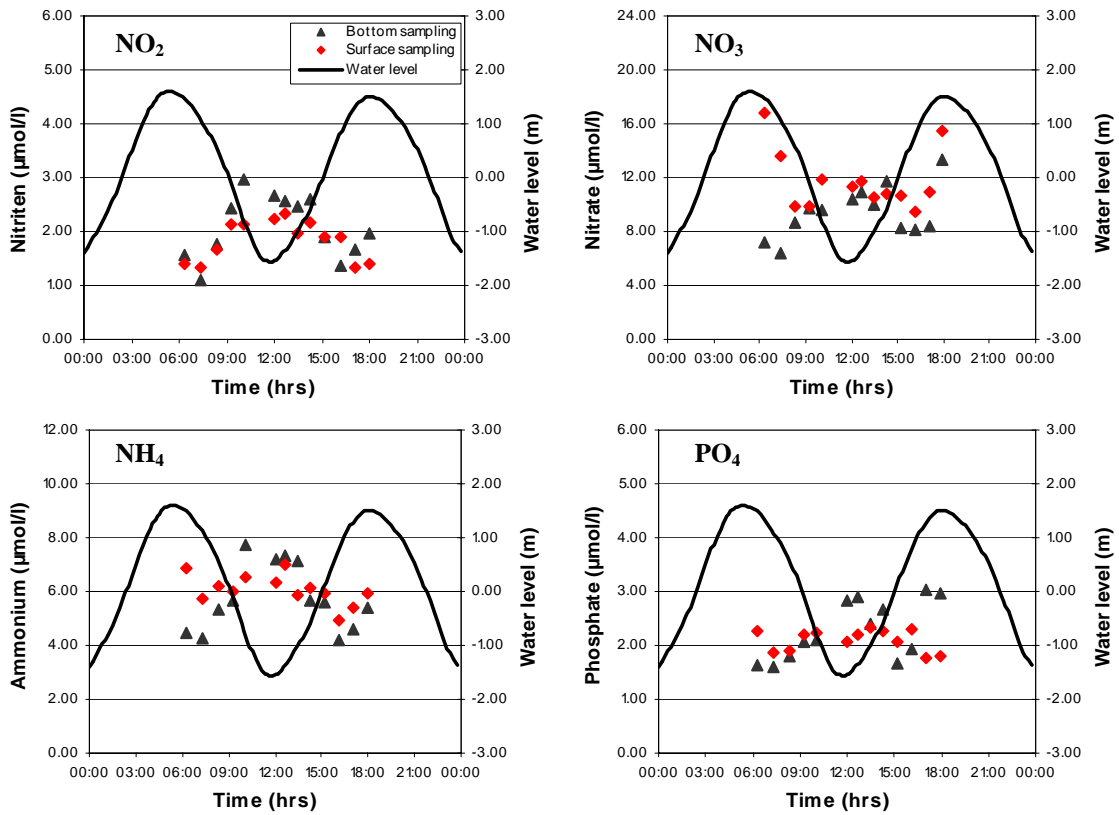


Figure 4.14: Vertical variation of NO_2 , NO_3 , NH_4 and PO_4 at station G on 12 September 2001

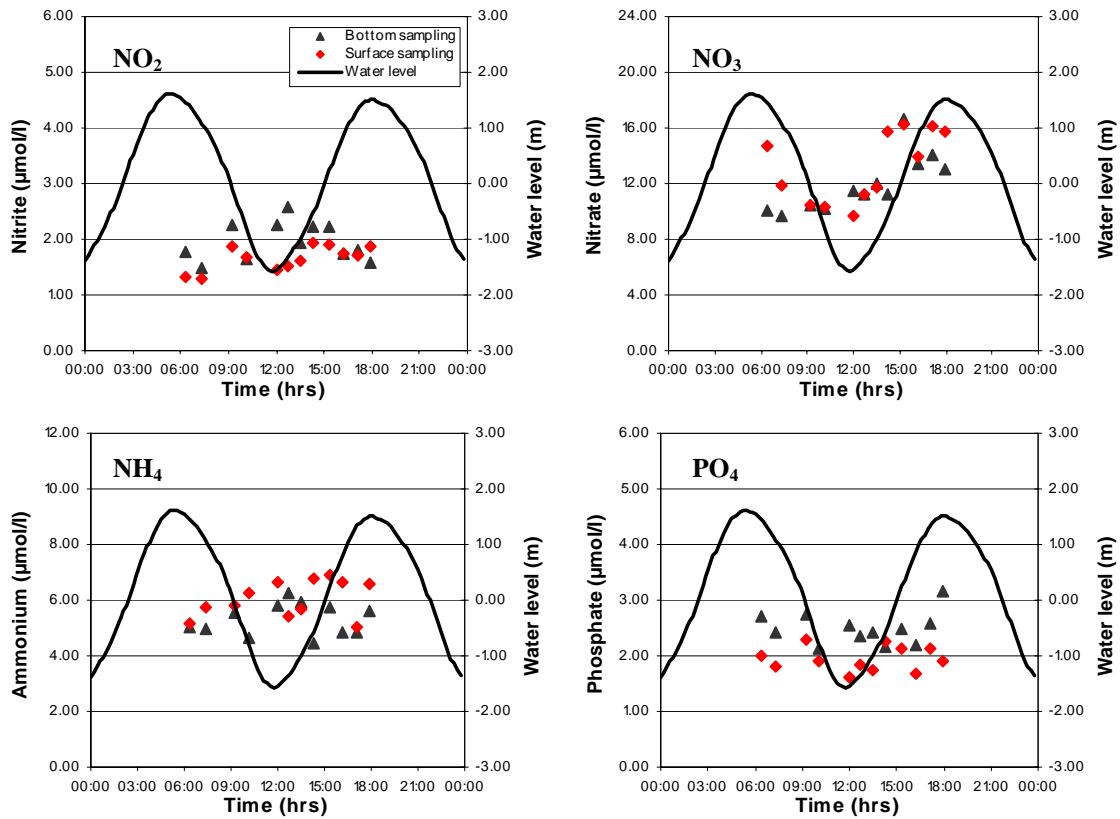


Figure 4.15: Vertical variation of NO_2 , NO_3 , NH_4 and PO_4 at station H on 12 September 2001

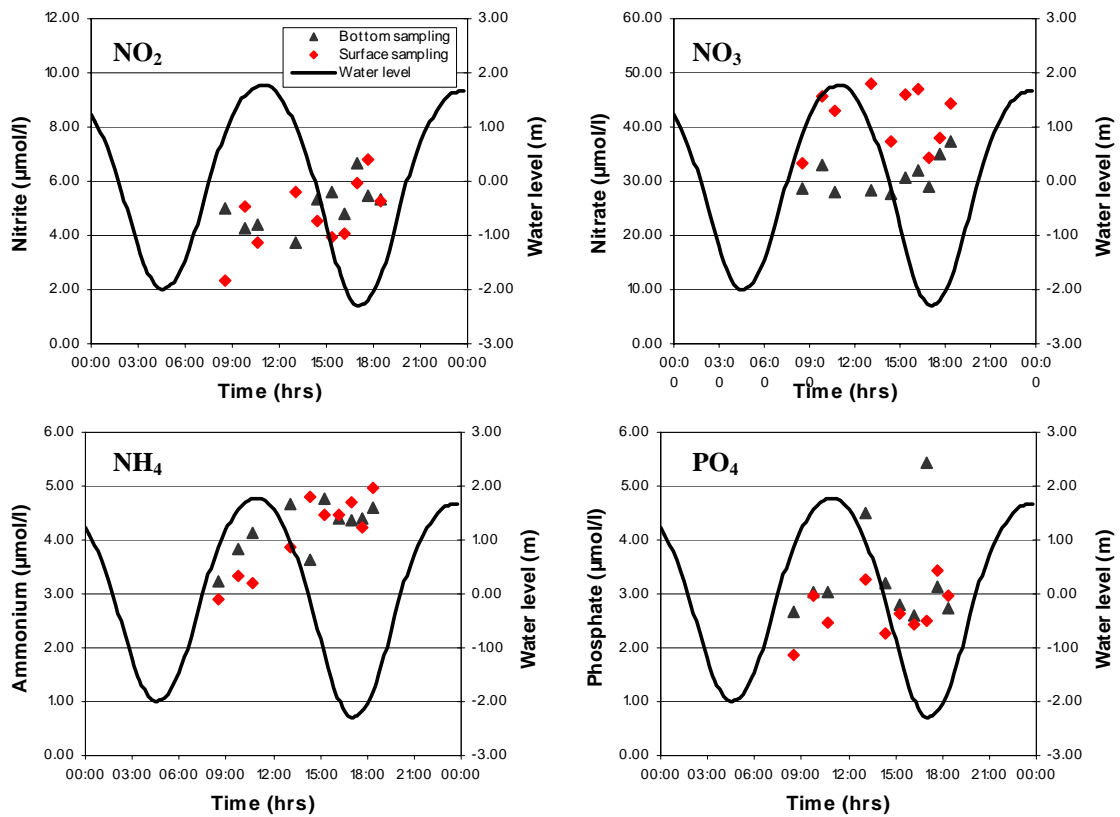


Figure 4.16: Vertical variation of NO_2 , NO_3 , NH_4 and PO_4 at station G on 14 November 2001

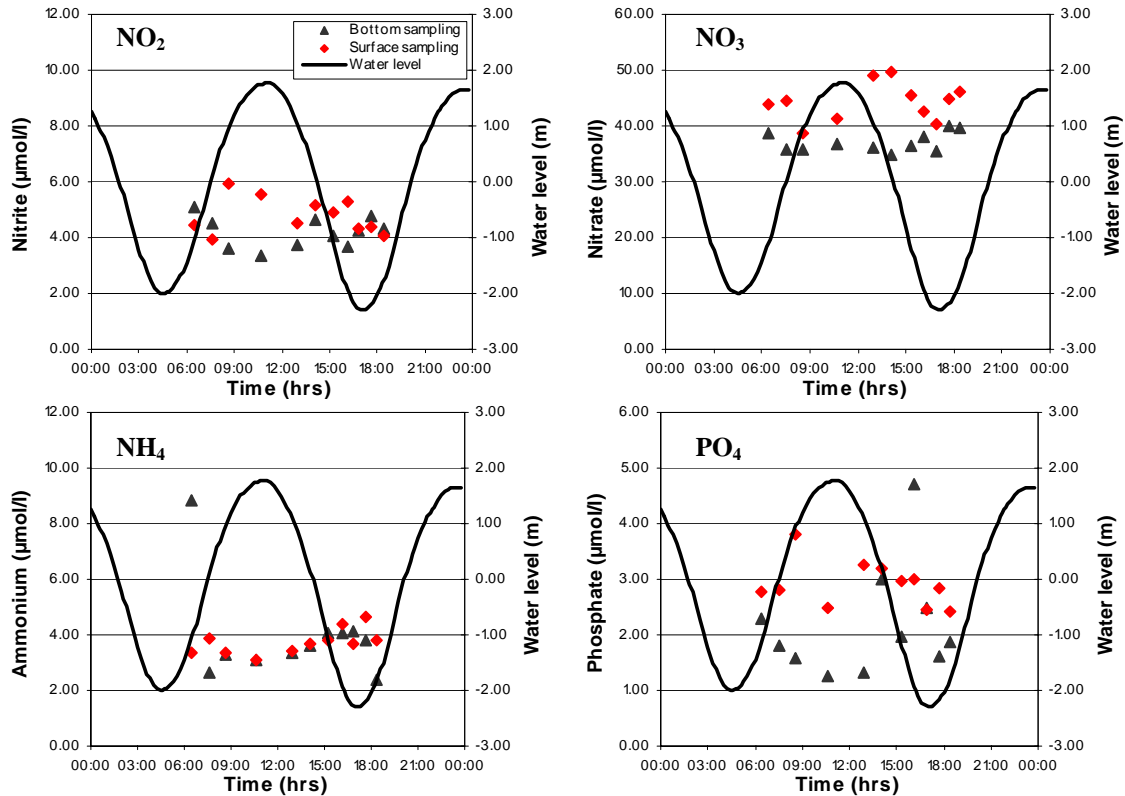


Figure 4.17: Vertical variation of NO_2 , NO_3 , NH_4 and PO_4 at station H on 14 November 2001

Seasonal variation and nutrient transports

Highest concentrations in dissolved inorganic nitrogen and in dissolved phosphate were observed in late autumn at the onset of the winter season indicating the advanced remineralisation of the organic material formed during the growing season. Highest ammonium concentrations were found in September as a result of ammonification of the fresh organic matter formed in late summer. Subsequent nitrification leads to the high nitrite and nitrate concentrations found in November.

Elevated phosphate concentrations were also found in September which may be a result of the massive remobilization of phosphate from anaerobic sediments in summer. The seasonal cycle of phosphate usually shows an annual maximum in August, however, this maximum is very broad and can extend until September.

Seasonal nutrient transports were calculated from the tidal nutrient measurements and the computed water transports over the cross section. Net transports were estimated from the difference between the inflow and outflow budgets.

Water transports were found to be rather balanced. Inflow increased slightly in November. Differences between the inflow and outflow were below 16% on average. Inflow increased slightly in November, resulting in highest net water transports during this period.

Nutrient transport budgets increased from June towards November in keeping with the seasonal variations of nutrient concentrations. Net budgets of nutrient transports entering

the Meldorf Bight fluctuated according to variations in net water transports and tidal nutrient concentrations.

During all measurement campaigns, a net import of dissolved inorganic nitrogen from the open Wadden Sea into the Meldorf Bight was observed. While the highest net import of nitrogen was found in November because of high water transports and high concentration during this time, the maximum net transport rate compared to the total import of dissolved nitrogen was found in June which may be due to increased nitrogen uptake and denitrification in the bight. Also for phosphate a net import was observed during most of the measurement campaigns. A moderate net export of phosphate was observed in early November even though there was a net import of water. This indicates the importance of phosphate production and release from local sources in the study area. Figures 4.18 to 4.20 give an overview of the water and nutrient transport budgets during the measuring campaigns.

A summary of time averaged mean values during flood and ebb phases and the standard deviations (SD) of the nutrient concentrations at stations G and H during the measuring campaigns, is presented in Table A.1-A.5 in Appendix A.

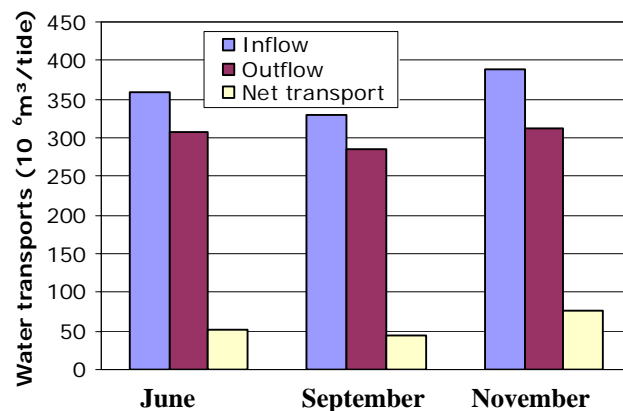


Figure 4.18: Water transports during the measurements in 2001 at the cross section G-H in the Piep intertidal channel

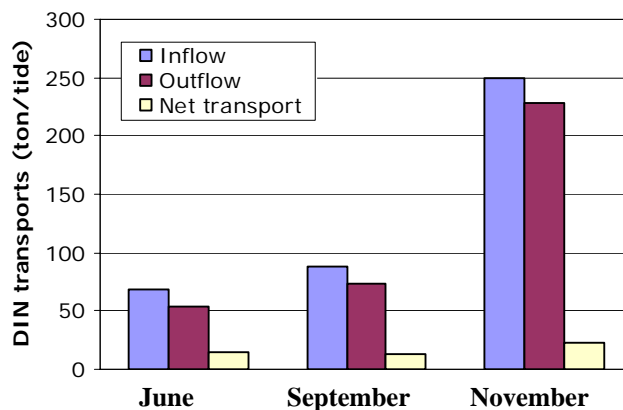


Figure 4.19: DIN transports at the cross section G-H in the Piep intertidal channel in 2001

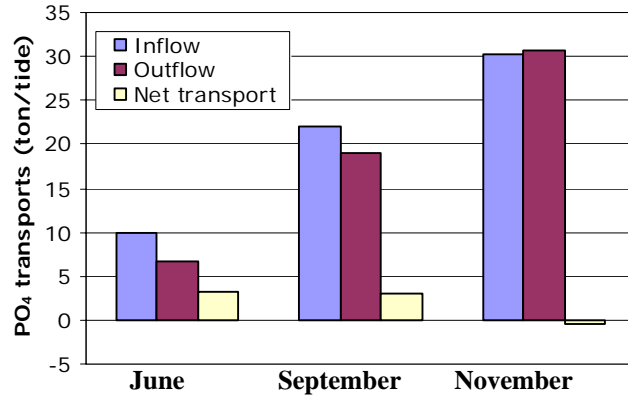


Figure 4.20: PO₄ transports at the cross section G-H in the Piep intertidal channel in 2001

4.3 Small scale nutrient distribution

4.3.1 Tidal conditions

As it was the case for the first measuring strategy, hydrodynamic conditions during the measurements were obtained from the Meldorf Bight Flow Model. Water level, current magnitude and direction of winter measurements are shown in Figures 4.21-4.22, Figures 4.23-4.24 for spring measurements and Figures 4.25-4.26 for summer measurements. The water sampling intervals of the grid measurements are also presented. The tidal range is between 3-4m and the maximum current magnitude is about 1.5m/s.

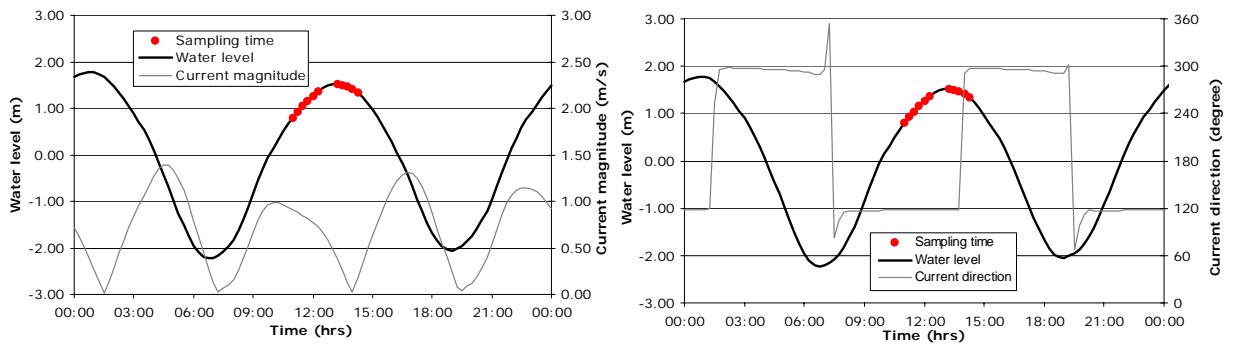


Figure 4.21: Water level, current magnitude and direction on 13 February 2002

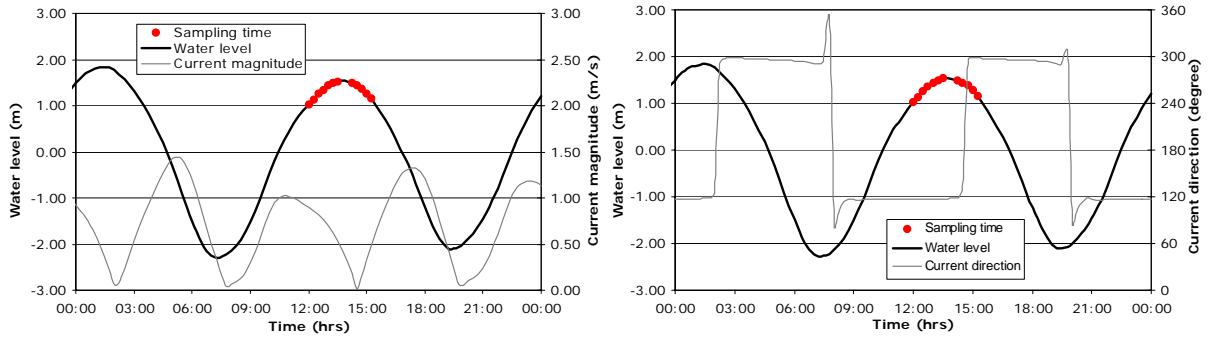


Figure 4.22: Water level, current magnitude and direction on 14 February 2002

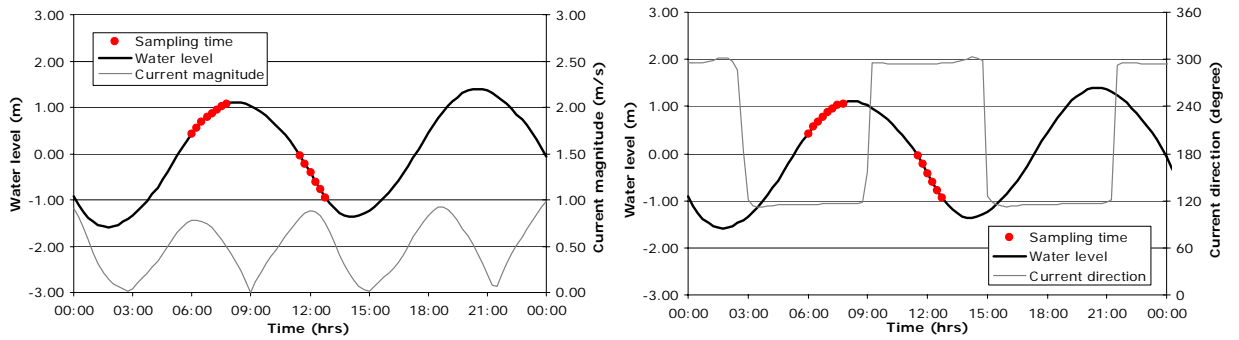


Figure 4.23: Water level, current magnitude and direction on 7 May 2002

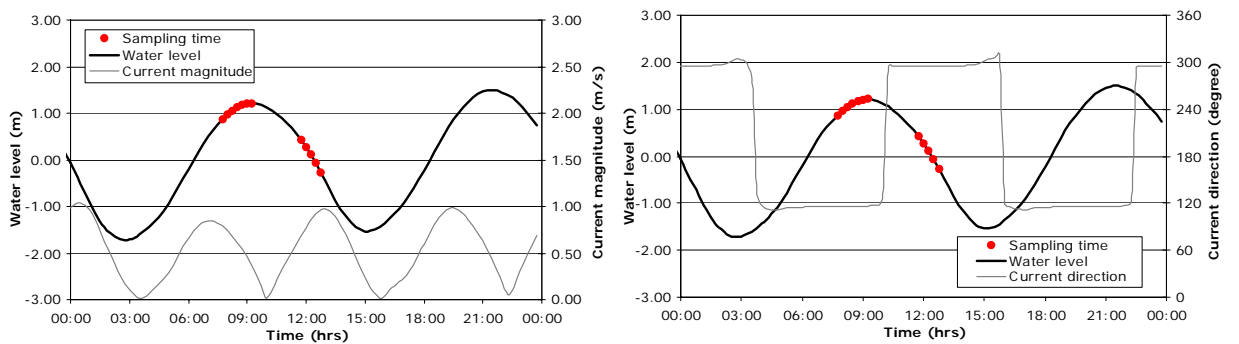


Figure 4.24: Water level, current magnitude and direction on 8 May 2002

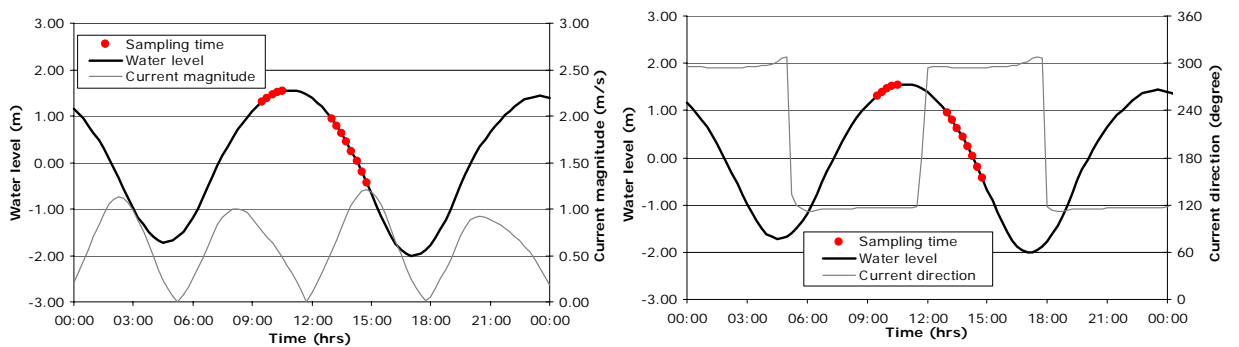


Figure 4.25: Water level, current magnitude and direction on 21 August 2002

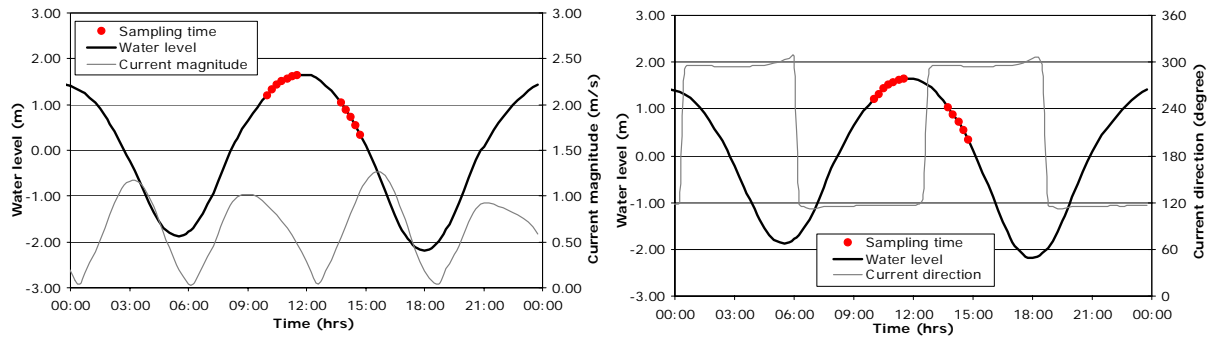


Figure 4.26: Water level, current magnitude and direction on 22 August 2002

4.3.2 Winter nutrient distribution

Grid measurements

A total of 8 grid stations were initially established to assess nutrient gradients and salinity before and after high water in the shallow area of the Meldorf Bight on February 13, 2002. The measurements were repeated on the consecutive day (Figure 4.27 and Figure 4.28). Locations of stations are indicated in Figure 4.3. In general, only minor differences in nutrient levels were found in the area. They range between 2.09 to 2.84gN/m³ for nitrate, 0.07 to 0.15gN/m³ for ammonium and 0.05 to 0.09gP/m³ for phosphate. Especially in the case of ammonium and phosphate, elevated concentrations prevailed during both of the spatial assessments at stations G4 and G5, along with a decrease in salinity of about 2-3 PSU. This indicates the influence of local freshwater discharge deriving from the polder basin adjacent to these sites.

Differences between the concentrations before and after high water were not significant. Also, nutrient and salinity patterns did not differ much between the two consecutive days of measurements. A compilation of the data obtained is given in Tables A.6-A.7, Appendix A.

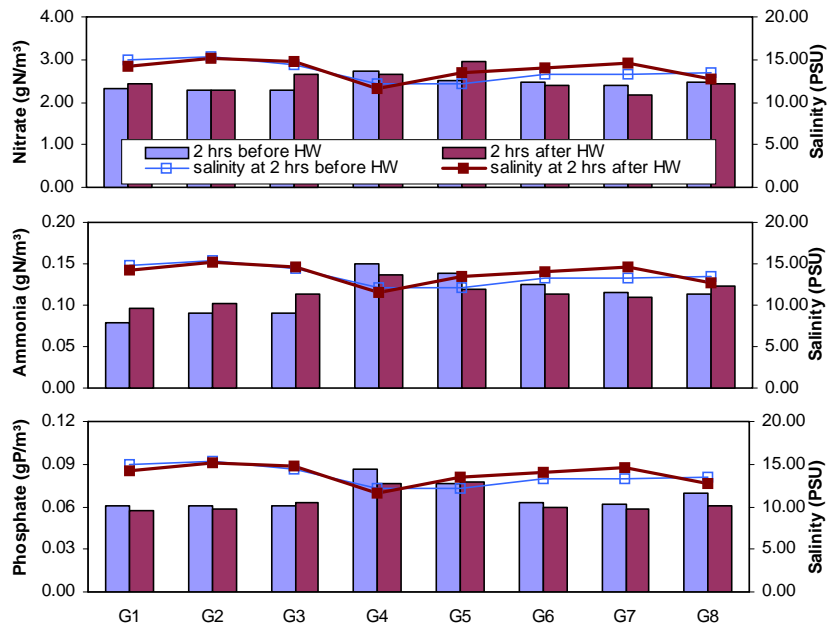


Figure 4.27: Nutrient concentrations at grid stations on 13 February 2002

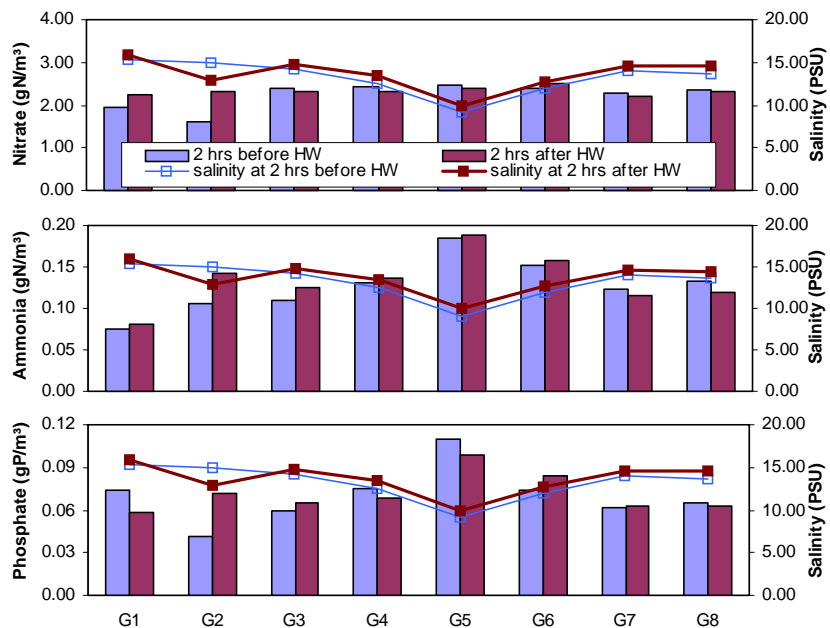


Figure 4.28: Nutrient concentrations at grid stations on 14 February 2002

Landbased measurements

Parallel to the grid measurements described above, landbased measurements of nutrient concentrations and salinity were performed in order to study in more details the potential of the local influences deriving from the hinterland.

High variations in nutrient levels were observed along the coastline during both days of measurements (Figure 4.29 and Figure 4.30). In general, the overall nutrient concentrations near the coast are found to be higher than in the more offshore area of the

bight. Elevated phosphate concentrations were observed at the south western part of the coast (stations L4 and L5) and at station L8-B, which were concomitant with a decrease in salinity. Also in the case of nitrate and ammonium higher levels usually prevailed at sites exhibiting lower salinity. These were related to freshwater input from the southern sluice and eastern polder basin. A similar relationship was found on the second day of measurements, but the water samples could not be taken at stations L8-A to L15, because the area was already fallen dry. Data of the measurements are presented in Table A.8, Appendix A.

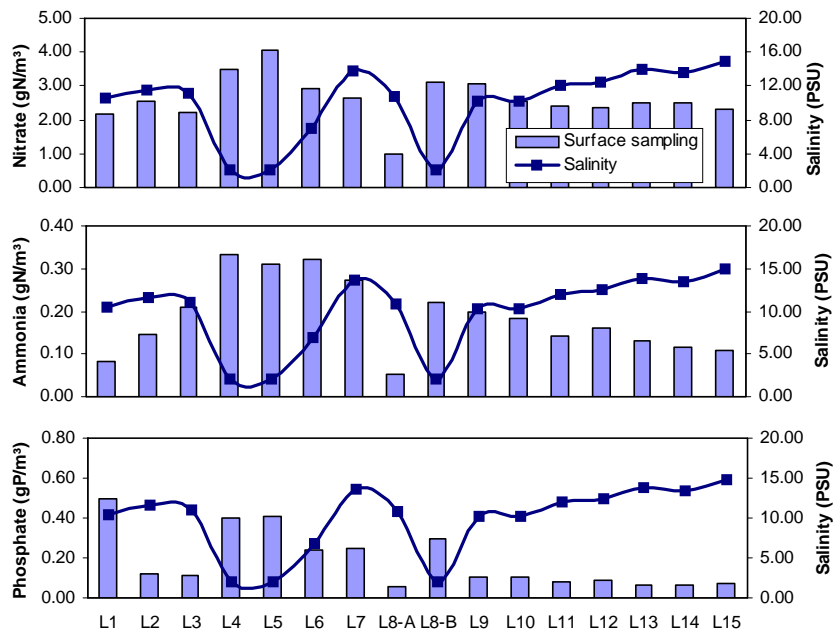


Figure 4.29: Nutrient concentrations at landbased stations on 13 February 2002

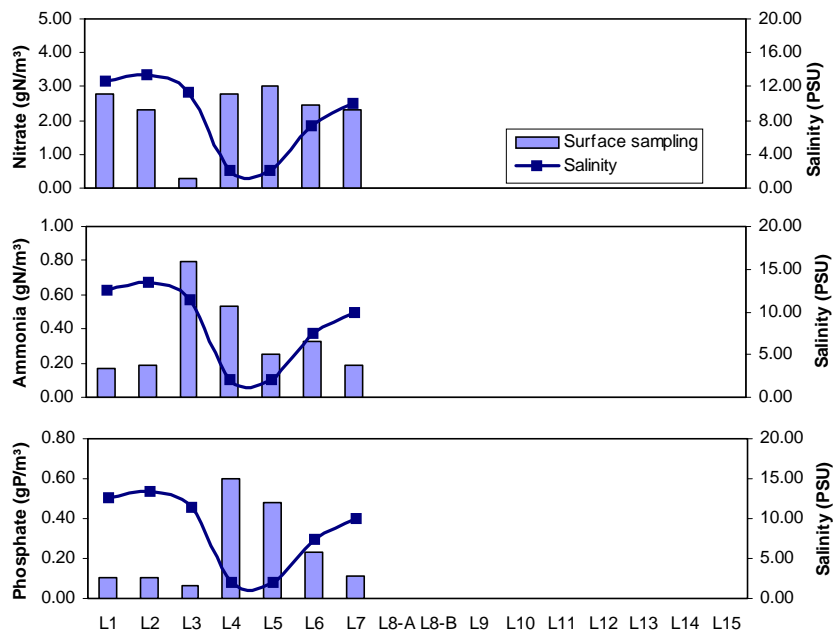


Figure 4.30: Nutrient concentrations at landbased stations on 14 February 2002

Figure 4.31 shows a comprehensive map of the gradients of dissolved inorganic nitrogen compounds and phosphate concentrations in the bight, as composed from the average concentrations at flood and ebb tides during the grid and the landbased measurements. The hot spots of high nutrient concentrations adjacent to sites of local freshwater influence in the eastern and southwestern area of the bight can be clearly traced from these figures. They were most pronounced in the pattern of nitrate levels. Lowest nutrient concentrations prevail in the center and near the open seaward border of the area.

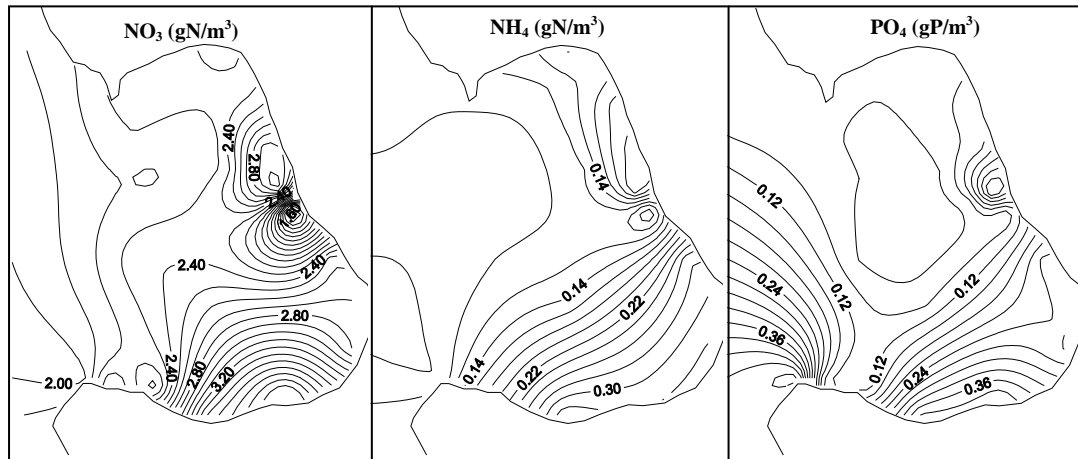


Figure 4.31: Distribution of NO_3 , NH_4 and PO_4 in winter 2002

There was a significant inverse relationship between total dissolved inorganic nitrogen and phosphate concentrations to salinity, indicating freshwater discharge as a major nutrient source in the area (Figure 4.32). The positive deviations in nutrient concentrations from this relationship suggest additional sources, such as different freshwater end members in the bight.

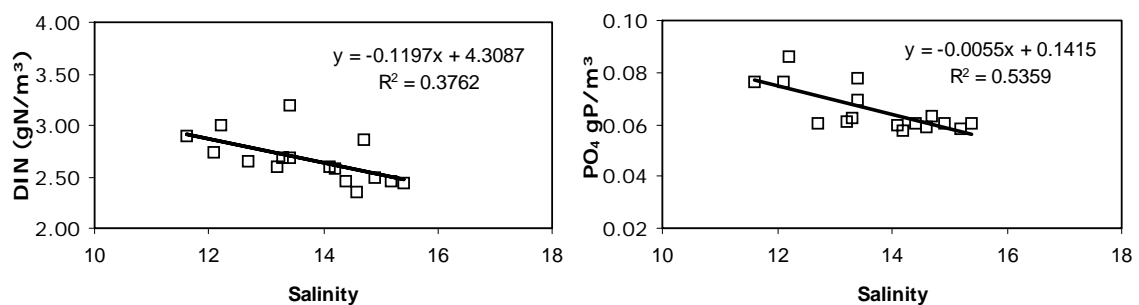


Figure 4.32: Correlation of DIN and PO_4 with salinity in winter 2002

The impact of the sewage discharge was also taken into account in this assessment (Figure 4.33). During the time of the measurements, this discharge accounted for about 13 l/s. Relatively high nitrogen concentrations were found in the outlet tank of the sewage plant. The mean concentration was about 4 times greater than the concentration obtained at the permanent station Buesum Mole. However, it was highly diluted already at the outfall pipe. Details of measured concentrations are presented in Table A.9, Appendix A.

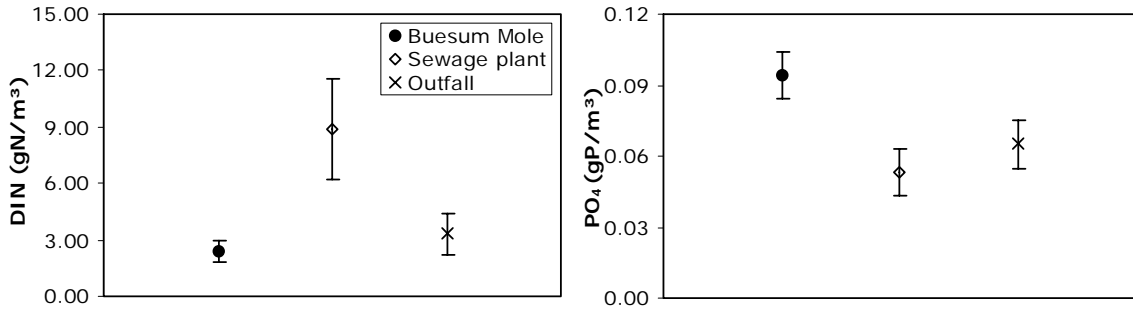


Figure 4.33: Comparisons of nutrient concentrations at the outlet and outfall of the sewage plant and at Buesum Mole in winter 2002

Ship stationary measurements at the open boundary of the study area

Figures 4.34 to 4.37 show the dissolved inorganic nutrient concentrations in the surface and bottom water at the tidal anchor stations on the seaward boundary of the bight. Nutrient concentrations show slight fluctuations over the tidal cycle with slightly higher mean levels during the ebb phase than during the flood phase, especially for ammonium. No significant vertical variation was observed. Means and standard deviation of the measured concentrations are presented in Table A.10, Appendix A.

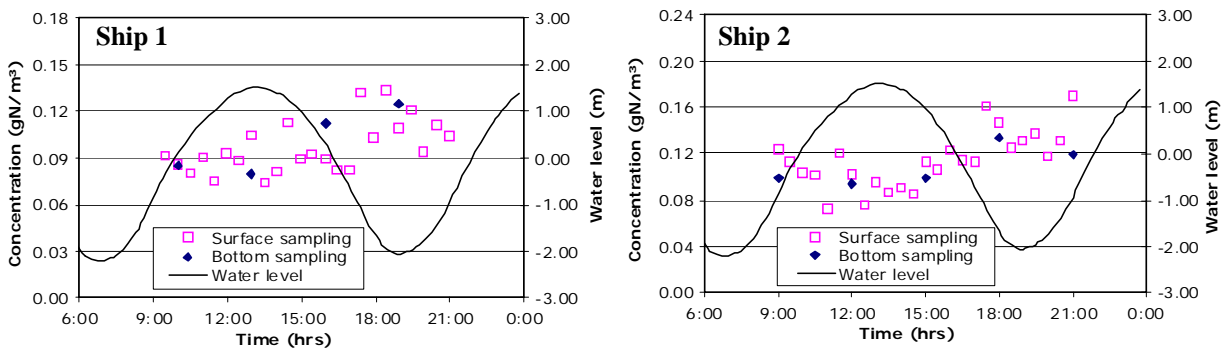


Figure 4.34: NO₂ concentration at ship 1 and ship 2 in winter 2002

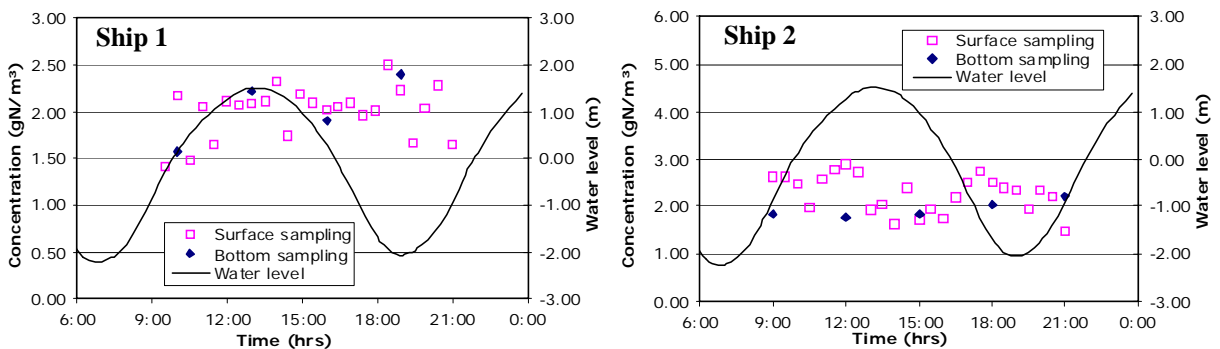


Figure 4.35: NO₃ concentration at station ship 1 and ship 2 in winter 2002

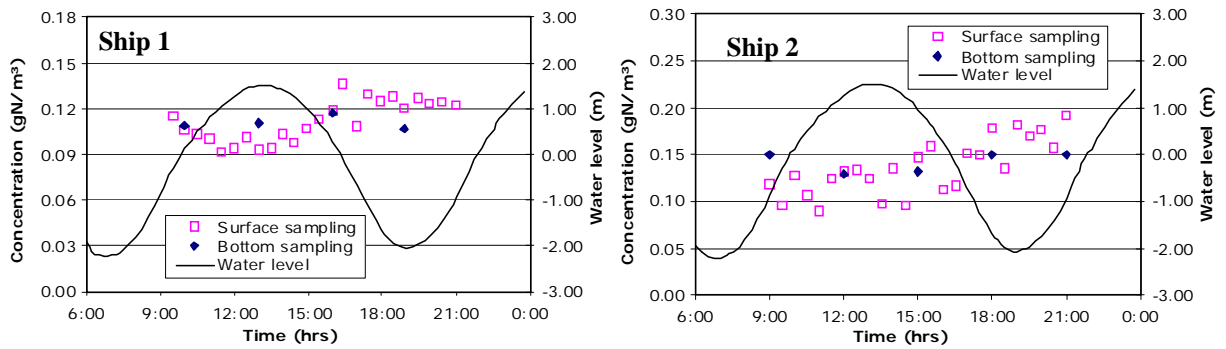


Figure 4.36: NH_4 concentration at station ship 1 and ship 2 in winter 2002

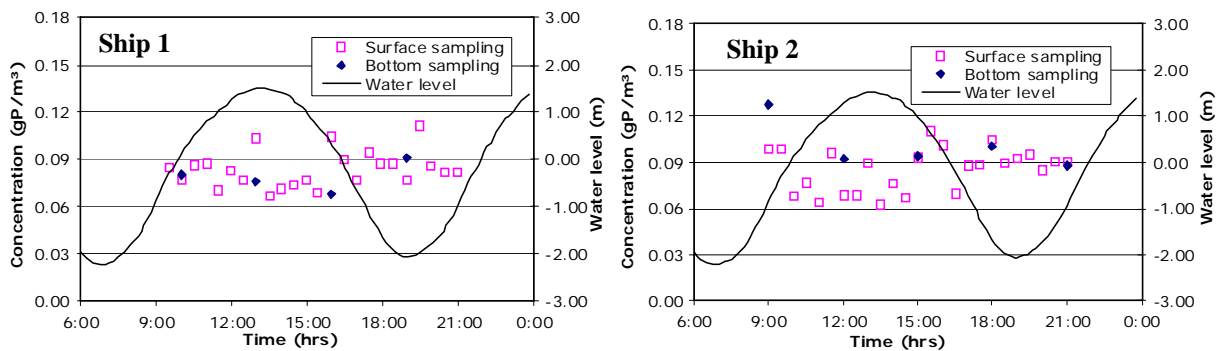


Figure 4.37: PO_4 concentration at station ship 1 and ship 2 in winter 2002

4.3.3 Spring nutrient distribution

Grid measurements

In the spring assessment, two additional stations were added to the initial grid of 8 stations sampled in the winter measurements. These stations were located at the end of a small tributary separated from the major channel in the middle of the bight (G9) and at the end of the tidal channel in front of the salt marshes (G10). Nitrate concentrations in spring differed slightly between 0.60-1.03gN/m³ (Figure 4.38 and Figure 4.39). High ammonium and phosphate concentrations were found at stations G4, G5, G6, G7 and G10 especially during low water with a maximum of 0.21gN/m³ and 0.13gP/m³, respectively. Concentrations before and after high water differed significantly at stations G4, G5 and G6 concomitant with a decrease in salinity as much as 5 PSU. This indicates the freshwater influence of the eastern polder adjacent to these stations. The evidence was more moderate on the second day of measurements. Details of the measurements are presented in Table A.11 and Table A.12 in Appendix A.

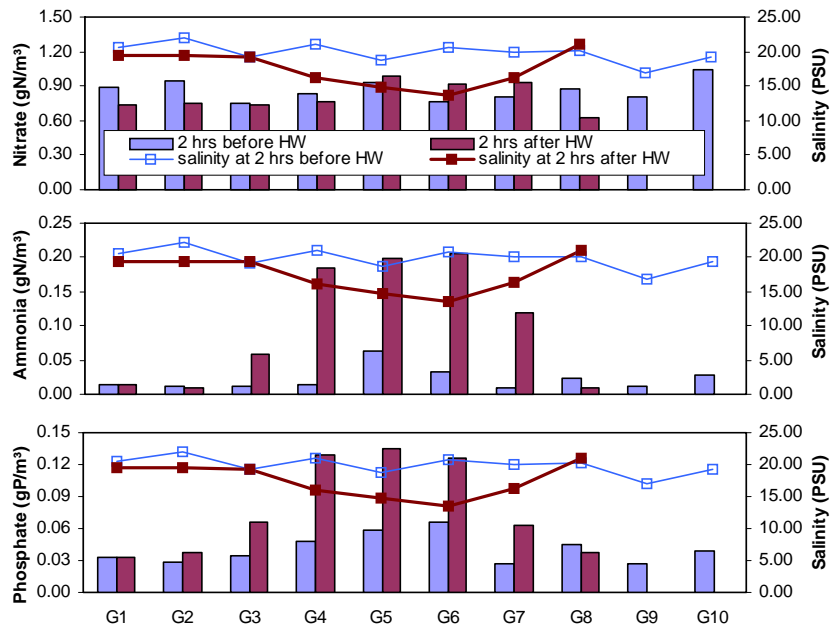


Figure 4.38: Nutrient concentrations at grid stations on 7 May 2002

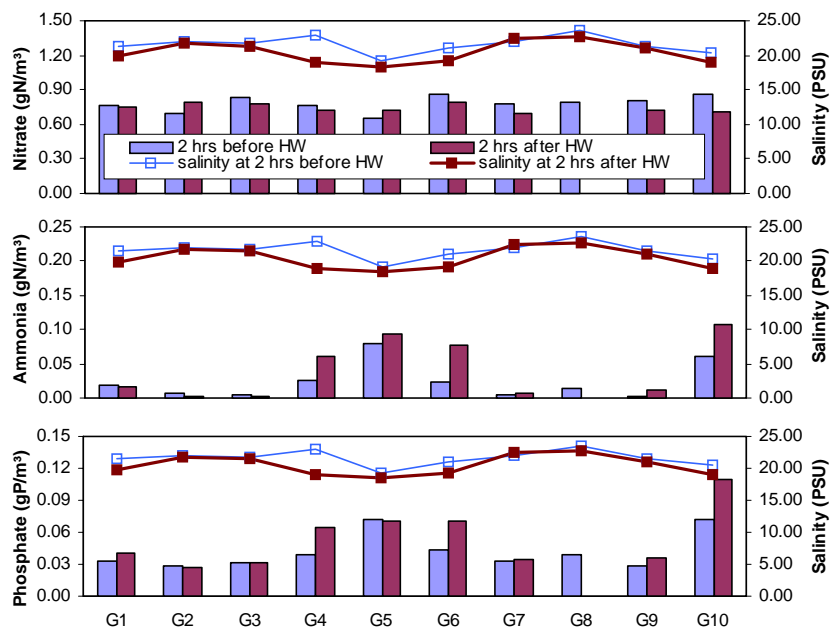


Figure 4.39: Nutrient concentrations at grid stations on 8 May 2002

Landbased measurements

Also in spring, nutrient concentrations in the very nearshore shallow water along the coastline exhibited marked variations, which were due to local influences from the coast. (Figure 4.40 and Figure 4.41). High nutrient levels appeared at stations L4, L5, L6, L7 and L10. In contrast, low concentrations were found at stations L1-L3 with slightly elevated ammonium at L2. Salinity dropped at two positions, L5 and L8-B indicating the freshwater inputs from the sluice and the polder basin. High nitrate concentrations were found at the stations close to these discharge locations. Variations of nutrient levels were

found to be smaller on the second day of measurements. Maxima prevailed at stations L5 for nitrate and L6 for phosphate. Measured concentrations and salinity are presented in Table A.13 in Appendix A.

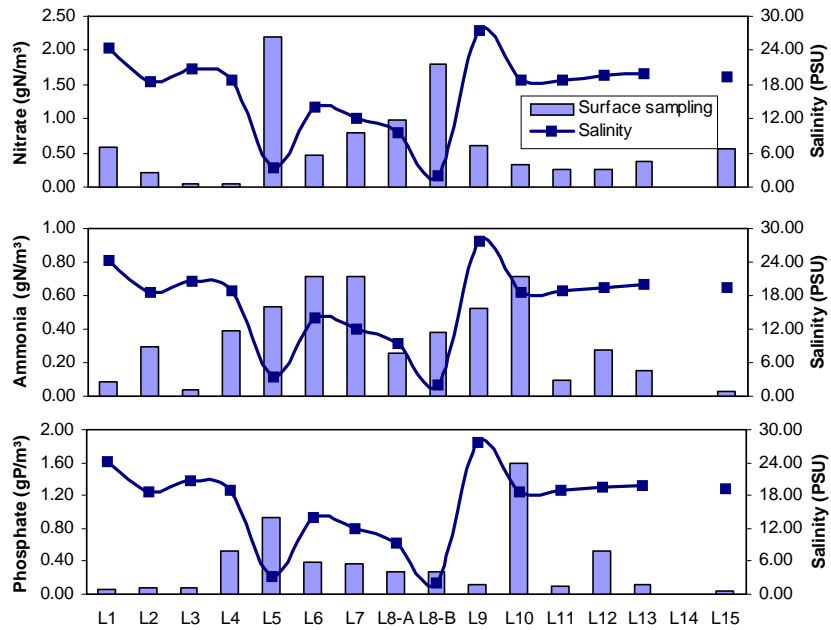


Figure 4.40: Nutrient concentrations at landbased stations on 7 May 2002

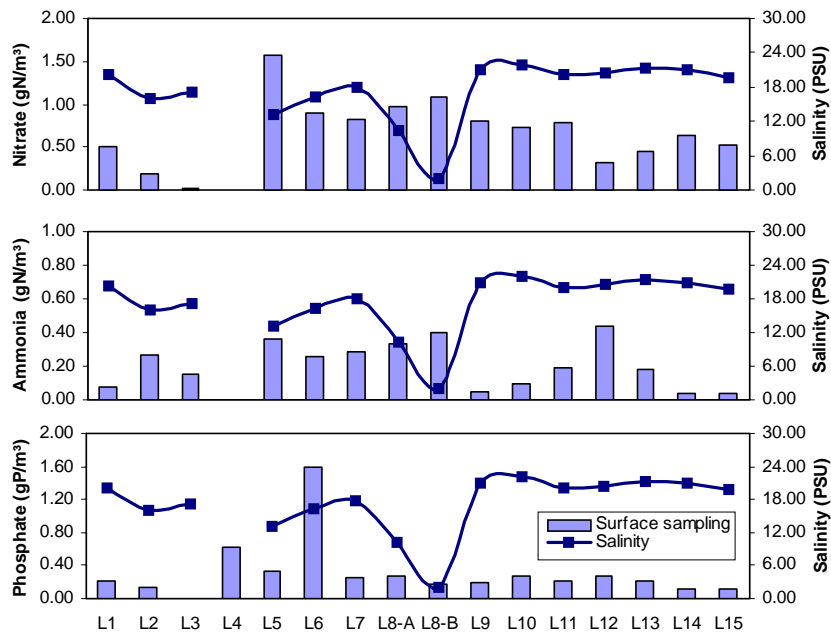


Figure 4.41: Nutrient concentrations at landbased stations on 8 May 2002

When compared to the winter situation, nutrient concentrations in spring showed a much higher variability. Figure 4.42 gives an overview of the spatial gradients of the dissolved inorganic nitrogen and phosphorus distribution in the area. As it was the case in winter, high concentrations of nitrate and ammonium were found in front of the local freshwater

sources. In the case of phosphate, a maximum occurred north of the outflow of the polder basin near the northeastern corner of the bight.

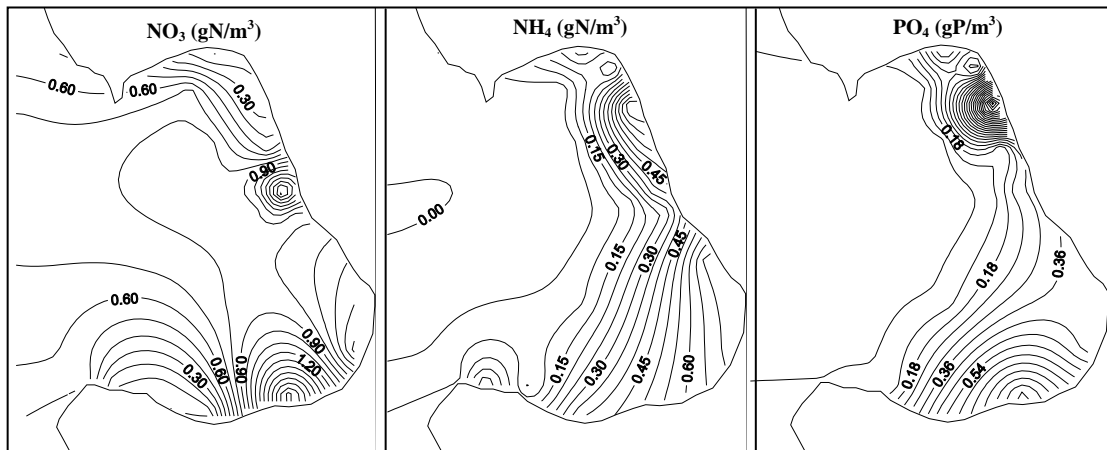


Figure 4.42: Distribution of NO_3 , NH_4 and PO_4 in spring 2002

Also in spring, total dissolved inorganic nitrogen and phosphate concentrations showed an inverse linear relationship with salinity (Figure 4.43). This underlines the importance of freshwater runoff as a major source. However, especially phosphate concentrations showed some deviations from this linear relationship, indicating additional internal sinks and sources in the area. Apart from uptake and remineralisation processes during the spring bloom, phosphate remobilization from the sediment on the muddy tidal flats in the northeast and southern part of the bight may play an important role for the modification of the nutrient pattern.

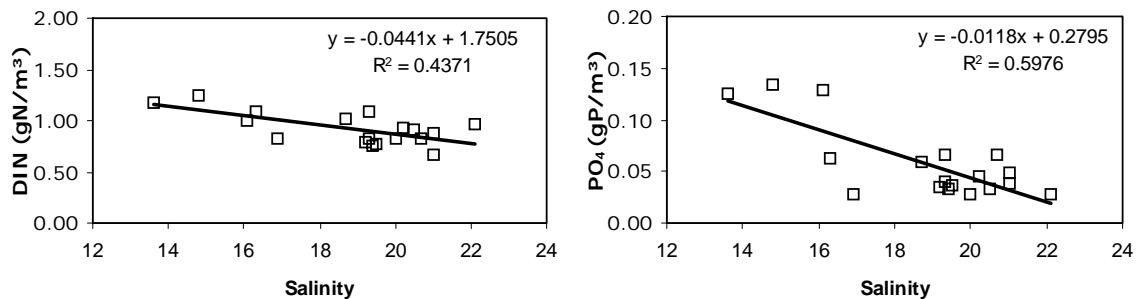


Figure 4.43: Correlation of DIN and PO_4 with salinity in spring 2002

Comparisons of nutrient concentrations at the sewage plant and at the outfall confirmed the insignificant importance of the sewage discharge to the Meldorf Bight (Figure 4.44). Approximate sewage discharge during the measurement period was 35 l/s, about 3 times higher than the discharge measured in winter. The mean concentration of dissolved nitrogen compounds in the outlet tank of the sewage plant was about 4 times greater than the mean concentrations measured at Buesum Mole. However, they were highly diluted at the outfall. Concentrations of phosphate were higher at the outfall when compared to the phosphate concentrations in the releasing tank of the sewage plant itself and also at the Buesum Mole. Remobilisation from the sediment could be the source for the higher values found at this station. The water depth at the outfall is very shallow and the tidal

flat area falls dry during low water which can stimulate the remobilisation process especially when the sediment is subjected to heating due to sunlight exposure. Details of the measured concentrations are presented in Table A.14 in Appendix A.

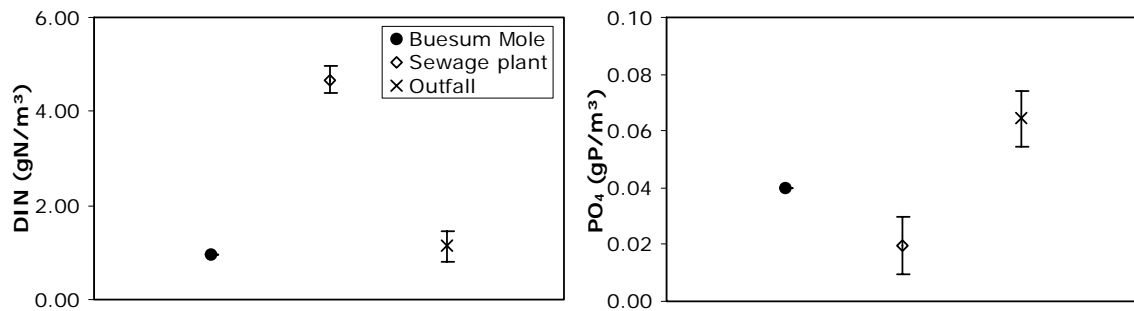


Figure 4.44: Comparisons of nutrient concentrations at the outlet and outfall of the sewage plant and at Buesum Mole in spring measurements 2002

Ship stationary measurements at the open boundary of the study area

Figure 4.45 to Figure 4.50 show the concentrations obtained from the stationary tidal measurements at the open seaward boundary of the bight. Details about the means and standard deviations of the measured concentrations are presented in Table A.15, Appendix A. Nutrient concentrations scattered over the tidal cycle with a tendency of slightly higher phosphate, nitrite and ammonium levels during the ebb phase. In the case of nitrate, concentrations were more or less equal or sometimes higher at high tide. Vertical variation was found to be not significant.

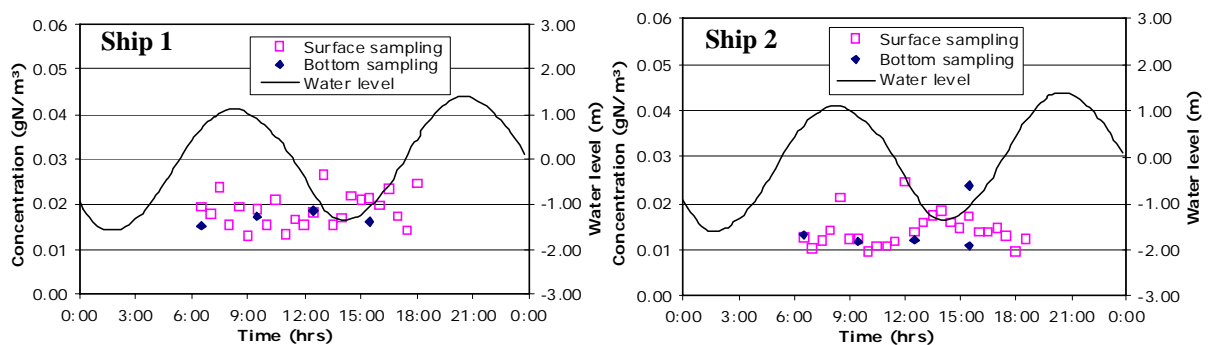


Figure 4.45: NO₂ concentration at station ship 1 and ship 2 in spring 2002

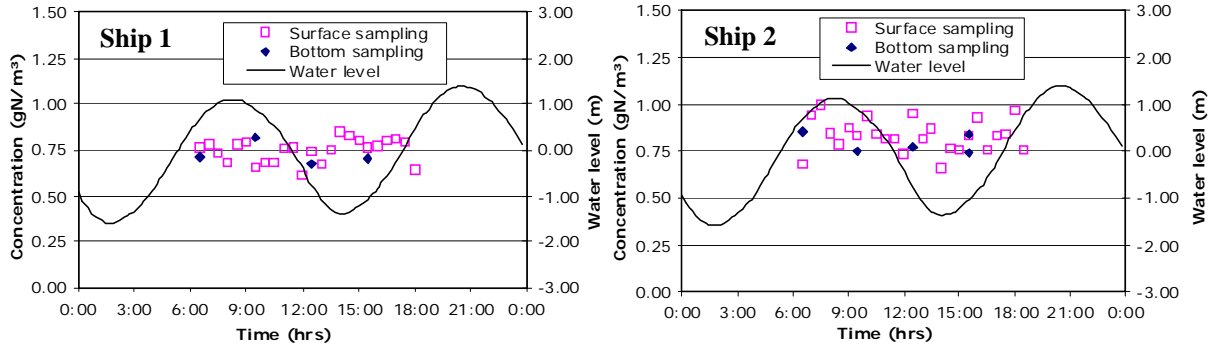


Figure 4.46: NO_3 concentration at station ship 1 and ship 2 in spring 2002

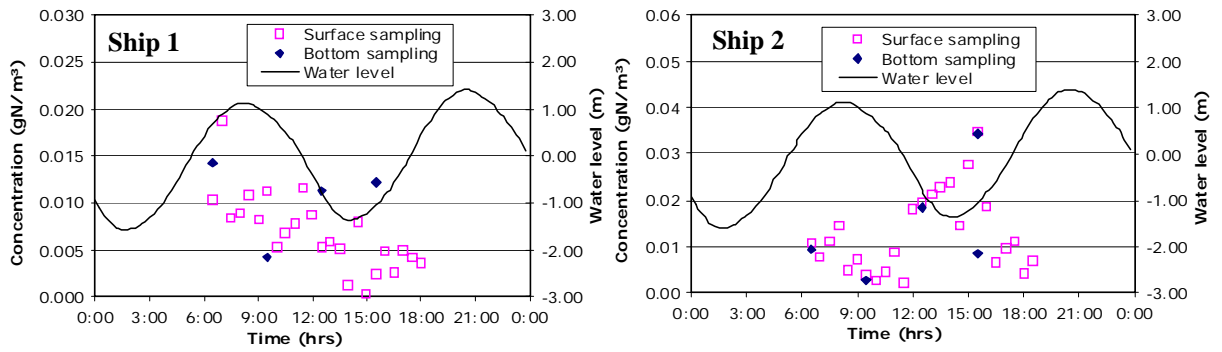


Figure 4.47: NH_4 concentration at station ship 1 and ship 2 in spring 2002

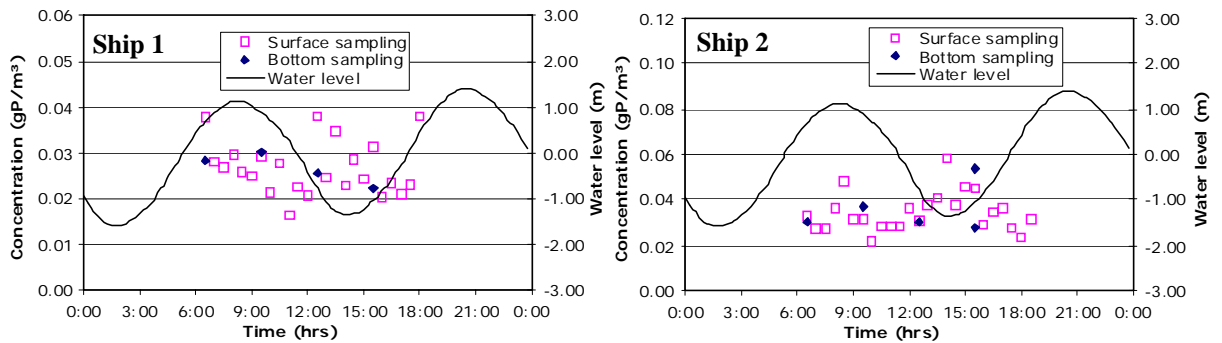


Figure 4.48: PO_4 concentration at station ship 1 and ship 2 in spring 2002

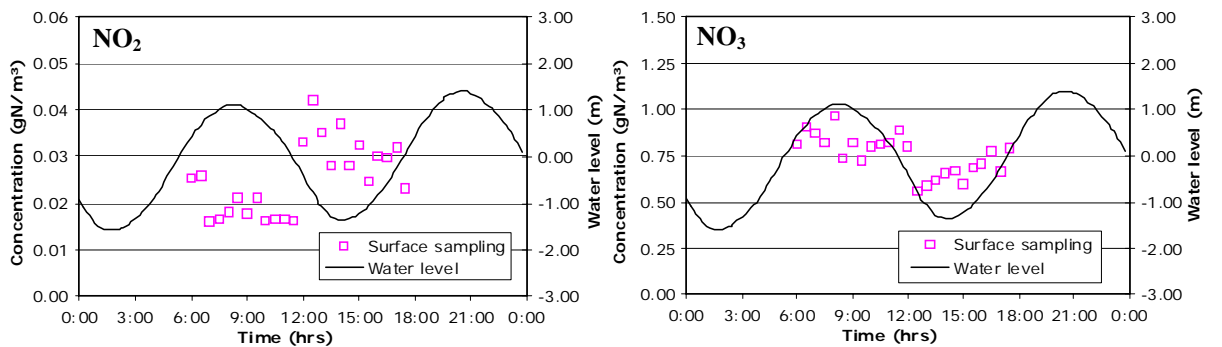


Figure 4.49: NO_2 and NO_3 concentrations at the automatic sampler station in spring 2002

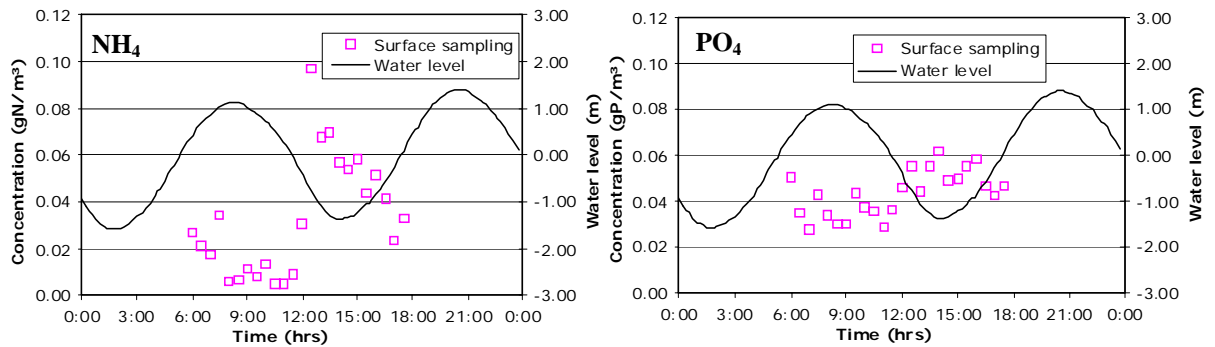


Figure 4.50: NH_4 and PO_4 concentrations at the automatic sampler station in spring 2002

4.3.4 Summer nutrient distribution

Grid measurements

In comparison with the situations in winter and spring, the summer nutrient distribution was found to be rather smooth (Figure 4.51 and Figure 4.52). The variations of nutrient levels were dominated by biochemical processes rather than by local freshwater influences as indicated by the relative uniform salinity pattern. Nitrate concentrations ranged between 0.12-0.28gN/m³ with slightly higher values at the seaside (G1, G2 and G3). Ammonium concentrations ranged between 0.01-0.05gN/m³ with highest concentrations mainly at the eastern part (G4, G5 and G6). High phosphate concentrations prevailed with maximum levels in the south eastern part at stations G4, G5, G8, G9 and G10 predominantly during low tide. Minimum and maximum concentrations of phosphate accounted for 0.07gP/m³ and 0.19gP/m³, respectively. The nutrient pattern on the two consecutive days of measurements was found to be rather similar. Measured concentrations are presented in Tables A.16 and A.17 in Appendix A.

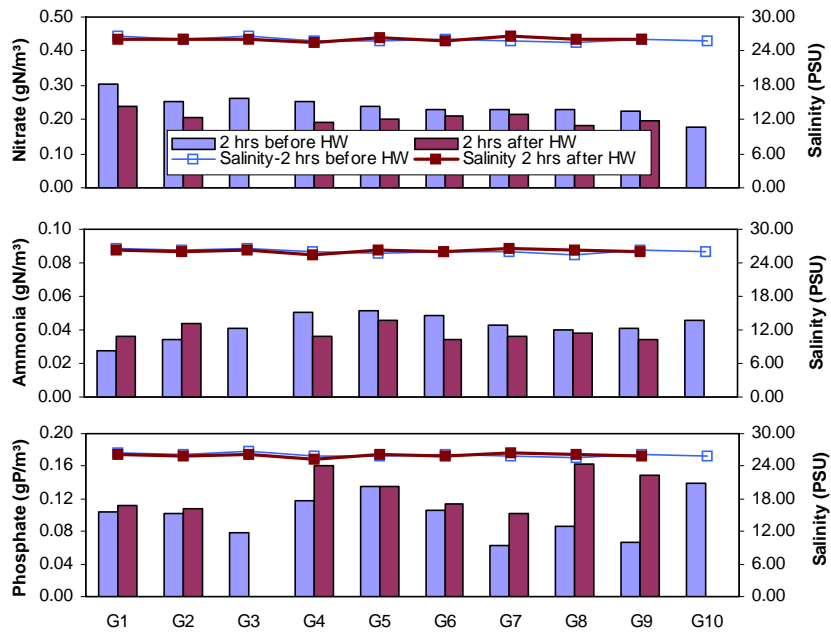


Figure 4.51: Nutrient concentrations at grid stations on 21 August 2002

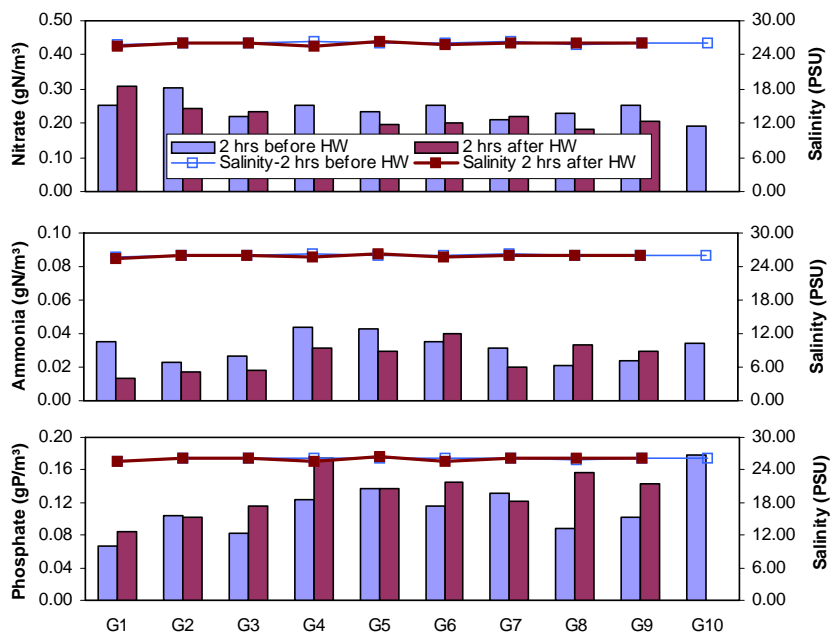


Figure 4.52: Nutrient concentrations at grid stations on 22 August 2002

Landbased measurements

High variations of nitrate and ammonium were found along the coastline (Figures 4.53-4.54). High nitrate levels were observed at stations L1, L7 and L15. Elevated concentrations of ammonium and phosphate at L4 may be related to intensified remineralisation and inadequate oxygen supply during summer in the sediment and shallow water of this location in front of the salt marshes. Salinity dropped significantly at L8-B near the polder basin but no depression of salinity was found between L4-L5 as observed in winter and spring. This is in keeping with reduced precipitation during the

summer season causing only a minor discharge from the sluice at the southern part. Nutrient discharge from the polder basin was also found to be minor since no significant increase of concentrations was found at station L8-B in contrast to the observations in spring. A very similar pattern of nutrient distributions was observed on the second day of measurements. High ammonium and phosphate still prevailed in the south (L4, L5 and L6). A compilation of the measured data is presented in Table A.18, Appendix A.

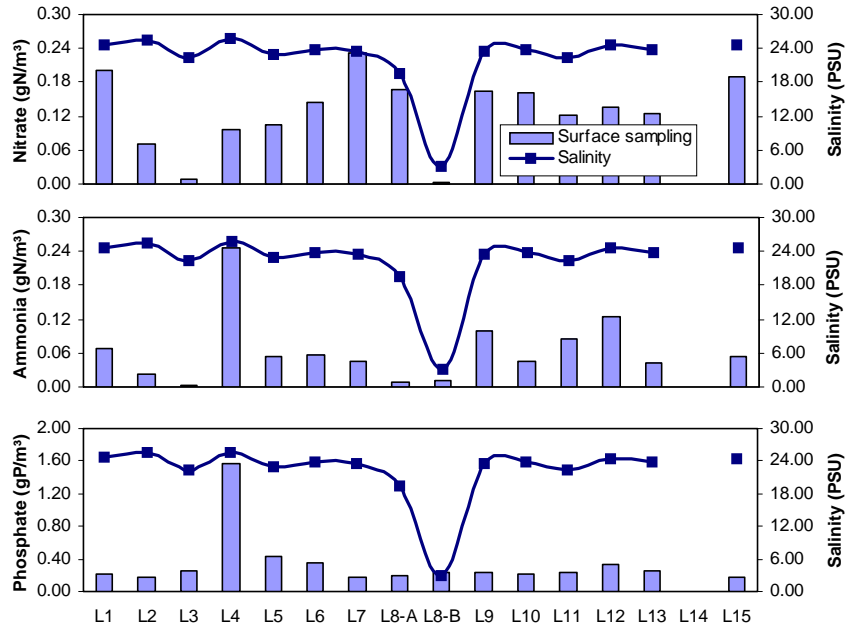


Figure 4.53: Nutrient concentrations at landbased stations on 21 August 2002

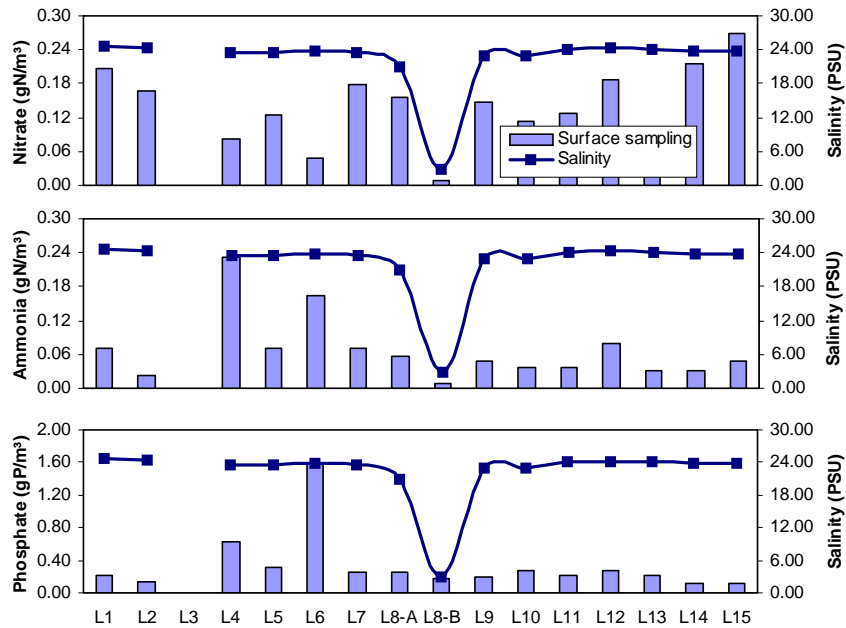


Figure 4.54: Nutrient concentrations at landbased stations on 22 August 2002

The comprehensive map of summer nutrient gradients in the Meldorf Bight illustrates well that the southern part is a local source of nutrients especially for ammonium and phosphate (Figure 4.55). These high gradients may be caused by enhanced remineralisation intensity in the high Wadden flats and the extended salt marsh in this area when they are subjected to high temperatures in summer. In the eastern part of the bight the discharge of the polder basin resulted in slightly elevated nitrate and ammonium concentrations but this impact was almost negligible for phosphate distribution.

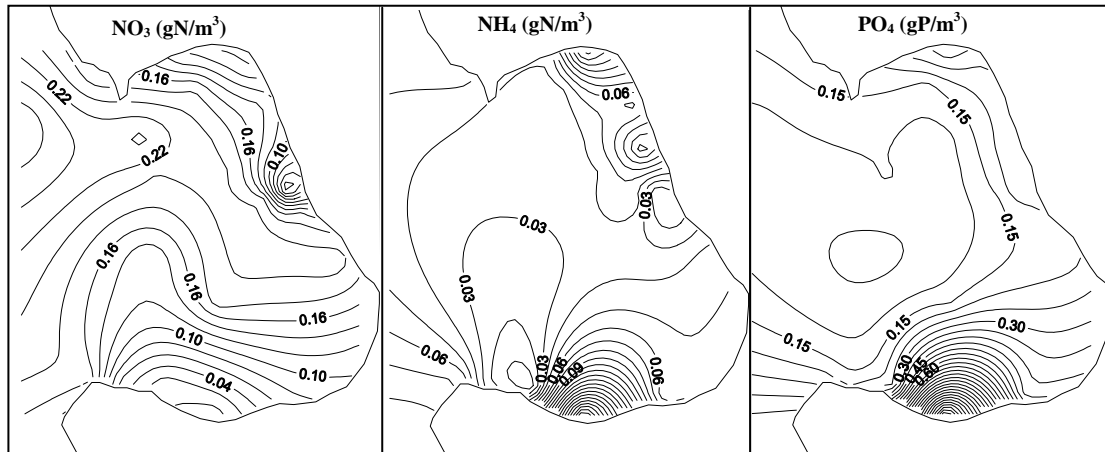


Figure 4.55: Distribution of NO_3 , NH_4 and PO_4 in summer 2002

As a consequence of reduced freshwater discharge and due to the dominance of internal transformation processes, the nutrient-salinity relationship was not significant in summer (Figure 4.56). Even DIN tends to increase with salinity suggesting an import of nitrogen rich seawater.

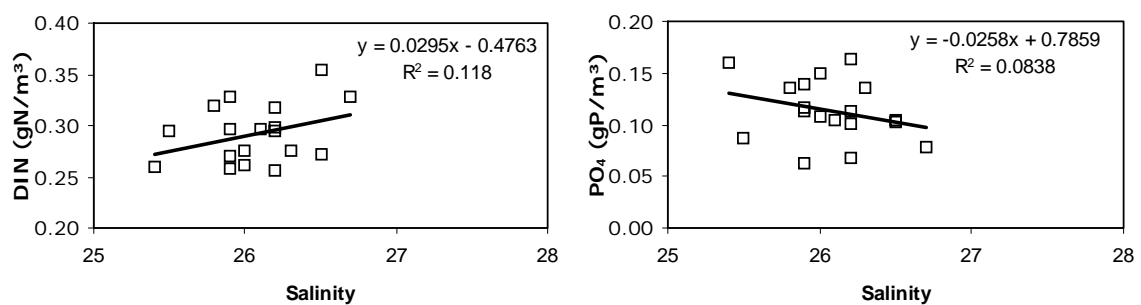


Figure 4.56: Correlation of DIN and PO_4 with salinity in summer 2002

Discharge from the Buesum sewage plant had only a minor influence on the nutrient conditions in the adjacent water of the Meldorf Bight (Figure 4.57). The approximate discharge of the sewage plant during the measurement period was about 40 l/s, which is distinctly more than in winter (13 l/s) and spring (35 l/s). A considerable increase in the population of the city of Buesum due to tourism is the reason for the increased amount of wastewater in summer. Dissolved nitrogen concentration in the outlet tank was almost 10 times greater than the mean value found at Buesum Mole. Phosphate concentration at the outfall was only slightly higher than the concentration in the treated sewage water, which

exhibited distinctly elevated levels when compared to those in winter and spring. Details of the measured concentrations are presented in Table A.19 in Appendix A.

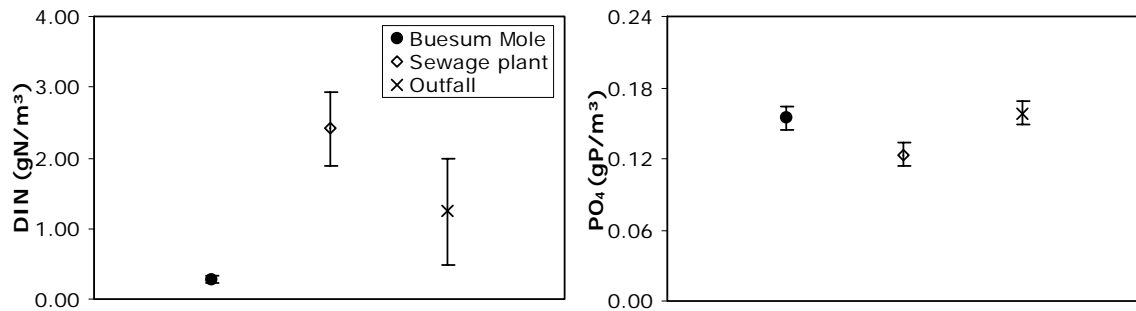


Figure 4.57: Comparisons of nutrient concentrations at the outlet and outfall of the sewage plant and at Buesum Mole in summer measurements 2002

Ship stationary measurements at the open boundary of the study area

As observed in the previous measurements, nutrient concentrations of the ship stationary measurements show slight fluctuations over the tidal cycle (Figures 4.58-4.63). Some scattered concentrations were observed but less than those found in spring. The concentrations during ebb phase were found to be slightly higher than the concentrations during flood phase except for nitrate which exhibited higher concentrations were found during high water. This may be associated with the transport of nitrate from the seaside. Details of the measured concentrations are presented in Table A.20, Appendix A.

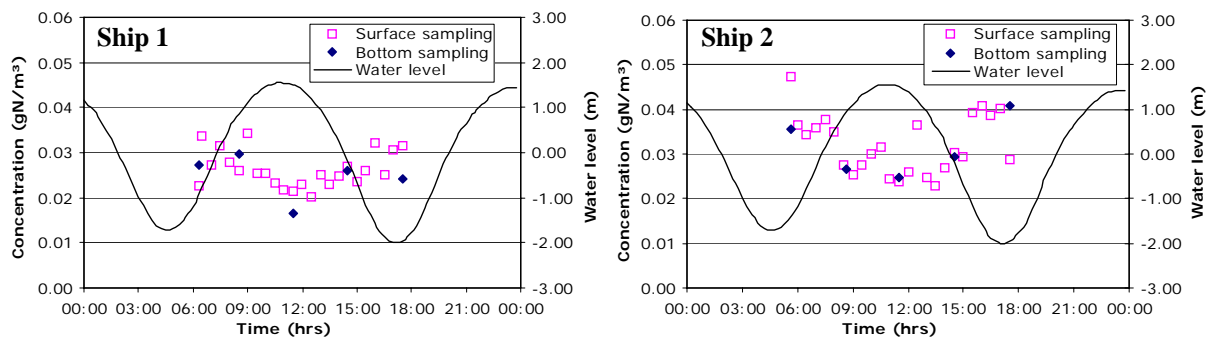


Figure 4.58: NO₂ concentration at stations ship 1 and ship 2 in summer 2002

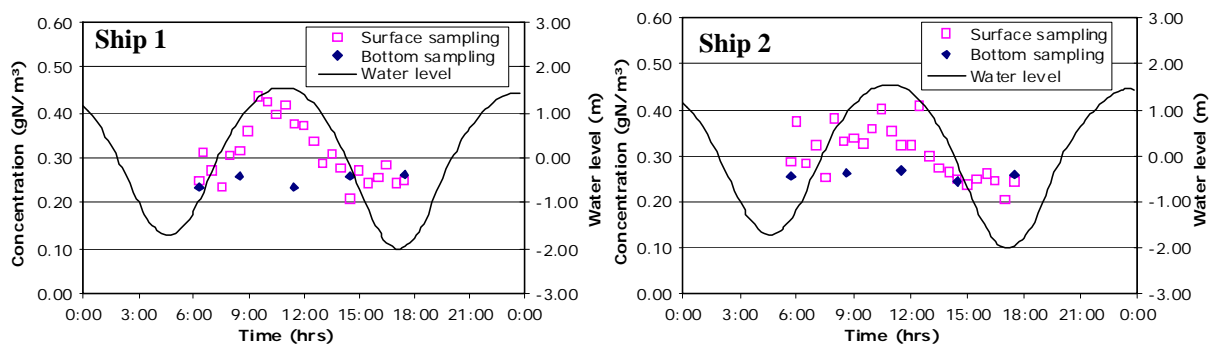


Figure 4.59: NO₃ concentration at stations ship 1 and ship 2 in summer 2002

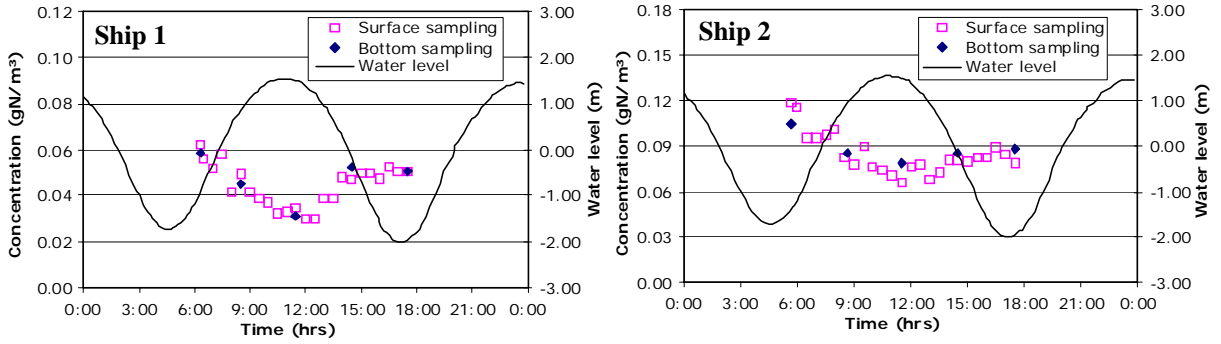


Figure 4.60: NH_4 concentration at stations ship 1 and ship 2 in summer 2002

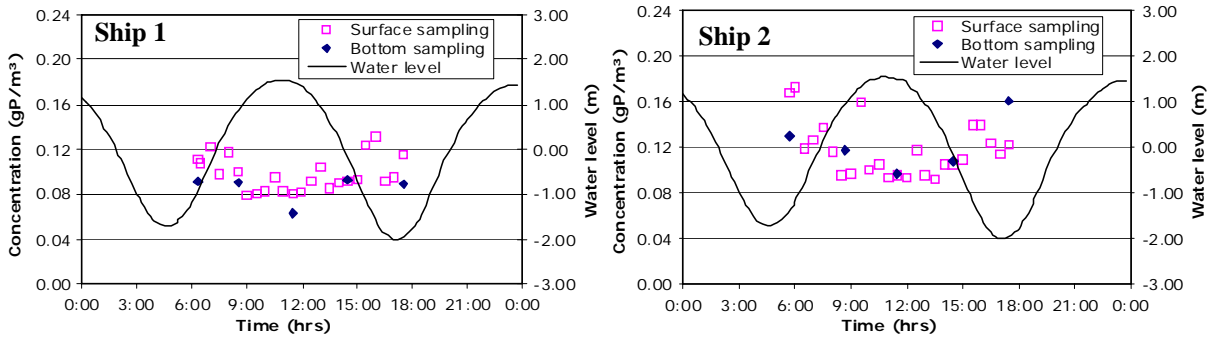


Figure 4.61: PO_4 concentration at stations ship 1 and ship 2 in summer 2002

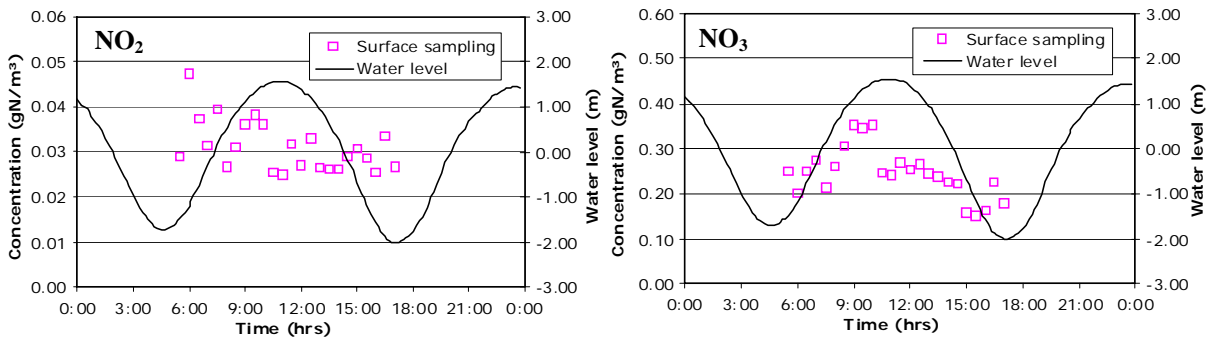


Figure 4.62: NO_2 and NO_3 concentrations at the automatic sampler station in summer 2002

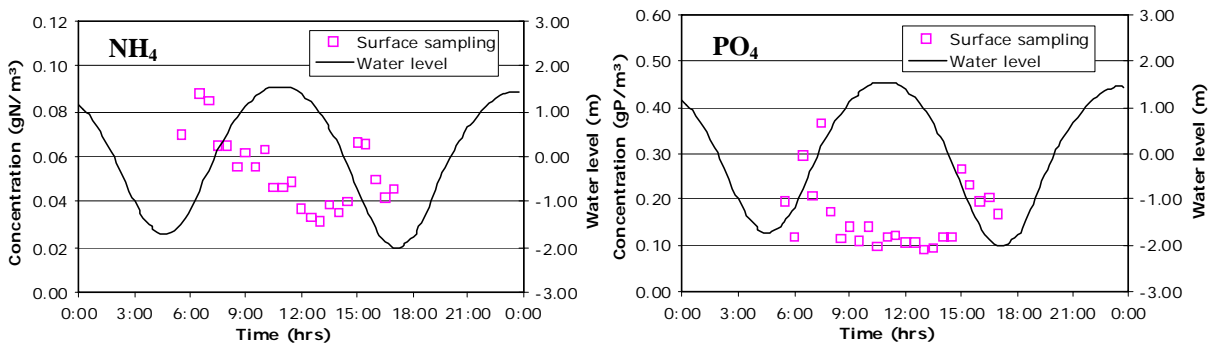


Figure 4.63: NH_4 and PO_4 concentrations at the automatic sampler station in summer 2002

4.4 Discussion of the measured results

After the two measurement strategies had been successfully performed, the measured nutrient dynamics were linked to additional data such as flow condition, salinity and additional freshwater discharge in order to detect causal relationships and to draw a conclusion on the nutrient conditions during the period of interest in the study area.

1. Preliminary measurements: Seasonal nutrient transports

Water transported in and out of the Meldorf Bight through the cross section of the Piep intertidal channel was estimated based on the measured nutrient concentrations and the computed flow discharges. The discharges were found to be slightly different for spring, summer and winter respectively. The net discharges show that water transport through the cross section during the measurement period was rather balanced. Inflows due to flood transports were found to be dominant during 4 periods of measurements with an approximate discharge of 360 million m³. About 15% (averaged) of total water transport was found to be imported into the Meldorf Bight. Various factors may cause this net import. In an idealized estuary, net transport over a tidal cycle in the absence of river input is zero. However, a net transport of zero rarely occurs. Instead, a substantial net import or export may occur during a tidal action which may be due to the specific bathymetry, the shape of the estuary and external factors such as riverine input.

Considering the seasonal transport of dissolved inorganic nutrients, nitrogen exhibited a net import during all seasons whereas this was the case for phosphate during June and September, but not in November. These import fluxes of nutrients into the Meldorf Bight are mostly due to the unbalance in water transports in conjunction with nutrient concentrations. Taking this into consideration by eliminating the influence of the water transport unbalance it appears that there remains a net import of nitrogen during early summer (June), an almost balanced nitrogen budget during late summer (September) and an export in autumn (November). DIN import from the Elbe estuary through the seaward border of the Meldorf Bight as observed in the spatial measurements during summer and dissolved inorganic nitrogen removal due to algal uptake and increased denitrification in the coastal muddy Wadden flats may be the reason for the net landward flux in June. By contrast, increased inputs from the agricultural hinterland and remineralisation of the organic material formed during the growth season may be the factors responsible for the outgoing nitrogen flux in November. In the case of dissolved phosphate, after the correction of unbalances in water transports, there is an almost balanced transport budget in June, a slight net export in September and a distinct export in November, which may be due to phosphate remobilisation from the sediments in the study area during this season. The enhanced remineralisation of an increased amount of organic matter deposited in the sediment during the growing season may lead to anaerobic conditions and result in an excess of phosphate. Seasonal transport patterns found in this study were largely in agreement with the patterns observed in the German Bight (DICK et. al., 1999).

2. Intensive measurements: Small scale seasonal nutrient distributions

Results of the seasonal small scale assessment suggest that two possible factors control the nutrient conditions in the coastal area of the Meldorf Bight which are: local freshwater discharge and release of nutrients from the remineralisation process in the sediment.

In addition to the input of particulate organic material from the coastal North Sea and the Elbe estuary, the polder basin at the east and the sluice in the southern corner of the coast are supplementary sources of particulate and dissolved nutrients in the Meldorf Bight. Freshwater of the numerous streams which drain the hinterland is rich in inorganic nitrogen and phosphate. This influence, however, is locally restricted and found at the more coastal sites mainly in the south-eastern region of the bight. A major source is the polder basin in the eastern part of the bight. The basin receives the water from the agricultural sector in the northern area (40,000 ha) and also from the sewage plants of the main inland towns, such as Heide and Meldorf. The second minor source, a sluice, is located at the southern corner of the bight and receives the water from the southern agricultural marshland (5,000 ha) without any sewage influence. However, results have shown that freshwater discharge alone can not account for the high concentrations of ammonium and phosphate observed in the southern area. These elevated concentrations rather derive from the accumulation of muddy sediments and the extended saltmarsh at this site, which constitute an internal diffuse source of nutrients for the bight. During ebb tide, the local nutrient plumes may spread further into the bight and also affect the central area. This effect was well observed in this study.

High ammonium and phosphate levels also prevailed above the shallow muddy flats near the north eastern coast without any relationship to freshwater influence. This was the case in spring and even more in summer. During this time of year, the remineralisation rate is intensified due to higher temperatures and an increase in organic loads deriving from intensified autochthonous primary production and an elevated import of particulate organic matter from the adjacent coastal North Sea. The phosphate is temporally stored in oxic sediments in form of an insoluble iron-hydroxide-P-complex and will be released as soon as anoxic conditions in the subsurface sediment layers proliferate. This process usually occurs in late summer. High concentrations of ammonium and phosphate at the coastal grid stations observed especially in summer may thus not be a result of local freshwater discharge only, but may partly be due to this sedimentary process, whereas in spring, freshwater discharge constitutes a major factor for the nutrient situation in the coastal area of the bight.

5 Numerical modelling

5.1 Introduction

In this chapter the set-up, calibration and validation of the nutrient dynamics model for the study site is described. The basic equations for flow and nutrient dynamics including the main assumption and simplification of biological processes are introduced. The settings of the two modules are also presented. Preliminary results of the models are presented and comparisons between modelled and measured nutrient concentrations were made. Discrepancies were analysed and the main reasons for the discrepancies were identified.

5.2 Modelling system

The Delft3D Modelling System developed by Delft Hydraulics in The Netherlands was employed. In this study only the flow and nutrient dynamics modules were used. Coupling of the results between these two modules ensures the representation of the physical process as required by the nutrient dynamics simulations. A description of the modules for simulations of flow and nutrient dynamics, their basic concepts and formulations are summarised below. Further information on the modelling system can be found in the Delft3D User Manual (WL Delft Hydraulics, 2003 and 2003a).

5.2.1 Flow model

The flow model can simulate the non steady flow condition in two- and three-dimensions resulting from tidal and meteorological forcing. The flow model results can be coupled with the nutrient dynamics model for the study of transport and mixing of substances. The model can account for the effect of stratification due to vertical salinity and/or temperature differences as well as for flooding and drying of the tidal flat. Source and sink terms are also included to model the discharge and withdrawal of water. In this study, the two-dimensional depth-integrated model was employed.

Basic equations

The two-dimensional depth-integrated continuity equation is given by:

$$\frac{\partial h}{\partial t} + \frac{\partial}{\partial x}(h\bar{u}) + \frac{\partial}{\partial y}(h\bar{v}) = 0 \quad (5.1)$$

where h = local water depth, \bar{u} and \bar{v} = depth-integrated fluid velocities in x and y directions, respectively, and t = time. The two-dimensional momentum balance equation for fluid can be expressed as:

in the x direction:

$$\frac{\partial}{\partial t}(h\bar{u}) + \frac{\partial}{\partial x}(h\bar{u}\bar{u}) + \frac{\partial}{\partial y}(h\bar{u}\bar{v}) + gh\frac{\partial}{\partial x}(h + z_b) - k_x h \left[\frac{\partial^2 \bar{u}}{\partial x^2} + \frac{\partial^2 \bar{v}}{\partial y^2} \right] - \frac{\tau_{bx}}{\rho} - \sum \frac{F_x}{\rho} = 0 \quad (5.2)$$

and in the y direction:

$$\frac{\partial}{\partial t}(h\bar{v}) + \frac{\partial}{\partial x}(h\bar{v}\bar{u}) + \frac{\partial}{\partial y}(h\bar{v}\bar{v}) + gh\frac{\partial}{\partial y}(h + z_b) - k_y h \left[\frac{\partial^2 \bar{v}}{\partial x^2} + \frac{\partial^2 \bar{u}}{\partial y^2} \right] - \frac{\tau_{by}}{\rho} - \sum \frac{F_y}{\rho} = 0 \quad (5.3)$$

in which g = gravitational acceleration, z_b = bed level above reference datum, k_x and k_y = effective dispersion coefficients representing the integration effects, ρ = fluid density and F = external driving forces e.g. wind, waves, Coriolis effect.

The bed shear stresses are usually related to the depth-integrated velocities:

$$\tau_{bx} = \rho g \frac{\bar{u} \bar{v}_r}{C^2} \quad (5.4)$$

$$\tau_{by} = \rho g \frac{\bar{v} \bar{v}_r}{C^2} \quad (5.5)$$

with C = Chezy coefficient and \bar{v}_r being the velocity vector magnitude defined as:

$$\bar{v}_r = \sqrt{\bar{u}^2 + \bar{v}^2} \quad (5.6)$$

Numerical solving method

A significant number of numerical schemes have been proposed to solve the partial derivative equations. Delft3D Modelling System uses the Finite difference method to solve these equations on a rectilinear or curvilinear grid. In the Finite difference scheme, the numerical solution is obtained by replacing the differential equation by a finite difference approximation for the variables involved in the system. The fundamental procedure for the synthesis of finite differences scheme is derived from the known expansion of the Taylor series. The solution domain is approximated by a grid of uniformly spaced nodes. At each node, the governing differential equation is approximated by an algebraic expression which references adjacent grid points as the

forward, central and backward finite difference approximations. Selection of the finite difference approximation can be critical, which can influence the computed results and the stability of the solution techniques. In Delft3D-Flow, the central finite difference is employed for the discretization of the advection in the vertical direction. In the horizontal direction, the so called alternating direction implicit (ADI) method utilizing both the upwind and the central finite difference approximation along the streamline is implemented to solve for the advective terms.

Numerical solution techniques can be classified as explicit or implicit. An implicit scheme computes the new value at time $t + \Delta t$ based on the coupling to the previous value computed at time t by solving difference equations including the boundary conditions. The most widely used term in computation of unsteady flow modelling, however, is the explicit term in which the new value at time $t + \Delta t$ is computed from the old values at time t . The stability of the explicit method is subjected to the Courant number:

$$\Delta t \leq \frac{\Delta x}{c_d} \quad (5.7)$$

where Δt = time step, Δx = grid spacing and c_d = wave celerity.

Boundary conditions

The boundary conditions can be specified into closed and open boundaries. A closed boundary means the boundary along the natural contour of land-water interface. Opposite to the closed boundary, an open boundary means the part across the flow field where water can move in and out of the model domain. In the flow model, the condition of the boundary must be described. For the closed boundary, the velocities normal to the closed boundary are set to zero to avoid flow going through the boundary. For large scale simulations the influence of the shear stress along the closed boundary can usually be neglected. In contrast, for a small scale simulation such as in a laboratory flume, the side walls can have an influence on the flow. For this case, the partial slip boundary is introduced. For the open boundary, the water level, velocity, discharge or partially reflective boundary conditions, can be prescribed. The data to impose for the open boundary can be obtained from the measurements, tide tables or from nesting of a larger model. The open boundary should be located as far as possible from the area of interest to avoid model instability.

For the boundary condition at the sea bed, usually the bed shear stress which can be combined with the effect of flow and wave is specified. As well as for the boundary at the free surface, the wind induced shear stress is taken into account. If there is no wind, the stress at the free surface is usually set to be zero.

Turbulence closure

The turbulence closure problem concerns the representation of the turbulent shear stress. The turbulence closure equations provide an estimate of the eddy coefficients to be used in the momentum and mass transport equations. Distinguished by the number of equations, the formulations are classified as zero-, one- and two order equations and

higher order methods. In the zero equation model, the closure term does not include a separate transport equation for turbulent energy. Therefore, the values of eddy coefficients must be specified or computed assuming that the dominant forces resulting in the production and dissipation of turbulent mixing are in equilibrium (Bedford, 1985). This is known as the algebraic equation. In the one equation model, the eddy coefficient is related to a turbulent kinetic energy and a length scale (Kolmogorov, 1942 and Prandtl, 1945). The equation is also known as the $k-l$ model. In this one equation model, the turbulence closure includes a separate transport equation for the kinetic energy density of the velocity fluctuations in three dimensions. The two equation turbulence closure models determine the length scale by introducing an additional equation which can compute the transport of turbulent energy and also its dissipation rate. The so called $k-\varepsilon$ turbulence-closure model is applied. For estuarine conditions where it is difficult to define a primary flow direction, this variable is normally ignored and the transverse and longitudinal eddy viscosities are set the same. In this study, an algebraic approach for the turbulence closure using a constant eddy viscosity in space and in time was considered.

Drying and flooding

The drying and flooding processes are taken into account in the computation of the flow model by removing grid points from the flow domain that become dry when the water level falls at low tide and by adding grid points that become wet when the tide rises. Dry cells are grid cells in which the bottom level is higher than the instantaneous water level. During each time step, the model determines if a cell is either included or excluded from the hydrodynamic computation. The criterion is based on the specification of the threshold depth (WL Delft Hydraulics, 2003a). When the total water depth is larger than the user-specified threshold depth, the cell is included in the hydrodynamic computation. If the total water depth becomes smaller than half the threshold depth, the cell is set dry. The definition of the flooding threshold to be twice as large as the drying threshold prevents changes of the cell's state in consecutive time steps.

5.2.2 Nutrient dynamics model

The nutrient dynamics module has been developed for the simulation of primary production including growth and mortality of algae taking into account the controlling biological and chemical processes. The module considers the dynamics and limitation of inorganic and organic nutrients, dissolved oxygen concentration and biochemical oxygen demand, suspended matter, temperature, salinity, light availability and phytoplankton composition.

The model equations can be formulated in two-and three-dimensions. In this study, the two-dimensional depth-integrated set of equations was used. The calculation of the equations takes the flow field obtained from the depth-averaged flow model, which has been set-up based on the assumption of a shallow water, incompressible flow and the total slip conditions, into consideration. Results on tidal flow conditions from the flow model are used in the nutrient dynamics model as the flow background for the calculation of transport and distribution of nutrients.

Basic equations

The two-dimensional nutrient dynamics model simulates the transport of the modelled substances by solving the advection–diffusion equation numerically. The advection–diffusion equation of the two-dimensional depth-integrated model can be written as:

$$\frac{\partial C}{\partial t} = \frac{\partial}{\partial x} \left(D_x \frac{\partial C}{\partial x} - \bar{u} C \right) + \frac{\partial}{\partial y} \left(D_y \frac{\partial C}{\partial y} - \bar{v} C \right) + S + f_R(C, t) \quad (5.8)$$

where C = concentration, D_x and D_y = dispersion coefficient in x and y directions, \bar{u} and \bar{v} = depth-integrated fluid velocities in x and y directions, S = additional inflows and $f_R(C, t)$ = reaction terms or processes which are described in terms of concentration and time.

The discharge term, S , is the additional discharge which is usually applied for a release of a small river or sewage plant. The reaction term, $f_R(C, t)$ is comprised both physical and biochemical reactions or processes. The description of the processes is described in the following sections.

Coupling of hydrodynamic data

The flow and nutrient dynamics models are separated modules. The nutrient dynamics model needs the flow conditions as a basis of transport calculations. Therefore, the hydrodynamic results from the flow module are continuously transferred to the nutrient module and used for further calculations for the distribution of nutrient concentrations.

Boundary conditions

The solution of the advection-diffusion equation requires the specification of concentration of the modelled substances along the open and closed (coastline) model boundaries. Along the open boundaries measured values are usually specified whereas along the coastline zero concentrations are imposed. The bottom boundary conditions are defined by the sedimentary processes. Surface boundary conditions are usually related to the atmospheric input. In a small study area, nutrient inputs from the atmosphere (wet deposition of nitrogen) are not of importance and therefore neglected.

Time step

The time step for the nutrient dynamics modelling is not restricted by the Courant number but by the stability reason of the numerical model (Rajar and Cetina, 1997). It is recommended to use the same time step as the hydrodynamic database to avoid interpolation.

Sources and sinks

Sources and sinks are known as the forcing function in the nutrient dynamics model as referred to the additional discharge S and the reaction term $f_R(C, t)$ in Eq. 5.8. The model takes into account the possible sources and sinks and then computes the changes to

the modelled substances. Important sources and sinks can be categorised into two groups, water mass and biochemical processes. The former is related to external forcing due to additional inflow (S). This flow may contain considerable amounts of nutrients and therefore impact the system. For the biological processes, concentrations of modelled substances are subjected to internal transformation such as phase transfer due to degradation or production processes ($f_R(C,t)$). The model only takes into account the changes and re-computes the total budget, but no new substance is formed.

Transformation of substances is mainly derived from the stoichiometry and molecular formula. Quantity of sources and sinks is defined as the zero-, first- and second- order approaches. A zero-order reaction means that the rate of change is constant in time while the first- and second- orders are dependent functions which take into account one and two parameters, respectively. Due to difficulties of non-linear relationships of the second-order approach, zero-and first-orders are commonly used.

Solution approaches

Two approaches based on the degree of sophistication of the modelling process can be adopted, i.e., DYNAMO and BLOOM approaches. In the DYNAMO approach, the primary production process is simplified and only two groups of algae are included. In this approach the two groups of algae considered are diatoms and non-diatoms (also referred as Greens). The main difference is that diatoms utilise silica as an essential nutrient in contrast to non-diatoms. A linear relationship is applied to all process parameters and only zero and first-order approaches are used in DYNAMO. The BLOOM approach is a more sophisticated one which accounts for the growth of algae including resources and growth limiting factors. Because the focus of the present investigation is not on algal bloom formation, the DYNAMO approach was used throughout this study.

Main assumptions

For the nutrient dynamics modelling, the following assumptions were made.

- In the water column, nutrients can be in the form of dissolved inorganic components (NO_3 , NH_4 , and PO_4), detritus components (DetN and DetP) and non-detritus organic components (OON and OOP). Parts of the nutrients are also incorporated in the algae and phosphorus can be adsorbed to particulate inorganic matter (AAP).
- In the bottom sediment, there are no dissolved nutrients. Nutrients can be in the form of detritus components and non-detritus organic components. Some nutrients are also incorporated in the algae at the bottom and phosphorus can be adsorbed to inorganic matter.
- Nutrients can be recycled for an infinite number of times without any losses other than those due to transport, chemical adsorption, denitrification and burial.

Processes

Processes including nitrification, denitrification, mineralisation, sedimentation, resuspension, burial and digging of nutrients in organic matter are accounted for in the modelling system. Since this study consider only the typical specific processes which

dominate in the area of investigation together with the measured results obtained during the field measurements, only denitrification of nitrate in sediment and the remineralisation of organic matter to ammonium and phosphate in the sediment were considered. Usually a critical temperature is defined to identify the computational process equations between zero- and first- order schemes. Descriptions of the selected processes are given as follows.

- **Denitrification in sediment**

Denitrification is the anaerobic bacterial process which transforms nitrate to nitrogen gas which leaves the system. It is sometimes referred to as 'dissimilatory' nitrate reduction because it occurs in association with the decomposition of organic matter. Denitrification can be described by the following reaction:



The sediment is usually anoxic below a certain depth. Therefore denitrification in the Wadden Sea sediments is more important than denitrification in the water column. In the model, denitrification in the sediment is solely orientated to nitrate removal from the water column. No oxygen is produced and no H^+ is removed. Computations of the denitrification flux depend on nitrate concentration in the water column and water temperature. Below a critical temperature, denitrification rate is low, the flux equals a user-specified constant (zero-order). Above the critical temperature the process is modelled as the sum of a constant and a function of the first order term which is corrected for temperature that stimulates the process rapidly. According to the well mixed of flow conditions in the study area, nitrate concentration is found to have no stratification and uniformly distributed along the vertical profile. Therefore, the depth-averaged concentrations of nitrate are used in the computations.

- **Mineralisation**

The decomposition of organic matter is referred to the process of mineralisation. This mineralisation process can take place in the water column and in the bottom sediment. Organic matter is first oxidised by molecular oxygen, final products of the reaction are carbon dioxide and nutrients. Nutrients deriving from remineralisation in the sediment are released from the pore water to the overlying water column. Computation of the mineralisation flux is temperature dependent. Below a critical temperature, the mineralisation flux is a user-defined constant. Above the critical temperature, the mineralisation flux is the sum of a constant and a first order equation which is the temperature dependent function. The specified critical temperature can have different values for the mineralisation in the water column and in the sediment.

Process equations and mass balance

The nutrient dynamics model calculates the total budget of the substances based on the mass balance equation. The process equations are introduced for the substances that are not conserved. The typical cycles of nitrogen and phosphorus are considered and the processes are simplified to a linear relationship. The substances are subjected to change by the process applied and the calculation is made using the basic critical factors such as

temperature or oxygen concentration, resulting in simplified cycles of nitrogen and phosphorus. The process equations used in the model are presented.

- **Nitrogen cycle**

Nitrogen is the most abundant gas comprising 78.084% by volume of the atmosphere. It is an essential nutrient for all organisms, but it only can be converted to protein by certain blue-green algae and bacteria that fix atmospheric nitrogen or by plants that use nitrate or ammonium for protein synthesis. In the model, the nitrogen cycle considers the following model variables in the water column and in the sediment.

In the water column, the model variables are ammonium (NH_4), nitrate (NO_3), nitrogen in non-diatom (Green), nitrogen in diatoms (Diat), in suspended detritus (DetN) and other organic nitrogen (OON). In this study all kinds of organic nitrogen are summarised as one pool of other organic nitrogen (OON).

The total nitrogen (TOTN) budget in the water column can be calculated as the sum of the following model variables:

$$\text{TOTN} = \text{NH}_4 + \text{NO}_3 + \text{Green (N)} + \text{Diat (N)} + \text{DetN} + \text{OON} \quad (5.10)$$

The mass balance for total nitrogen in the water column can be written as:

$$\frac{d\text{TOTN}}{dt} = \text{resuspension} + \text{mineralisation} - \text{sedimentation} - \text{denitrification} \quad (5.11)$$

In this study, only NH_4 , NO_3 , OON, **mineralisation** and **denitrification** processes are considered.

In the bottom sediment, the model variables are nitrogen in diatoms (Diat), nitrogen in non-diatoms (Green), bottom detritus (DetN) and other organic nitrogen (OON). The pool of all organic nitrogen considered in this study is described as one pool of other organic nitrogen (OON). The total nitrogen (BotN) budget can be calculated as the sum of the following model variables:

$$\text{BotN} = \text{Green (N)} + \text{Diat (N)} + \text{DetN} + \text{OON} \quad (5.12)$$

The mass balance for total nitrogen in the sediment can be written as:

$$\frac{d\text{BotN}}{dt} = \text{sedimentation} - \text{mineralisation} - \text{mortality} - \text{resuspension} - \text{burial} + \text{digging} \quad (5.13)$$

In this study, only OON and **mineralisation** processes are considered.

- **Phosphorus cycle**

The phosphorus cycle is a simplified version of the nitrogen cycle. There is only one dissolved pool and only one removal process. Inorganic phosphorus can be presented as dissolved ortho-phosphate (PO_4) or can be reversibly adsorbed to inorganic matter. The adsorbed form of PO_4 is modelled explicitly and is called inorganic adsorbed phosphorus (AAP). This is a different approach from the adsorption of micro-pollutants, which are adsorbed to both inorganic and organic substances. In the model, the phosphorus cycle considers the model variables both in the water column and in the sediment.

In the water column, model variables are ortho-phosphate (PO_4), phosphorus in algae (Green), phosphorus in diatom (Diat), in suspended detritus (DetP), other organic phosphorus (OOP), and inorganic adsorbed phosphorus (AAP). In this study all kinds of organic phosphorus are summarised as one pool of other organic phosphorus (OOP).

In the water column, the total phosphorus (TOTP) budget can be calculated as the sum of following model variables:

$$\text{TOTP} = \text{PO}_4 + \text{Green (P)} + \text{Diat (P)} + \text{DetN} + \text{OOP} + \text{AAP} \quad (5.14)$$

The mass balance for total phosphorus in the water column can be written as:

$$\frac{dTOTP}{dt} = \text{resuspension} + \text{mineralisation} - \text{sedimentation} \quad (5.15)$$

In this study, only **PO₄**, **OOP** and **mineralisation** processes are considered.

In the bottom sediment, model variables are phosphorus in diatoms (Diat), phosphorus in algae (Green), bottom detritus (DetP), other organic phosphorus (OOP) and bottom inorganic adsorbed phosphorus (AAP). The organic pool is summarised as one pool of other organic phosphorus (OOP) in this study. The total phosphorus (BotP) budget can be calculated as the sum of following model variables:

$$\text{BotP} = \text{Green (P)} + \text{Diat (P)} + \text{DetP} + \text{OOP} + \text{AAP} \quad (5.16)$$

The mass balance for total phosphorus in the sediment can be written as:

$$\frac{dBotP}{dt} = \text{sedimentation} - \text{mineralisation} - \text{resuspension} - \text{burial} + \text{digging} \quad (5.17)$$

In this study, only **OOP** and **mineralisation** processes are considered.

5.3 Meldorf Bight Model

In this section, the set-up, sensitivity studies, calibration and validation of the flow and nutrient dynamics models for the Meldorf Bight are presented. The model has been set-up

within the DELFT3D Modelling System, developed by Delft Hydraulic, The Netherlands. In this study only the flow and nutrient dynamics models were employed.

5.3.1 Model domain, grid and bathymetry

The Meldorf Bight Flow model developed by Corelab, University of Kiel, Germany (Palacio et. al., 2001, Mayerle and Palacio, 2002) was adopted in this study. The model domain covers an area of about 280km² which includes the two major tidal channels (Norderpiep and Suederpiep) and the adjacent tidal flats. These two tidal channels intersect within the Bight and from the main Piep channel system. The grid was defined in the previous study on the basis of the sensitivity studies (Palacio et. al., 2001). A curvilinear grid consisting of about 21,000 cells adjusted to the bathymetry with spacing ranging from 50m to 120m has been used.

The bathymetry used to set-up the Meldorf Bight flow model was obtained from measurements in 1998 by the Federal Maritime and Hydrographic Agency (BSH) in Hamburg, Germany. In the tidal flat regions the bathymetry was obtained from the bathymetrical maps of 1990 from the Office of the Rural Development in Husum, Germany. The grid and bathymetry used in this study are shown in Figure 5.1. The deepest part at the middle of the Piep intertidal channel ranges up to 25m and about half of the area falls dry at low water conditions.

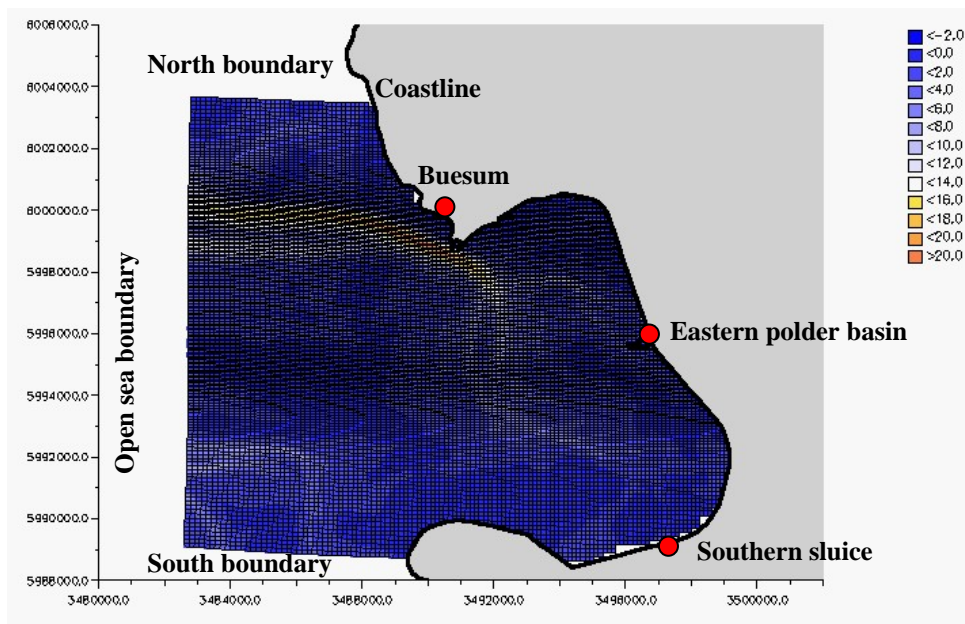


Figure 5.1: Grid and bathymetry of the Meldorf Bight model

5.3.2 Model dimensions

Due to a strong tidal mixing, the flow is well mixed and no stratification occurs. Therefore, the simulations were carried out with the two-dimensional depth-integrated approach for the period of interest (Palacio et al., 2001). The analysis focuses on the flow processes of the tidal channel in which the influence of wind and wave are less important and were not taken into account.

5.3.3 Tidal flow model

An extensive investigation on the open sea boundary conditions led to several approaches such as the application of measured water levels, the application of astronomical constituents and the application of the results of a large scale model nesting covering the entire continental shelf area. In the present study, the astronomical constituents were imposed at the open sea boundaries of the Meldorf Bight model. This is acceptable since the measurements were made under calm weather conditions in which the astronomical effects are predominant.

5.3.3.1 Model set-up

The details of the model set-up are referred to Palacio et. al. (2001). The initial velocity field was taken to be zero and the water surface elevation was set-up to zero elevation relative to the mean sea level. To avoid the effects of artificial values on the computational results, a sufficient warming-up period of about 48 hours was applied to obtain a steady state. Physical parameters such as gravity acceleration, water density, temperature and salinity were defined.

5.3.3.2 Sensitivity studies

The effect of time step, grid spacing, eddy viscosity, wind conditions, bottom roughness, morphology and approaches for prescribing the open sea boundary conditions on water levels and flow velocities at several locations were investigated (Palacio et. al., 2001). The investigations were carried out by comparing computed water levels and velocities obtained by changing the model settings and parameters. The results lead to the main model settings in terms of time step (0.5 min), eddy viscosity (constant in time and space: $1\text{m}^2/\text{s}$). A grid with a resolution of 60-180m was found to be adequate for the model domain.

5.3.3.3 Model calibration

After the main model settings were obtained from the sensitivity studies, the Meldorf Bight flow model was calibrated. This was done by changing the bathymetry and bed roughness using extensive field measurement data. The influence of bathymetrical changes and the influence of bed roughness, including the temporal and spatial variability of the equivalent bed roughness, were studied. The model results in terms of water levels, depth-integrated velocities and flow discharges over the cross-section were compared with the measurements and a good agreement was obtained.

5.3.3.4 Model validation

The validation of the Meldorf Bight Model has been made on the basis of short term simulations of about one day for the reproduction of flow velocities for spring and neap tides and long term simulations of about two months for the determination of tidal constituents. The model was verified with the measured data. It was found that it is

capable of capturing water levels and currents in good agreement with observations. The reproduction of tidal constituents is well achieved. RMS-error of the discrepancies of the depth-integrated velocities between the field measurements and model results of 0.19m/s was obtained.

5.3.4 Nutrient dynamics model

A two-dimensional depth integrated set of equations was considered. The solution of the equations uses the flow field obtained from the tidal flow model. Simulations begin with the flow model and are carried out for the entire period. The results in terms of current velocities and water levels are then transferred to the nutrient dynamics model.

Simulations were assigned for the analysis of dissolved inorganic nutrient distributions for three periods in winter, spring and summer 2002. Simulation was first done for winter nutrient distributions by assuming a conservative behaviour of nutrients, because during this season biological processes are not significant. Effects of sediment remineralisation, denitrification and of local discharges along the coastline have only minor influence on the nutrient distributions and transports during this time. This can be accepted since the temperature during winter is very low and all related agricultural and biological activities are at minimum. In the first stage, this assumption was also applied for the simulations in spring and summer. Preliminary results were obtained and discrepancies between model and measurement results show clearly the need to calibrate the model with the dominant processes. Therefore the importance of the chemical and physical processes in spring and summer was analysed and applied in the calibration. Details of model settings are described in the following sections.

5.3.4.1 Model set-up

Flow conditions obtained from the tidal flow model during the periods of interest were transferred to the nutrient dynamics module for further calculation of the nutrient distribution. These are velocities, water elevations, density, salinity, vertical eddy viscosity and vertical eddy diffusivity. Further settings are described as below.

Substances

Modelled substances are nitrate, ammonium and phosphate. In the first stage of simulations, no process was selected. The substances were assumed to be conservative. The model computed the distributions of the selected substances according to the transport of the nutrient concentrations from the open sea boundaries. Discrepancies between the computed and the measured nutrient concentrations were later analysed and the major sources and sinks responsible for the discrepancies were identified. The calibration strategy was designed to incorporate these major sinks and sources into the model. Details are discussed in the calibration process.

Boundary conditions

Concentrations of all substances are prescribed at the open boundaries of the model. Zero concentration is applied at the closed boundary. In this study, the range of constants based

on mean absolute deviations of the measured nutrient concentrations were used (Falconer and Lin, 1997). For the initial setting, no bottom boundary conditions were specified. The input of the nutrients from the atmosphere was found to be insignificant and therefore disregarded (Drago et. al., 2001).

Initial conditions and physical parameters

Initial conditions are concentrations of all substances at the start of the calculation. The importance of initial conditions depends on the length of the simulation in relation to retention time and boundary conditions. Retention time is the average time that a molecule of water remains in a water body. In this study the initial conditions of all substances were set as zero concentration. Simulations were run until steady state fields were reached and the effect of initial conditions disappeared. A sufficient time of about 2 days was found to be necessary. Physical parameters such as temperature and salinity were set-up based on the physical conditions of the study area during the period of interest. Constant values in time and space were considered throughout this study.

5.3.4.2 Sensitivity studies

Sensitivity analysis was made in order to study the effect of certain parameters on the computed results. The parameters were systematically varied based on the initial given default or general values and the results in terms of computed concentrations at Buesum Mole were compared with the standard runs, which were simulated without the process to be tested. Results of computed nutrient concentrations were plotted against the water level to see the effect over the tidal cycle at Buesum Mole. In this study, the effect of the dispersion coefficient, time step, open sea boundary conditions, denitrification rate and remineralisation rates were investigated as discussed in the following sections.

Effect of time step

Time steps of 5, 15 and 30 minutes were considered in the simulations. The time step for the nutrient dynamics modelling is not restricted by the Courant number but by the stability reason of the numerical model (Rajar and Cetina, 1997). It is recommended to use the same time step as the hydrodynamic database to avoid interpolation. Results are presented in Figures 5.2-5.4 for nitrate, ammonium and phosphate, respectively. It is found that the concentrations produced during high water are rather similar. During low water, the smaller time step produced slightly lower concentration values compared to the concentrations obtained by considering a higher time step. In this study, a time step of 30 minutes was selected and used for further simulations.

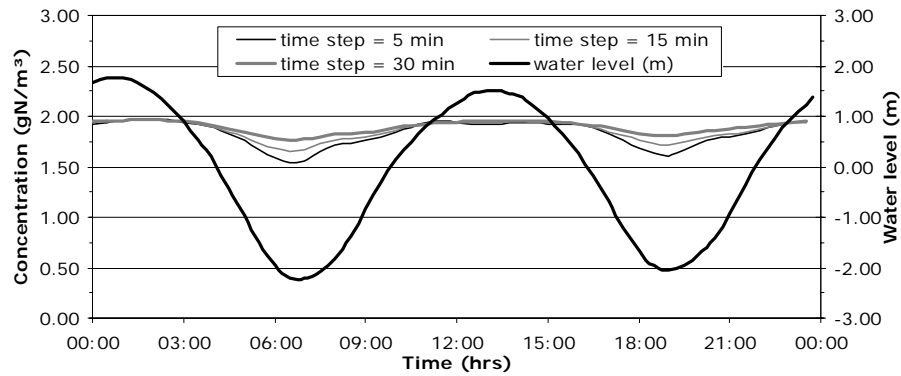


Figure 5.2: Effect of time step on NO_3 concentrations

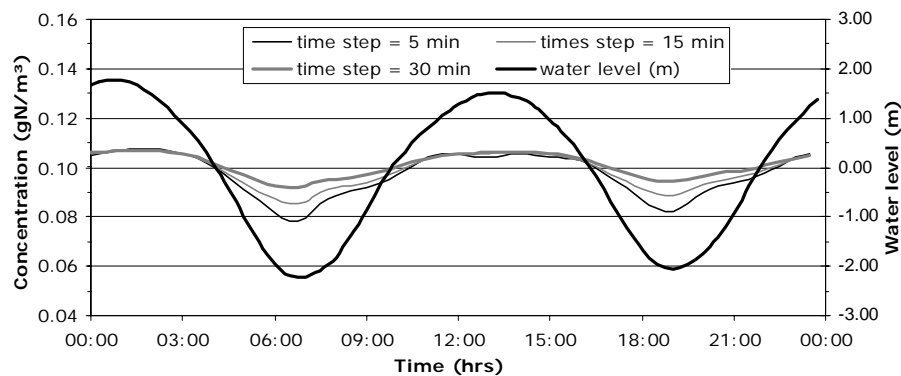


Figure 5.3: Effect of time step on NH_4 concentrations at Buesum Mole

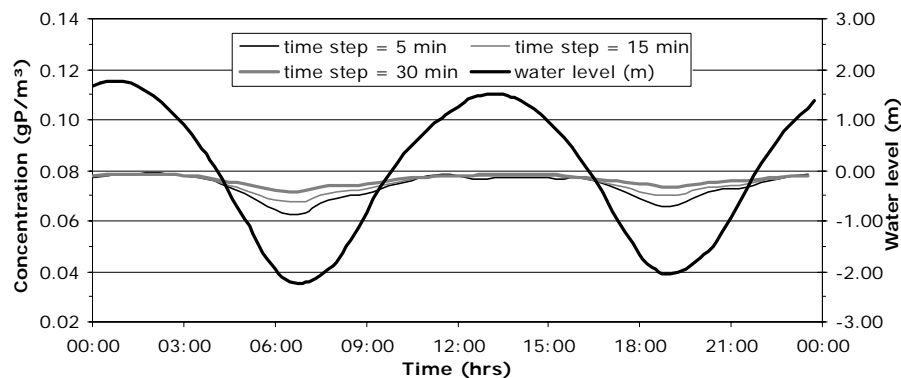


Figure 5.4: Effect of time step on PO_4 concentrations

Effect of the open sea boundary conditions

Concentrations of the considered substances have to be specified at the open boundaries of the model grid. In this case, the mean concentration was applied as a constant value in time and space at the open sea boundaries. Together with its standard deviation, the upper and lower mean boundary conditions were also specified as a constant. Computed concentrations based on three different boundary conditions are shown in Figures 5.5-5.7 for nitrate, ammonium and phosphate, respectively. It is found that the range of the constant nutrient concentrations applied at the open boundary is significantly related to the concentrations produced by the model. For each open boundary value, the simulations

produced rather uniform concentrations which slightly fluctuated with the water level. Selection of appropriate boundary conditions is discussed in section 5.3.4.3.

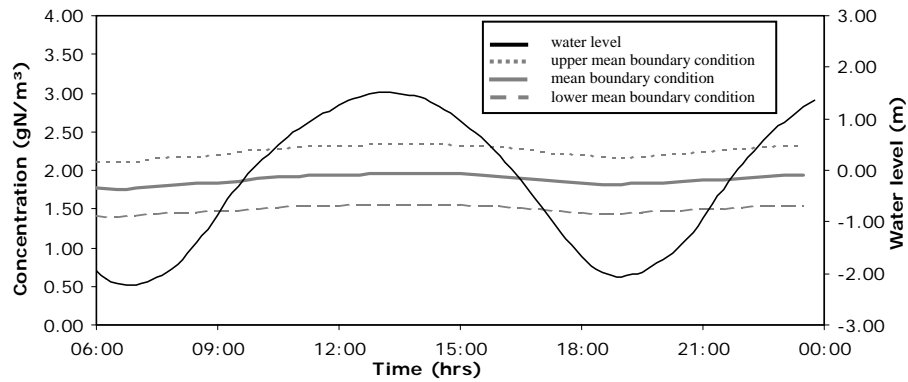


Figure 5.5: Effect of the open boundary on NO_3 concentrations

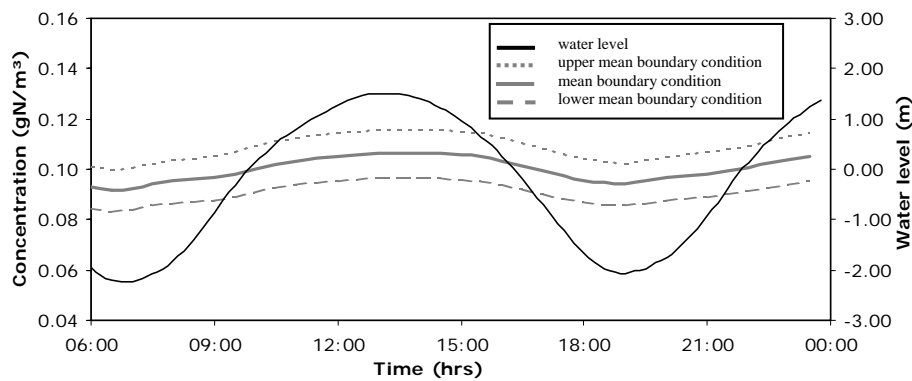


Figure 5.6: Effect of the open boundary on NH_4 concentrations

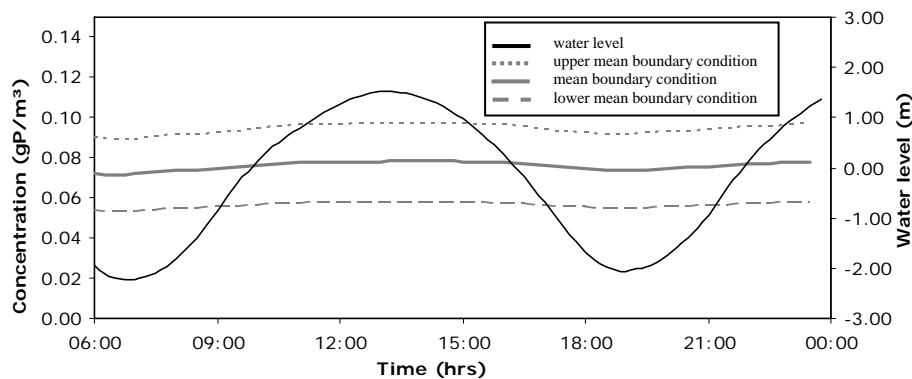


Figure 5.7: Effect of the open boundary on PO_4 concentrations

Effect of the dispersion coefficient

The effect of the dispersion coefficient on the concentrations of nutrients was investigated. Simulations were carried out considering three different uniform dispersion coefficients. These consider between the recommended value $1\text{m}^2/\text{s}$ and the values of 10 and $20\text{m}^2/\text{s}$. The simulation results are shown in Figures 5.8-5.10 for nitrate, ammonium and phosphate respectively. It can be seen that the dispersion coefficients have

insignificant influence on the computed nutrient concentrations with relatively small discrepancies during low water. A recommended uniform dispersion coefficient of $1\text{m}^2/\text{s}$ was selected throughout this study (see DELFT3D-WAQ, User Manual, 2003).

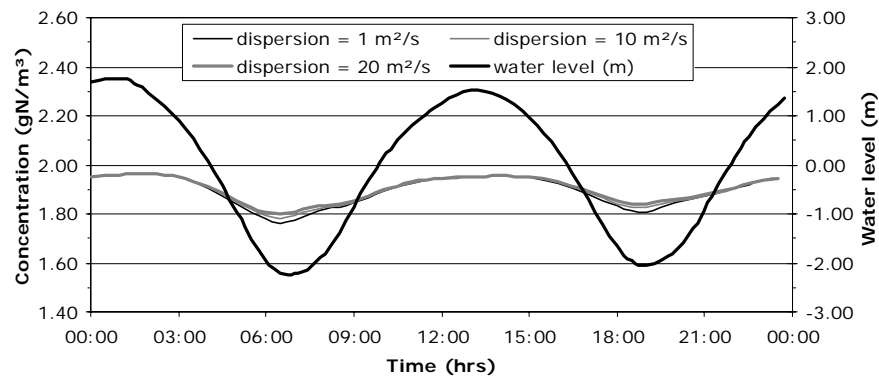


Figure 5.8: Effect of the dispersion coefficients on NO_3 concentrations

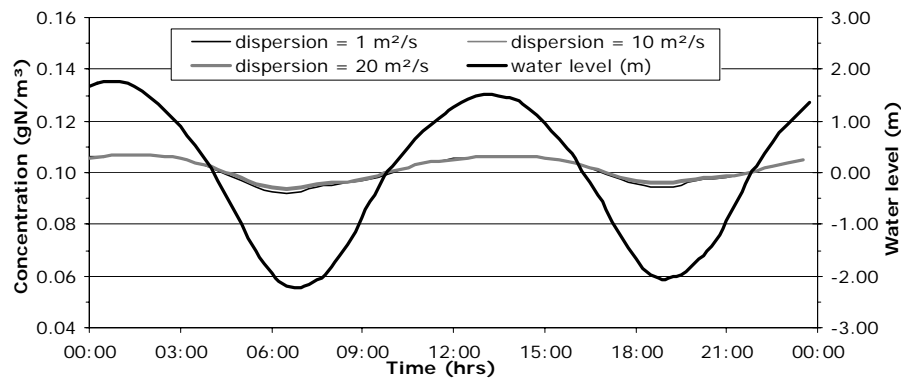


Figure 5.9: Effect of the dispersion coefficients on NH_4 concentrations

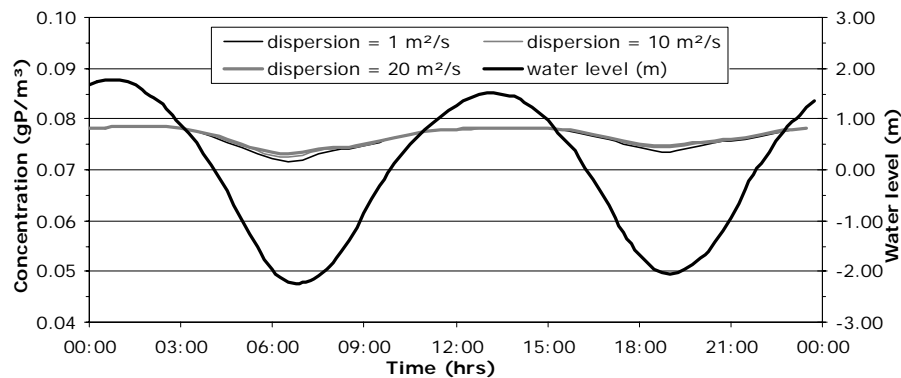


Figure 5.10: Effect of the dispersion coefficients on PO_4 concentrations

Effect of denitrification rate

The denitrification process removes nitrate from the system. A simplified form of the equation is as follows. If the temperature is below a critical value, then a constant flux for denitrification is applied. For values above this limit a temperature dependent function with a specified denitrification rate is considered. Denitrification rate is the specific coefficient at a specific temperature (20°C) determined in the laboratory (see DELFT3D-WAQ, User Manual, 2003). In this study different values for the denitrification rate were

considered. The results of the simulation in terms of nitrate concentrations at Buesum Mole are shown in Figure 5.11. Higher denitrification rates lead to a distinct reduction in nitrate concentrations. For values of the order of 0.01d^{-1} only minor differences with the standard run resulted. In this study the default value of 0.1d^{-1} (see DELFT3D-WAQ. User Manual, 2003) was applied for the calculation of the denitrification process.

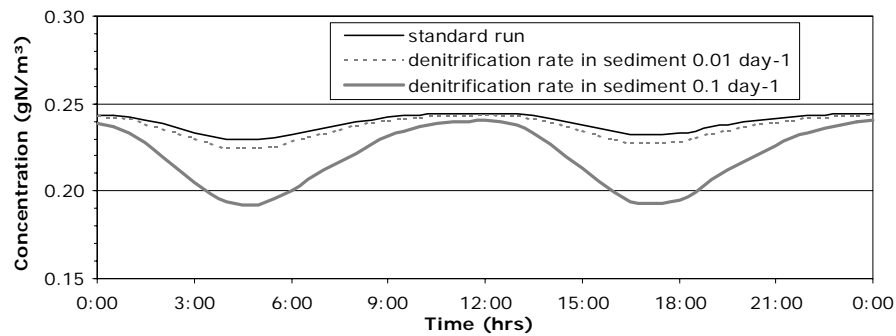


Figure 5.11: Effect of the denitrification rate on NO_3 concentrations

Effect of the phosphate remineralisation rate in the sediment

Remineralisation is a slow process when compared to the effects of transport and dispersion. A simplified equation of the nutrient dynamics model uses the critical temperature to identify the computational functions. Remineralisation rate is tested here by modelling phosphate concentration with remineralisation rate values equal to 1d^{-1} and 10d^{-1} . Results were compared with the standard run (Figure 5.12). It is found that higher remineralisation rates tend to increase the computed phosphate concentrations. The process occurs slowly as the rates applied produced only a minor difference.

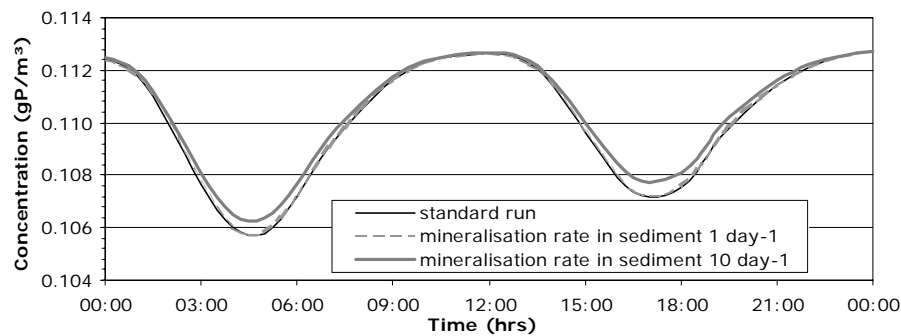


Figure 5.12: Effect of the remineralisation on PO_4 concentrations

5.3.4.3 Selection of open sea boundary conditions

The solution of the advection-diffusion equation requires the specification of concentration of the modelled substances along the model boundaries. Along the open boundaries measured values are usually specified whereas along the coastline zero values of concentrations are imposed. The measured concentrations are usually scattered due to various physical and biochemical conditions (see section 4.3.2 to 4.3.4: Ship stationary measurements at the open boundary of the study area). Therefore, an appropriate value must be selected to prevent disturbance from the scattering on the computed results. In

this study the mean absolute deviations were used to define the boundary conditions. The simulations were performed by applying the measured nutrient concentrations as a constant value at the model boundaries. By considering the mean value and its standard deviation, the mean, upper and lower mean boundary conditions were defined.

Preliminary model settings were obtained based on the assumption of conservative behaviour of nutrient dynamics; no biological processes were applied in the model. Therefore, simulation results represent only the distribution of nutrients from the open sea boundary without disturbance of any biochemical processes. Averaged discrepancies at all grid stations in the study area were considered. Details of comparison results with mean absolute deviation boundary conditions are shown in Appendix B. The boundary conditions which give the minimum discrepancies will be selected and will be used for further studies on the calibration and validation of the model.

Winter distribution

Table 5.1 shows the averaged discrepancies of the simulation results with different boundary conditions compared with the in-situ measurements of all grid stations. It is found that by using the mean absolute deviations at the open boundaries, the simulation results could cover the scattered range of the nutrients in the field. Considering nitrate and ammonium concentrations of the grid measurements, the upper mean and mean standard deviations applied at the open boundaries were appropriate to simulate the nutrient distributions with minimum discrepancies of 10.44% and 14.30% respectively. In the case of phosphate, the lower mean standard deviation applied at the open boundaries was appropriate to simulate the nutrient distributions with the minimum discrepancies of 16.30%. Some discrepancies were observed at grid stations G4, G5 and G6 at which the measurements indicated rather high concentrations for all substances (Figures 5.13-5.15).

Table 5.1: Selection of boundary condition for the nutrient simulation in winter

Substances	Measured boundary condition		Range of boundary condition			Comparison with in-situ measurements		
	Mean	SD	Lower	Mean	Upper	Lower	Mean	Upper
	g/m ³	g/m ³	g/m ³	g/m ³	g/m ³	Discrepancies = $\frac{\text{Model} - \text{Measured}}{\text{Measured}}$ (%)		
Nitrate	1.906	0.267	1.639	1.906	2.173	32.24	21.20	10.44
Ammonium	0.112	0.013	0.099	0.112	0.125	15.39	14.30	17.43
Phosphate	0.084	0.011	0.073	0.084	0.095	16.30	28.24	43.62

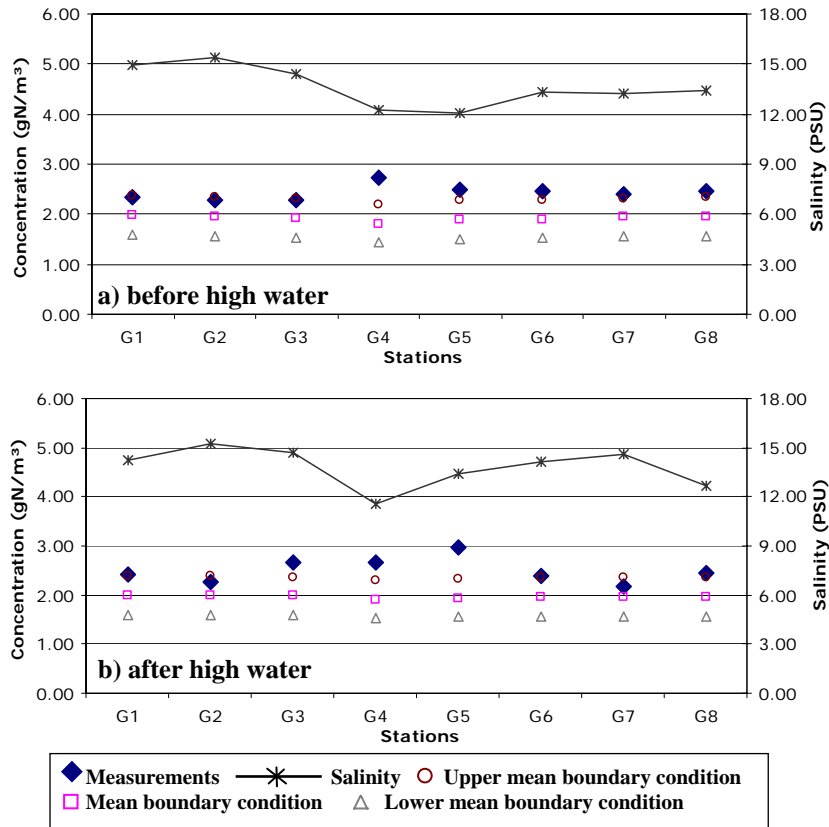


Figure 5.13: Comparison of measured and computed NO_3 concentrations before high water (a) and after high water (b) in winter 2002

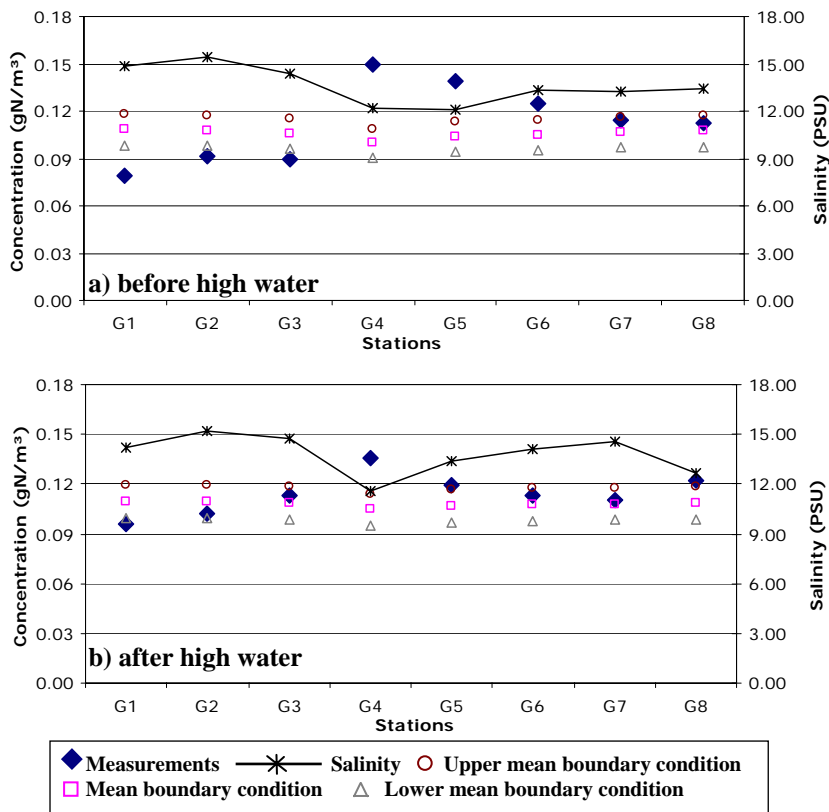


Figure 5.14: Comparison of measured and computed NH_4 concentrations before high water (a) and after high water (b) in winter 2002

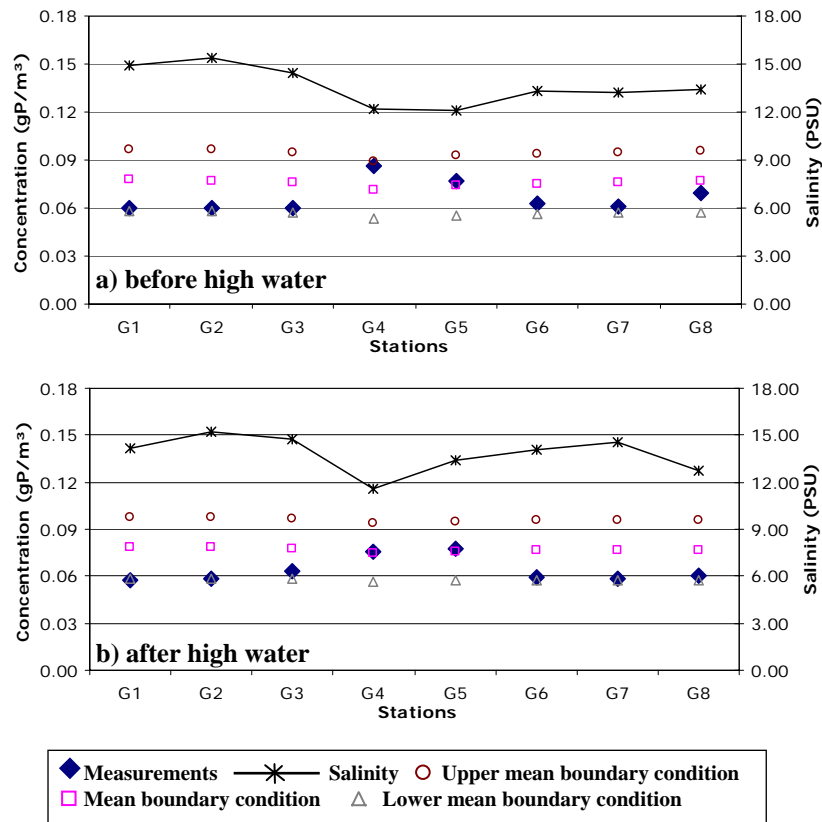


Figure 5.15: Comparison of measured and computed PO_4 concentrations before high water (a) and after high water (b) in winter 2002

Spring distribution

Simulation results revealed the capability of the model to simulate the spring distributions of nutrients in the area. By using the mean absolute deviations at the open boundaries, the simulation results appear to cover the scattered range of the nutrients in the field. Comparison of results with the in-situ measurements shows an agreement between the model and measured data. It is found that the upper mean standard deviations applied at the open boundaries were appropriate to simulate the nutrient concentrations with averaged discrepancies of 11.05%, 47.29%, and 32.50% for nitrate, ammonium and phosphate respectively (Table 5.2). High discrepancies were found coinciding with the indication of low salinity at some stations. Figures 5.16-5.18 show the simulated results of nitrate, ammonium and phosphate with different boundary conditions in spring.

Table 5.2: Selection of boundary condition for the nutrient simulation in spring

Substances	Measured boundary condition		Range of boundary condition			Comparison with in-situ measurements		
	Mean	SD	Lower	Mean	Upper	Lower	Mean	Upper
	g/m^3	g/m^3	g/m^3	g/m^3	g/m^3	Discrepancies = $\frac{\text{Model} - \text{Measured}}{\text{Measured}}$ (%)		
Nitrate	0.728	0.064	0.664	0.728	0.792	19.49	12.97	11.05
Ammonium	0.007	0.004	0.003	0.007	0.011	83.97	62.59	47.29
Phosphate	0.027	0.006	0.021	0.027	0.033	53.34	40.01	32.50

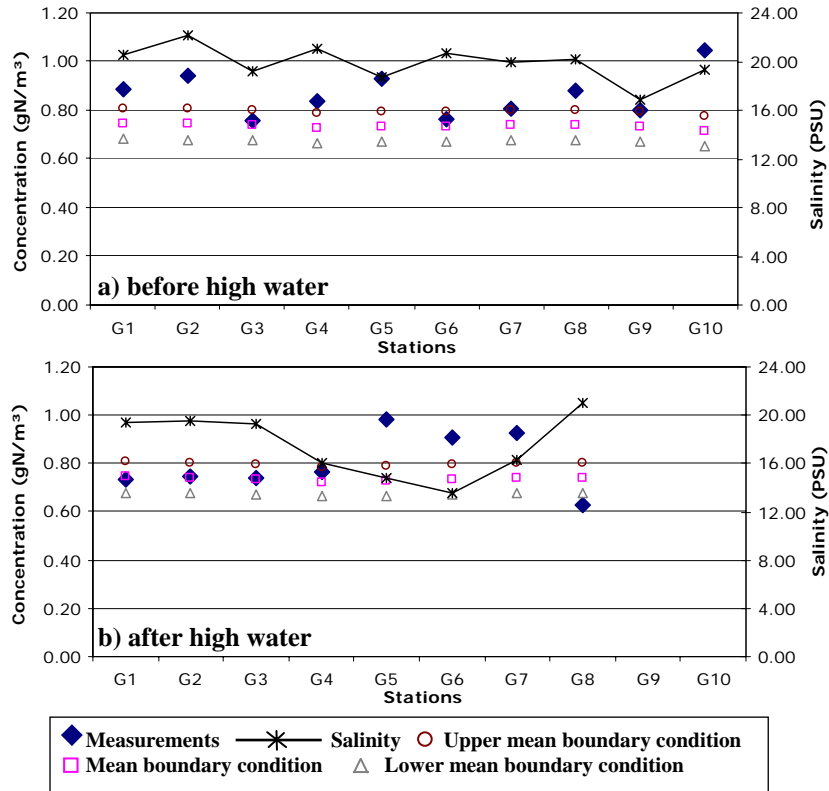


Figure 5.16: Comparison of measured and computed NO_3 concentrations before high water (a) and after high water (b) in spring 2002

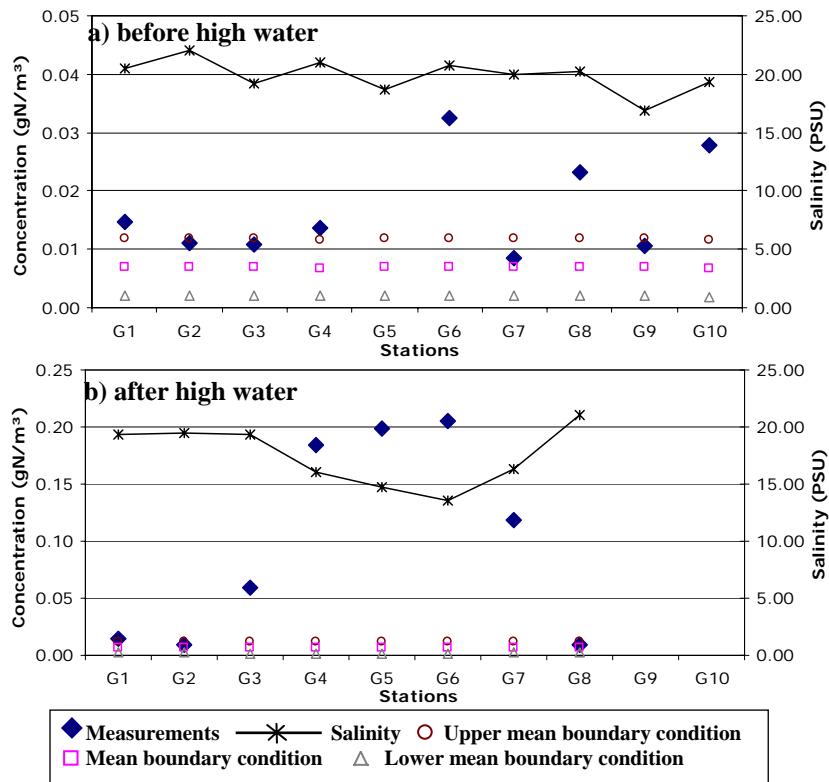


Figure 5.17: Comparison of measured and computed NH_4 concentrations before high water (a) and after high water (b) in spring 2002

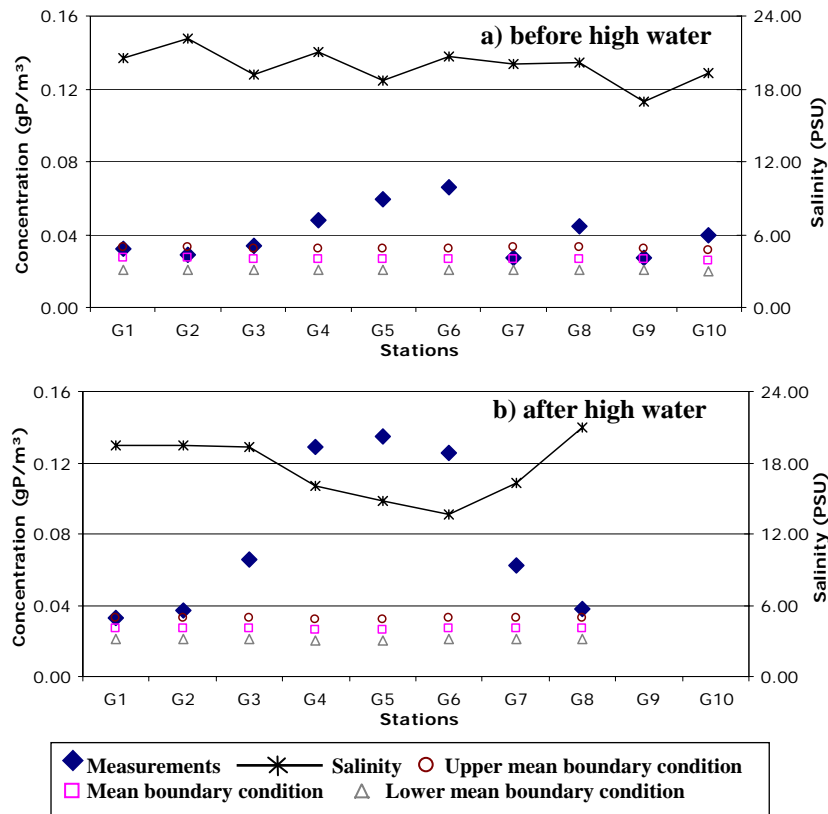


Figure 5.18: Comparison of measured and computed PO_4 concentrations before high water (a) and after high water (b) in spring 2002

Summer distribution

Summer distribution appeared to be rather uniform compared to the distribution in spring therefore less discrepancies were obtained when comparing the results between the model and measured data. Table 5.3 shows the averaged discrepancies of the simulated results with different boundary conditions. It is found that the lower mean standard deviations applied at the open boundaries were appropriate to simulate the nutrient distributions with the errors of 14.94% and 15.75% for nitrate and ammonium respectively. In the case of phosphate, the mean standard deviation applied at the open boundaries was appropriate to simulate the nutrient distributions with an error of 22.90%. Figures 5.19-5.21 show the simulated results of nitrate, ammonium and phosphate with different boundary conditions in summer.

Table 5.3: Selection of boundary condition for the simulation in summer

Substances	Measured boundary condition		Range of boundary condition			Comparison with in-situ measurements		
	Mean	SD	Lower	Mean	Upper	Lower	Mean	Upper
	g/m^3	g/m^3	g/m^3	g/m^3	g/m^3	Discrepancies = $\frac{\text{Model} - \text{Measured}}{\text{Measured}}$ (%)		
Nitrate	0.284	0.067	0.217	0.284	0.351	14.94	44.21	78.23
Ammonium	0.045	0.009	0.036	0.045	0.054	15.75	16.92	33.15
Phosphate	0.098	0.015	0.083	0.098	0.113	28.28	23.02	22.90

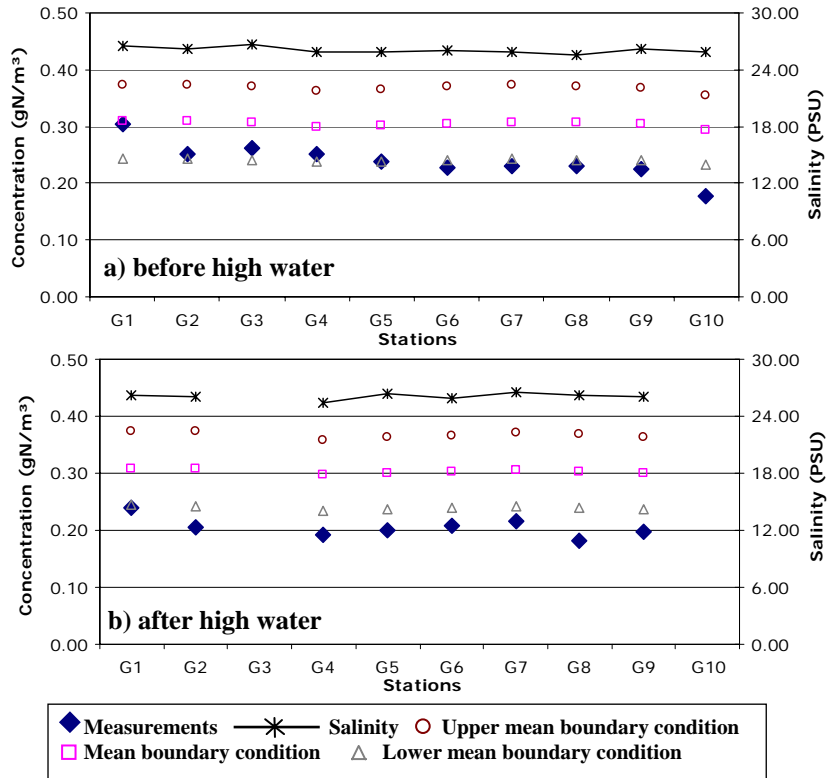


Figure 5.19: Comparison of measured and computed NO_3 concentrations before high water (a) and after high water (b) in summer 2002

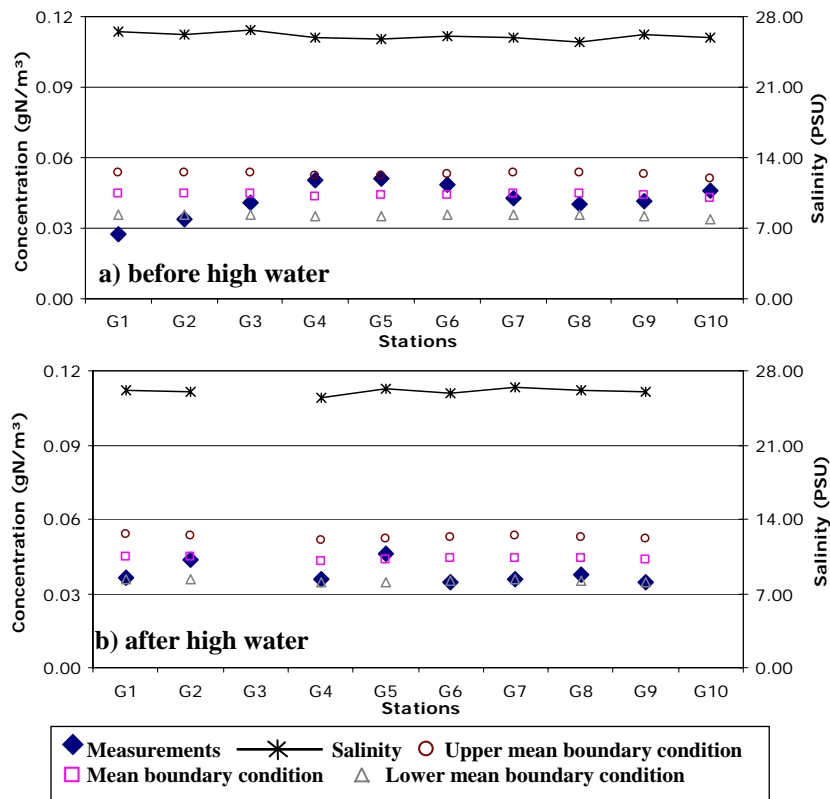


Figure 5.20: Comparison of measured and computed NH_4 concentrations before high water (a) and after high water (b) in summer 2002

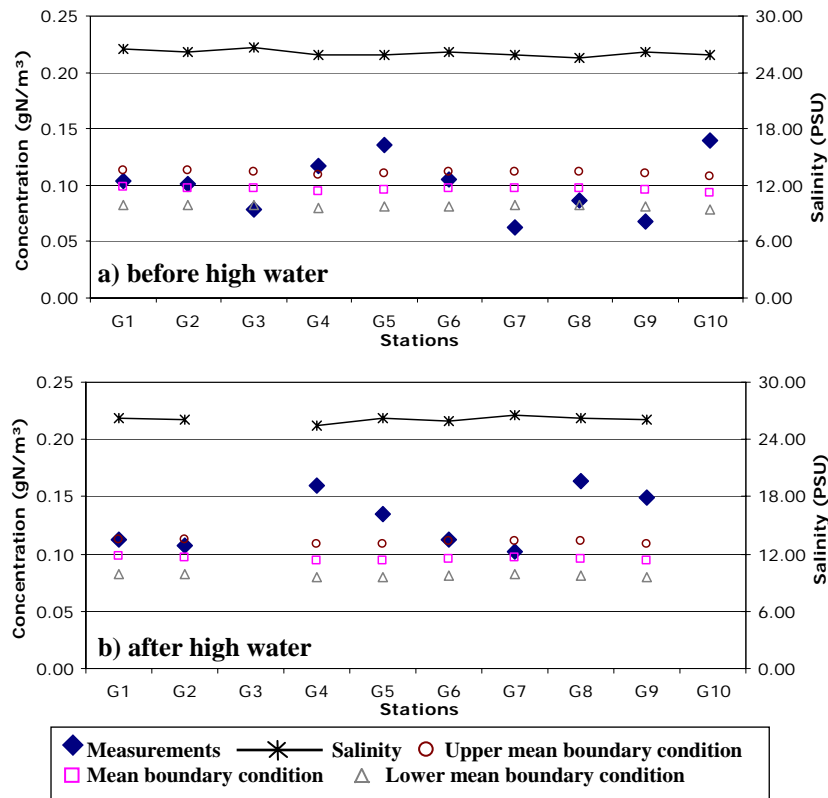


Figure 5.21: Comparison of measured and computed PO_4 concentrations before high water (a) and after high water (b) in summer 2002

5.3.4.4 Model calibration

As discussed in chapter 4, results of the seasonal small scale spatial assessments suggest that at least two factors are of seasonally varying importance in this area. One factor is the local freshwater discharge from the polder basin and the sluice (Figure 5.1) which are located at the eastern and southern corner of the bight. The other factor is the release of ammonium and phosphate from the muddy Wadden sea sediments. This is of particular importance during summer where the sediments get increasingly anoxic together with an increase of organic load and temperature. This evidence was confirmed by the results obtained from the preliminary measurements in 2001 at the cross section of the Piep intertidal channel. A small amount of phosphate produced specifically from the tidal flat was found in late summer (Figure 4.20).

Another important process related to the loss of nitrate from the system is denitrification which is well documented in the investigations of the German Bight. Denitrification provides a sink for nitrogen in estuarine systems and has been shown to be proportional to the rate of organic nitrogen remineralisation in the sediment. Denitrification of nitrate was estimated to account for an average loss of 8-16% of the total nitrogen influx into the German Bight and the adjacent Wadden Sea. Low nitrate concentrations occur in summer in large parts of the German Bight (Beusekom et al., 1999).

In this study the model calibration was carried out bearing in mind the dominant processes corresponding to the specific local processes which prevailed during field measurements. Together with the discrepancies obtained between the preliminary model

settings and measured concentrations, dominant processes were clearly identified. Calibration strategies were defined to take into account these processes in the model computations. In spring, additional discharges from the polder basin and the sluice were taken into account. Approximate discharges and measured nutrient concentrations were considered. Enhanced mineralisation of nutrients in the sediment during summer is a well known process in this region. This process was applied for the calibration of ammonium and phosphate in the summer. In addition, denitrification in the sediment during the summer was also assigned for the calibration of nitrate. Denitrification and mineralisation rates were obtained partly from the measurements in the tidal flat area of the Meldorf Bight and also from the available literature data on the German Bight. Table 5.4 summarises the calibration strategy that was considered in this study. The calibration takes into account the feasible ranges of parameters both from direct measurements and also from literature.

Table 5.4: Calibration strategy

Season	Dominant process	Data required	Calibrated Parameters (rates)	Notes
Winter	Nutrients are conservative and the biological processes are minimal	no	no	To test the accuracy and capability of the model in computing the distributions of nutrients based on the transport process
Spring	Freshwater influence	Flow discharges and nutrient concentrations at the polder basin and the sluice	Discharges at the eastern polder basin = 10 m ³ /s with NO ₃ = 0.8 gN/m ³ NH ₄ = 1.0 gN/m ³ PO ₄ = 1.0 gP/m ³ Discharges at the southern sluice = 2 m ³ /s with NO ₃ = 0.2 gN/m ³ NH ₄ = 0.5 gN/m ³ PO ₄ = 0.5 gP/m ³	Flow discharges were calibrated based on the measured nutrient concentrations
Summer	Denitrification of NO ₃ in sediment	Denitrification rate of NO ₃ in sediment	Zero order = 0.0006 gN/m ² /d First order = 0.1 1/d	Denitrification rate = 0.00007-0.00064 gN/m ² /d in the German Bight
	Mineralisation of NH ₄ in sediment	Mineralisation rate of NH ₄ in sediment	NH ₄ in sediment 0.04 gN Zero order = 0.008 gN/m ² /d First order = 0.03 1/d	NH ₄ in porewater of sandy sediment = 0.07-2.26 gN/m ³ NH ₄ in porewater of mixed sediment = 0.81-1.12 gN/m ³
	Mineralisation of PO ₄ in sediment	Mineralisation rate of PO ₄ in sediment	PO ₄ in sediment 0.25 gP Zero order min. in sed = 0.03 gP/m ² /d First order min. in sed = 0.01 1/d	PO ₄ in porewater of sandy sediment = 0.15-0.32 gP/m ³ PO ₄ in porewater of mixed sediment = 0.16-0.28 gP/m ³ PO ₄ released from sediment = 0.0124 – 0.0155 gP/m ² /d in the German Bight

The model was calibrated based on the selected dominant process as presented in Table 5.4. The model performance was determined by comparing the modelled nutrient concentrations with the observed concentrations. Discrepancies in terms of percentage (%) were evaluated between the computed and measured values. Simulation results in winter are presented in Figures 5.22-5.27. Results from the preliminary set-up without any biochemical processes included are also presented for spring (Figures 5.28-5.33) and summer (Figures 5.34-5.39) in order to compare the influence of the applied calibrated process on the modelled concentrations. The model was calibrated for three different seasons. Results are described as follows:

Winter distribution

Due to the conditions in winter, no special biochemical processes were considered in the calibration. Nutrient concentrations were computed based on the transport of nutrient from the open sea boundary. The agreement between measured and computed values at the measuring locations is within 10 to 20%. The computed concentrations show more uniform concentrations compared with those obtained from the measurements. Comparisons between the measurements and the preliminary model results of nutrient concentrations are presented in Figures 5.22 to 5.24. Although the model is unable to capture the high gradients near the coastline, the distribution and computed concentrations are in good agreement.

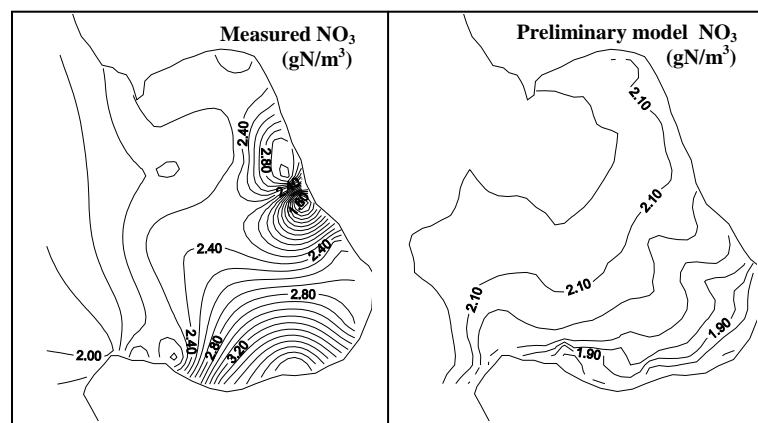


Figure 5.22: Measured data versus preliminary model results for NO_3 on 13 February 2002

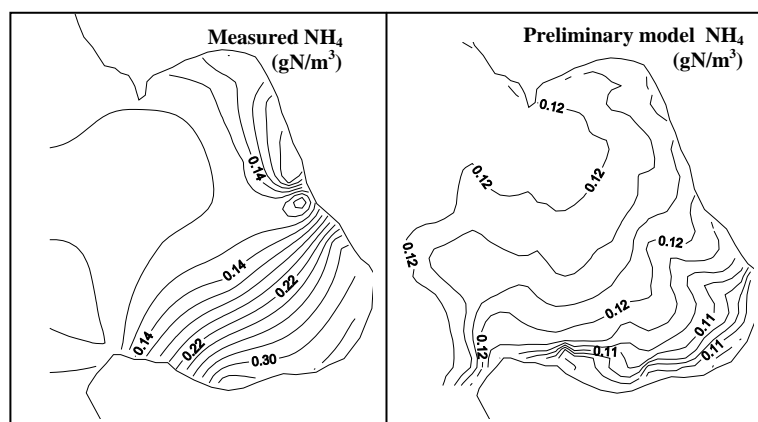


Figure 5.23: Measured data versus preliminary model results for NH_4 on 13 February 2002

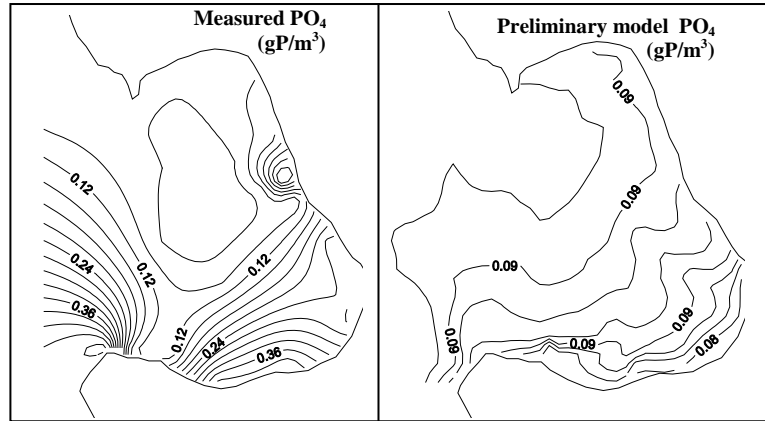


Figure 5.24: Measured data versus preliminary model results for PO₄ on 13 February 2002

Computed results were further compared to the measurements obtained from the grid measurements. The comparisons were carried out for the conditions before and after high tides (Figures 5.25 to 5.27). A good agreement between measured and computed values resulted. Best agreement was found for the modelling of nitrate.

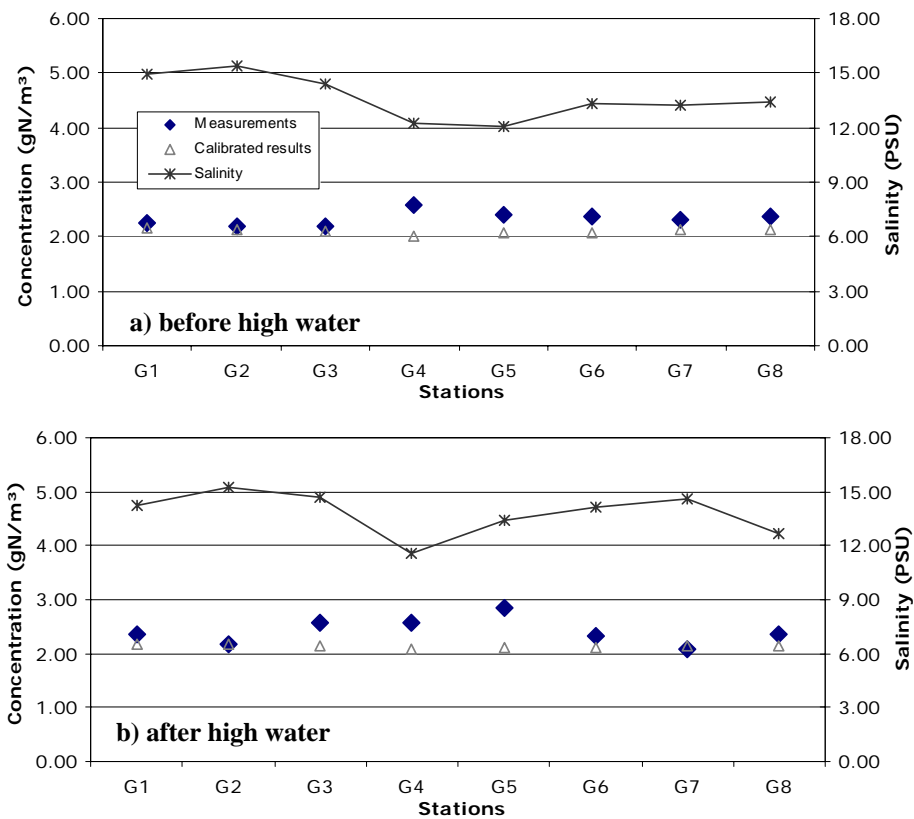


Figure 5.25: Comparisons of measured and computed concentrations of NO₃ at the grid stations before high water (a) and after high water (b) on 13 February 2002

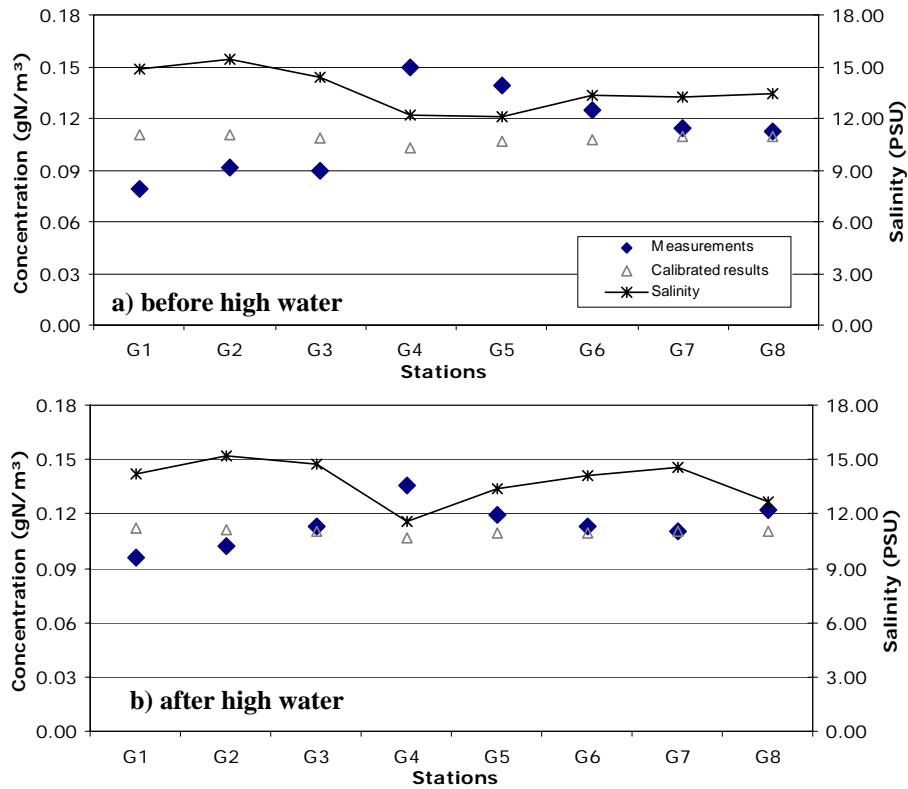


Figure 5.26: Comparisons of measured and computed concentrations of NH_4 at the grid stations before high water (a) and after high water (b) on 13 February 2002

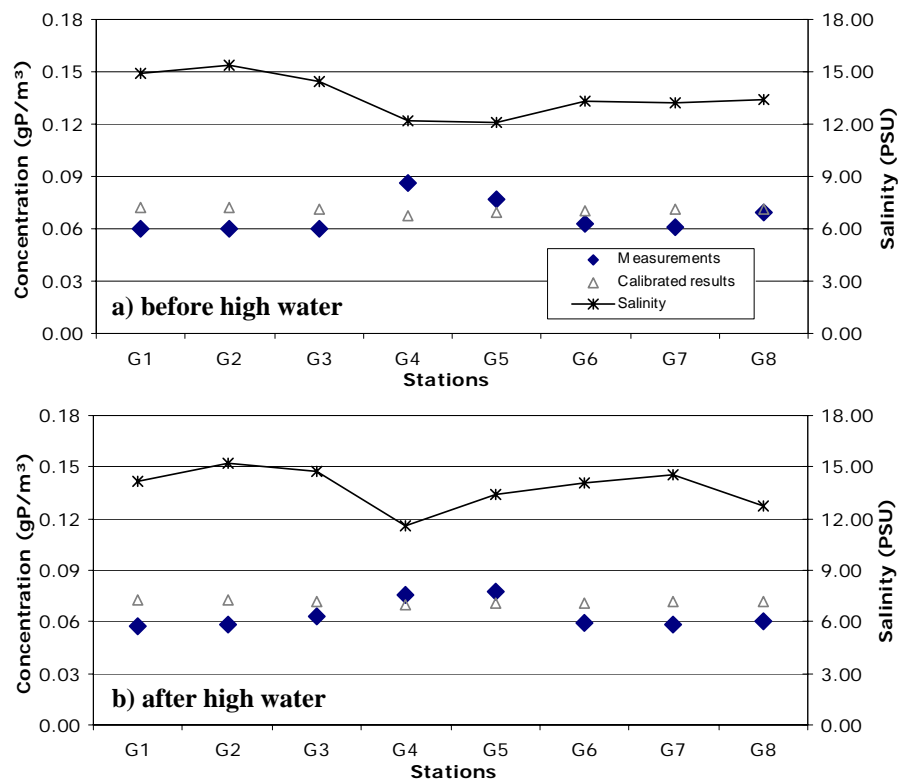


Figure 5.27: Comparisons of measured and computed concentrations of PO_4 at the grid stations before high water (a) and after high water (b) on 13 February 2002

Spring distribution

The additional flow discharge from the polder basin and the sluice containing high nutrient concentrations was taken into account in the model calibration for the spring period. Distributions of measured concentrations, preliminary and calibrated model results were compared (Figures 5.28 to 5.30). It is clearly seen that the influences of freshwater input were captured in the calibration results. Compared to the preliminary results, the calibrated results show a more realistic concentration pattern with higher gradients in the vicinity of the point sources.

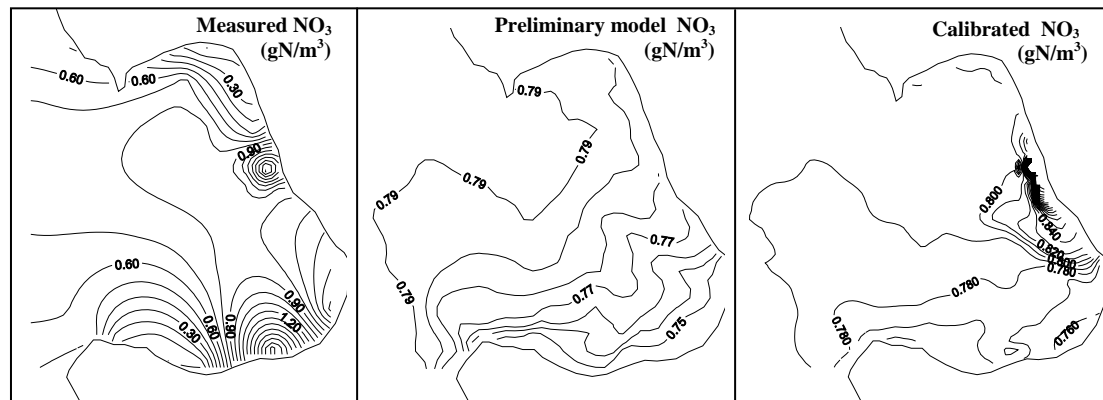


Figure 5.28: Measured data versus preliminary and calibrated model results for NO_3 on 7 May 2002

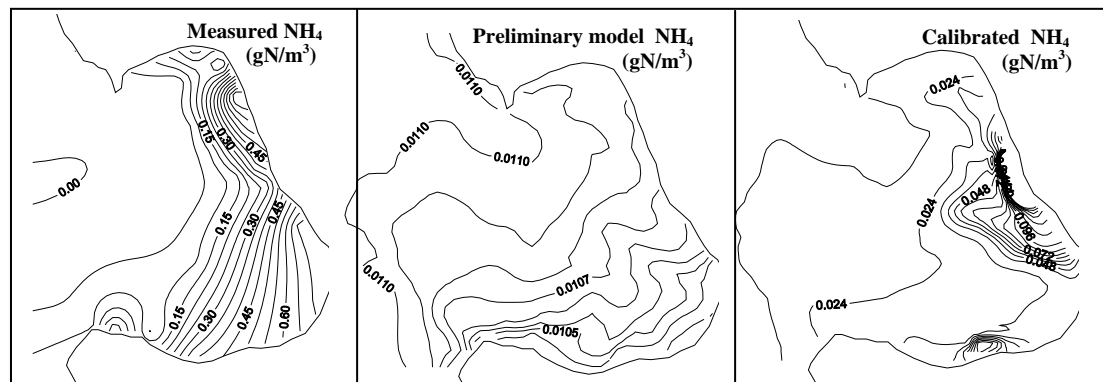


Figure 5.29: Measured data versus preliminary and calibrated model results for NH_4 on 7 May 2002

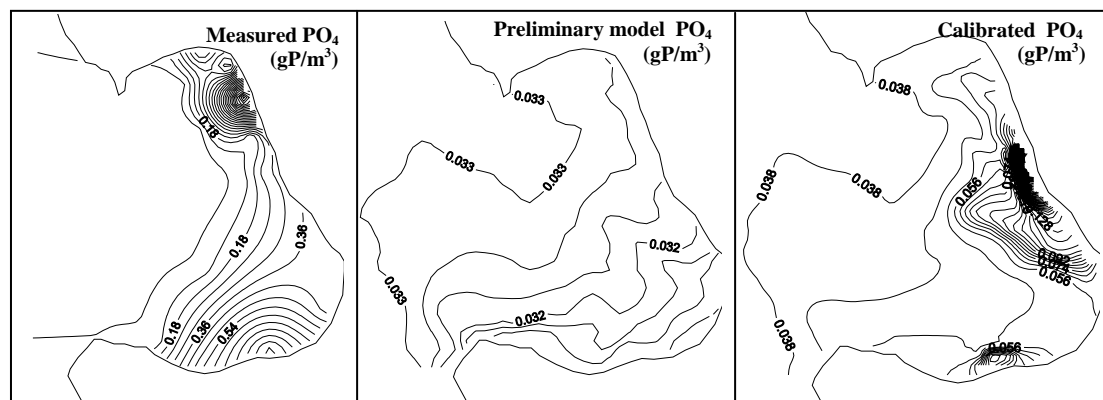


Figure 5.30: Measured data versus preliminary and calibrated model results for PO_4 on 7 May 2002

The model performances were determined by comparing the calibrated model results with the measured concentrations at the grid stations (Figures 5.31 to 5.33). Increases in concentrations can be clearly seen in the vicinity of freshwater discharges (G4 and G10 for the southern sluice and G5-G7 for the eastern polder basin). Computed nitrate concentrations increased slightly near the discharge locations. The increases of ammonium and phosphate concentrations near the discharge locations were well estimated. The overall measured trend is relatively well reproduced by the computed nutrient concentrations. However the model performance in simulating the concentrations at the grid stations near the coast is still rather poor especially for ammonium. Measured concentrations during low water are not well captured by the model. Underestimation of calibrated simulations was found for ammonium and phosphate during low water. Discrepancies range between 10% for nitrate and 30% for phosphate.

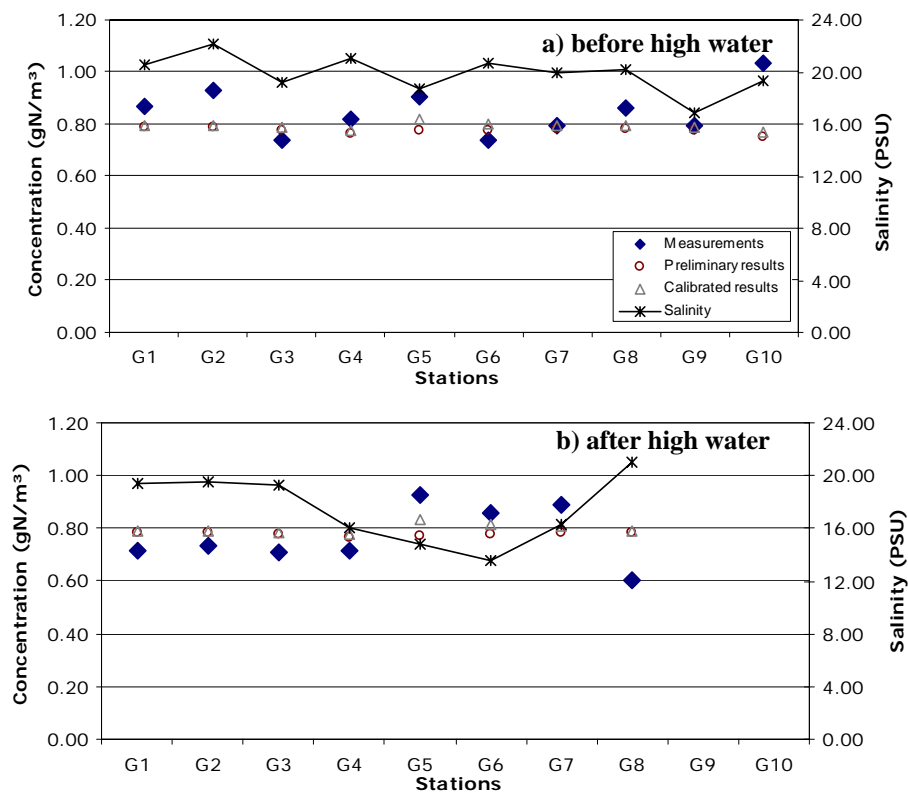


Figure 5.31: Comparisons of measured data, preliminary and calibrated model results for NO₃ at the grid stations before high water (a) and after high water (b) on 7 May 2002

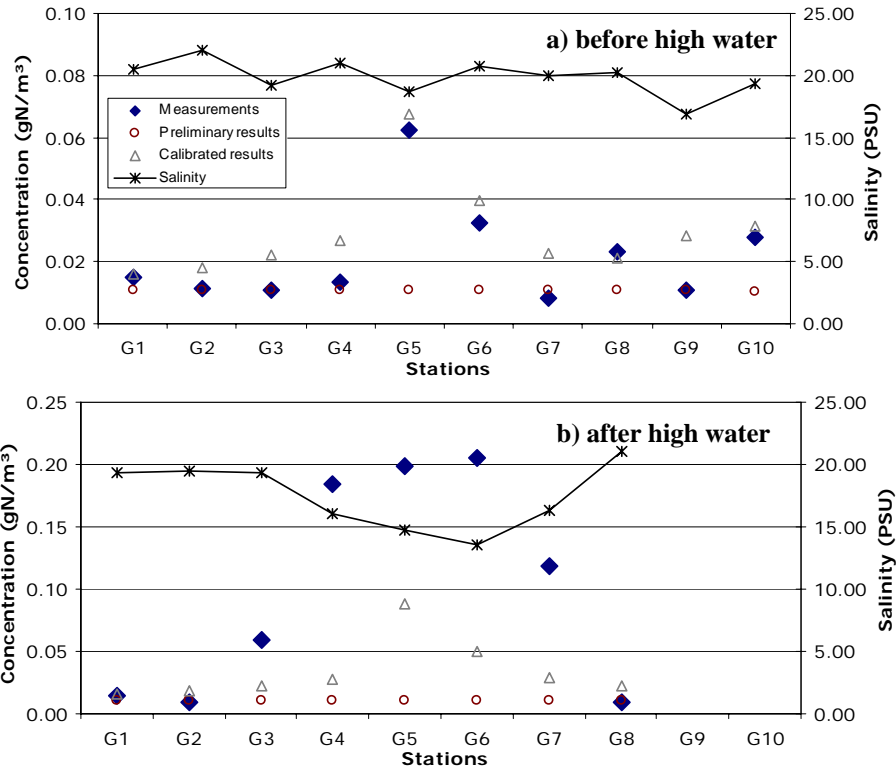


Figure 5.32: Comparisons of measured data, preliminary and calibrated model results for NH_4 at the grid stations before high water (a) and after high water (b) on 7 May 2002

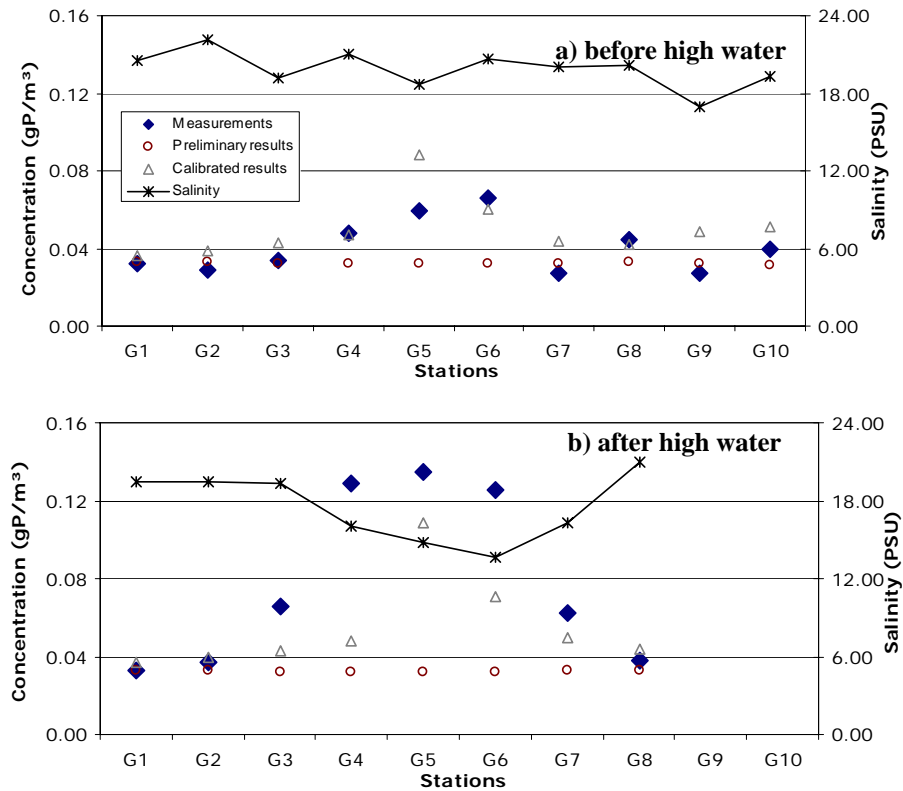


Figure 5.33: Comparisons of measured data, preliminary and calibrated model results for PO_4 at the grid stations before high water (a) and after high water (b) on 7 May 2002

Summer distribution

For the summer period, the effect of denitrification of nitrate and remineralisation of phosphate and ammonium in the sediment were taken into account. Distributions of measured concentrations, preliminary and calibrated model results were compared (Figures 5.34 to 5.36). The calibrated results reflect the general nutrient levels, however only moderate agreements were found for the spatial pattern. Especially at the coastline accuracy was not satisfactorily achieved.

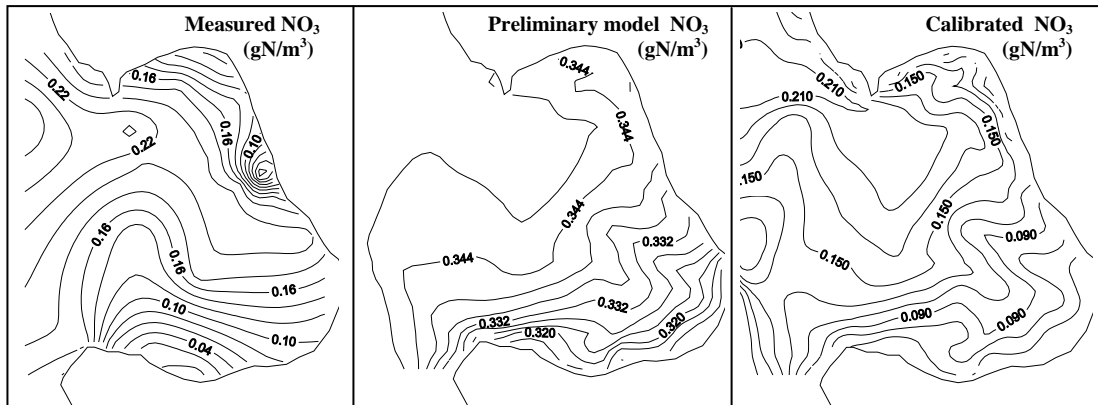


Figure 5.34: Measured data versus preliminary and calibrated model results for NO₃ on 21 Aug. 2002

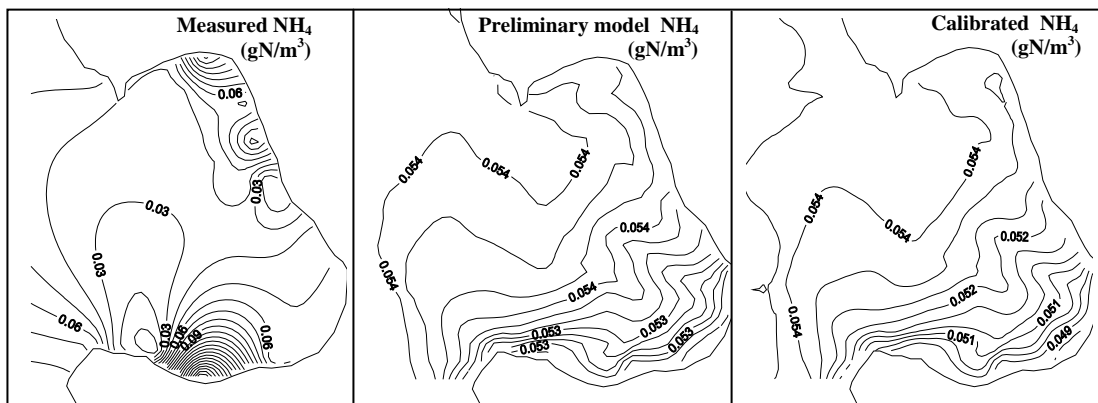


Figure 5.35: Measured data versus preliminary and calibrated model results for NH₄ on 21 Aug. 2002

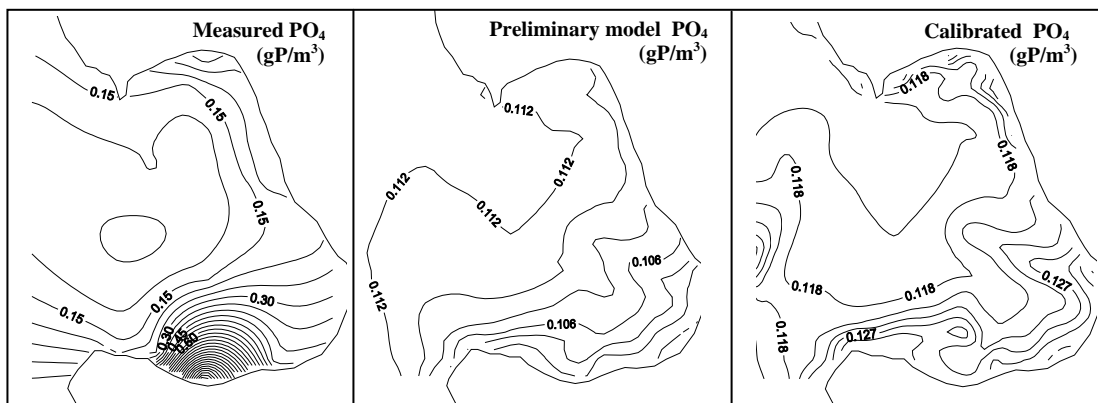


Figure 5.36: Measured data versus preliminary and calibrated model results for PO₄ on 21 Aug. 2002

Calibrated results were further evaluated for the ability to simulate nutrient concentrations in the shallow area of the grid measurements (Figures 5.37 to 5.39). The results show a good agreement between model and measured nitrate concentrations with discrepancies of about 9%. Concentrations of nitrate were found to decrease with the applied denitrification rate. The standard runs provide reasonable results but with a more uniform trend. Calibrated concentrations of ammonium and phosphate were found to be elevated especially near the coast with the specified mineralisation rates. The results show a good agreement between the simulation and the measured data. However, the accuracy of the model for ammonium is still rather poor especially during low water. The observed ammonium concentrations are rather scattered and increased at the stations near the coast in which the selected remineralisation process only may not be able to entirely cover. In general, measured phosphate concentrations are scattered and show an increasing trend in the shallow area. The simulations with the calibrated settings show the ability of the model in capturing the dominant processes especially during low water. During high water, measured phosphate concentrations were found to be rather scattered and hard to be captured by the model. The discrepancies for nitrate and phosphate concentrations range between 9-25%.

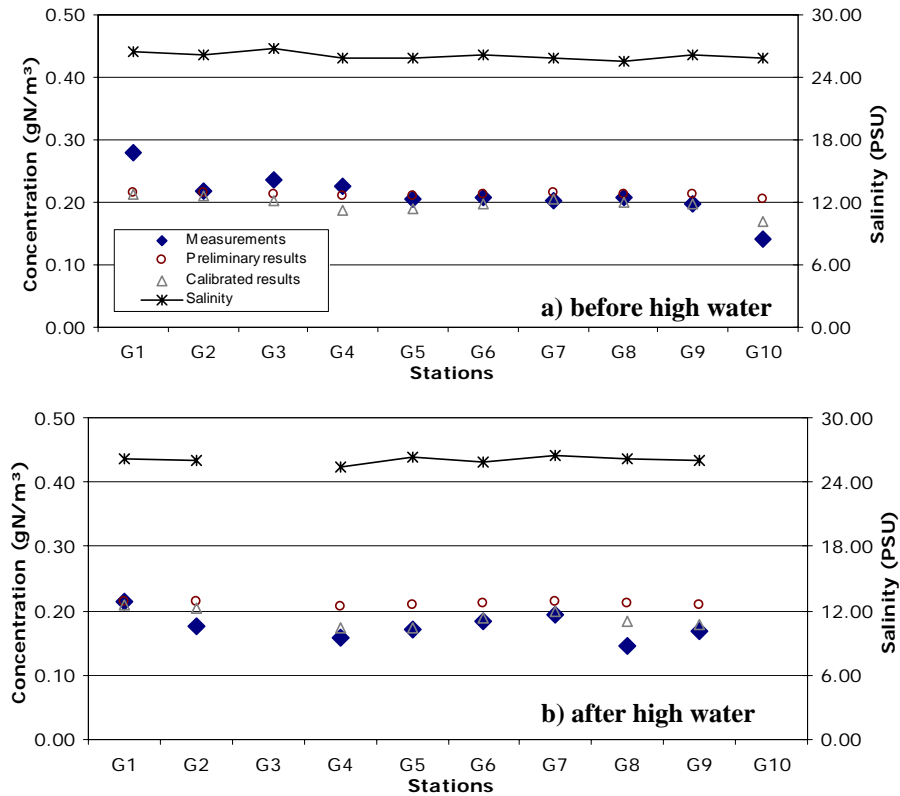


Figure 5.37: Comparisons of measured and computed concentrations of NO_3 at the grid stations before high water (a) and after high water (b) on 21 August 2002

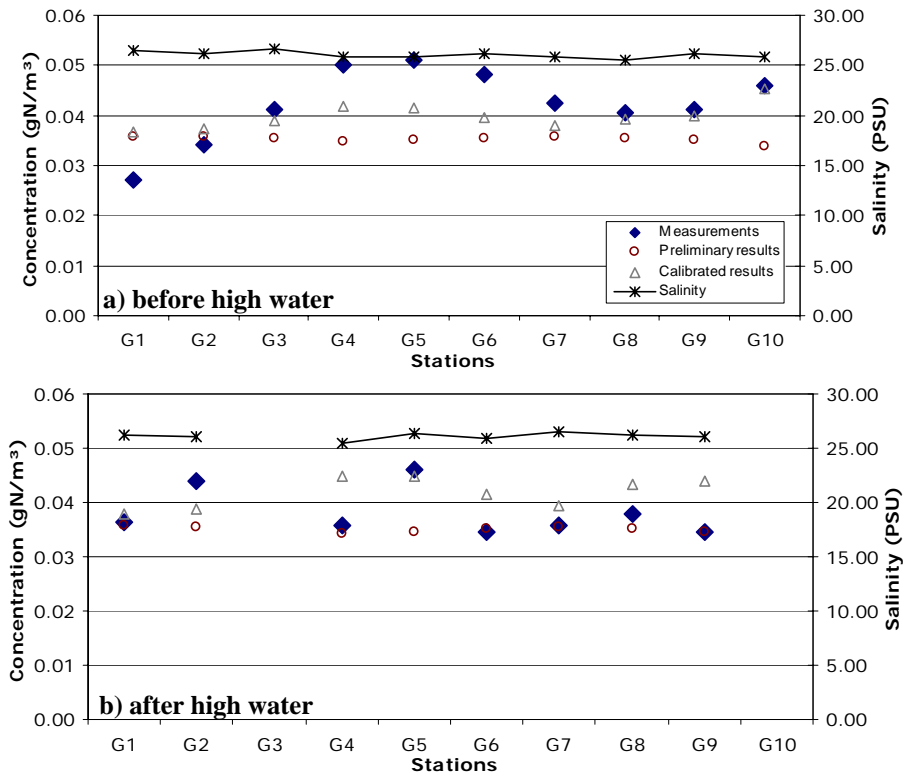


Figure 5.38: Comparisons of measured and computed concentrations of NH_4 at the grid stations before high water (a) and after high water (b) on 21 August 2002

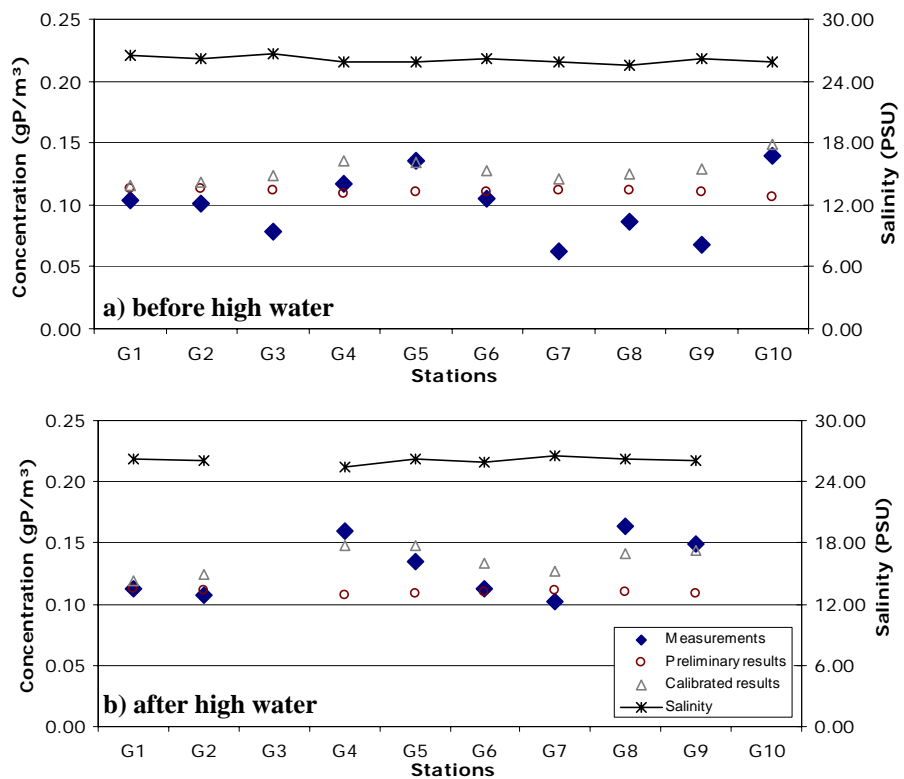


Figure 5.39: Comparisons of measured and computed concentrations of PO_4 at the grid stations before high water (a) and after high water (b) on 21 August 2002

5.3.4.5 Model validation

In this section, results of the model validation are presented. The model settings defined in the calibration were considered through the validation. The model was validated with the field measurements obtained from the grid measurements on the next consecutive day of each seasonal measuring campaigns at similar tidal and weather conditions (winter simulations: 14 February 2002, spring simulations: 8 May 2002 and summer simulations 22 August 2002). Table 5.5 summarises the averaged discrepancies of all grid stations from the calibration and validation results. The ranges of discrepancies of the validation are between 8-15% for nitrate and 17-32% for phosphate, but for ammonium relatively high discrepancies especially in spring still prevailed. The best agreement between measured and modelled results for ammonium was found in winter though model results were still less accurate than for nitrate and phosphate. However, a rather good agreement for distribution trends was achieved. This confirms that the validated model is capable of reproducing the nutrient distribution in the study area with a drawback in the estimation of ammonium concentrations in spring and summer.

Table 5.5: Summary of the discrepancies obtained from calibration and validation results

Seasons	Discrepancies = $\frac{\text{Model} - \text{Measured}}{\text{Measured}}$ (%)					
	Calibration			Validation		
	NO ₃	NH ₄	PO ₄	NO ₃	NH ₄	PO ₄
Winter	10.44	14.30	16.30	8.49	21.15	17.57
Spring	10.10	69.30	29.06	9.68	210.30	32.23
Summer	9.23	13.10	25.61	15.19	51.48	19.42

Measured and computed nutrient concentrations are compared in Figures 5.40 to 5.42 for winter, spring and summer simulations, respectively. It is found that the model is able to capture the main trends quite well. The steep gradients of nutrients resulting from freshwater input along the coastline in spring are fairly well estimated. However, in most cases, computed concentration values still underestimate the measured ones, especially in the nearshore region. The model shows thus a moderate agreement for predicting the gradients resulting from internal sources and sinks due to the dominating biochemical processes in summer.

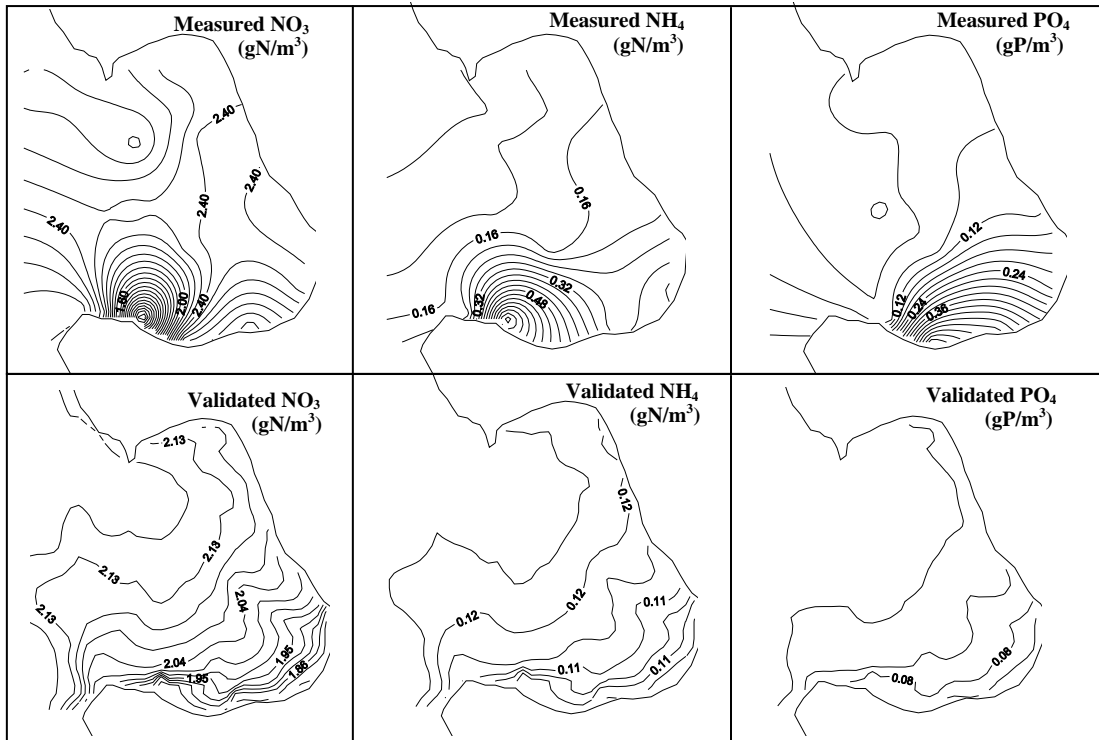


Figure 5.40: Measured data versus validated model results for NO_3 , NH_4 , PO_4 on 14 February 2002

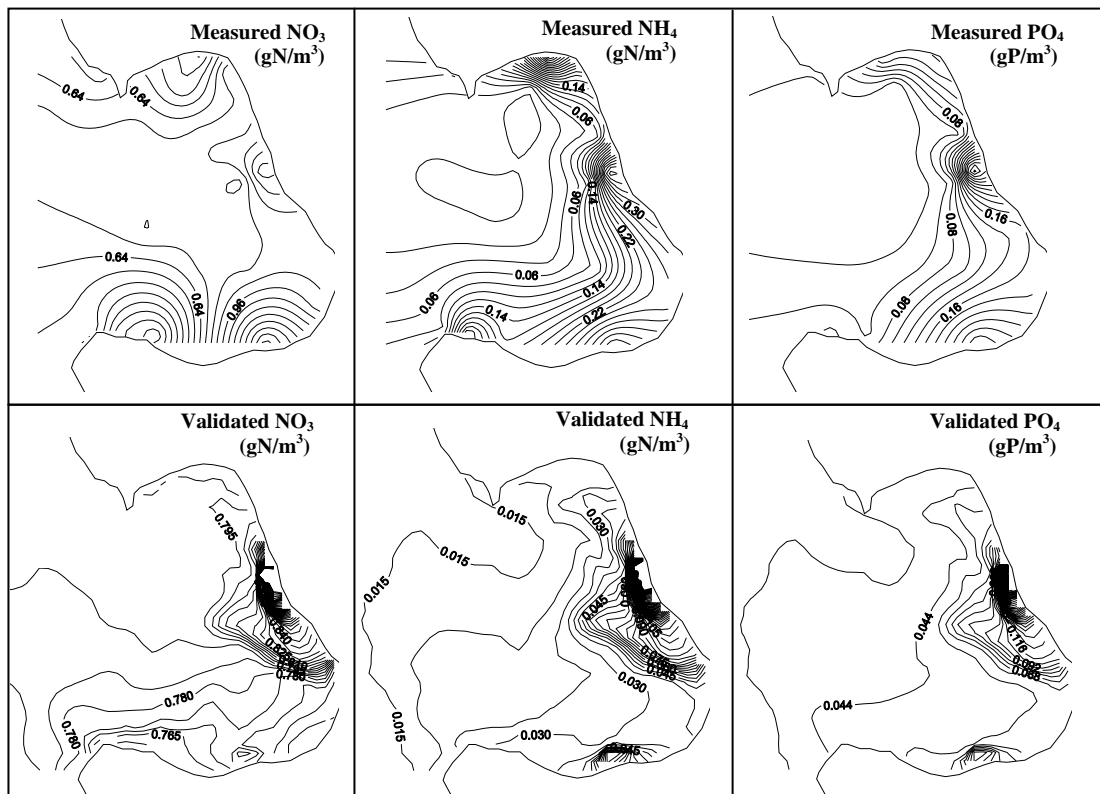


Figure 5.41: Measured data versus validated model results for NO_3 , NH_4 and PO_4 on 8 May 2002

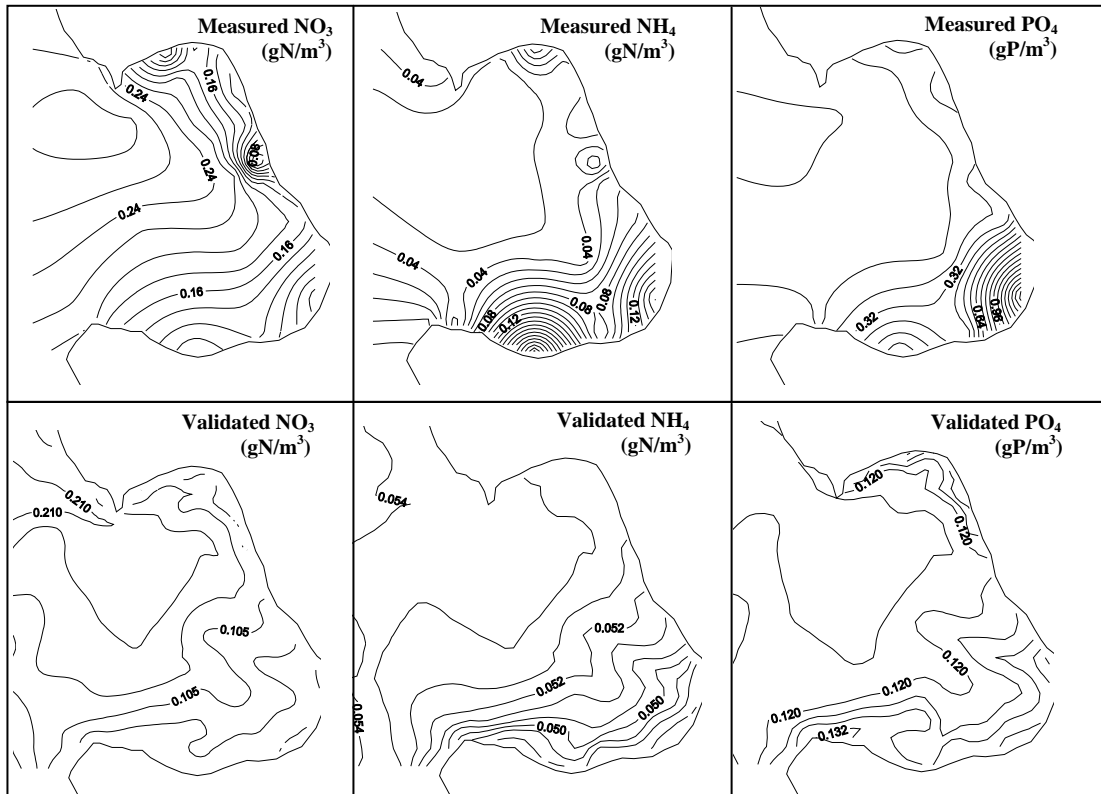


Figure 5.42: Measured data versus validated model results for NO_3 , NH_4 and PO_4 on 22 August 2002

The model was further evaluated with the grid stations data (G1-G10) in the shallow waters. Comparisons between the model and measurement results at the grid stations are presented in Figures 5.43 to 5.51. It is found that the model can predict the distribution tendency with moderate agreement. However, accuracy for ammonium is still not satisfactory. The effect of the freshwater discharge was predicted with good agreement both at high and low waters. As well as for the assigned biochemical processes, predicted concentrations fit well with the situation in the field although some scatters can not be captured. The validation results and discrepancies in terms of percentage are summarised in Appendix B for winter, spring and summer simulations respectively.

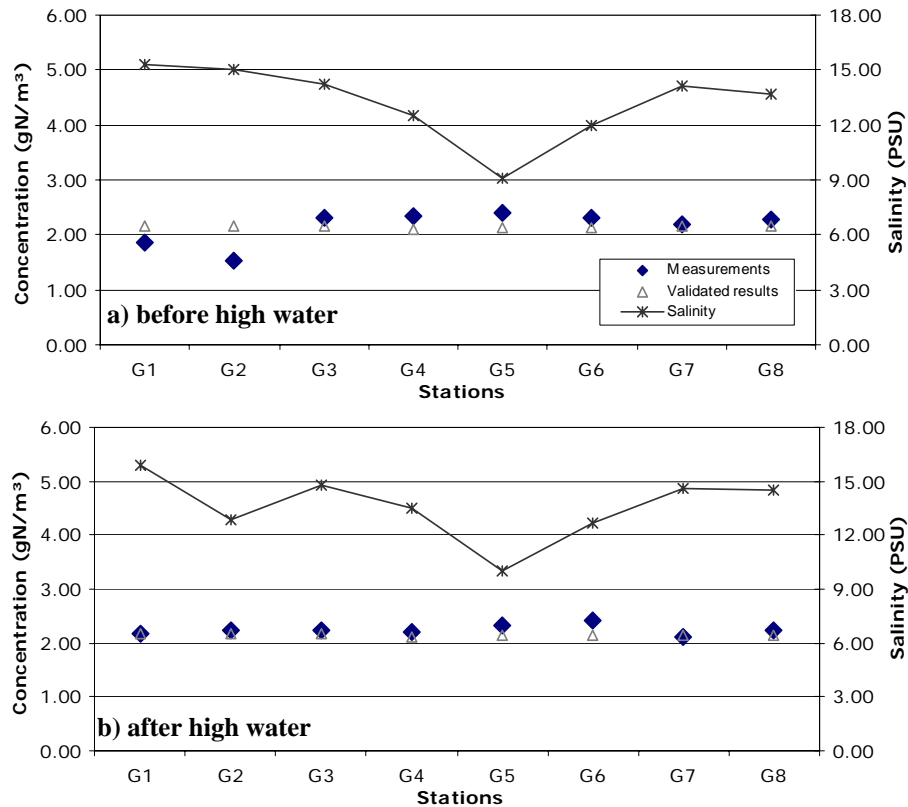


Figure 5.43: Comparisons of measured and validated concentrations of NO_3 at the grid stations before high water (a) and after high water (b) on 14 February 2002

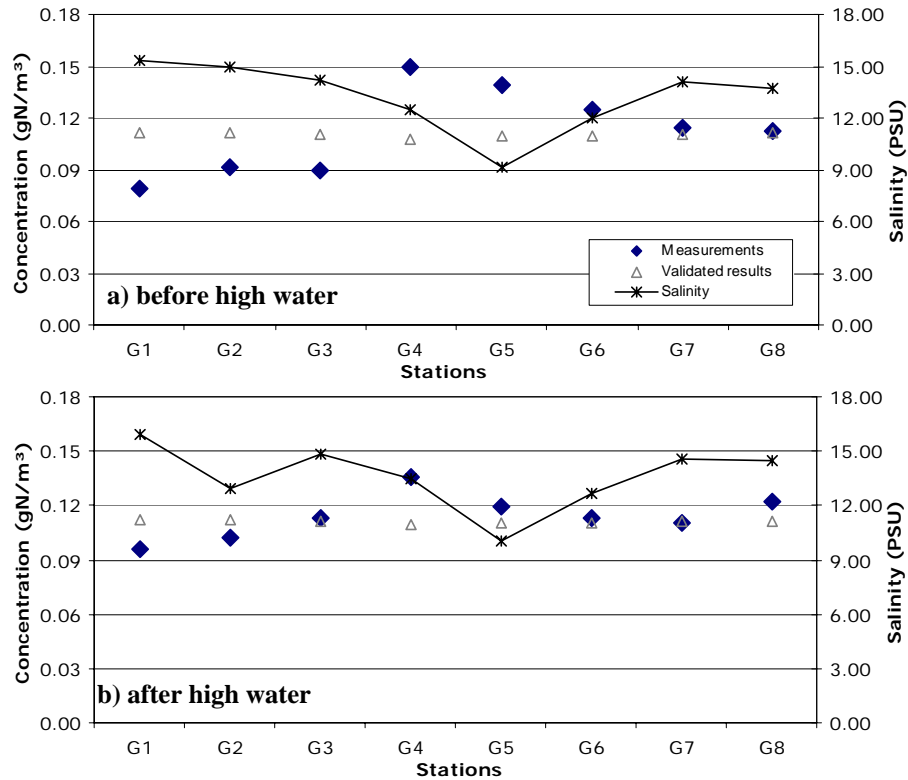


Figure 5.44: Comparisons of measured and validated concentrations of NH_4 at the grid stations before high water (a) and after high water (b) on 14 February 2002

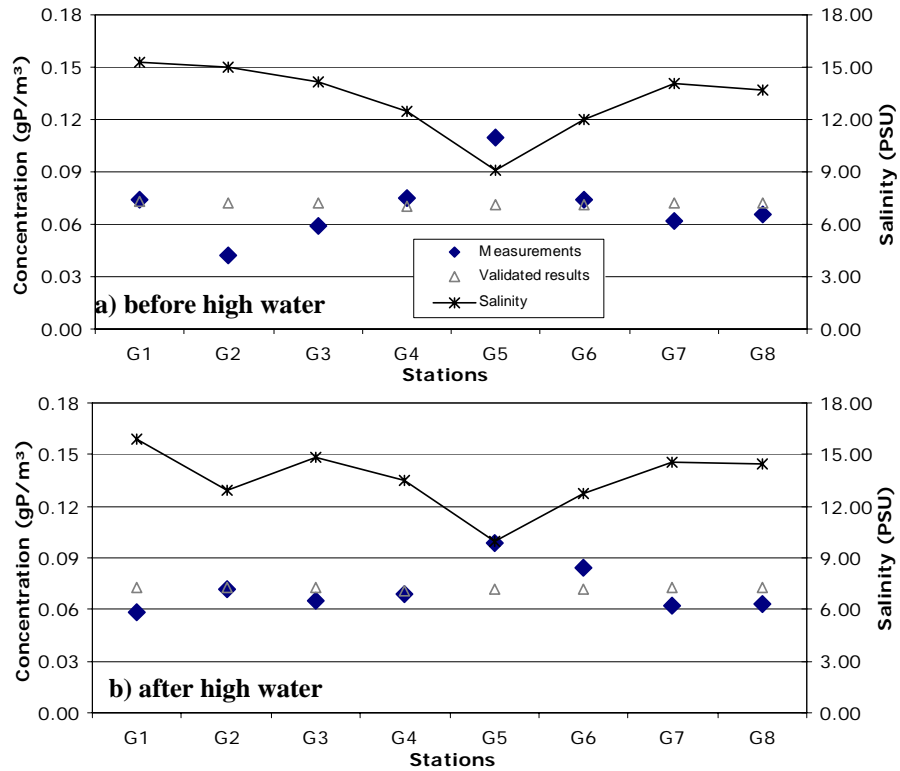


Figure 5.45: Comparisons of measured and validated concentrations of PO₄ at the grid stations before high water (a) and after high water (b) on 14 February 2002

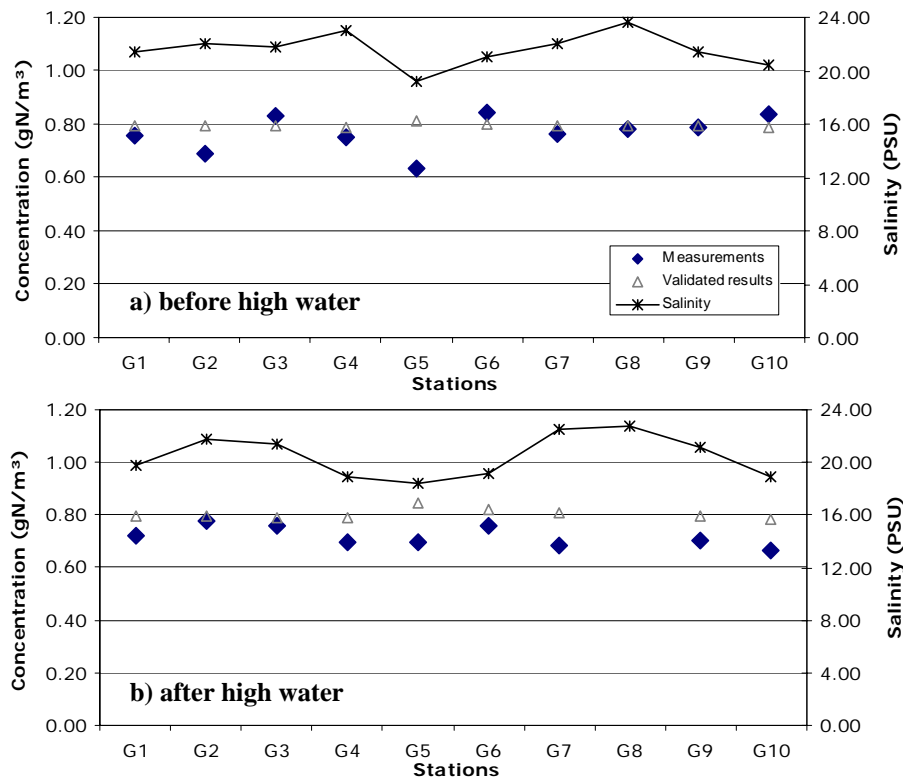


Figure 5.46: Comparisons of measured and validated concentrations of NO₃ at the grid stations before high water (a) and after high water (b) on 8 May 2002

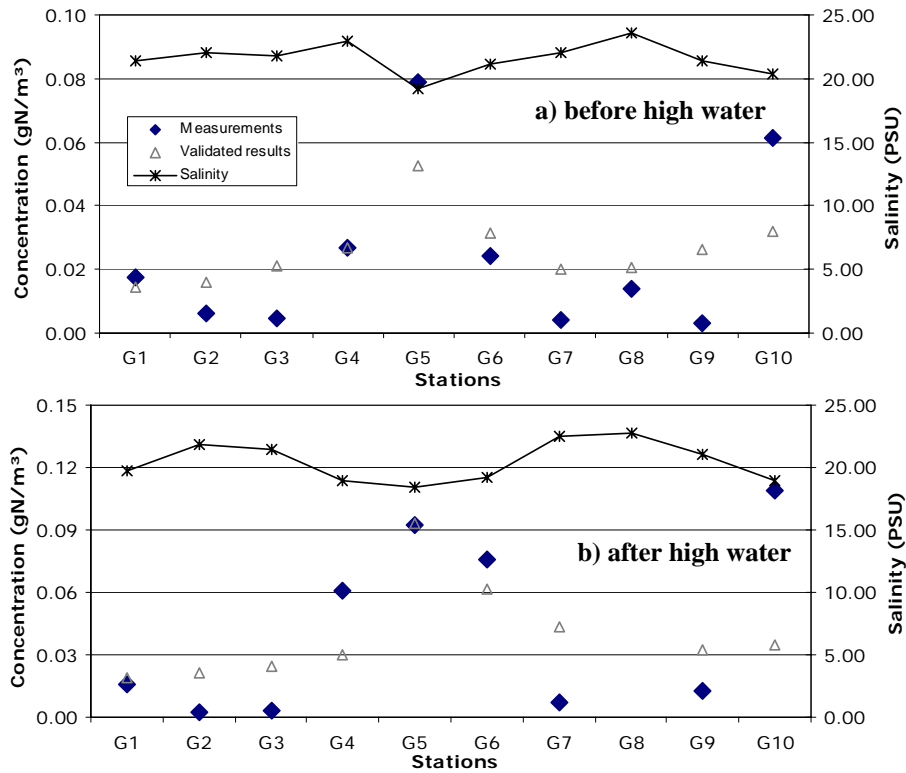


Figure 5.47: Comparisons of measured and validated concentrations of NH_4 at the grid stations before high water (a) and after high water (b) on 8 May 2002

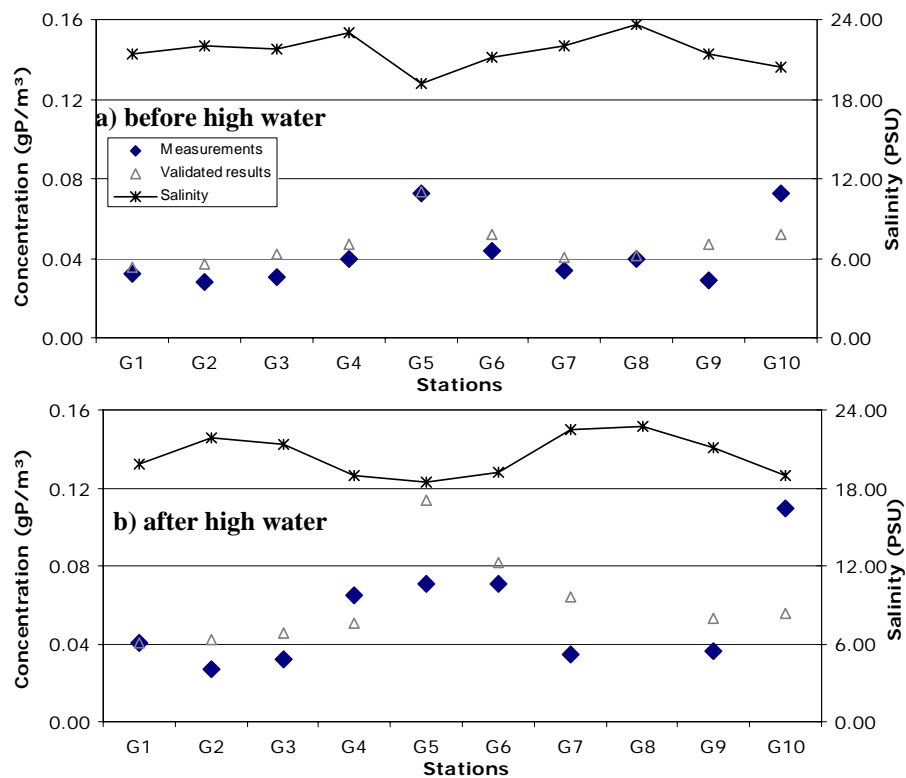


Figure 5.48: Comparisons of measured and validated concentrations of PO_4 at the grid stations before high water (a) and after high water (b) on 8 May 2002

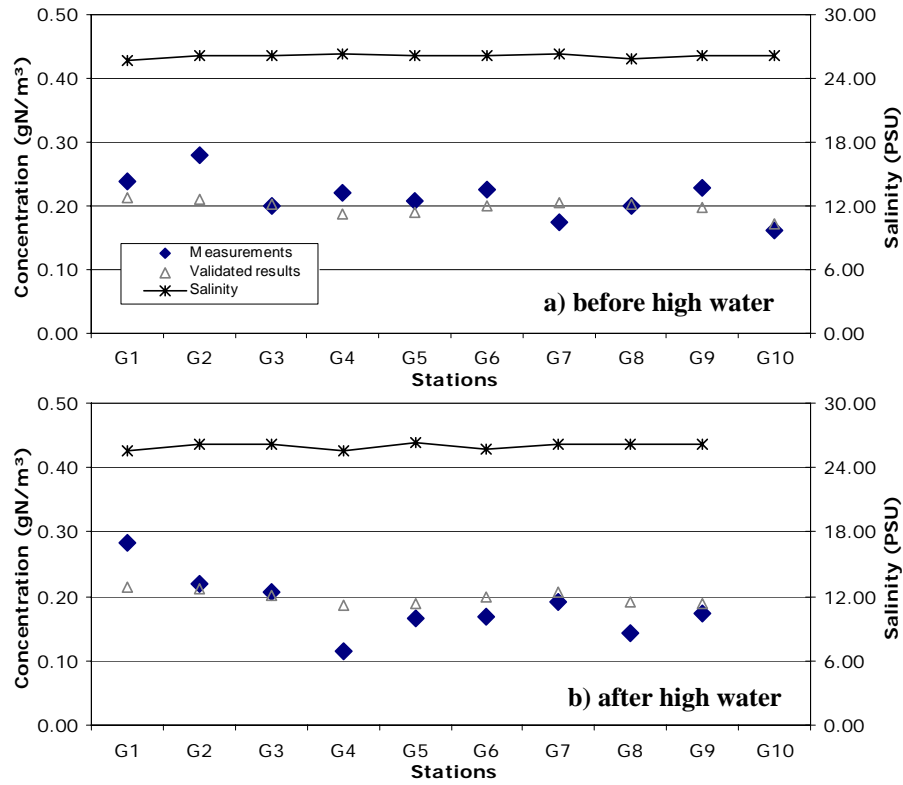


Figure 5.49: Comparisons of measured and validated concentrations of NO_3 at the grid stations before high water (a) and after high water (b) on 22 August 2002

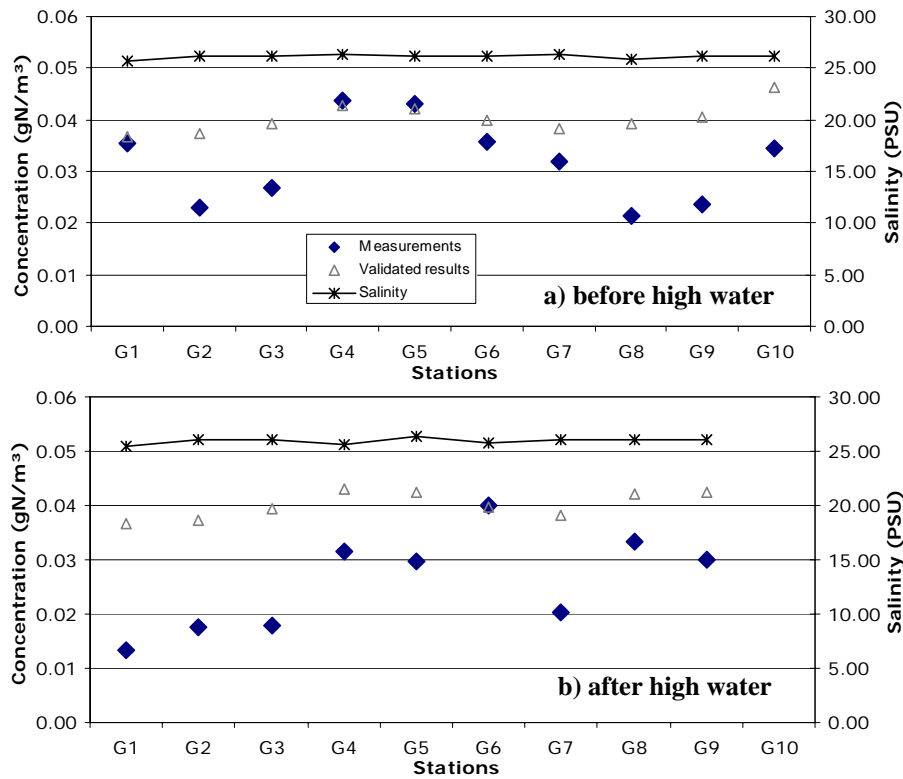


Figure 5.50: Comparisons of measured and validated concentrations of NH_4 at the grid stations before high water (a) and after high water (b) on 22 August 2002

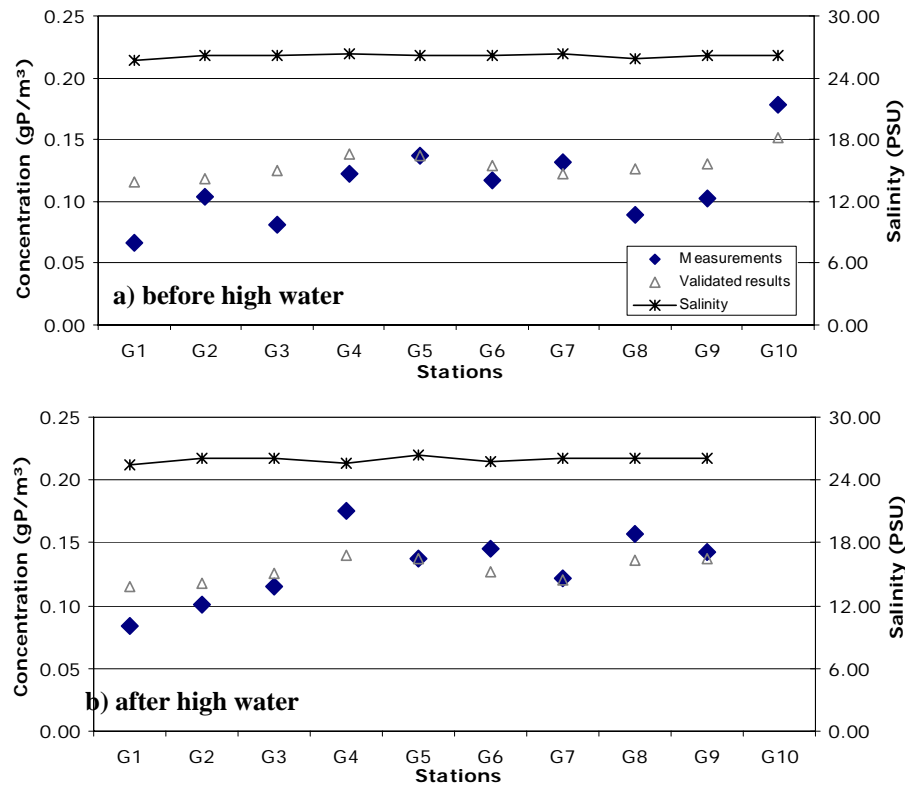


Figure 5.51: Comparisons of measured and validated concentrations of PO_4 at the grid stations before high water (a) and after high water (b) on 22 August 2002

5.3.4.6 Discussion of the results

In general, the nutrient dynamics model shows a satisfying performance to capture the distribution of nutrient concentrations in the study area and also shows the ability to capture the effects due to local sinks and sources such as the freshwater influence in spring and the biochemical transformation process in summer.

In winter, even though slight fluctuations of salinity were observed, nutrient concentrations were rather uniform. Assuming that the nutrients in winter behave conservatively because biological activity is minimal, the model was set-up without accounting for any biochemical processes. Satisfactory results were obtained. Applying this model set-up to the spring and summer situation, discrepancies occur, which were sometimes, but not always in keeping with salinity depression at the relevant stations.. These discrepancies were used as the key to define the strategy to calibrate the model. On the basis of the discrepancies the dominant processes were selected and the parameters required were taken from measurements and literature. This strategy has shown its effectiveness in calibrating the model to enhance its performance. Satisfactory results within a realistic range were achieved. In general, the model can produce the trends in nutrient distributions relatively well but results still can not entirely explain the situation in the direct vicinity of the coastline (landbased stations) and during low water in the shallow water area where nutrient concentrations were underestimated in most cases. This points out that freshwater influence should also be considered in winter and in summer and that biochemical processes should be addressed for the spring situation as well. In addition there may be other relevant processes especially during low water which were

not accounted for in the simulations. Pore water release due to gravity flow and erosion including tidal pumping resulting from the changing tide may be relevant processes which were not considered here. Further investigations into the importance of these processes are required.

Results from the validation confirm that the model is also capable of predicting the nutrient distributions on the next consecutive day under similar weather and tidal conditions. The simulation results fit rather well with the observed nutrient concentrations at the grid stations, especially for the winter simulations. Nitrate is found to be well simulated for all seasons. Trends of elevated nutrient concentrations during spring simulations due to the influence of freshwater discharges are well predicted. Also in summer, the nutrient dynamics model shows a good agreement with the observations by taking into account the dominant biochemical processes which naturally occur in the study area. Predicted nitrate concentrations decreased in the shallow water area due to denitrification which fits well with the situation occurring in the field. The remineralisation process improves the ability of the model to compute the nutrient distributions especially in the shallow water area. Not only the accuracy that has been achieved but also the computed results are more realistic. However, spatial variability of observed ammonium and phosphate concentrations cannot be covered by the predicted results entirely. From the validation results, it can be concluded that for short-term modelling, with similar weather and tidal conditions, the nutrient dynamics model is capable of predicting the trends of nutrient distributions satisfactorily.

6 Model application

6.1 Introduction

In this chapter, several hypothetical scenarios of interests are investigated through the use of a validated model, which are the effects resulting from an increased sewage water release in the Meldorf Bight, an increased local freshwater input from the hinterland and an intensified remineralisation in the sediment. Simulations were done by considering typical or measured values and by considering their impact on the nutrient distribution in the area.

6.2 Sewer station

The Buesum sewage plant is located at the northwestern corner of the Meldorf Bight (Figures 3.2 and 3.4). The pipe outfall is shallowly buried with the outfall placed about 30m from the coastline. The averaged effluents discharge is 800,000m³/year with daily volume ranging between 1,500 to 5,000m³. From the measurements, it is found that the wastewater in the outlet tank particularly contains high nitrate concentration. However the concentration is diluted and reduced at the outfall due to a strong tidal mixing. The influence of the current wastewater discharge on the nutrient concentrations in the Meldorf Bight is found to be insignificant (see section 4.3). The surrounding area is hardly affected by the released concentrations.

The model was used to simulate the hypothetical condition that the released nutrient concentrations in summer at the outfall are doubled. How will this effluent discharge affect the surrounding area? Details of the measured discharge and concentrations are described in section 4.3.4 (more details of measured data are also given in Table A.19, Appendix A) for the summer measurement. Designed scenarios are presented in Table 6.1 and Figure 6.1. They show that a doubling in nutrient discharge results in the formation of a distinct wastewater plume in front of the outfall location. This is especially the case for nitrate. By contrast, the ammonium and phosphate plumes in the southern part of the bay are due to high nutrient release from the extended southern mud flats during this time. It can be seen clearly that the impact of the sewer station is of minor importance for the N and P levels in the bay when compared to that of intensified nutrient release from the sediment.

Table 6.1: Scenarios of sewage water release into the Meldorf Bight

Scenario	Description
Scenario 1	Simulation with the effluent nutrient discharge at the outfall based on the field measurement in summer 2002 (Discharge = 40l/s, NO ₃ = 1.16gN/m ³ , NH ₄ = 0.05gN/m ³ , PO ₄ =0.16gP/m ³)
Scenario 2	Simulation with doubly increasing of nutrient concentrations at the outfall from scenario 1

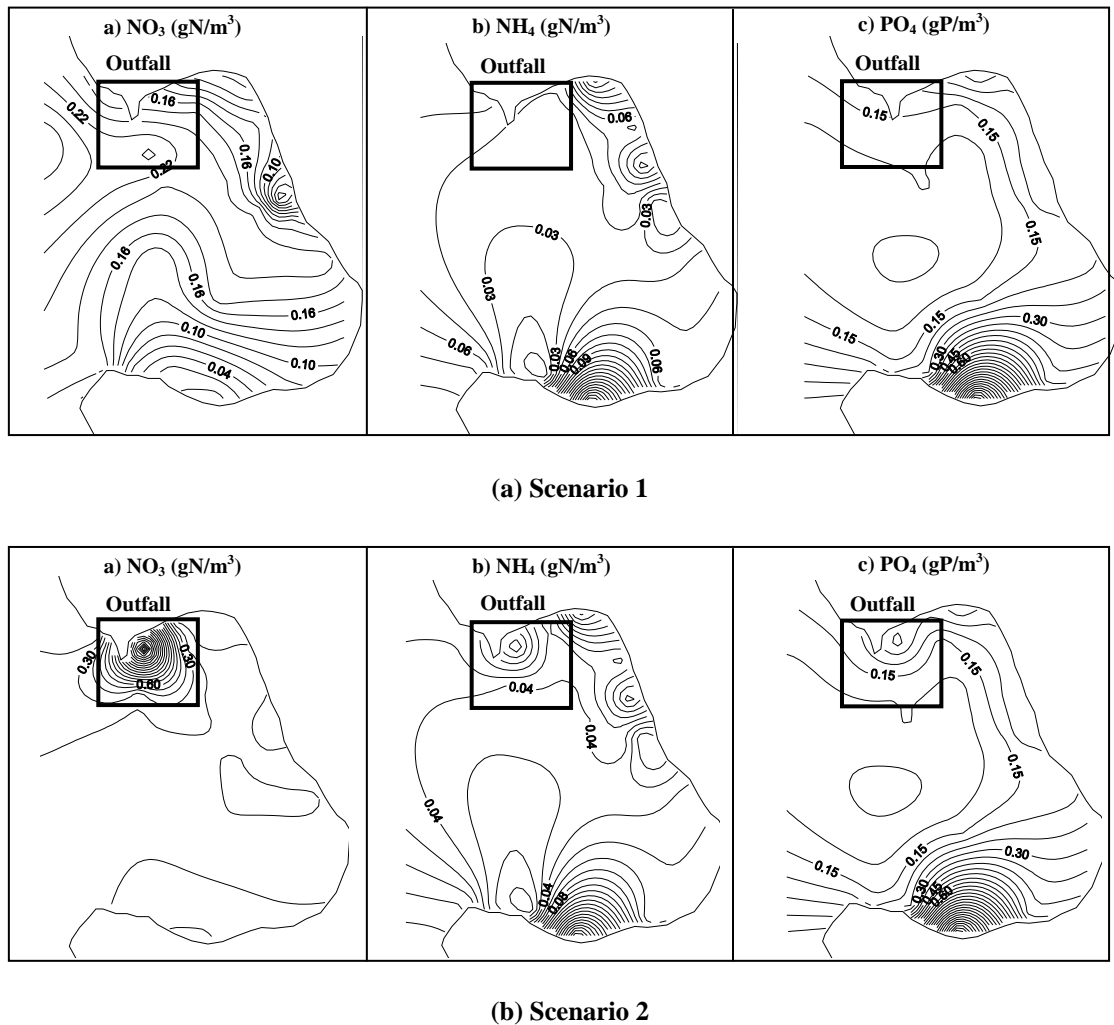


Figure 6.1: Effect of increased nutrient discharge from the sewage plant on nutrient levels on the surrounding area (a) nitrate (b) ammonium (c) phosphate concentrations of scenarios 1 and 2

6.3 Freshwater input

The major freshwater input to the study area is the discharge from the polder basin on the eastern side of the Meldorf Bight. This discharge originates from the drainage of the agricultural hinterland and the sewage effluents from different wastewater treatment plants in the vicinity of the area. There is another minor freshwater input from the sluice gate at the southern part which receives water from the agricultural sector. These discharges are of local importance since they contain high nutrient concentrations and are released to the bight directly. The discharge rate depends mainly on the meteorological conditions such as rainfall. The locations of the polder basin and the sluice are shown in Figure 3.2. To evaluate the impact of increased freshwater discharges to the study area, the gradients resulting from several hypothesis scenarios were simulated with the model. Approximated freshwater discharges and nutrient concentrations obtained from the measurements in spring 2002 were used as a basis for the design of the scenarios. Details of the measured discharge and concentrations are described in section 4.3.3. Table 6.2

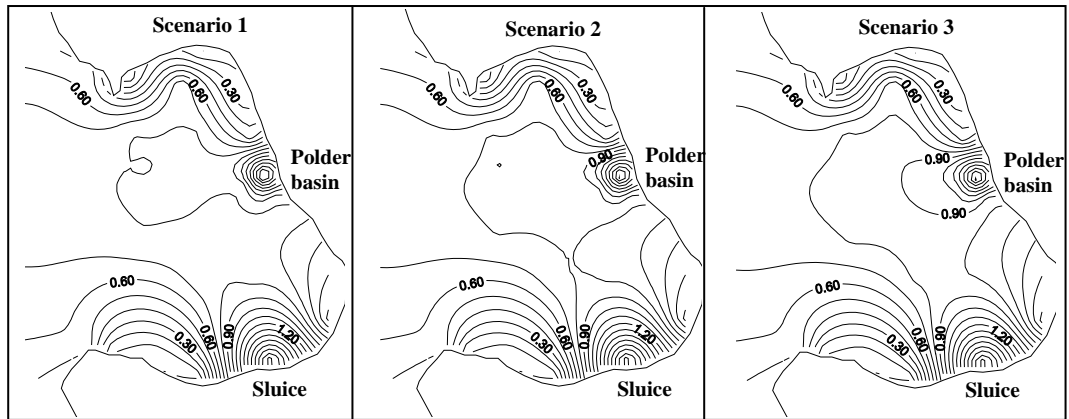
shows the details of the designed scenarios of changes in freshwater discharges. Simulation results are shown in Figure 6.2.

Table 6.2: Scenarios of freshwater discharges into the Meldorf Bight

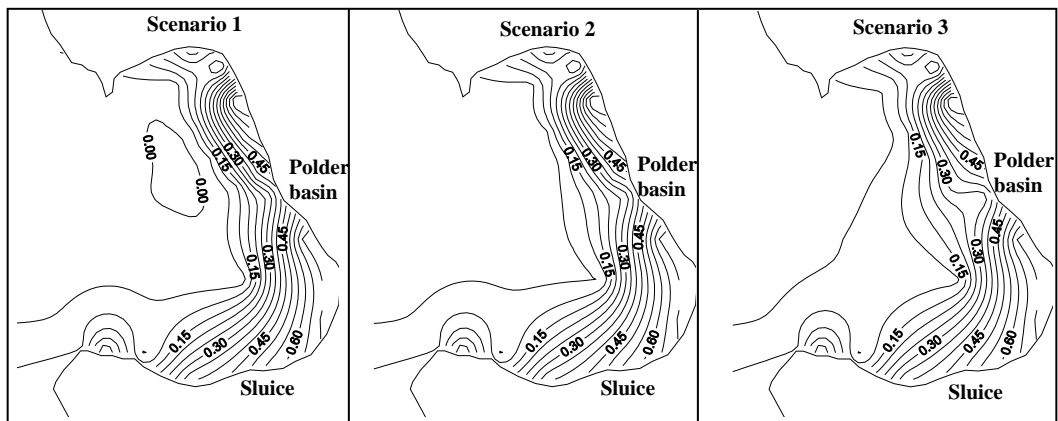
Scenario	Description
Scenario 1	Simulation with the additional freshwater discharges based on the field measurement in spring 2002: - The polder basin: discharge = 10m ³ /s, NO ₃ = 0.8gN/m ³ , NH ₄ = 1.0gN/m ³ , PO ₄ =1.0gP/m ³ - The southern sluice: discharge = 2m ³ /s, NO ₃ = 0.2gN/m ³ , NH ₄ = 0.5gN/m ³ , PO ₄ =0.5gP/m ³
Scenario 2	Increasing of freshwater discharges (at the polder basin and at the sluice) of scenario 1 by a factor of two
Scenario 3	Increasing of freshwater discharges and nutrient concentrations (at the polder basin and at the sluice) of scenario 1 by a factor of two.

It can be observed from the simulations that the level of nutrient gradients and their spatial distribution differ slightly in each scenario. Concentrations are significantly elevated especially near the discharge locations (the polder basin and the sluice). The nutrient plume increases considerably along with an increase of freshwater discharge. It is clearly seen from the scenario results that the major impact is from the polder basin on the eastern side of the bight. It impacts even the central area of the bight while the influence of the southern sluice is restricted only to the southern corner.

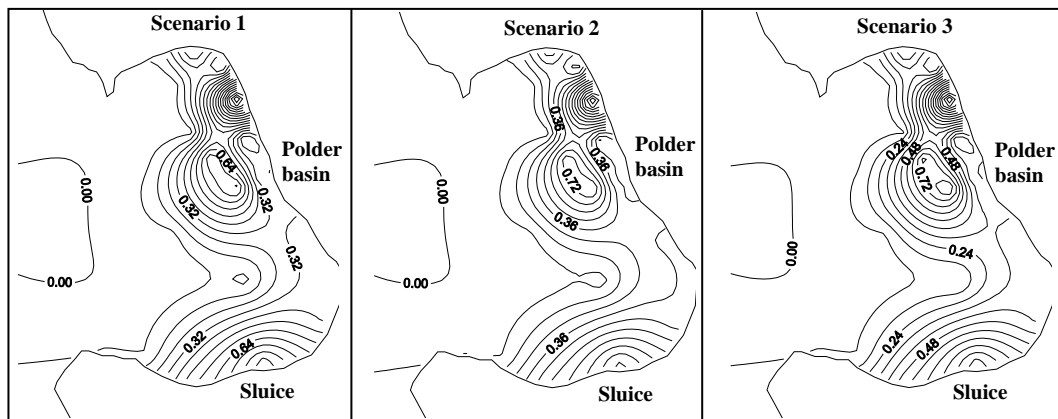
On the basis of these simulation results, it is recommended that care must be taken for the operation of the polder basin and nutrient concentrations should be regularly monitored to prevent eutrophication problems due to hypernutrification resulting from the spreading of local nutrient plumes in the area. Critical nutrient thresholds should be set in combination with scenario runs in order to provide the operational regulations to keep the area safe within the acceptable limits.



(a) NO_3 (gN/m^3)



(b) NH_4 (gN/m^3)



(c) PO_4 (gP/m^3)

Figure 6.2: Effect of freshwater input on (a) nitrate (b) ammonium (c) phosphate concentration on the Meldorf Bight

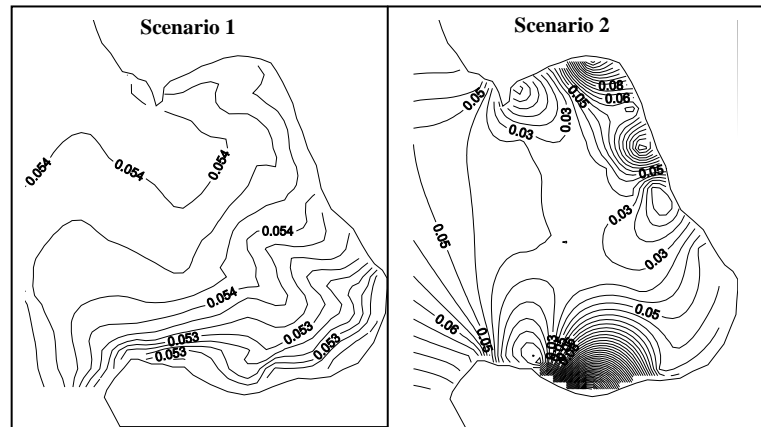
6.4 Remineralisation of ammonium and phosphate in sediment

Remineralisation of organic matter in the Wadden Sea sediment is usually most intense in late summer resulting in an increase of phosphate and ammonium concentrations without any sign of freshwater input. Ammonium is released from the sediment to the water column predominantly during anoxic condition going along with an increasing organic load and temperature. Under oxic conditions, ammonium derived from the remineralisation of organic matter is rapidly transformed to nitrite and nitrate by nitrifying bacteria, while phosphate is adsorbed to insoluble particulate iron hydroxide and temporarily stored in the sediments. Under anoxic condition, phosphate is remobilized from its particulate form and released into the water column while nitrification activity ceases and the dissimulative reduction of oxidised nitrogen to ammonium becomes important.

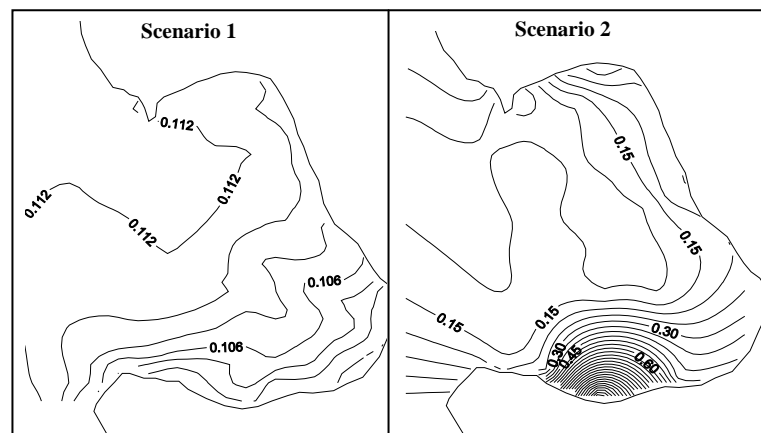
Due to limitation of direct measurements of the remineralisation rate and the limited ability to determine the impact of benthic nutrient release on the spatial nutrient gradients in the Wadden Sea water under different physical conditions, the nutrient dynamics model was applied to get an idea of the importance of this process. The model was set-up with and without the remineralisation process (scenarios 1 and 2) for the summer situation 2002 as presented in Table 6.3. Different remineralisation rates for ammonium and phosphate were applied in the simulations based on the spatial gradient adapted from the relationship between grain size distribution (see Figure 3.8) and measured nutrient concentrations in sediment porewater (Schroeder, 2002 and see Table 5.4). The remineralisation rates applied in this study are in the ranges of 0.004 – 0.018 gN/m²/d for NH₄ and 0.0124 – 0.0155 gP/m²/d for PO₄. Discrepancies obtained from the comparisons between the two scenarios show clearly the impact of ammonium and phosphate release from the sediment on the nutrient concentrations in the water. Simulation results are shown in Figure 6.3 and the discrepancies between these two scenarios at each of the grid stations (see Figure 4.3) are illustrated in Figure 6.4.

Table 6.3: Scenarios of the remineralisation of NH₄ and PO₄ in sediment at the Meldorf Bight

Scenario	Description
Scenario 1	Simulation settings based on the field measurement in summer 2002 without the remineralisation process
Scenario 2	Simulation settings based on the field measurement in summer 2002 with applied spatial gradient of remineralisation rates in sediment for NH ₄ and PO ₄



(a) NH_4 (gN/m^3)



(b) PO_4 (gP/m^3)

Figure 6.3: Effect of nutrient release from the sediment on (a) ammonium and (b) phosphate concentrations in sediment of scenarios 1 and 2

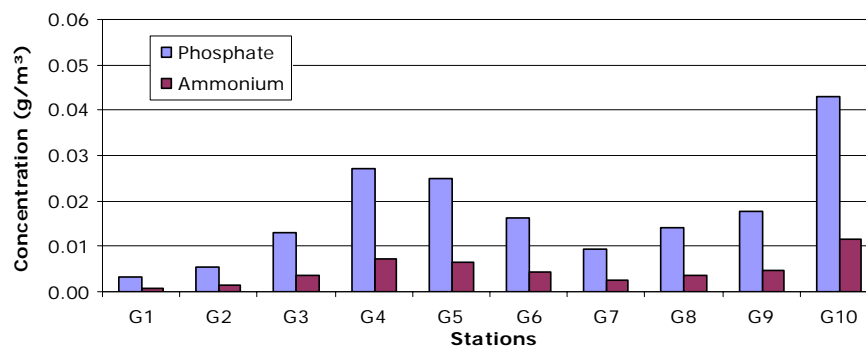


Figure 6.4: Discrepancies between scenarios 1 and 2 for ammonium and phosphate concentrations

The results show that with a given spatial remineralisation rate, the concentrations of ammonium and phosphate are elevated differently. High gradients appear in the southern part and also along the north-eastern part for ammonium. Considering the discrepancies at each measuring stations, it is found that the discrepancies are increasing towards shallow areas (G4, G5, G6, G9 and G10). In the deeper channel (G1-G3) the discrepancies are less. Concentrations increase significantly especially at station G10 which is located at

the end of the tidal channel in front of the salt marshes. It becomes thus obvious that the physicochemical sediment conditions have a strong effect on the nutrient release to the water column. Elevated ammonium concentrations appear in front of the polder basin and the sluice, which is well in keeping with the field measurements. However, freshwater inputs containing high nutrient loads may also contribute to the observed nutrient pattern. With the knowledge of the discrepancies, remineralisation fluxes can be estimated. Since measurements of the remineralisation rate are relatively difficult to perform on a large spatial scale, model application can help to assess the impact of this process to the overall area. Differing from the influence of freshwater input, the shallow water areas in the southern part of the Meldorf Bight play a substantial role for the nutrient situation due to an enhanced nutrient release resulting from the benthic remineralisation process.

6.5 Discussion of the model application

In different model applications, the influences of sewer discharge, freshwater input and benthic remineralisation on the distribution pattern of ammonium and phosphate in the water of Meldorf Bight were tested. It is shown in the simulated results that the impact of a twofold increase of nutrient loads from the sewer station is restricted to the direct vicinity of the outfall and effects mainly the nitrate concentrations. Results from the scenarios tested also show clearly the importance of freshwater discharge from the eastern polder basin as the major additional nutrient source. In contrast, the shallow water area in the southern part becomes more important as the major site for nutrient release from the sediment due to increased remineralisation intensity. From the computed gradients and the spatial field measurements it can thus be concluded that the model proves to be capable of simulating the changes in nutrient concentrations due to a specific process. From the discrepancies obtained by comparing the model results with and without the simulated process the nutrient loads induced by the process can be estimated quantitatively for the whole study area, which is hard to obtain from field measurements.

7 Conclusions and recommendations

The main objective of this study is to set-up, calibrate, validate and apply a nutrient dynamics model for the simulation of the seasonal nutrient distribution in a coastal area of the German Wadden Sea. The study area is the Meldorf Bight, situated in the south of the Northern Wadden Sea region which is subjected to a strong estuarine influence deriving from the Elbe. To fulfill this objective, purposely designed measurements were carried out. These were divided into two phases. Preliminary measurements were conducted to determine the seasonal nutrient status in terms of transported budgets at a cross-section of the main tidal channel over the tidal cycle. In a second phase intensive measuring campaigns were designed in order to assess the seasonal small scale nutrient distribution especially in the more shallow water area in which information is still inadequate. Major sinks and sources were deduced from these measurements and results were used to set-up, calibrate and validate the nutrient dynamics model.

A short-term modelling can easily capture the physical influences and provides the nutrient dynamics due to the daily tidal variation. Investigations on a longer time scale will improve our understanding of variations due to meteorological changes and estuarine processes, such as the variable discharge of the Elbe river. Additional biological and chemical processes of low intensity but high persistence will gain importance in long term modelling and should hence be taken into account. If they prove to be a key factor, a systematic monitoring should be performed. Also, a specific process may be temporarily turned off and is therefore lacking in a short term simulation. On a longer time scale, the dynamics of this process can be precisely studied and the transformation rates can be analyzed with the help of the model. In the Wadden Sea, this holds especially true for coupled benthic-pelagic processes. Results from the present investigation show clearly the importance of sedimentary processes for nutrient release, especially in the shallow tidal flat region, but the availability of information is still rather poor.

Considering the diversity of possible nutrient sinks and sources in the coastal Wadden Sea, only a limited number of processes were taken into consideration in model calibration. However, the approach adopted appears to be sufficient for the simulation of nitrate distribution. In the case of ammonium and phosphate, on the other hand, significant negative and positive discrepancies between model results and field data indicate that localized and additional sink and source processes must be taken into account in future efforts to improve the numerical model. Results of the model application show that a local specification of benthic transformation rates such as remineralisation according to the spatial sediment structure has a significant impact on the simulated concentrations in the water column. The onshore residual transport of particulate organic matter due to tidal asymmetry (Dronkers et al., 1990) in the shallow Wadden Sea results in coastal mud accumulation sites exhibiting a high remineralisation intensity with a subsequent release of high amounts of ammonium and phosphate, especially in summer. This process is enhanced by the numerous brushwood groins bordering the coastline, especially in the southern part of the study area. Further, increasing anoxia in these muddy sediments, concomitant with a seasonal increase in temperature, leads to local desorption of phosphate from the temporary iron hydroxide

sediment buffer, producing distinct spatial gradients in the Wadden Sea without the influence of freshwater discharges.

Rapid physical nutrient exchange processes between seabed sediment and the water column due to pore water leakage during the ebb tide, tidal pumping and erosion should be included in a local parametrisation. Furthermore, and in particular in long-term modelling, the uptake of nutrients by the phytoplankton and phytobenthos should be addressed as a sink during the entire growth season. This process also exhibits a pronounced spatial heterogeneity, generally depending on light availability and hence on turbidity and water depth (Tillmann et al., 2000). In a recent paper on a strategic model for nutrient simulation in the Wadden Sea, Ebenhoeh et al. (2004) has demonstrated that increasing sedimentation of particulate matter and removal of phytoplankton in the near-shore shallow parts of the area may alone produce the observed steep nutrient gradients directed towards the shoreline. The overestimation of ammonium concentrations, especially in the summer simulations, further suggests that nitrification of this nutrient species in well-oxygenated water must also be taken into consideration, as the intensity of this process is largely governed by temperature. In spring, the importance of freshwater discharge from the southern sluice should be accounted for more precisely in the ammonium and phosphate simulations.

Integration of the above-mentioned processes requires further field studies, especially regarding the identification and quantification of benthic-pelagic processes in shallow Wadden Sea areas. The intensity of gravity-driven pore water leakage on sediment slopes during the ebb tide exhibits a pronounced spatial heterogeneity and is highly dependent on the composition of benthic infauna and bioturbation (Schroeder, K., 2003). The importance of other physical exchange processes, such as density-driven osmotic exchange reactions due to evaporation in the shallow tidal pools and ditches of the intertidal area during the ebb tide, is largely unknown. The same holds true for the magnitude of direct coastal nutrient inputs by groundwater intrusion through porous sediments.

The present study indicates that scattered freshwater discharges originating from the drainage of agricultural hinterland and the release of nutrients due to the decomposition of accumulated organic matter as well as phosphate desorption from iron-hydroxides are the main reasons why riverine nutrient reduction has no effect on the hypertrophic nutrient status of the Meldorf Bight, as pointed out by Ladwig et al. (2003). It may hence be assumed that eutrophication will continue to persist in the study area. A reorientation in agricultural practice towards organic farming and crop rotation may well mitigate this problem. Modelled scenarios may also help to verify the efficiency of such countermeasures.

References

- Agatha, S., Hesse, K.-J., Nehring, S. and Lorjé, J.C., 1994. Plankton und Nährstoffe in Brackwasserbecken am Rande des Schleswig-Holsteinischen Wattenmeeres unter besonderer Berücksichtigung der Ciliaten und Dinoflagellaten-Dauerstadien sowie blütenbildender und toxischer Formen. UBA-Forschungsbericht Nr. 10802085/01.
- Aksnes, D.L., Ulvestad, K.B., Balino, B.M., Berntsen, J., Egge, J.K. and Svendsen, E., 1995. Ecological modelling in coastal waters: towards predictive physical-chemical-biological simulation models. *Ophelia*, 41, 5-35.
- Allen, J.I., Blackford, J., Holt, J., Proctor, R., Ashworth, M. and Siddorn, J., 2001. A highly spatially resolved ecosystem model for the North West European Continental Shelf. *Sarsia*, 86, 423-440.
- Anonymous, 1993. Quality status report of the North Sea. Subregion 10. The Wadden Sea, Common Wadden Sea Secretariat, Wilhelmshaven, 174 pp.
- Bedford, K.W., 1985. Selection of turbulence and mixing parameterizations for estuary water quality models. Misc. Paper, EL-85-2, U.S. Army Engineer Waterways Experiment Station, Vicksburg, MS.
- Behrendt, H., Bach, M. and Kunkel, R., 2003. Deutschlands = Nutrient emissions into river basins of Germany on the basis of a harmonized procedure, Internationale Harmonisierung der Quantifizierung von Nährstoffeeinträgen aus diffusen und punktuellen Quellen in die Oberflächengewässer e, CD-ROM, Umweltbundesamt.
- Berg van den, A.J., Ridderinkhof, H., Riegman, R., Ruurdij, P. and Lenhart, H.-J., 1996. Influence of variability in water transport on phytoplankton biomass and composition in the southern North Sea: A modelling approach(FYFY). *Continental Shelf Research*, 16(7), 907-931.
- Beusekom, J.E.E. van. and Brockmann, U.H., 1998. Transformation of phosphorus in the Elbe Estuary. *Estuaries*, 21, 518-526.
- Beusekom, J.E.E. van, Brockmann, U.H., Hesse, K.-J., Hickel, W., Poremba, K. and Tillmann, U., 1999. The importance of sediments in the transformation and turnover of nutrients and organic matter in the Wadden Sea and German Bight. *German Journal of Hydrography*, 51(2/3), 245-266.
- Beusekom, J.E.E. van, Fock, H., Jong, F. de, Diehl-Christiansen, S. and Christiansen, B., 2001. Wadden Sea Specific Eutrophication Criteria. *Wadden Sea Ecosystem*, 14, 1-115.
- Beusekom, J.E.E. van. and Jong, V.N. de, 1997. Transformation of phosphorus in the Wadden Sea: appetite formation. *German Journal of Hydrography*, 49, 297-305.
- Beusekom, J.E.E. van. and Jong, V.N. de, 1998. Retention of phosphorus and nitrogen in the Ems estuary. *Estuaries*, 21, 527-539.

Blumberg, A.F. and Mellor, G.L., 1980. A coastal numerical model, *Mathematical Modelling of Estuarine Physics*. J. Sundermann and K. Holz, Springer-Verlag, New York, 202-218.

Blumberg, A.F. and Mellor, G.L., 1987. A description of a three-dimensional coastal ocean circulation model, in *Three-Dimensional Coastal ocean Models*. Coastal and Estuarine Sciences, vol. 4, Heaps, AGU, Washington, DC, 1-16.

Boyd, C.E., 2000. *Water Quality: An Introduction*. Kluwer Academic Publishers, Massachusetts, USA.

Brow, J. and Bearman, G., 1989. *Ocean chemistry and deep-sea sediments*. Open University, Oceanography Course Team, Pergamon Press, Oxford.

Chapra, S.C., 1997. *Surface water-quality modeling*. McGraw-Hill series in water resources and environmental engineering, New York.

Delhez, E.J.M. and Martin, G., 1994. 3D modelling of hydrodynamic and ecohydrodynamic processes on the north-western European continental shelf. *Bulletin de la Societe Royale des Sciences de Liege*, 63(1-2), 5-64.

Dick, S. and Schönfeld, W., 1996. Water Transport and Mixing in the North Frisian Wadden Sea-Results of Numerical Investigations. *German Journal of Hydrography*, 48(1), 27-48.

Dick, S., Brockmann, U.H., Beusekom, J.E.E. van, Fabiszisky, B., George, M., Hentschke, U., Hesse, K-J., Mayer, B., Nitz, T., Polhmann, T., Poremba, K., Schaumann, K., Schönfeld, W., Starke, A., Tillmann, U. and Weide, G., 1999. Exchange of matter and energy between the Wadden Sea and the coastal waters of the German Bight—Estimations based on numerical simulations and field measurements. *German Journal of Hydrography*, 51(2/3), 181-219.

Dickinson, R.E., Huber, W.C., and Pollman, C.D., 1992. *Lake Okeechobee phosphorus dynamics study-Volume X: Modelling of phosphorus dynamics in the water column*. West Palm Beach, FL: South Florida Water Management District.

Drago, M., Cescon, B. and Iovenitti, L., 2001. A three dimensional numerical model for eutrophication and pollutant transport. *Ecological Modelling*, 145, 17-34.

Dronkers, J., van Alphen, J.S. and Borst, J.C., 1990. Suspended sediment transport processes in the Southern North Sea. In: Cheng, R.T. (Ed.), *Residual Currents and Long-term Transport*, Coastal and Estuarine Studies 38, American Geophysical Union, Washington, DC.

Ebenhoeh, W., Kohlmeier, C., Baretta, J.W. and Flöser, G., 2004. Shallowness may be a major factor generating nutrient gradients in the Wadden Sea. *Ecological Modelling*, 174.

Ehlers, J., 1988, *The morphodynamics of the Wadden Sea*, A. A. Balkema, Rotterdam.

Environmental and Hydraulics Laboratories, 1986. CE-QUAL-W2: A numerical two-dimensional, laterally averaged model of hydrodynamics and water quality. Instruction Report E-86-5, U.S. Army Corps of Engineers Waterways Experiment Station, Vicksburg, MS.

Falconer, R.A. and Lin, B., 1997. Three-dimensional modelling of water quality in the Humber Estuary. *Wat. Res.*, 31(5), 1092-1102.

Fasham, M.J.R., Ducklow, H.W. and McKelvie, S.M., 1990. A nitrogen-based model of plankton dynamics in the oceanic mixed layer. *Journal of Marine Research*, 48, 591-639.

Fennel, K., 1999. Convection and the Timing of Phytoplankton Spring Blooms in the Western Baltic Sea. *Estuarine, Coastal and Shelf Sciences*, 49, 113-128.

Fennel, W. and Naumann, T., 1996. The mesoscale variability of nutrients and plankton as seen in a coupled model. *German Journal of Hydrography*, 48(1), 49-71.

Fock, H., Jong, F. de, Diehl-Christiansen, S. and Christiansen, B., 2001. Wadden Sea Specific Eutrophication Criteria. *Wadden Sea Ecosystem*, 14, 1-115.

Gewässerbeobachtung Zahlentafel, 1999-2001. Landesamt für Natur und Umwelt des Landes Schleswig-Holstein, Germany.

Grasshoff, K., 1983. *Methods of Seawater Analysis*. 2nd Revised and Extended Edition, Verlag Chemie GmbH, Germany.

Hall, R.W., 1987. Application of CE-QUAL-W2 to the Savannah River Estuary. Technical Report EL-87-4, U.S. Army Corps of Engineers Waterways Experiment Station, Vicksburg, MS.

Hartsuiker, G., 1997. Deutsche Bucht and Dithmarschen Bucht: Set-up and calibration of tidal flow models. Delft, DELFT HYDRAULICS, Report z428.

Helder, W., 1974. The cycle of dissolved inorganic nitrogen compounds in the Wadden Sea. *Neth. J. Sea Res.*, 8, 154-173.

Hesse, K-J., Hentschke, U. and Brockmann, U., 1992. A synoptic study of nutrient and phytoplankton characteristics in the German Wadden Sea with respect to coastal eutrophication. *Marine Eutrophication and Population Dynamics*, 25th European Marine Biology Symposium, Ferrara, 45-53.

Hesse, K-J., Tillmann, U. and Brockmann, U. H., 1995. Nutrient-phytoplankton relations in the German Wadden Sea. *ICES CM/T*, 8-13.

Hickel, W., 1989. Temporal variability of micro and nanoplankton in the German Bight. *ICES J. Mar. Sci.*, 55, 600-609.

Hydroqual, 1987. A steady state coupled hydrodynamic/water quality model of the eutrophication and anoxia process in Chesapeake Bay, Prepared for the U.S. Environmental Protection Agency Chesapeake bay program, Annapolis, MD.

Jørgensen, S.E., 1994. Models as instruments for combination of ecological theory and environmental practice. *Ecological Modelling*, 75/76, 5-20.

Jørgensen, S.E., 1996. *Handbook of environmental and ecological modeling*. Lewis.

Johnson, B.H., Trawie, M.J. and Kee, P.G., 1989. A numerical study of the effect of channel deepening on shoaling and salinity intrusion in the Savannah Estuary. Technical Report HL-89-26, U.S. Army Corps of Engineers Waterways Experiment Station, Vicksburg, MS.

Jonge, V.N. de. and Postma, H., 1974. Phosphorus compounds in the Dutch Wadden Sea. *Journal of Sea Research*, 8, 139-153.

Jørgensen, S.E., 1994. Models as instruments for combination of ecological theory and environmental practice. *Ecological Modelling*, 75/76, 5-20.

Kishi, M.J. and Ikeda, S., 1986. Population dynamics of red tide organisms in eutrophicated coastal waters-numerical experiment of phytoplankton bloom in the East Seto Inland Sea. *Ecological Modelling*, 31, 145-174.

Kolmogorov, A., 1942. Equations of turbulence motion of an incompressive fluid. *Izv. Akad. Nauk. SSR., Seria Fizicheska Vi*, No. 1-2, 56-58. (English translation: Imperial College, Mechanical Engineering Department Report. ON/6, 1968).

Kühn, W. and Radach, G., 1997. A one-dimensional physical-biological model study of the pelagic nitrogen cycling during the spring bloom in the northern North Sea (FLEX'76). *Journal of Marine Research*, 55, 687-734.

Ladwig, N., Hesse, K.-J., Colijn, F. and Tillmann, U., 2003. Has the eutrophic state of German Wadden Sea waters changed over the past 10 years due to nutrient reduction?, *ICES Marine Science Symposia*, 219.

Lalli, C.M. and Parsons, T., 1993. *Biological oceanography: an introduction*. Pergamon Press, Oxford.

Lenhart H.J., 1999. Eutrophierung im kontinentalen Küstenbereich der Nordsee, Reduktionsszenarien der Flusseinträge von Nährstoffen mit dem Ökosystem-Modell ERSEM. *Berichte aus dem Zentrum für Meeres- und Klimaforschung, Reihe B: Ozeanographie*, 35, 169.

Lenhart H.J., Radach, G. and Ruardij, P., 1997. The effects of river input on the ecosystem dynamics in the continental coastal zone of the North Sea using a box refined ecosystem model ERSEM. *Journal of Sea Research*, 38, 249-274.

Lewis, E.L., 1980. The Practical Salinity Scale 1978 and its antecedents. *IEEE Journal of Ocean Engineering*, 5(1), 3-8.

Lohse, L., Kloosterhuis, H.T., Raaphorst van, W. and Helder, W., 1996. Denitrification rates as measured by the isotope pairing method and by the acetylene inhibition technique

in continental shelf sediments of the North Sea. *Marine Ecology Progress Series*, 132, 169-179.

Los, F.J., 1991. Mathematical simulation of algae blooms by the model BLOOM II. Documentation report, Delft Hydraulics Laboratory, The Netherlands.

Luyten, P.J., Jones, J.E., Proctor, R., Tabor, A., Tett, P. and Wild-Allen, K., 1999. COHERENS – A Coupled Hydrodynamical – Ecological Model for Regional and Shelf Seas. User Documentation. MUMM Report, Management Unit of the Mathematical Models of the North Sea, Belgium.

MANS, 1991. MANS-Management analysis of the North Sea: Scientific workshop on eutrophication models. Report Rijkswaterstaat, GWW(91. 213), 26.

Martin, J.L. and McCutcheon, S.C., 1999. Hydrodynamics and Transport for Water Quality Modeling. Lewis Publishers, USA.

Mayerle, R. and Palacio, C., 2002. Open boundary condition approaches for near coastal area models. Proceedings of the 13th congress of the Asia and Pacific division of IAHR.

Mayerle, R., Razakafoniaina, N., Palacio, C. and Pramono, G.H., 2002. Bedforms and Equivalent Roughness Sizes in tidal channel. River Flow 2002, IAHR, Louvain-la-Neuve, Belgium.

Meeder, J.P., 1998. Numerical simulation of chemical reactions in point-source plumes. Dissertation, Delft University Press, The Netherlands.

Mellor, G.L. and Yamada, T., 1982, Development of a turbulence closure model for geophysical fluid problems. *Reviews of Geophysics and Space Physics*, 20 (4), 851-875.

Moll, A., 1995. Regionale Differenzierung der Primärproduktion in der Nordsee: Untersuchungen mit einem drei-dimensionalen Modell. *Berichte aus dem Zentrum für Meeres- und Klimaforschung. Reihe B: Ozeanographie*, 19, 151.

Moll, A., 1997b, Modelling primary production in the North Sea. *Oceanography*, 10(1), 24-26.

Moll, A. and Radach G., 2001. Synthesis and New Conception of North Sea Research (SYCON): Review of three-dimensional ecological modelling related to the North Sea shelf system. Zentrum für Meeres – und Klimaforschung der Universität Hamburg, Germany.

Moll, A., 1998a. Assessment of three-dimensional physical-biological ECOHAM1 simulations by quantified validation for the North Sea with ICES and ERSEM data. *ICES CM 1998 (Q5)*, 1-14.

Moll, A., 1998b. Regional distribution of primary production in the North Sea simulated by a three-dimensional. *Journal of Marine Systems*, 16(1-2), 151-170.

Neumann, T., 2000. Toward a 3D – ecosystem model of the Baltic Sea. *Journal of Marine Systems*, 25, 405-419.

OSPAR et al., 1988. Report of the ASMO modelling workshop on eutrophication issues, The Hague, The Netherlands, OSPAR Commission Report, 102.

Palacio, C., Winter, C. and Mayerle, R., 2001. Set-up of a hydrodynamic model for the Meldorf Bight. World water & environmental resources congress, ASCE/EWRI, Orlando, USA.

Pätsch, J. and Radach, G., 1997. Long-term simulation of the eutrophication of the North Sea: Temporal development of nutrients, chlorophyll and primary production in comparison to observations. *Journal of Sea Research*, 38, 275-310.

Poebandono and Mayerle, R., 2003. Effectiveness of acoustic backscatter measurements from acoustical profilers for estimation of suspended sediment concentration. Proceedings of the IEEE 7th Working Conference on Current Measurement Technology, San Diego, USA.

Poerbandono, 2003. Measurement and Modelling of Sediment Transport in the Meldorf Bight Tidal Channels,, German North Sea coast. Ph.D thesis, University of Kiel, Germany.

Postma, H., 1954. Hydrography of the Dutch Wadden Sea. *Archives néerlandaises de Zoologie*, 10, 405-511.

Postma, H., 1966. The cycle of nitrogen in the Wadden Sea and adjacent areas. *Neth. J. Sea. Res.*, 3, 186-221.

Postma, H., 1983. Hydrography of the Wadden Sea: Movements and properties of water and particulate matter. *Ecology of the Wadden Sea*, A.A. Balkema, Rotterdam, 1(I), Rep. 2, 1-75.

Prandtl, L., 1945. Über ein neues Formelsystem für die ausgebildete Turbulenz. *Nachr. Akad. Wiss., Gottingen, Math-Phy. Klasse*, 6.

Radach G. and Moll, A., 1990. State of the art in algal bloom modelling. *Water pollution Research Report*, 12, 115-149.

Radach, G. and Lenhart, H.-J., 1995. Nutrient dynamics in the North Sea: Fluxes and budgets in the water column derived from ERSEM. *Netherlands Journal of Sea Research*, 33 (3-4), 301-335.

Radach, G. and Moll, A., 1993, Estimation of variability of production by simulating annual cycles of phytoplankton in the central North Sea. *Progress in Oceanography*, 31(4), 339-419.

Rajar, R. and Cetina, M., 1997. Hydrodynamic and water quality modelling: An experience. *Ecological Modelling*, 101, 195-207.

Reimers, H.C., 1999. Wirkungsweise von Buschlahnungen auf den Sedimenthaushalt von aufwachsenden Deichvorländern, Research and Technology Centre Westcoast, University of Kiel, Büsum Germany, Report no. 17, In German.

Reineck, H.E., 1978. Dass Watt, Ablagerungs und Lebensraum, Kramer, Frankfurt, Second edition, In German.

Rick, H.-J., Baumann, M.E.M., Beil, J., Brasse, S., Brockmann, U.H., Buchholz, F., Diel-Christiansen, S., Duerselen, C.-D., Fehner, U., Gaertner, U., George, M., Goebel, A., Hesse, K.-J., Kabatnik, C., Klawon, A., Kopp, R., Koschinski, P., Krause, M., Ladwig, N., Mehrkuehler, C., Mueller, R., Poremba, K., Raabe, T., Reimer, A., Rieling, T., Rick, S., Schaumann, K., Schuett, M., Suedermann, J., Tillmann, A., Tillmann, U., Weber, A., Weide, G. and Wolff, C., 1999. Balances and imbalances of production and respiration in German Bight pelagic systems. *Dt. Hydrogr. Z.*

Ruardij, P., Haren van, H., and Ridderinkhof, H., 1997. The impact of thermal stratification on phytoplankton and nutrient dynamics in shelf seas: a model study. *Journal of Sea Research*, 38, 311-331.

Schnoor, J.L., 1996. Environmental modeling: fate and transport of pollutants in water, air and soil. A Wiley-interscience publication, New York.

Schröder, K., 2002. Sediment-Pore water analysis at the tidal flat area of the Meldorf Bight. Training report, Università Ca' Foscari di Venezia, Italy.

Schröder, K., 2003. Eutrophic phenomena in the Wadden Sea of Schleswig-Holstein, Germany: assessment and quantification of the porewater leakage process in the intertidal flat. Master thesis, Università Ca' Foscari di Venezia, Italy.

Skogen, M.D. and Moll, A., 2000. Interannual variability of the North Sea primary production: comparison from two model studies. *Continental Shelf Reseach*, 20(2), 129-151.

Skogen, M.D., Aure, J., Danielssen, D. and Svendsen, E., 1998a. Natural fertilisation of the marine environment – modelling of Glomma Flood 1995. *Sarsia*, 83, 361-372.

Skogen, M.D., Eriksrod, G. and Svendsen, E., 1997. Quantification of transports to Skagerrak. In E. Özsoy, & A. Mikaelyan (Eds.), *Sensitivity to change: Black Sea, Baltic Sea, North Sea*, Amsterdam:Kluwer Academic Publishers, 327-339.

Skogen, M.D., Svendsen, E. and Ostrowski, M., 1998b. Quantifying volume transports during SKAGEX with the Norwegian ecological model system. *Continental Shelf Research*, 17(5), 1817-1837.

Spiegel, F., 1997. Die Tidebecken des Schleswig-holsteinischen Wattenmeers: Morphologische Strukturen und Anpassungsbedarf bei weiter steigendem Meeresspiegel. Bericht Nr. 14, Forschungs und Technologies zentrum Westküste, Germany.

Streeter, V. L. and Wylie, E.B., 1985. *Fluid mechanics*, McGraw-Hill, New York.

Sündermann, J., Hesse, K.-J. and Beddig, S., 1999. Coastal mass and energy fluxes in the southeastern North Sea, *German Journal of Hydrography*, 51(2/3), 113-132.

SYNDWATT, 1992. Interim Report SYNDWAT. 124-132.

Tamasalu, R., 1996. Coupled 3D hydrodynamic and ecosystem model finest. EMI Report Series – Estonian Marine Institute, 5, 113.

Tamasalu, R., 1998. The coupled 3D hydrodynamic and ecosystem model finest. MERI Report Series of the Finnish Institute of Marine Research, 35, 166.

Tillmann, U., Hesse, K.-J. and Colijn, F., 2000. Planktonic primary production in the German Wadden Sea. *Journal of Plankton Research*, 22(7), 1253-1276.

Topçu, D.H. and Brockmann, U., 2001. Synthesis and New Conception of North Sea Research (SYCON): Fluxes of Matter. Zentrum für Meeres – und Klimaforschung der Universität Hamburg, Germany.

Verboom, G.K., Ronde, J.G. de. and Dijk, R.P. van, 1992. A fine grid tidal flow and storm surge model of the North Sea. *Continental Shelf Research*, 12, 213-223.

Walsh, J. J., Dieterle, D.A. and Meyers, M.B., 1988. A simulation analysis of the fate of phytoplankton within the Mid-Atlantic Bight. *Continental Shelf Research*, 8(5-7), 757-787.

WL Delft Hydraulics, 1996a. GPP. User Manual.

WL Delft Hydraulics, 1996b. QUICKIN. User Manual.

WL Delft Hydraulics, 1996c. RGFGRID. User Manual.

WL Delft Hydraulics, 2003. DELFT3D-WAQ. User Manual, release 4.00.

WL Delft Hydraulics, 2003a. DELFT3D-FLOW. User Manual, release 3.10.

Appendix A

Results of field measurements

Table A.1: NO₂ concentrations at stations G and H of the measuring campaigns performed in 2001

Date	Tide	Concentration (µmol/l)							
		Station G				Station H			
		Free Surface		Bottom		Free Surface		Bottom	
		Mean	SD	Mean	SD	Mean	SD	Mean	SD
21.06.01	Flood	1.05	0.49	0.75	0.13	0.70	0.2	1.01	0.23
	Ebb	0.72	0.23	0.75	0.19	0.64	0.14	0.93	0.24
29.06.01	Flood	0.22	0.09	0.33	0.09	-	-	-	-
	Ebb	0.17	0.03	0.28	0.11	0.25	0.14	0.28	0.07
12.09.01	Flood	1.90	0.36	2.15	0.49	1.72	0.18	2.04	0.33
	Ebb	1.74	0.38	1.97	0.74	1.53	0.28	1.79	0.34
14.11.01	Flood	4.64	1.69	4.89	0.54	4.71	0.82	4.72	0.67
	Ebb	4.83	0.89	5.23	1.10	4.84	0.42	4.08	0.40

Table A.2: NO₃ concentration at stations G and H of the measuring campaigns performed in 2001

Date	Tide	Concentration (µmol/l)							
		Station G				Station H			
		Free Surface		Bottom		Free Surface		Bottom	
		Mean	SD	Mean	SD	Mean	SD	Mean	SD
21.06.01	Flood	14.64	4.89	18.34	3.60	20.65	3.63	21.36	3.69
	Ebb	17.68	5.99	19.27	4.65	21.67	4.84	18.94	2.82
29.06.01	Flood	0.44	0.17	1.60	0.17	-	-	-	-
	Ebb	0.70	0.32	1.44	0.39	0.62	0.29	1.84	1.17
12.09.01	Flood	11.38	1.80	10.18	1.86	13.79	2.59	12.90	1.84
	Ebb	12.41	2.91	8.31	1.52	11.84	2.04	10.10	0.33
14.11.01	Flood	40.83	5.20	32.28	4.11	43.21	2.70	37.75	1.91
	Ebb	42.57	6.22	29.50	1.74	45.38	4.08	36.19	1.14

Table A.3: NH₄ concentration at stations G and H of the measuring campaigns performed in 2001

Date	Tide	Concentration (µmol/l)							
		Station G				Station H			
		Free Surface		Bottom		Free Surface		Bottom	
		Mean	SD	Mean	SD	Mean	SD	Mean	SD
21.06.01	Flood	1.69	0.69	2.03	0.59	1.97	0.44	1.77	0.77
	Ebb	0.97	0.39	1.24	0.51	1.35	0.62	1.09	0.39
29.06.01	Flood	0.18	0.08	0.16	0.08	-	-	-	-
	Ebb	0.34	0.12	0.09	0.08	0.22	0.06	0.38	0.25
12.09.01	Flood	5.94	0.61	5.90	1.21	6.20	0.70	5.43	0.65
	Ebb	5.50	1.38	6.26	0.45	5.75	0.46	5.05	0.38
14.11.01	Flood	3.72	0.85	4.04	0.54	3.69	0.55	4.01	2.42
	Ebb	4.46	0.36	4.37	0.45	3.79	0.34	3.82	0.34

Table A.4: DIN concentration at stations G and H of the measuring campaigns performed in 2001

Date	Tide	Concentration ($\mu\text{mol/l}$)			
		Station G		Station H	
		Free Surface	Bottom	Free Surface	Bottom
21.06.01	Flood	17.38	21.12	23.32	24.14
	Ebb	19.37	21.26	23.66	20.96
29.06.01	Flood	0.84	2.09	-	-
	Ebb	1.21	1.81	1.09	2.5
12.09.01	Flood	19.22	18.23	21.71	20.37
	Ebb	19.65	16.54	19.12	16.94
14.11.01	Flood	49.19	41.21	51.61	46.48
	Ebb	51.86	39.1	54.01	44.09

Table A.5: PO₄ concentration at stations G and H of the measuring campaigns performed in 2001

Date	Tide	Concentration ($\mu\text{mol/l}$)							
		Station G				Station H			
		Free Surface		Bottom		Free Surface		Bottom	
		Mean	SD	Mean	SD	Mean	SD	Mean	SD
21.06.01	Flood	1.19	1.01	1.11	0.37	0.76	0.12	1.11	0.38
	Ebb	0.71	0.57	0.90	0.25	0.74	0.39	0.99	0.43
29.06.01	Flood	0.60	0.21	0.82	0.21	-	-	-	-
	Ebb	0.45	0.10	0.82	0.18	0.45	0.10	0.82	0.18
12.09.01	Flood	2.09	0.22	2.55	0.51	1.91	0.24	2.49	0.31
	Ebb	2.10	0.20	1.83	0.24	2.00	0.20	2.49	0.29
14.11.01	Flood	2.75	0.59	2.92	0.19	2.85	0.49	1.74	0.36
	Ebb	2.63	0.38	3.70	1.22	2.97	0.32	2.69	1.28

Table A.6: Nutrient concentrations of the grid measurement of the measuring campaigns performed in winter 2002

Date	Stations	NO ₂ (gN/m ³)		NO ₃ (gN/m ³)		NH ₄ (gN/m ³)		PO ₄ (gP/m ³)	
		Before HW	After HW	Before HW	After HW	Before HW	After HW	Before HW	After HW
13-02-02	G1	0.0856	0.0709	2.2423	2.3453	0.0787	0.0961	0.0603	0.0578
	G2	0.0793	0.0898	2.1935	2.1739	0.0913	0.1023	0.0603	0.0583
	G3	0.0819	0.0816	2.2014	2.5828	0.0898	0.1128	0.0603	0.0632
	G4	0.1273	0.0982	2.5908	2.5594	0.1495	0.1359	0.0861	0.0760
	G5	0.0945	0.1207	2.4085	2.8368	0.1393	0.1192	0.0765	0.0777
	G6	0.0972	0.0818	2.3702	2.3195	0.1248	0.1131	0.0627	0.0594
	G7	0.0845	0.0764	2.3041	2.0965	0.1147	0.1100	0.0612	0.0587
	G8	0.1025	0.0869	2.3678	2.3563	0.1127	0.1224	0.0693	0.0605
14-02-02	G1	0.0713	0.0705	1.8684	2.1674	0.0754	0.0812	0.0738	0.0581
	G2	0.0822	0.0819	1.5246	2.2471	0.1049	0.1414	0.0417	0.0722
	G3	0.0760	0.0822	2.3192	2.2204	0.1093	0.1245	0.0594	0.0654
	G4	0.0933	0.0885	2.3278	2.2138	0.1306	0.1358	0.0749	0.0685
	G5	0.0771	0.0879	2.4088	2.3168	0.1850	0.1886	0.1100	0.0986
	G6	0.0838	0.0809	2.3006	2.4126	0.1523	0.1585	0.0744	0.0840
	G7	0.0783	0.0777	2.1958	2.1218	0.1233	0.1158	0.0620	0.0626
	G8	0.0843	0.0806	2.2670	2.2490	0.1324	0.1185	0.0655	0.0629

Table A.7: Salinity analysis of the grid measurement of the measuring campaigns performed in winter 2002

Date	Stations	Salinity (PSU)	
		Before high water	After high water
13-02-02	G1	14.90	14.20
	G2	15.40	15.20
	G3	14.40	14.70
	G4	12.20	11.60
	G5	12.10	13.40
	G6	13.30	14.10
	G7	13.20	14.60
	G8	13.40	12.70
14-02-02	G1	15.30	15.90
	G2	15.00	12.90
	G3	14.20	14.80
	G4	12.50	13.50
	G5	9.10	10.00
	G6	12.00	12.70
	G7	14.10	14.60
	G8	13.70	14.50

Table A.8: Nutrient concentrations of the landbased measurements of the measuring campaigns performed in winter 2002

Date	Stations	Salinity	NO ₂	NO ₃	NH ₄	PO ₄
		(PSU)	gN/m ³	gN/m ³	gN/m ³	gP/m ³
13-02-02	L1	10.5	0.1918	2.1486	0.0812	0.4978
	L2	11.6	0.1299	2.5452	0.1457	0.1213
	L3	11.1	0.1864	2.2278	0.2088	0.1081
	L4	2	0.0765	3.4880	0.3334	0.3965
	L5	2	0.0734	4.0587	0.3095	0.4096
	L6	6.9	0.1240	2.9252	0.3227	0.2384
	L7	13.7	0.0836	2.6522	0.2745	0.2501
	L8-A	10.8	0.0825	0.9772	0.0526	0.0594
	L8-B	2	0.0491	3.1085	0.2223	0.2951
	L9	10.2	0.0965	3.0524	0.1989	0.1078
	L10	10.2	0.1127	2.5584	0.1836	0.1080
	L11	12	0.1028	2.4080	0.1408	0.0772
	L12	12.5	0.1095	2.3727	0.1621	0.0868
	L13	13.9	0.0943	2.4920	0.1323	0.0621
	L14	13.5	0.0938	2.4777	0.1173	0.0675
L15	14.9	0.0853	2.3144	0.1078	0.0731	
14-02-02	L1	12.6	0.1117	2.7632	0.1676	0.1031
	L2	13.4	0.1272	2.3064	0.1846	0.1027
	L3	11.4	0.0219	0.2850	0.7961	0.0622
	L4	2.1	0.0646	2.7812	0.5281	0.5961
	L5	2	0.0658	3.0369	0.2558	0.4778
	L6	7.4	0.1277	2.4314	0.3275	0.2334
	L7	10	0.0900	2.3023	0.1873	0.1152

Table A.9: Nutrient concentrations at landbased stationary measurements of the measuring campaigns performed in winter 2002

Stations	NO ₂ (gN/m ³)		NO ₃ (gN/m ³)		NH ₄ (gN/m ³)		PO ₄ (gP/m ³)	
	Mean	SD	Mean	SD	Mean	SD	Mean	SD
Buesum Mole	0.1110	0.0146	2.1617	0.5234	0.1273	0.0166	0.0944	0.0124
Sewage plant	0.0702	0.0123	8.7207	2.6230	0.0705	0.0210	0.0534	0.0126
Outfall	0.0816	0.0138	3.1174	1.0359	0.1071	0.0204	0.0650	0.0081

Table A.10: Means and standard deviations of nutrient concentrations at the ship stationary stations of the measuring campaigns performed in winter 2002

Stations	Sampling Type	NO ₂ (gN/m ³)		NO ₃ (gN/m ³)		NH ₄ (gN/m ³)		PO ₄ (gP/m ³)	
		Mean	SD	Mean	SD	Mean	SD	Mean	SD
Ship 1	Surface	0.0948	0.0214	2.0028	0.2689	0.1119	0.0133	0.0835	0.0113
	Bottom	0.1005	0.0218	2.0275	0.3605	0.1109	0.0044	0.0784	0.0099
Ship 2	Surface	0.1146	0.0242	2.1408	0.5197	0.1362	0.0293	0.0854	0.0139
	Bottom	0.1090	0.0170	1.9320	0.1833	0.1424	0.0108	0.1005	0.0159

Table A.11: Nutrient concentrations of the grid measurement of the measuring campaigns performed in spring 2002

Date	Stations	NO ₂ (gN/m ³)		NO ₃ (gN/m ³)		NH ₄ (gN/m ³)		PO ₄ (gP/m ³)	
		Before HW	After HW	Before HW	After HW	Before HW	After HW	Before HW	After HW
7-05-02	G1	0.0164	0.0153	0.8692	0.7161	0.0147	0.0143	0.0325	0.0332
	G2	0.0129	0.0169	0.9313	0.7308	0.0112	0.0097	0.0286	0.0368
	G3	0.0154	0.0310	0.7400	0.7096	0.0109	0.0594	0.0340	0.0656
	G4	0.0182	0.0532	0.8198	0.7121	0.0136	0.1845	0.0481	0.1284
	G5	0.0253	0.0554	0.9048	0.9278	0.0624	0.1993	0.0592	0.1344
	G6	0.0236	0.0548	0.7374	0.8555	0.0325	0.2048	0.0663	0.1253
	G7	0.0112	0.0394	0.7942	0.8897	0.0084	0.1185	0.0276	0.0623
	G8	0.0198	0.0250	0.8619	0.6037	0.0233	0.0097	0.0445	0.0376
	G9	0.0095	-	0.7915	-	0.0107	-	0.0271	-
	G10	0.0156	-	1.0326	-	0.0278	-	0.0396	-
8-05-02	G1	0.0103	0.0212	0.7585	0.7222	0.0176	0.0156	0.0324	0.0404
	G2	0.0107	0.0109	0.6875	0.7802	0.0061	0.0027	0.0279	0.0272
	G3	0.0092	0.0135	0.8285	0.7585	0.0047	0.0035	0.0309	0.0318
	G4	0.0198	0.0284	0.7509	0.6970	0.0268	0.0604	0.0392	0.0645
	G5	0.0216	0.0312	0.6318	0.6971	0.0789	0.0928	0.0723	0.0711
	G6	0.0186	0.0282	0.8456	0.7583	0.0242	0.0762	0.0441	0.0709
	G7	0.0104	0.0150	0.7628	0.6838	0.0042	0.0072	0.0334	0.0345
	G8	0.0135	-	0.7814	-	0.0138	-	0.0397	-
	G9	0.0123	0.0187	0.7902	0.6996	0.0029	0.0125	0.0287	0.0360
	G10	0.0251	0.0420	0.8388	0.6661	0.0613	0.1086	0.0724	0.1096

Table A.12: Salinity analysis of the grid measurement of the measuring campaigns performed in spring 2002

Date	Stations	Salinity (PSU)	
		Before high water	After high water
7-05-02	G1	20.50	19.40
	G2	22.10	19.50
	G3	19.20	19.30
	G4	21.00	16.10
	G5	18.70	14.80
	G6	20.70	13.60
	G7	20.00	16.30
	G8	20.20	21.00
	G9	16.90	-
	G10	19.30	-
8-05-02	G1	21.40	19.80
	G2	22.00	21.80
	G3	21.80	21.40
	G4	23.00	18.90
	G5	19.20	18.40
	G6	21.10	19.20
	G7	22.00	22.50
	G8	23.60	-
	G9	21.40	21.10
	G10	20.40	18.90

Table A.13: Nutrient concentrations of the landbased measurements of the measuring campaigns performed in spring 2002

Date	Stations	Salinity	NO ₂	NO ₃	NH ₄	PO ₄	
		(PSU)	gN/m ³	gN/m ³	gN/m ³	gP/m ³	
7-05-02	L1	24.3	0.0251	0.5790	0.0819	0.0577	
	L2	18.6	0.0944	0.2072	0.2975	0.0872	
	L3	20.7	0.0086	0.0421	0.0335	0.0851	
	L4	18.8	0.0442	0.0448	0.3915	0.5242	
	L5	3.3	0.1904	2.1988	0.5346	0.9296	
	L6	14	0.1172	0.4785	0.7096	0.3911	
	L7	12	0.1514	0.7953	0.7096	0.3762	
	L8-A	9.4	0.1166	0.9717	0.2593	0.2670	
	L8-B	2	0.0894	1.8098	0.3847	0.2738	
	L9	27.6	0.1713	0.6183	0.5233	0.1186	
	L10	18.7	0.0886	0.3272	0.7096	1.5897	
	L11	18.9	0.0266	0.2459	0.0946	0.0999	
	L12	19.5	0.1744	0.2629	0.2785	0.5162	
	L13	19.9	0.1169	0.3848	0.1486	0.1217	
	L14			-	-	-	-
L15	19.3	0.0180	0.5565	0.0323	0.0484		
8-05-02	L1	20.2	0.0272	0.5037	0.0808	0.0695	
	L2	16	0.0787	0.1849	0.2645	0.0849	
	L3	17.2	0.0055	0.0195	0.1517	0.0564	
	L4			-	-	-	-
	L5	13.1	0.0779	1.5672	0.3594	0.2785	
	L6	16.4	0.0920	0.8923	0.2533	0.1850	
	L7	17.9	0.0594	0.8170	0.2868	0.1450	
	L8-A	10.3	0.0916	0.9805	0.3303	0.2343	
	L8-B	2	0.1330	1.0893	0.3974	0.3834	
	L9	21	0.0272	0.8082	0.0458	0.0560	
	L10	22	0.0305	0.7260	0.0958	0.1111	
	L11	20.1	0.0556	0.7785	0.1920	0.1511	
	L12	20.5	0.1598	0.3118	0.4377	0.1477	
	L13	21.3	0.1274	0.4461	0.1787	0.1546	
	L14	20.9	0.0245	0.6384	0.0370	0.0496	
L15	19.7	0.0173	0.5326	0.0342	0.0397		

Table A.14: Nutrient concentrations at landbased stationary measurements of the measuring campaigns performed in spring 2002

Stations	NO ₂ (gN/m ³)		NO ₃ (gN/m ³)		NH ₄ (gN/m ³)		PO ₄ (gP/m ³)	
	Mean	SD	Mean	SD	Mean	SD	Mean	SD
Sewage plant	0.0838	0.0298	4.4680	0.2142	0.1188	0.0311	0.0196	0.0085
Outfall	0.0315	0.0101	0.9461	0.2157	0.1537	0.1094	0.0643	0.0125

Table A.15: Nutrient concentrations at the ship stationary stations of the measuring campaigns performed in spring 2002

Stations	Sampling Type	NO ₂ (gN/m ³)		NO ₃ (gN/m ³)		NH ₄ (gN/m ³)		PO ₄ (gP/m ³)	
		Mean	SD	Mean	SD	Mean	SD	Mean	SD
Ship 1	Surface	0.0188	0.0037	0.7468	0.0632	0.0071	0.0047	0.0267	0.0059
	Bottom	0.0169	0.0015	0.7266	0.0622	0.0105	0.0044	0.0266	0.0035
Ship 2	Surface	0.0142	0.0036	0.8337	0.0872	0.0130	0.0087	0.0343	0.0084
	Bottom	0.0144	0.0053	0.7916	0.0535	0.0162	0.0137	0.0359	0.0107
Automatic Sampler	Surface	0.0252	0.0077	0.7544	0.1077	0.0348	0.0254	0.0433	0.0099
	Bottom	-	-	-	-	-	-	-	-

Table A.16: Nutrient concentrations of the grid measurement of the measuring campaigns performed in summer 2002

Date	Stations	NO ₂ (gN/m ³)		NO ₃ (gN/m ³)		NH ₄ (gN/m ³)		PO ₄ (gP/m ³)	
		Before HW	After HW	Before HW	After HW	Before HW	After HW	Before HW	After HW
21-08-02	G1	0.0244	0.0238	0.2785	0.2144	0.0273	0.0363	0.1038	0.1123
	G2	0.0318	0.0278	0.2191	0.1762	0.0341	0.0439	0.1011	0.1075
	G3	0.0253	-	0.2360	-	0.0410	-	0.0782	-
	G4	0.0265	0.0334	0.2250	0.1574	0.0503	0.0357	0.1169	0.1601
	G5	0.0310	0.0286	0.2059	0.1717	0.0512	0.0459	0.1353	0.1351
	G6	0.0205	0.0266	0.2066	0.1825	0.0482	0.0344	0.1050	0.1130
	G7	0.0258	0.0212	0.2031	0.1941	0.0425	0.0357	0.0621	0.1023
	G8	0.0233	0.0369	0.2078	0.1455	0.0404	0.0377	0.0869	0.1633
	G9	0.0282	0.0293	0.1963	0.1682	0.0413	0.0347	0.0676	0.1496
	G10	0.0358	-	0.1410	-	0.0461	-	0.1394	-
22-08-02	G1	0.0151	0.0264	0.2393	0.2838	0.0355	0.0134	0.0670	0.0839
	G2	0.0245	0.0240	0.2800	0.2201	0.0231	0.0176	0.1033	0.1011
	G3	0.0172	0.0265	0.2002	0.2061	0.0267	0.0179	0.0815	0.1158
	G4	0.0318	0.0249	0.2210	0.1136	0.0437	0.0315	0.1227	0.1750
	G5	0.0284	0.0279	0.2074	0.1669	0.0431	0.0297	0.1373	0.1372
	G6	0.0268	0.0300	0.2264	0.1689	0.0356	0.0400	0.1166	0.1447
	G7	0.0362	0.0296	0.1744	0.1918	0.0319	0.0202	0.1318	0.1222
	G8	0.0303	0.0401	0.1994	0.1441	0.0214	0.0333	0.0885	0.1567
	G9	0.0239	0.0321	0.2275	0.1726	0.0238	0.0299	0.1023	0.1427
	G10	0.0305	-	0.1616	-	0.0345	-	0.1780	-

Table A.17: Salinity analysis of the grid measurement of the measuring campaigns performed in summer 2002

Date	Stations	Salinity (PSU)	
		Before high water	After high water
21-08-02	G1	26.50	26.20
	G2	26.20	26.00
	G3	26.70	26.20
	G4	25.90	25.40
	G5	25.80	26.30
	G6	26.10	25.90
	G7	25.90	26.50
	G8	25.50	26.20
	G9	26.20	26.00
	G10	25.90	-
22-08-02	G1	25.70	25.50
	G2	26.10	26.10
	G3	26.10	26.10
	G4	26.30	25.60
	G5	26.10	26.40
	G6	26.10	25.70
	G7	26.30	26.10
	G8	25.90	26.10
	G9	26.10	26.10
	G10	26.10	-

Table A.18: Nutrient concentrations of the landbased measurements of the measuring campaigns performed in summer 2002

Date	Stations	Salinity	NO ₂	NO ₃	NH ₄	PO ₄
		(PSU)	gN/m ³	gN/m ³	gN/m ³	gP/m ³
21-08-02	L1	24.6	0.0316	0.1999	0.0685	0.2215
	L2	25.5	0.0119	0.0695	0.0225	0.1782
	L3	22.5	0.0032	0.0093	0.0020	0.2629
	L4	25.7	0.1077	0.0976	0.2466	1.5712
	L5	22.8	0.0252	0.1037	0.0536	0.4303
	L6	23.7	0.0260	0.1431	0.0554	0.3552
	L7	23.4	0.0221	0.2332	0.0463	0.1824
	L8-A	19.5	0.0064	0.1669	0.0096	0.1880
	L8-B	3	0.0076	0.0029	0.0124	0.2425
	L9	23.5	0.0441	0.1649	0.0978	0.2275
	L10	23.9	0.0218	0.1618	0.0457	0.2177
	L11	22.3	0.0392	0.1224	0.0863	0.2431
	L12	24.5	0.0557	0.1369	0.1251	0.3359
	L13	23.8	0.0207	0.1245	0.0430	0.2526
	L14			-	-	-
L15	24.5	0.0250	0.1889	0.0531	0.1770	
22-08-02	L1	24.6	0.0289	0.2075	0.0709	0.2215
	L2	24.3	0.0104	0.1674	0.0213	0.1417
	L3	23.1	0.0024	0.0112	-	0.4304
	L4	23.4	0.0891	0.0827	0.2325	0.6230
	L5	23.6	0.0285	0.1241	0.0698	0.3232
	L6	23.9	0.0632	0.0490	0.1629	1.5872
	L7	23.6	0.0289	0.1770	0.0710	0.2568
	L8-A	21	0.0238	0.1565	0.0573	0.2622
	L8-B	2.8	0.0059	0.0073	0.0093	0.1737
	L9	23	0.0205	0.1486	0.0484	0.1863
	L10	22.8	0.0164	0.1137	0.0374	0.2782
	L11	24.1	0.0161	0.1277	0.0367	0.2067
	L12	24.2	0.0316	0.1866	0.0783	0.2702
	L13	24.1	0.0139	0.0754	0.0308	0.2139
	L14	23.9	0.0143	0.2145	0.0317	0.1166
L15	23.8	0.0207	0.2681	0.0490	0.1094	

Table A.19: Means and standard deviations of nutrient concentrations at landbased stationary measurements of the measuring campaigns performed in summer 2002

Stations	NO ₂ (gN/m ³)		NO ₃ (gN/m ³)		NH ₄ (gN/m ³)		PO ₄ (gP/m ³)	
	Mean	SD	Mean	SD	Mean	SD	Mean	SD
Buesum Mole	0.0282	0.0040	0.2189	0.0422	0.0375	0.0076	0.1546	0.0378
Sewage plant	0.0272	0.0104	2.3346	0.4876	0.0491	0.0326	0.1236	0.0335
Outfall	0.0316	0.0105	1.1610	0.7211	0.0508	0.0158	0.1585	0.0440

Table A.20: Nutrient concentrations at the ship stationary stations of the measuring campaigns performed in summer 2002

Stations	Sampling Type	NO ₂ (gN/m ³)		NO ₃ (gN/m ³)		NH ₄ (gN/m ³)		PO ₄ (gP/m ³)	
		Mean	SD	Mean	SD	Mean	SD	Mean	SD
Ship 1	Surface	0.0264	0.0040	0.3103	0.0652	0.0446	0.0091	0.0981	0.0154
	Bottom	0.0247	0.0050	0.2512	0.0139	0.0475	0.0105	0.0850	0.0125
Ship 2	Surface	0.0321	0.0065	0.3040	0.0558	0.0848	0.0135	0.1177	0.0235
	Bottom	0.0314	0.0066	0.2579	0.0090	0.0884	0.0111	0.1225	0.0249
Automatic Sampler	Surface	0.0311	0.0056	0.2454	0.0558	0.0541	0.0158	0.1626	0.0710
	Bottom	-	-	-	-	-	-	-	-

Appendix B

Calibration and validation results

Table B.1: Calibrated results of nitrate for winter measurements

Stations	Tide	Measured data (gN/m ³)	Calibrated results (gN/m ³)	Discrepancies (%)
G1	2 hours before high water	2.2423	2.1521	4.02
G2		2.1935	2.1351	2.66
G3		2.2014	2.1084	4.22
G4		2.5908	2.0043	22.64
G5		2.4085	2.0768	13.77
G6		2.3702	2.0803	12.23
G7		2.3041	2.1175	8.10
G8		2.3678	2.1296	10.06
G1	2 hours after high water	2.3453	2.1681	7.56
G2		2.1739	2.1610	0.59
G3		2.5828	2.1457	16.92
G4		2.5594	2.0714	19.07
G5		2.8368	2.1182	25.33
G6		2.3195	2.1217	8.53
G7		2.0965	2.1434	2.24
G8		2.3563	2.1409	9.14
Average				10.44

Table B.2: Validated results of nitrate for winter measurements

Stations	Tide	Measured data (gN/m ³)	Validated results (gN/m ³)	Discrepancies (%)
G1	2 hours before high water	1.8684	2.1656	15.91
G2		1.5246	2.1582	41.55
G3		2.3192	2.1457	7.48
G4		2.3278	2.0971	9.91
G5		2.4088	2.1326	11.46
G6		2.3006	2.1321	7.32
G7		2.1958	2.1502	2.08
G8		2.2670	2.1528	5.04
G1	2 hours after high water	2.1674	2.1709	0.16
G2		2.2471	2.1678	3.53
G3		2.2204	2.1594	2.75
G4		2.2138	2.1193	4.27
G5		2.3168	2.1402	7.62
G6		2.4126	2.1472	11.00
G7		2.1218	2.1542	1.53
G8		2.2490	2.1556	4.15
Average				8.49

Table B.3: Calibrated results of ammonium for winter measurements

Stations	Tide	Measured data (gN/m ³)	Calibrated results (gN/m ³)	Discrepancies (%)
G1	2 hours before high water	0.0787	0.1109	40.96
G2		0.0913	0.1100	20.55
G3		0.0898	0.1087	21.04
G4		0.1495	0.1033	30.92
G5		0.1393	0.1070	23.13
G6		0.1248	0.1072	14.09
G7		0.1147	0.1091	4.85
G8		0.1127	0.1098	2.63
G1	2 hours after high water	0.0961	0.1117	16.29
G2		0.1023	0.1114	8.89
G3		0.1128	0.1106	1.99
G4		0.1359	0.1068	21.43
G5		0.1192	0.1092	8.42
G6		0.1131	0.1094	3.34
G7		0.1100	0.1105	0.44
G8		0.1224	0.1103	9.86
Average				14.30

Table B.4: Validated results of ammonium for winter measurements

Stations	Tide	Measured data (gN/m ³)	Validated results (gN/m ³)	Discrepancies (%)
G1	2 hours before high water	0.0754	0.1116	48.13
G2		0.1049	0.1112	6.07
G3		0.1093	0.1106	1.18
G4		0.1306	0.1081	17.25
G5		0.1850	0.1099	40.59
G6		0.1523	0.1099	27.86
G7		0.1233	0.1108	10.13
G8		0.1324	0.1110	16.17
G1	2 hours after high water	0.0812	0.1119	37.88
G2		0.1414	0.1117	20.97
G3		0.1245	0.1113	10.59
G4		0.1358	0.1092	19.54
G5		0.1886	0.1103	41.50
G6		0.1585	0.1107	30.18
G7		0.1158	0.1110	4.13
G8		0.1185	0.1111	6.24
Average				21.15

Table B.5: Calibrated results of phosphate for winter measurements

Stations	Tide	Measured data (gP/m ³)	Calibrated results (gP/m ³)	Discrepancies (%)
G1	2 hours before high water	0.0603	0.0723	19.91
G2		0.0603	0.0717	18.93
G3		0.0603	0.0708	17.51
G4		0.0861	0.0673	21.76
G5		0.0765	0.0698	8.86
G6		0.0627	0.0699	11.44
G7		0.0612	0.0711	16.15
G8		0.0693	0.0715	3.20
G1	2 hours after high water	0.0578	0.0728	26.12
G2		0.0583	0.0726	24.46
G3		0.0632	0.0721	14.01
G4		0.0760	0.0696	8.49
G5		0.0777	0.0712	8.43
G6		0.0594	0.0713	20.08
G7		0.0587	0.0720	22.61
G8		0.0605	0.0719	18.91
Average				16.30

Table B.6: Validated results of phosphate for winter measurements

Stations	Tide	Measured data (gP/m ³)	Validated results (gP/m ³)	Discrepancies (%)
G1	2 hours before high water	0.0738	0.0728	1.38
G2		0.0417	0.0725	73.73
G3		0.0594	0.0721	21.42
G4		0.0749	0.0704	5.91
G5		0.1100	0.0716	34.88
G6		0.0744	0.0716	3.67
G7		0.0620	0.0722	16.55
G8		0.0655	0.0723	10.35
G1	2 hours after high water	0.0581	0.0729	25.54
G2		0.0722	0.0728	0.89
G3		0.0654	0.0725	10.87
G4		0.0685	0.0712	3.99
G5		0.0986	0.0719	27.11
G6		0.0840	0.0721	14.15
G7		0.0626	0.0724	15.52
G8		0.0629	0.0724	15.13
Average				17.57

Table B.7: Calibrated results of nitrate for spring measurements

Stations	Tide	Measured data (gN/m ³)	Computed results (gN/m ³)		Discrepancies (%)	
			Standard Model	Calibrated Model	Standard Model	Calibrated Model
G1	2 hours before high water	0.8692	0.7869	0.7911	9.47	8.98
G2		0.9313	0.7847	0.7907	15.75	15.10
G3		0.7400	0.7783	0.7867	5.18	6.32
G4		0.8198	0.7638	0.7752	6.84	5.44
G5		0.9048	0.7730	0.8263	14.56	8.67
G6		0.7374	0.7775	0.8063	5.44	9.34
G7		0.7942	0.7817	0.7931	1.56	0.13
G8		0.8619	0.7831	0.7909	9.14	8.24
G9		0.7915	0.7732	0.7875	2.31	0.51
G10		1.0326	0.7532	0.7672	27.07	25.70
G1	2 hours after high water	0.7161	0.7864	0.7920	9.82	10.60
G2		0.7308	0.7834	0.7902	7.20	8.14
G3		0.7096	0.7768	0.7856	9.46	10.71
G4		0.7121	0.7649	0.7768	7.41	9.09
G5		0.9278	0.7709	0.8359	16.91	9.91
G6		0.8555	0.7770	0.8171	9.17	4.49
G7		0.8897	0.7820	0.8060	12.11	9.41
G8		0.6037	0.7822	0.7911	29.55	31.03
G9		-	-	-	-	-
G10		-	-	-	-	-
Average					11.05	10.10

Table B.8: Validated results of nitrate for spring measurements

Stations	Tide	Measured data (gN/m ³)	Validated results (gN/m ³)	Discrepancies (%)
G1	2 hours before high water	0.7585	0.7924	4.47
G2		0.6875	0.7927	15.31
G3		0.8285	0.7932	4.26
G4		0.7509	0.7898	5.18
G5		0.6318	0.8144	28.90
G6		0.8456	0.8000	5.39
G7		0.7628	0.7939	4.07
G8		0.7814	0.7941	1.62
G9		0.7902	0.7946	0.55
G10		0.8388	0.7873	6.14
G1	2 hours after high water	0.7222	0.7942	9.97
G2		0.7802	0.7935	1.71
G3		0.7585	0.7915	4.35
G4		0.6970	0.7874	12.98
G5		0.6971	0.8430	20.93
G6		0.7583	0.8214	8.32
G7		0.6838	0.8104	18.51
G8		-	-	-
G9		0.6996	0.7934	13.39
G10		0.6661	0.7849	17.84
Average				9.68

Table B.9: Calibrated results of ammonium for spring measurements

Stations	Tide	Measured data (gN/m ³)	Computed results (gN/m ³)		Discrepancies (%)	
			Standard Model	Calibrated Model	Standard Model	Calibrated Model
G1	2 hours before high water	0.0147	0.0109	0.0157	25.90	6.71
G2		0.0112	0.0109	0.0179	2.75	59.43
G3		0.0109	0.0108	0.0221	0.78	102.54
G4		0.0136	0.0106	0.0266	21.87	95.69
G5		0.0624	0.0107	0.0673	82.80	7.81
G6		0.0325	0.0108	0.0395	66.74	21.55
G7		0.0084	0.0109	0.0227	29.31	169.87
G8		0.0233	0.0109	0.0210	53.30	9.87
G9		0.0107	0.0107	0.0282	0.61	164.06
G10		0.0278	0.0105	0.0312	62.38	12.15
G1	2 hours after high water	0.0143	0.0109	0.0164	23.68	14.48
G2		0.0097	0.0109	0.0186	12.61	92.04
G3		0.0594	0.0108	0.0223	81.83	62.36
G4		0.1845	0.0106	0.0273	94.24	85.22
G5		0.1993	0.0107	0.0880	94.63	55.85
G6		0.2048	0.0108	0.0497	94.73	75.72
G7		0.1185	0.0109	0.0290	90.83	75.56
G8		0.0097	0.0109	0.0229	12.17	136.40
G9		-	-	-	-	-
G10		-	-	-	-	-
Average					47.29	69.30

Table B.10: Validated results of ammonium for spring measurements

Stations	Tide	Measured data (gN/m ³)	Validated results (gN/m ³)	Discrepancies (%)
G1	2 hours before high water	0.0176	0.0144	18.66
G2		0.0061	0.0161	164.44
G3		0.0047	0.0214	355.24
G4		0.0268	0.0266	0.68
G5		0.0789	0.0528	33.12
G6		0.0242	0.0313	29.18
G7		0.0042	0.0199	369.64
G8		0.0138	0.0207	50.23
G9		0.0029	0.0261	816.09
G10		0.0613	0.0318	48.15
G1	2 hours after high water	0.0156	0.0193	24.22
G2		0.0027	0.0211	692.37
G3		0.0035	0.0245	601.19
G4		0.0604	0.0304	49.71
G5		0.0928	0.0934	0.73
G6		0.0762	0.0612	19.68
G7		0.0072	0.0432	496.83
G8		-	-	-
G9		0.0125	0.0321	157.58
G10		0.1086	0.0349	67.86
Average				210.30

Table B.11: Calibrated results of phosphate for spring measurements

Stations	Tide	Measured data (gP/m ³)	Computed results (gP/m ³)		Discrepancies (%)	
			Standard Model	Calibrated Model	Standard Model	Calibrated Model
G1	2 hours before high water	0.0325	0.0328	0.0366	0.86	12.72
G2		0.0286	0.0327	0.0387	14.46	35.55
G3		0.0340	0.0324	0.0428	4.71	25.64
G4		0.0481	0.0318	0.0469	33.89	2.52
G5		0.0592	0.0322	0.0878	45.63	48.26
G6		0.0663	0.0324	0.0601	51.15	9.36
G7		0.0276	0.0326	0.0434	18.13	57.52
G8		0.0445	0.0326	0.0418	26.72	6.17
G9		0.0271	0.0322	0.0488	18.90	79.95
G10		0.0396	0.0314	0.0513	20.71	29.56
G1	2 hours after high water	0.0332	0.0328	0.0373	1.43	12.16
G2		0.0368	0.0326	0.0394	11.34	7.00
G3		0.0656	0.0324	0.0430	50.63	34.38
G4		0.1284	0.0319	0.0476	75.19	62.92
G5		0.1344	0.0321	0.1085	76.09	19.26
G6		0.1253	0.0324	0.0704	74.17	43.85
G7		0.0623	0.0326	0.0497	47.68	20.14
G8		0.0376	0.0326	0.0436	13.33	16.07
G9		-	-	-	-	-
G10		-	-	-	-	-
Average					32.50	29.06

Table B.12: Validated results of phosphate for spring measurements

Stations	Tide	Measured data (gP/m ³)	Validated results (gP/m ³)	Discrepancies (%)
G1	2 hours before high water	0.0324	0.0353	8.87
G2		0.0279	0.0371	32.97
G3		0.0309	0.0422	36.66
G4		0.0392	0.0472	20.43
G5		0.0723	0.0735	1.63
G6		0.0441	0.0521	18.07
G7		0.0334	0.0408	22.10
G8		0.0397	0.0416	4.73
G9		0.0287	0.0469	63.66
G10		0.0724	0.0523	27.79
G1	2 hours after high water	0.0404	0.0402	0.47
G2		0.0272	0.0420	54.06
G3		0.0318	0.0453	42.23
G4		0.0645	0.0509	21.10
G5		0.0711	0.1141	60.40
G6		0.0709	0.0819	15.63
G7		0.0345	0.0640	85.30
G8		-	-	-
G9		0.0360	0.0527	46.70
G10		0.1096	0.0553	49.54
Average				32.23

Table B.13: Calibrated results of nitrate for summer measurements

Stations	Tide	Measured data (gN/m ³)	Computed results (gN/m ³)		Discrepancies (%)	
			Standard Model	Calibrated Model	Standard Model	Calibrated Model
G1	2 hours before high water	0.2785	0.2163	0.2130	22.34	23.53
G2		0.2191	0.2158	0.2106	1.50	3.86
G3		0.2360	0.2137	0.2018	9.45	14.50
G4		0.2250	0.2091	0.1861	7.06	17.32
G5		0.2059	0.2107	0.1886	2.34	8.41
G6		0.2066	0.2130	0.1982	3.07	4.07
G7		0.2031	0.2147	0.2059	5.70	1.36
G8		0.2078	0.2140	0.2009	2.98	3.36
G9		0.1963	0.2124	0.1964	8.19	0.06
G10		0.1410	0.2047	0.1699	45.14	20.47
G1	2 hours after high water	0.2144	0.2155	0.2082	0.50	2.92
G2		0.1762	0.2143	0.2029	21.66	15.17
G3		-	-	-	-	-
G4		0.1574	0.2062	0.1735	31.02	10.22
G5		0.1717	0.2081	0.1744	21.18	1.52
G6		0.1825	0.2114	0.1896	15.81	3.88
G7		0.1941	0.2137	0.1996	10.13	2.86
G8		0.1455	0.2123	0.1841	45.84	26.49
G9		0.1682	0.2083	0.1785	23.85	6.11
G10		-	-	-	-	-
Average					15.43	9.23

Table B.14: Validated results of nitrate for summer measurements

Stations	Tide	Measured data (gN/m ³)	Validated results (gN/m ³)	Discrepancies (%)
G1	2 hours before high water	0.2393	0.2131	10.95
G2		0.2800	0.2108	24.71
G3		0.2002	0.2021	0.95
G4		0.2210	0.1873	15.22
G5		0.2074	0.1898	8.49
G6		0.2264	0.1988	12.16
G7		0.1744	0.2063	18.28
G8		0.1994	0.2022	1.42
G9		0.2275	0.1971	13.36
G10		0.1616	0.1729	7.00
G1	2 hours after high water	0.2838	0.2141	24.57
G2		0.2201	0.2119	3.73
G3		0.2061	0.2017	2.10
G4		0.1136	0.1861	63.80
G5		0.1669	0.1887	13.06
G6		0.1689	0.1999	18.35
G7		0.1918	0.2077	8.25
G8		0.1441	0.1913	32.79
G9		0.1726	0.1890	9.51
G10		-	-	-
Average				15.19

Table B.15: Calibrated results of ammonium for summer measurements

Stations	Tide	Measured data (gN/m ³)	Computed results (gN/m ³)		Discrepancies (%)	
			Standard Model	Calibrated Model	Standard Model	Calibrated Model
G1	2 hours before high water	0.0273	0.0359	0.0368	31.60	34.88
G2		0.0341	0.0358	0.0372	4.89	9.07
G3		0.0410	0.0354	0.0389	13.64	5.20
G4		0.0503	0.0347	0.0420	30.95	16.49
G5		0.0512	0.0350	0.0416	31.74	18.78
G6		0.0482	0.0353	0.0396	26.73	17.78
G7		0.0425	0.0356	0.0381	16.27	10.36
G8		0.0404	0.0355	0.0393	12.09	2.82
G9		0.0413	0.0352	0.0400	14.68	3.22
G10		0.0461	0.0340	0.0454	26.31	1.42
G1	2 hours after high water	0.0363	0.0358	0.0378	1.47	4.07
G2		0.0439	0.0356	0.0388	19.00	11.55
G3		-	-	-	-	-
G4		0.0357	0.0342	0.0448	4.28	25.47
G5		0.0459	0.0345	0.0449	24.83	2.23
G6		0.0344	0.0351	0.0415	1.91	20.56
G7		0.0357	0.0355	0.0395	0.73	10.51
G8		0.0377	0.0352	0.0434	6.68	14.93
G9		0.0347	0.0346	0.0439	0.38	26.46
G10		-	-	-	-	-
Average					14.90	13.10

Table B.16: Validated results of ammonium for summer measurements

Stations	Tide	Measured data (gN/m ³)	Validated results (gN/m ³)	Discrepancies (%)
G1	2 hours before high water	0.0355	0.0368	3.81
G2		0.0231	0.0374	61.98
G3		0.0267	0.0393	47.00
G4		0.0437	0.0427	2.32
G5		0.0431	0.0421	2.16
G6		0.0356	0.0400	12.46
G7		0.0319	0.0383	20.37
G8		0.0214	0.0393	84.06
G9		0.0238	0.0404	70.13
G10		0.0345	0.0462	33.92
G1	2 hours after high water	0.0134	0.0366	172.50
G2		0.0176	0.0371	111.11
G3		0.0179	0.0394	119.39
G4		0.0315	0.0431	36.74
G5		0.0297	0.0424	42.86
G6		0.0400	0.0398	0.49
G7		0.0202	0.0380	88.21
G8		0.0333	0.0421	26.64
G9		0.0299	0.0424	41.96
G10		-	-	-
Average				51.48

Table B.17: Calibrated results of phosphate for summer measurements

Stations	Tide	Measured data (gP/m ³)	Computed results (gP/m ³)		Discrepancies (%)	
			Standard Model	Calibrated Model	Standard Model	Calibrated Model
G1	2 hours before high water	0.1038	0.1126	0.1160	8.48	11.71
G2		0.1011	0.1124	0.1177	11.14	16.42
G3		0.0782	0.1113	0.1243	42.37	58.98
G4		0.1169	0.1089	0.1362	6.84	16.47
G5		0.1353	0.1097	0.1346	18.87	0.48
G6		0.1050	0.1109	0.1271	5.64	21.06
G7		0.0621	0.1118	0.1212	80.19	95.39
G8		0.0869	0.1115	0.1255	28.28	44.45
G9		0.0676	0.1106	0.1284	63.57	89.82
G10		0.1394	0.1066	0.1496	23.52	7.33
G1	2 hours after high water	0.1123	0.1122	0.1198	0.10	6.61
G2		0.1075	0.1116	0.1239	3.85	15.25
G3		-	-	-	-	-
G4		0.1601	0.1074	0.1473	32.95	8.04
G5		0.1351	0.1084	0.1473	19.76	9.06
G6		0.1130	0.1101	0.1341	2.59	18.70
G7		0.1023	0.1113	0.1263	8.77	23.47
G8		0.1633	0.1105	0.1411	32.32	13.59
G9		0.1496	0.1085	0.1434	27.51	4.17
G10		-	-	-	-	-
Average					23.15	25.61


Table B.18: Validated results of phosphate for summer measurements

Stations	Tide	Measured data (gP/m ³)	Validated results (gP/m ³)	Discrepancies (%)
G1	2 hours before high water	0.0670	0.1162	73.51
G2		0.1033	0.1182	14.43
G3		0.0815	0.1254	53.84
G4		0.1227	0.1386	12.94
G5		0.1373	0.1364	0.68
G6		0.1166	0.1284	10.14
G7		0.1318	0.1220	7.46
G8		0.0885	0.1257	42.04
G9		0.1023	0.1298	26.96
G10		0.1780	0.1522	14.50
G1	2 hours after high water	0.0839	0.1154	37.53
G2		0.1011	0.1173	15.99
G3		0.1158	0.1259	8.66
G4		0.1750	0.1399	20.06
G5		0.1372	0.1375	0.27
G6		0.1447	0.1274	11.96
G7		0.1222	0.1208	1.18
G8		0.1567	0.1362	13.13
G9		0.1427	0.1375	3.64
G10		-	-	-
Average				19.42

Erklärung

Hiermit erkläre ich an Eides statt, dass ich die vorliegende Dissertation mit dem Titel "*Process based modelling of the nutrient dynamics in a tidal dominated coastal area*" selbständig angefertigt habe und dabei nur Daten und Informationen der genannten Quellen benutzt habe. Weiterhin versichere ich, dass die vorliegende Dissertation weder ganz noch zum Teil bei einer anderen Stelle im Rahmen eines Prüfungsverfahrens vorgelegt wurde.

Kiel, den 17.09.2004

A handwritten signature in blue ink, appearing to be 'P. Leangruxa', written in a cursive style.

Piyamarn Leangruxa

Lebenslauf

Name: Piyamarn Leangruxa
Date of Birth: 26 August 1975
Place of Birth: Nakhonratchasima, Thailand
Nationality: Thai
Marital status: Single

2000-2004	PhD Student:	Coastal Research Laboratory, University of Kiel, Germany.
1998-2000	M. Eng (Civil Engineering)	Department of Civil Engineering Sirindhorn International Institute of Technology, Thammasat University, Thailand.
1994-1998	B. Eng (Civil Engineering)	Department of Civil Engineering Sirindhorn International Institute of Technology, Thammasat University, Thailand.
1994	Grade 12	St. Lambutus School, Antwerpen, Belgium Exchanged student by AFS program.
1993	Secondary	Suranareewittaya school, Nakhonratchasima, Thailand.

